Mineral Industries Experiment Station

Bulletin No.62

Seventeenth Technical Conference

On Petroleum Production

In co-operation with the

Pennsylvania Grade Crude Oil Association

FOREWORD

This bulletin, presented by the Mineral Industries Experiment Station of the School of Mineral Industries, is a record of the proceedings of the 17th Technical Conference on Petroleum Production which was held on the campus of The Pennsylvania State University on October 28, 29 and 30, 1953.

Neither the conference nor this bulletin could be possible without the help of many persons and organizations, whose aid we wish to acknowledge. We are particularly indebted to those who undertook preparation of manuscripts and presentation of technical discussions. This includes staff members of Divisions of Petroleum and Natural Gas Engineering, Geophysics and Geochemistry, and Mineralogy at the University; The United States Bureau of Mines Station at Bartlesville, Oklahoma; and the Pennsylvania Grade Crude Oil Association Laboratory at Bradford, Pennsylvania.

The conference could not have proceeded successfully without the help of those persons who very willingly acted as co-chairmen for the technical sessions. We acknowledge the assistance of Mr. W. S. Lytle, Dr. E. J. Moore, Dr. E. T. Heck, Mr. P. T. Bail, Dr. J. N. Breston, Dr. A. T. Corey, Mr. C. S. Skow and Mr. W. T. Paynter in this capacity.

A record of the attendance at the conference is contained in the bulletin. We express our appreciation to those from outside the State of Pennsylvania and the Appalachian Area who had sufficient confidence in the success of the conference to travel considerable distances in order to attend.

CONTENTS

LABORATORY EXPERIMENTS WITH DETERGENTS AS WATER-FLOODING ADDITIVES

H.N. Dunning*and Lun Hsiao*

Introduction

The considerable amount of petroleum remaining in producing formations after water flooding is terminated has stimulated research in water-flooding additives. The effects of many types of substances on the efficiency of water flooding have been investigated in laboratory studies.[1, 2, 3, 4] A few of the additives that appeared most promising in laboratory studies have been tested in the field.[5] Of the wide variety of additives tested, water-soluble detergents have shown the most consistent effectiveness in increasing petroleum recovery.

These detergents commonly are effective in lowering the interfacial tension at the oil-water interface and in promoting the wetting of solid surfaces by an aqueous phase. The effect of relative reservoir wettability on the action of these additives has received recent attention.[2, 6] Although laboratory media may be prepared with surfaces distinctly hydrophobic or hydrophilic, the relative wettability of reservoir formations under natural conditions if of a more problematic nature. The ability of a detergent solution to displace petroleum from solid surfaces is a primary requirement if the detergent is to aid more complete recovery of petroleum from reservoirs that have hydrophobic surfaces. The efficiency with which detergent solutions displace petroleum from oil-wet sand surfaces has been investigated by a centrifugal-displacement method.[4, 7] This method was used because the determinations may be made rapidly enough to permit a large number of samples to be tested.

The loss of detergent by adsorption at solid-liquid interfaces and the dilution of detergent solutions by connate water have caused serious doubt that detergents can be used economically as water-flooding additives. However, considerations of the chromatographic theory show that it should be possible to cause a "zone" of detergent to move through the producing formation. This theory originally was developed to explain and predict the movement of "bands" or zones of colored substances through adsorbent columns as the result of flowing a solvent through the columns. Recently the chromatographic theory has been applied to the movement of detergent zones through porous media.[2] The movement of these zones occurs by a continuing process of adsorption and desorption. In effect, this process would allow repeated use of the original quantity of detergent. Few tests of the applicability of the chromatographic theory to the movement of detergent zones have been made. Therefore, the adsorption of typical non-ionic detergents at the sand-water interface was investigated. These studies supplied the data necessary to calculate the rate of detergent-zone movement in porous media. Experimental studies of the rate of detergent-zone movement were made and the results compared with the theoretical values.

Experimental

Petroleum Displacement Efficiencies

A synthetic "oil sand" was prepared by mixing 2 kilograms of Railroad White Sand (40-70 mesh) with 135 grams of crude oil. This was about the maximum quantity of crude oil that could be used without excessive gravity drainage of the oil. The surface area of the sand was 110 $cm.^2/gm.$ The petroleum sample was obtained from the Rio Bravo field, Kern County, Calif., and had a specific gravity of 0.828, 60/60° F. (39.4° API) and a viscosity of 2.68 cp. (37.4 Saybolt seconds at 77° F.) The interfacial tension of this crude oil at a water interface after 1 hour was 19.8 dynes/cm. as determined by the pendent-drop method.

The sand initially was cleaned with hot chromic acid, washed extensively with tap water, distilled water, and acetone, and dried at 110° C. The crude oil was "topped" at 50° C. to remove the more volatile components. This treatment minimized erratic results due to evaporation during the determinations and caused only minor changes in the properties of the crude oil. The synthetic oil sand prepared by this method exhibited a porosity of about 35 percent with normal conditions of packing and about 25 percent of the pore space was filled with crude oil. Samples of the oil sand were removed from the container only after thorough mixing. Between tests, the oil sand was agitated intermittently.

Thirty grams of the synthetic oil sand was placed in a centrifuge tube having a small-diameter calibrated neck. The tube then was filled to a reference mark high on the neck with the detergent solution to be tested. Triplicate tests were made on groups of eight in which one of the tubes contained distilled water as a standard. The tubes initially were centrifuged for 15 minutes; then they were removed from the centrifuge, tilted to about 45°, swirled gently to allow release of trapped oil drops, and centrifuged for another 10 minutes. This treatment was repeated four times, and after each

* Petroleum Experiment Station, Bureau of Mines, Bartlesville, Oklahoma

centrifuging the amount of oil displaced from the sand was measured directly in the calibrated neck. Although the amount of crude oil produced usually reached a constant value after two treatments, this procedure was adopted to insure that equilibrium was attained. The centrifuge was operated at 2500 r.p.m. in these tests. The radial distance from the center of the shaft to the center of the sand sample was 17.3 cm. The application of the centrifuge to the testing of consolidated reservoir materials has been described by Slobod et al. [8]

Results of this type of test are subject to random errors in sampling of the sand. Since no means has been found to eliminate these errors completely, it is essential that conclusions be drawn from statistical calculations rather than from the observations of a single test.

Detergent Adsorption

The adsorption of several non-ionic detergents on Tip Top Sand (140-200 mesh) was investigated. The surface area of this sand was 305 $cm.^2/gm.$ Methods of analysis based on surface-tension and ultraviolet-absorption measurements were used to corroborate and supplement each other. Surface tension values at 25° C. were determined by the du Nouy ring method with a modified chainomatic balance and a combination thermostat-elevating platform. [11] The instrument was calibrated over the range of surface tension to be investigated by measuring the surface tensions of purified benzene and nitrobenzene. In this range

$$\gamma_{corr.} = \gamma_{obs.} \times 0.93$$

where γ = surface tension (dynes/cm.). In the ultraviolet-absorption method the maximum in absorbance at 276 mμ for detergents containing a phenyl group was used. Aqueous detergent solutions of known concentration were prepared, and a calibration curve of absorbance versus concentration was determined. Then detergent solutions of known volume and various known concentrations were shaken with weighed amounts of sand until equilibrium was established. The equilibrium concentrations were determined from the calibration curves by determining the absorbance of the supernatant solutions after centrifuging to remove as much of the suspended matter as possible. The amount of detergent adsorbed (removed from solution) was calculated from the observed change in concentration.

Detergent Zone Movement

The applicability of the chromatographic theory to calculation of the rate of zone movement was investigated. Columns having internal dimensions of 1.0 cm. x 34.0 cm. were packed with Tip Top Sand (140-200 mesh). The porosity of these packed columns was about 35 percent. In a typical determination the column initially was wet with water. Then 3.6 ml. of Igepal CO-630 solution (400 p.p.m.) was put on the column. Then the detergent was eluted with water and the zone movement determined by frontal analysis of the eluent produced.

Results and Discussion

Petroleum Displacement Efficiencies

The relative effectiveness with which a detergent solution displaces petroleum from a solid surface is reported as "displacement efficiency". The term "displacement efficiency" is defined as the amount of oil displaced from a synthetic oil sand by a detergent solution relative to the amount displaced from corresponding sand samples by distilled water. The average displacement efficiency for 0.1 wt.-percent solutions of 54 non-ionic detergents tested [4, 7] was 1.24, while the range in efficiency was 1.02 to 1.38. The average standard deviation of displacement efficiency values was 0.095. The average displacement efficiency for 0.1 wt.-percent solutions of 20 anionic detergents tested was 1.09. Although the anionic detergents were generally inferior to non-ionic types, the "built" anionic detergent formulations, such as Tide, the Nacconols, and Ahcol 350 were as effective as the average non-ionic detergent. Only a few cationic detergents were tested. Of these, only the Ethomeens were effective in displacing petroleum from sand. The Ethomeens tested had only moderate cationic tendencies. The major part of the study was centered on non-ionic detergents, because these substances appeared most promising in displacement efficiencies, are quite inert chemically, and may be prepared with a wide variation in properties.

The hydrophilic portion of many non-ionic detergents is a polyoxyethylene chain. Displacement efficiencies and standard deviation values for 0.1 wt.-percent solutions of 16 effective detergents, formed by condensing ethylene oxide with a variety of hydrophobic groups, are summarized in Table I.

It is observed that these detergent solutions are generally effective in displacing petroleum from sand. The surface tensions of 1.0 wt.-percent solutions of these detergents ranged from 29.5 to 38.3 dynes/cm. and averaged 33.8 dynes/cm. These detergents contained essentially 100 percent of the active ingredients and were water-soluble at room temperature. Previous studies showed that a series of

detergents containing an alkyl phenol as the hydrophobic group and varying amounts of ethylene oxide in the hydrophilic chain exhibited maxima in displacement efficiency when their polyoxyethylene chain was of a length to bestow limited water solubility on them. [4] This indicated that the HLB (Hydrophilic-lipophilic balance) of a detergent is an important factor in determining its efficiency in displacing petroleum.

The average amount of petroleum displaced from 30 grams of synthetic oil sand by distilled water was 1.43 ml., or 63.0 percent of the total petroleum present. The average amount of petroleum displaced from corresponding sand samples by the 16 detergents listed in Table I was 1.81 ml. or 79.7 percent of the total petroleum present.

It is evident that these detergents increase the efficiency of water in displacing petroleum from sand under the test conditions. Therefore, they meet a primary requirement of water-flooding additives. However, this is not the only requirement since better displacement from reservoir surfaces may not necessarily result in more complete petroleum recovery. After an effective displacement of petroleum from reservoir surfaces by the aqueous phase, the residual oil may be present in drops or irregular masses lodged in the porous medium. In the centrifugal displacement method used in these studies, oil drops that have been displaced from the sand surface are subjected to a centrifugal force that tends to eject them from the medium. The removal of displaced oil is expedited by agitation of the sand between applications of centrifugal force. These conditions are not encountered in actual water-flooding operations.

A few linear flood tests using columns packed with the synthetic oil sand were conducted in order to investigate the relationship of results from centrifugal methods to those from flooding studies. In these tests the sand columns were flooded with distilled water until oil production ceased. Then floods consisting of dilute solutions of the detergents that appeared promising in the centrifugal displacement tests were initiated and continued until production of oil again ceased. In each case there was observed a considerable increase in oil recovery as a result of using detergents in the aqueous phase that had proved effective in centrifugal studies.

This type of test is not similar to field conditions for several reasons. In these packed columns, the porosity was relatively high, the clean sand was wet originally with the crude oil before water was introduced, and a very low pressure gradient was used. However, the results indicate that the increased petroleum displacement observed in the centrifugal test is reflected by a more complete recovery of crude oil in linear floods of unconsolidated material. These results are in agreement with the conclusions of other investigators. [3]

Detergent Adsorption

Another consideration in the application of detergents to water-flooding operations is their inherent tendency to be adsorbed at solid-liquid interfaces. The resulting loss in detergent may be sufficient to make the use of detergents uneconomical. From considerations based on the chromatographic theory, Preston and Calhoun [9] and others [10] have shown theoretically that it should be possible to cause a detergent "zone" to move through porous materials by following the detergent solution with water. Trueblood and Malmberg [10] conducted studies of the applicability of this theory to the movement of nitroaniline and substituted nitroaniline through a silicic acid-celite medium. Their results gave evidence in substantiation of the theory.

The adsorption of some typical non-ionic detergents on sand was determined. The adsorption isotherms of Oronite NI-W, Oronite 52555, and Igepal CA-630 on sand from aqueous solutions are shown in Figure 1. The adsorption of each non-ionic detergent investigated could be described by an isotherm resembling one of these three curves. The adsorption of Oronite NI-W can be described by the Langmuir equation while the adsorption of Oronite 52555 appears to be of the BET or multimolecular-layer type. The Igepal CA-630 adsorption isotherm does not fit a general adsorption equation since the adsorption appears to decrease at higher equilibrium concentrations. Although the higher concentration range is less accurately determined than the middle region, the experimental error can hardly account for the rather large decrease in adsorption of Igepal CA-630 as the equilibrium concentration is increased above 200 p.p.m. This decrease was observed using the surface-tension method of analysis as well as the ultraviolet absorption method and it also has been observed in other laboratories. It must be remembered that a sample of polyoxyethylated detergent having a given average mole ratio of ethylene oxide to phenol actually contains molecules with a considerable range in polyoxyethylene chain length. The number of molecules of varying size is represented by Poisson's distribution formula. [12] Therefore, their adsorption characteristics may be influenced by this mole ratio distribution. If real, this decrease in detergent adsorption at higher concentrations may be of considerable importance.

Detergent Zone Movement

According to the chromatographic theory, the rate of zone movement can be calculated from the

constants of the adsorption isotherm and the porosity of the porous medium. 9, 10/ The rate equations show that substances that are adsorbed more strongly may be expected to move more slowly than less strongly adsorbed substances. Further, the shape of the adsorption isotherm determines the tendency of the zone to become diffuse or to resist decreases in concentration. All these detergents have adsorption isotherms that are concave toward the abscissa at the lower concentrations. Therefore, the leading boundary of the zone should exhibit "self-sharpening" tendencies, 9, 10/ thus resisting decreases in concentration while the trailing boundary should tend to spread out spontaneously. These theories are strictly applicable only if equilibrium is established instantaneously. A finite rate of establishment of equilibrium would tend to result in a gradual broadening of the zone with a consequent lowering in concentration.

Since Oronite NI-W is adsorbed according to the Langmuir equation, the rate of detergent-zone movement can be calculated rather accurately for various concentrations. Such calculations indicate that the ratio of zone movement to front movement through porous media of this porosity and surface characteristics should vary from about 0.05 at 25 p.p.m. to 0.32 at 500 p.p.m. and 0.46 at 1000 p.p.m. Since the Igepal isotherms determined are not readily described by a common adsorption equation, the calculation of their movement at concentrations above about 50 p.p.m. involves large assumptions. Calculations assuming that the three isotherms shown in Figure 1 are linear below 50 p.p.m. indicate that the ratio of zone movement to flood movement should be about 0.07 at this concentration.

The applicability of the chromatographic theory to calculating rate of zone movement was checked by frontal analysis of the eluent from a chromatographic column in which 3.6 ml. of Igepal CO-630 solution was put on the column at a concentration of 400 p.p.m. and eluted with water. The adsorption isotherm of this detergent resembled that of Igepal CA-630 (Fig.1). If it is assumed that Igepal CO-630 actually obeys the Langmuir equation and if the constants are evaluated from the portion of the isotherm below the "hump", the ratio of zone movement to flood movement should be about 0.3. This result is only approximate because the isotherms of the Igepals actually show considerable deviations from the Langmuir equation as mentioned previously.

Figure 2 shows the shape of the detergent zone as determined experimentally (curve 1), as injected (curve 2), and as predicted from the chromatographic theory (curve 3) with the above assumptions. It is observed that the peak concentration was reached after about the calculated amount of eluent had been produced. The peak concentration is much less than the concentration of the solution put on the column (about 30 p.p.m. compared to 400 p.p.m.). Since the volume of solution put on the column was much less than the calculated minimum volume to allow elution of a zone of the original concentration, the theoretical zone also has a considerably lower peak concentration than the injected solution. The experimental zone is considerably more diffuse than was predicted from the theory assuming instantaneous establishment of equilibrium. This behavior would be expected if the eluent flowed through the column at a rate much greater than that required for the establishment of equilibrium conditions. The production of eluent at about 20 ml. per hour is probably one of the causes of the diffuse experimental zone. A slower rate of elution might be expected to allow the formation of a much sharper zone. Later semiquantitative experiments indicate that this is indeed the case. It might be pointed out that movement of a water flood at perhaps 1 foot a day represents about 1/20 the rate that was used in this study. Therefore, it would be expected that the actual zone obtained in water-flooding operations would resemble the theoretical zone more closely than did the zone (curve 1) determined experimentally.

Moore and Blum 2/ report some microscopic observations of the effect of a sharp interfacial-tension change on the displacement of oil by an aqueous phase. They observed that parts of the irregular oil masses lodged in irregular pores were broken off and moved through the medium when a sharp change in interfacial tension occurred. A gradual change in interfacial tension did not have this effect. If the detergent zone moving through a porous medium has a sharp leading boundary, as predicted from the above isotherms, such a sudden change in interfacial tension may occur. However, these workers were unable to obtain such a high interfacial-tension gradient in experiments with long cores. 2/

The adsorption isotherms and chromatographic determinations discussed above were determined with a carefully cleaned sand. Similar experiments with sand that has contacted crude petroleum may give results with a closer resemblance to actual conditions. Experiments of this type are included in the proposed research program of this laboratory.

Conclusions

A centrifugal method has been used to evaluate the efficiencies with which aqueous solutions of detergents displace petroleum from sand surfaces. The results of these tests with 0.1 wt.-percent solution of 16 polyoxyethylated detergents summarized in this report show that they are effective for this purpose. These detergents displaced 1.15 to 1.33 times the amount of petroleum from synthetic oil-sand samples that was displaced by water from corresponding samples. The average displacement efficiency was 1.265. The average amount of petroleum displaced from 30 grams of synthetic oil sand by distilled water was 1.43 ml. or 63 percent of the total petroleum present. The average

amount of petroleum displaced from corresponding sand samples by the 16 detergents listed was 1.81 ml. or 79.7 percent of the total petroleum present.

The adsorption of several non-ionic detergents at the sand-water interface was determined. The adsorption isotherms were of varying forms, although all were concave toward the abscissa at the lower concentrations. The adsorption of Oronite NI-W can be described by the Langmuir equation, while the adsorption of Oronite 52555 appears to be of the BET or multimolecular type. The adsorption isotherm of Igepal CA-630 is not readily described by the common adsorption equations.

The applicability of the chromatographic theory to the prediction of detergent-zone movement and shape was tested experimentally. Theoretical considerations show that for Igepal CO-630 the ratio of zone movement to flood movement through the porous medium used should be about 0.3 at a concentration of 400 p.p.m. This detergent and the others studied would be expected to form zones that were self-sharpening at the leading boundary and diffuse at the trailing boundary. Experimental results were in general agreement with predictions based on the chromatographic theory.

Bibliography

1. Terwilliger, P. L., and Yuster, S. T., "Chemical Agents in Water-Flooding," Producers Monthly, vol. XI, No. 1, 1946, pp. 42-45.

2. Moore, T. F., and Blum, H. A., "Wettability in Surface-active Agent Water Flooding," Oil and Gas Journal, vol. 51, No. 31, 1952, pp. 108-111.

3. Calhoun, J. C., Stahl, C. D., Preston, F. W., and Nielsen, R. F., "A Review of Laboratory Experiments on Wetting Agents for Water Flooding," Producers Monthly, vol. 16, No. 1, 1951, pp. 15-23.

4. Dunning, H. N., Gustafson, H. J., and Johansen, R. T., "Displacement of Petroleum from Sand by Solutions of Polyoxyethlated Detergents," presented: 124th. American Chemical Society National Meeting, Chicago, Ill., Sept. 8, 1953.

5. Breston, J. N., and Johnson, W. E., "Experiments with Wetting Agents in the Bradford Field," Producers Monthly, vol. 16, No. 1, 1951, pp. 24-30.

6. Caro, R. A., Calhoun, J. C., and Nielsen, R. F., "Experiments Using Surface Active Agents to Increase Oil Recovery," Pennsylvania State College, Mineral Industries Experiment Satation, Bulletin No. 60, 1952, pp. 57-59.

7. Dunning, H. N., Hsiao, Lun, and Johansen, R. T., "Petroleum Displacement by Detergent Solutions," Bureau of Mines Report of Investigations, to be published.

8. Slobod, R. L., Chambers, Adele, and Prehn, W. L., "Use of Centrifuge for Determining Connate Water, Residual Oil, and Capillary Pressure Curves of Small Core Samples," Journal of Petroleum Technology, vol. 3, No.4, 1951, pp. 127-134.

9. Preston, F. W., and Calhoun, J. C., "Applications of Chromatography to Petroleum Production Research," Producers Monthly, vol.16, No. 5, 1952, pp. 22-31.

10. Trueblood, K. N., and Malmberg, E. W., "An Experimental Study of Chromatography on Silicic Acid-Celite. The Applicability of the Theory of Chromatography," Journal of the American Chemical Society, vol. 72, No. 9, 1950, pp. 4112-4124.

11. Dunning, H. N., and Johansen, R. T., "A Combination Thermostat and Elevating Platform for the Surface-Tension Balance," Review of Scientific Instruments, vol. 24, September 1953, to be published.

12. Mayhew, R. L., and Hyatt, R. C., "The Effect of Mole Ratio Distribution on the Physical Properties of Poloyoxyethylated Alkylphenol," Journal of the American Oil Chemists' Society, Vol. XXIX, No. 9, 1952, pp. 357-362.

TABLE I

Petroleum Displacement Efficiencies of Polyoxyethylated Detergents

Detergent	Manufacturer	Hydrophobic constituent	Displacement efficiency	Standard deviation
Emulphor ON-870	General Dyestuff Corp.	Oleic acid (ether)	1.24	0.086
Emulphor EL-719	do.	Castor oil (ester-ether)	1.26	.059
Ethofat C/25	Armour and Co.	Coco fatty acids (ester)	1.30	.001
Ethomeen 18/20	do.	Stearyl amine	1.28	.001
Ethomid HT/25	do.	Hydrogenated tallow amide	1.26	.001
Ethomid C/25	do.	Coco amide	1.15	.114
Ethomid RO/25	do.	Red 611 amide	1.26	.087
Igepal CA-630	General Dyestuff Corp.	Alkyl phenol	1.28	.094
Igepal CO-710	do.	do.	1.28	.161
Lissapol N-380	Arnold Hoffman and Co., Inc.	do.	1.33	.038
Lubrol W.	do.	Fatty alcohol	1.24	.022
Dispersant NI-W	Oronite Chemical Co.	Alkyl phenol	1.29	.161
Nonic 218	Sharples Chemicals, Inc.	Tert. dodecylthioether	1.29	.192
Synthetics B-79	Hercules Powder Co.	Alkyl phenol	1.28	.069
Synthetics B-48	do.	Rosin (ester)	1.30	.001
Tween 80	Atlas Powder Co.	Sorbitan Mono-oleate (ester-ether)	1.21	.190
Average			1.265	0.080

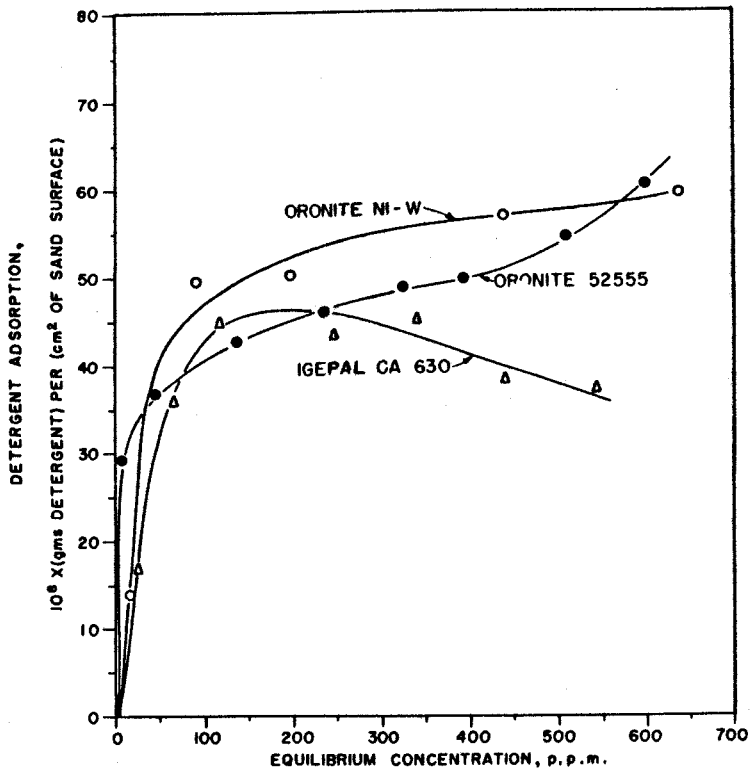

Figure 1.— Examples of adsorption isotherms of polyoxyethylated detergents.

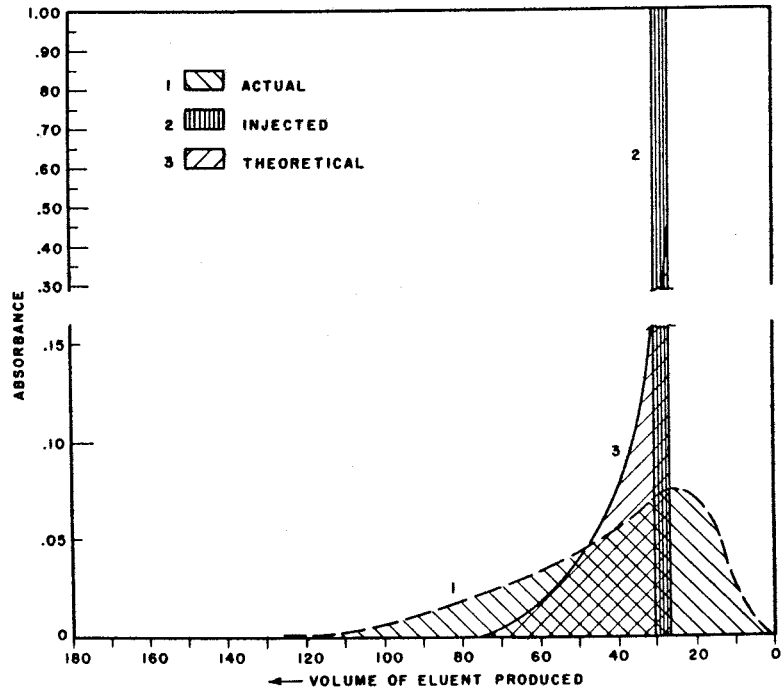

Figure 2.—Theoretical and experimental detergent zones

CORRELATION OF OIL RESIDUALS FOLLOWING SURFACTANT FLOODS

Edmundo Ojeda*, Floyd Preston** and J. C. Calhoun**

The petroleum industry has for some years been intrigued by the possible use of surface active agents as additives in water flooding for the recovery of oil. Although a reasonable amount of laboratory effort has been expended on this problem the effort has usually led to conjecture rather than to sound conclusions. The barrier to a lack of understanding has in a large measure been due to an inadequate knowledge of those variables which have control over oil recovery. Consequently, it has been hard to evaluate test results or to know what properties of a surface active agent to stress for accomplishing additional oil recovery.

Increased knowledge about porous materials and the nature of capillary forces within them, coupled with controlled tests, have brought about progress on use of surface active agents within the past year or two. In 1952, Caro, et al[1], reported that oil recoveries might be effected differently from oil-wet and water wet systems and indicated that removal in a specific water wet system was accomplished with less additive material than in an oil wet system. The presentation in this report is a continuation of Caro's work to cover more specifically the variables indicated by him. A general correlation of variables is possible for the water wet system studied although the scope of the work does not permit the determination of a specific surface active agent to effect oil recovery in a given instance.

Experimental Procedure:

Because the work of Caro and that of Moore[2], as well as general work on porous materials, has indicated a basic difference in oil retention in oil-wet and water-wet systems, a decision was made to segregate the two efforts. A series of water-wet consolidated sandstone specimens were obtained by acid-treating natural Berea sandstone. Berea sand was deemed to be naturally water wet, but it was felt that acid treatment should be used to reduce the surface variation to a minimum. The individual samples were radial, flood pot type samples which had been cut from a diamond drill core.

The fluids used were n-octane and water. All core samples were first saturated with water, then were flooded with n-octane at 50 cm. Hg pressure to obtain a specimen with a simulated interstitial water and original oil saturation. The specimens were flooded with distilled water and then with solutions of surfactant. The surfactant was Igepal CA Extra Concentrated # in all cases. Figure 1 shows a flow diagram of the apparatus used.

Two different flooding procedures were employed. In the first procedure, distilled water flood was followed by a flood with a water solution of 0.001% agent by weight, which in turn was followed by floods with .01% and 0.1% solutions. Upon completion of this sequence the pressure of flood was raised in increments. Finally, the core was dismounted and analyzed for residual n-octane content by ASTM methods.

This procedure proved to be unsatisfactory for determination of residual n-octane content at intermediate pressures or with intermediate solution concentrations because the recovered increments of n-octane could not be measured accurately. For determining residual n-octane content as a function of applied pressure and concentration, therefore, a given water flood was followed by a given solution flood at a given pressure and concentration. ASTM extraction then was used to determine residual n-octane content.

The residual n-octane content following straight water flooding was always determined by subtracting produced n-octane by water flood from the original n-octane content. Water floods were terminated when fluid rates became constant and no additional oil production was evident.

Contribution Number 53-17, School of Mineral Industries, The Pennsylvania State College.

* Former graduate student, Division of Petroleum and Natural Gas Engineering, The Pennsylvania State College, now of Creole Petroleum Corporation, Venezuela.

** Division of Petroleum and Natural Gas Engineering, The Pennsylvania State College.

The General Dyestuff, Inc. condensation product of ethylene oxide with an alkyl phenol. Similar material is supplied under other trade names, for example, Hercules B-79.

In all floods, the effluent water was collected and periodic surface tension readings were made. Each flood was continued until it was judged that the effluent stream had reached substantially the same surface tension as the solution being used for injection. Figure 2 shows the surface tensions of the surfactant solutions and their interfacial tensions against n-octane. All tension readings were made at 31°C.

Following the termination of a solution flood and prior to the determination of octane residual by ASTM extraction, the test sample was flooded again with distilled water at the same applied pressure as had been used on the solution flood. The object was to desorb the surface active agent so that it did not interfere with weight determination for the ASTM test. In no instance was oil recorded as having been produced during this water flushing period.

After extraction and before being resaturated for another run each core was again cleaned of any possible residual surfactant by the passage of large volumes of distilled water. Each core was used several times. The consistency which was obtained on initial octane content prior to water flooding on successive uses attests to the sufficiency of the cleaning method and indicates that wetting properties of the surface were consistent.

Experimental Results on Octane Residuals:

In Table I are listed the results of the individual tests. Listed are (1) the applied pressure for the test (which would be the final applied pressure in those instances where the pressure was raised during the run; this applied to runs Nos. 1-6), (2) the interfacial tension between n-octane and the solution used for flood (which would be the final solution used in those cases where the concentration was increased during the test; this applied to runs Nos. 1-4 and 7), (3) the permeabilities, (4) the porosities, (5) the quantity $(k/\phi)^{1/2}$, (6) the residual n-octane values, and (7) the quantity $\gamma/\Delta P$.

Figure 3 shows three of the typical relationships found when the residual n-octane saturation values are plotted versus $\gamma/\Delta P$ for an individual core. These plots include the residual values following straight water flood as well as those following surfactant flood. It is not certain from these curves what the value of residual n-octane should be for $\gamma/\Delta P$ equal to zero.

It was noted that the individual plots of residual n-octane versus $\gamma/\Delta P$ are almost parallel, and that the variation depended upon the pore geometry constants of the specimens. Consequently, in Figure 4, residual n-octane has been plotted versus $(k/\phi)^{1/2}$ using $\gamma/\Delta P$ as a constant parameter. A family of parallel lines is deduced. $(k/\phi)^{1/2}$ is used to indicate the complexity of porous structure. This is a commonly used quantity for the correlation of residual wetting fluids, but has not been used for correlation of non-wetting residual fluids. The parallelism of the relationships at constant $\gamma/\Delta P$ would be indicative of a consistent contribution of the pore matrix to residual under any flow conditions.

Other more complex correlations were sought to bring all data to a common curve, or to explain a given mechanism of oil retention by virtue of the variables being grouped. None of the relationships tried appeared to give a better understanding of the variables to be grouped. Two of the attempts will be shown.

Should one consider the dimensional number which results from capillary pressure terminology, the result is,

$$P_c = \frac{\gamma}{(k/\phi)^{1/2}} J(S_w)$$

or

$$\frac{1}{J(S_w)} = \frac{\gamma}{P_c}\left(\frac{\phi}{k}\right)^{1/2}$$

If one considers the applied pressure to be proportional to the capillary pressure which would result at oil residual then a plot of $(\gamma/\Delta P)(\phi/k)^{1/2}$ versus residual oil might be useful. The log-log curves of Figure 5, with a variation at constant $\gamma/\Delta P$ again being evident, is the result of this relationship.

Brown, et al[3] have deduced a dimensionless number for correlating of residual liquid content of porous media. His number

$$\frac{k(-\Delta P)}{L g_c \gamma \cos\theta}$$

is obtained by balancing the driving force $\Delta P/L$ against the restraining force $\gamma \cos\theta/k$; g_c is a units conversion factor. This might be thought of as a modification of the previous correlation.

In Figure 6 this type plot has been used for all the data taken. The correlation given by Brown for residuals in different porous matrixes is drawn also on Figure 6. The spread of residual values from the average is quite large.

Experimental Results on Surfactant Required:

In all instances the change in surface tension of the effluent stream was used as a measure of the amount of solution required to effect oil recovery. The behavior of the effluent surface tensions was as would be inferred from adsorption theory.(4) This theory indicates that the advance of surface active material should be slower than the carrying stream, that the lag should be least for the highest concentration solution and that the lag should be proportional to the internal surface area for adsorption. All of these observations are substantiated by the data taken.

Figures 7 and 7A give plots of the successive reductions in effluent surface tension when the inlet concentrations were successively raised from .001% by weight, to .01% by weight and then 0.1% by weight. This behavior is shown for three separate cores. During this sequence the applied pressures were constant. In all cases the number of pore volumes required to reach equilibrium is less as the concentration increases.

The same effect is shown in Figure 9 which is a typical plot of the results when three successive runs were made on a single core; each time surfactant flood started after the water flood. Pressure may have been different on two such instances as are shown here but if so the relative positions of the curves were not changed. Again, these data show that the solution front lags behind the water advance least for the highest concentration solution. Similar data were obtained on four cores, and the average amounts of fluid required for the effluent surface tension to reach equilibrium were used to construct Figure 10, a plot of R versus solution concentration. R is defined(4) as the rate at which the solution front advances relative to the rate at which fluid is injected. It is of interest to note that a 1% solution would bring this value to greater than .50 which is definitely encouraging for commercial application.

In Figure 8 the increased loss of surfactant with increased surface area is shown, $(k/\phi)^{1/2}$ being cited as inversely proportional to the internal surface area per unit of pore volume. These graphs were taken for runs on different cores for which the concentration of solution was a constant. An exact value for R in a given situation would require taking into account the internal surface area of the particular formation under discussion.

Experimental Results on Fluid Rates:

Effluent rates were not measured continuously, but sufficient spot readings were made to indicate that the effluent rates were increased as concentration of the surfactant solution was increased. This observation indicates that octane was being continuously moved by the solution. Table II gives a list of the effluent rates at the start and end of the surfactant floods. In spite of the increases in fluid rate due to removal of octane it is evident that the surfactant solutions were producing some plugging, as evidenced by a decline in rates over long periods when little octane was being moved. Figure 1 gives spot rate readings on Run No. 1. Although the fluid rate gradually increased as octane was removed, the rate declined over short intervals when the octane content remained relatively constant. This behavior was found in several similar runs.

Discussion of Results on Water Wet System:

It is encouraging that variables centributing to oil recovery can be grouped to yield consistent correlations such as Figures 3-6. However, it is not possible to say from the work thus far, that any particular grouping so far advanced is any better than another particular grouping.

Interfacial tension is only one of the characteristics of surfactant solution in the presence of oil that might be considered as a correlating parameter. It was, however, the only variable considered to date. The inference of the correlations presented is that γ is the only required parameter of the surfactant solution. The inference is supported by the fact that interfacial tensions between octane and distilled water (no surfactant) also fall in line. However, it is reemphasized that only one

surfactant was used and further work must be done to prove that interfacial tension suffices to correlate residuals in water wet systems.

It is also implied in the present work that cos $\theta = 1.0$ for all runs made. Although it is felt that this condition was adhered to, there is no proof of it. Consistency of interstitial water by octane displacement is perhaps the best proof that each core was brought back to a standard surface condition before water flooding. It would be expected that the use of a surfactant giving low γ but a change in wettability such that cos $\theta \neq 1.0$ would give residuals not correlatable with residuals when cos $\theta = 1.0$. The consistency of oil residuals may also be taken as evidence of consistent surface conditions, therefore.

As indicated in Figure 3, the values of residual octane might go to zero when $\gamma/\Delta P$ goes to zero. This need not be so, and additional data would be required to prove the point. A given pore geometry could be such that at $\gamma/\Delta P = 0$ a properly oriented residual octane content could remain. Correlations such as Figure 4, therefore, are not expressable in equation form except over the specific range of $\gamma/\Delta P$ values examined here.

Since the size of flood pot sample was not varied in the present work it is impossible to say whether ΔP or $\Delta P/L$ should be the proper parameter to use in correlations. This point must be examined further.

According to the data cited here, residual oil could be taken low enough in this porous system to be of definite commercial significance. Probably the importance of the value of ΔP (or $\Delta P/L$) in a given instance would be equal to or greater than the value of γ in determining the commercial use of surfactants.

Also according to the data cited here, the adsorption characteristics of the system studied are in the commercial range, or at least indicate that they may be brought into the commercial range by the choice of a surfactant having better adsorption properties than the one used.

Acknowledgment:

The experimental apparatus with which this work was performed was contributed by the research project of The Pennsylvania Grade Crude Oil Association. The data and techniques are reported in greater detail in the M. S. thesis of Edmundo Ojeda, from which this paper is condensed.

References:

1. R. A. Caro, J. C. Calhoun and R. F. Nielsen, "Experiments Using Surface Active Agents to Increase Oil Recovery", 16th Annual Technical Meeting and Bull. 60, Mineral Industries Experiment Station, State College, Pennsylvania, October 1952.

2. T. F. Moore and H. A. Blum, "Importance of Wettability in Surface Active Agent Water Flooding", 16th Annual Technical Meeting and Bull. 60, Mineral Industries Experiment Station, State College, Pennsylvania, October 1952.

3. Brown and Associates, Unit Operations, Chapter 17, page 223, John Wiley and Son.

4. F. W. Preston and J. C. Calhoun, "Application of Chromatography to Petroleum Production Research", 15th Technical Meeting and Bull. 59, Mineral Industries Experiment Station, State College, Pennsylvania, October 1951.

TABLE I

SUMMARY OF DATA FOR WATER WET SYSTEM

Core	K(mds)	ϕ	ΔP cm hg	γ	S_{OR}	Initial Oil (%)	Run No.
			1.2	37.8	45.4	68.2	1
MO14-78	512	.239	5.3	37.8	34.8	68.2	16
			5.3	37.8	33.9	68.2	8
			5.3	11.9	24.1		16
			5.3	3.4	19.5		8
			15.3	3.4	13.1		1
MO16-13	317	.213	5.3	37.8	37.8	63.9	17
			5.3	37.8	38.6	63.9	9
			5.3	11.9	26.8		17
			5.3	3.4	20.1		9
			1.2	37.8	43.8	63.9	2
			15.3	3.4	14.9		
Berea 4	487	.237	5.3	37.8	35.4	64.6	18
			5.3	37.8	34.6	64.6	10
			5.3	11.9	24.0		18
			5.3	3.4	20.3		10
			1.2	37.8	46.4	64.6	3
			15.3	3.4	17.1		3
MO14-106	323	.235	5.3	37.8	40.3	66.0	19
			5.3	37.8	41.3	66.0	4
			5.3	11.9	26.2		19
			5.3	3.4	23.3		4
			5.3	37.8	41.3	66.0	11
			15.3	3.4	18.4		11
MO14-102	220	.225	5.3	37.8	43.1	66.0	20
			5.3	37.8	51.0	66.0	5
			5.3	11.9	29.2		20
			5.3	3.4	25.7		5
			5.3	37.8	44.9	66.0	12
			15.3	3.4	21.3		12
MO16-21	200	.214	5.3	37.8	39.4	63.4	21
			5.3	37.8	51.6	63.4	6
			5.3	11.9	30.5		21
			5.3	3.4	27.7		6
			5.3	37.8	40.4	63.4	13
			15.3	3.4	23.0		13
BE-24	190	.216	5.3	37.8	41.6	61.5	14
			5.3	3.4	27.7		14
			5.3	37.8	41.9	61.5	23
			15.3	3.4	22.3		23
BE-25	485	.257	5.3	37.8	37.6	66.2	15
			5.3	3.4	21.1		15
			5.3	37.8	39.0	66.2	22
			15.3	3.4	15.1		22
			5.3	37.8	39.0	66.2	7
			10.3	21.7	30.3		7

TABLE II

INCREASE IN WATER RATES DURING SURFACTANT FLOOD

Run No.	Core	cc/min At Start Of Flood	cc/min At End Of Flood	Pore Volumes Of Flood
8	MO14-78	9.0	16.0	66.1
16	MO14-78	8.5	12.0	181
9	MO16-13	5.3	7.96	47.8
17	MO16-13	1.65	2.68	148
10	Berea #4	8.13	15.4	46.0
18	Berea #4	4.26	8.75	137
11	MO14-106	7.66	19.8	46.4
19	MO14-106	1.54	2.05	137
12	MO14-102	5.0	15.5	53.7
20	MO14-102	1.25	1.64	120
13	MO16-21	6.25	15.3	51.6
21	MO16-21	.87	1.77	97.4
14	Be-24	2.75	2.23	40.5
23	Be-24	7	15.0	62.8
15	Be-25	13.0	14.3	53.2
22	Be-25	19	49.6	64.0

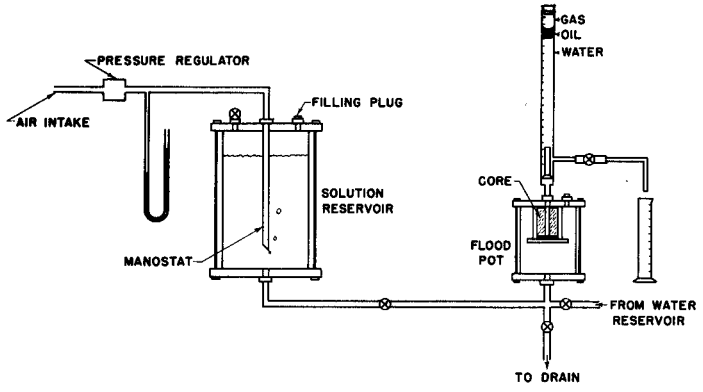

FIGURE 1 WATER FLOOD APPARATUS

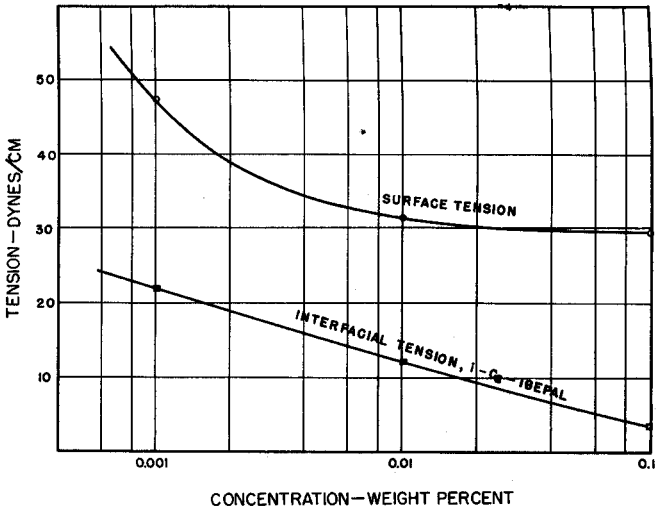

FIGURE 2. SURFACE AND INTERFACIAL TENSION OF IGEPAL CA EXTRA

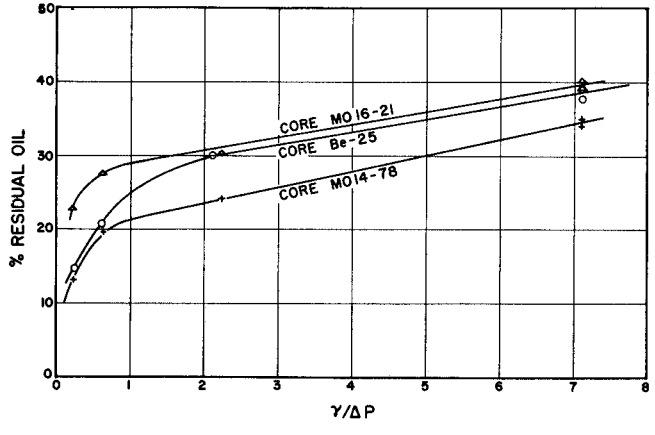

FIGURE 3 RESIDUAL OIL SATURATIONS vs. $\gamma/\Delta P$

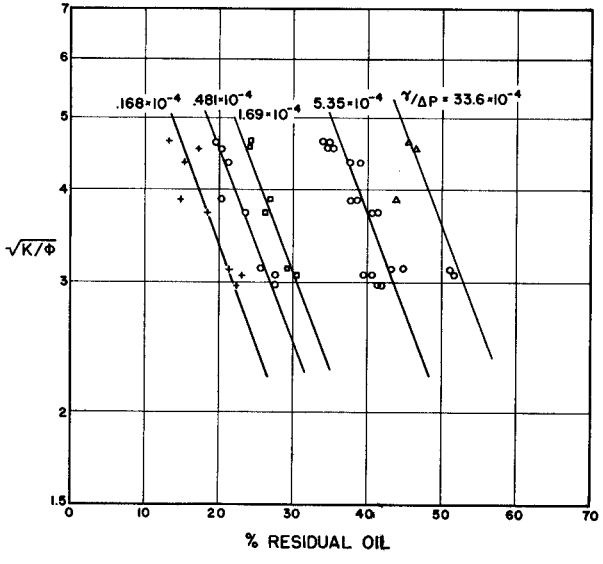

FIGURE 4 CORRELATION OF RESIDUAL OIL SATURATIONS

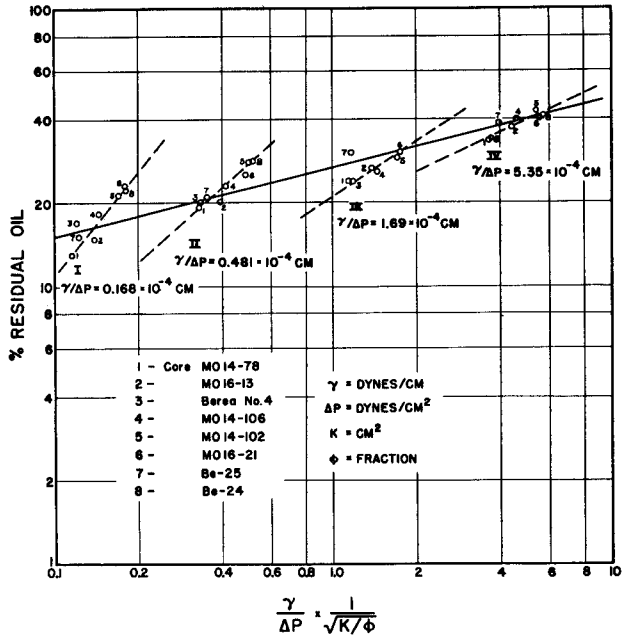

FIGURE 5 RESIDUAL OIL CORRELATION

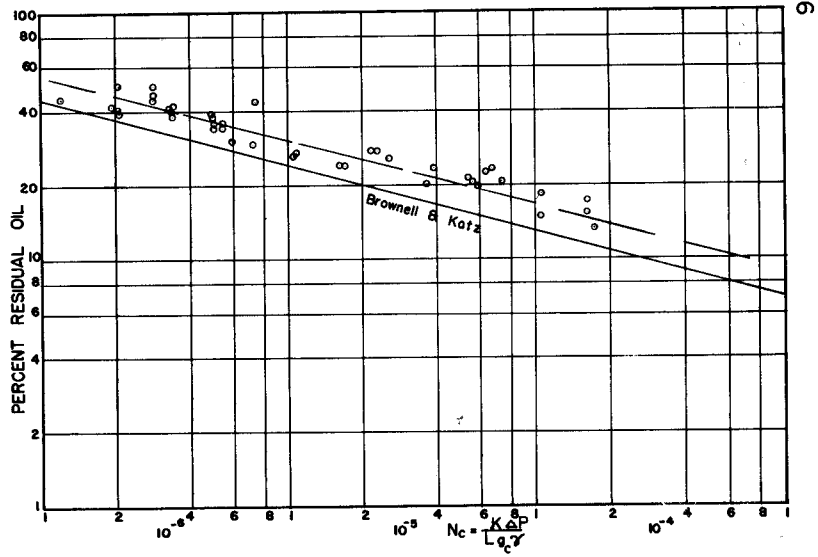

FIGURE 6. CORRELATION OF RESIDUAL OIL SATURATION

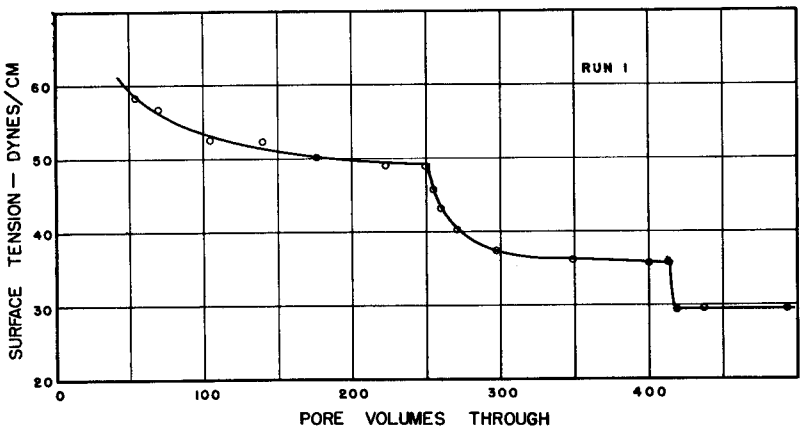

FIGURE 7. SURFACE TENSION VS PORE VOLUMES THROUGH

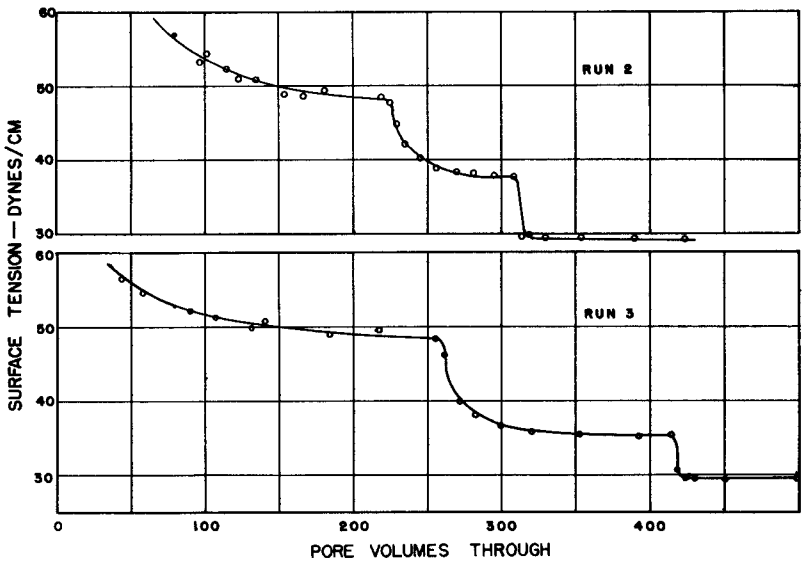

FIGURE 7A. SURFACE TENSION VS PORE VOLUMES THROUGH

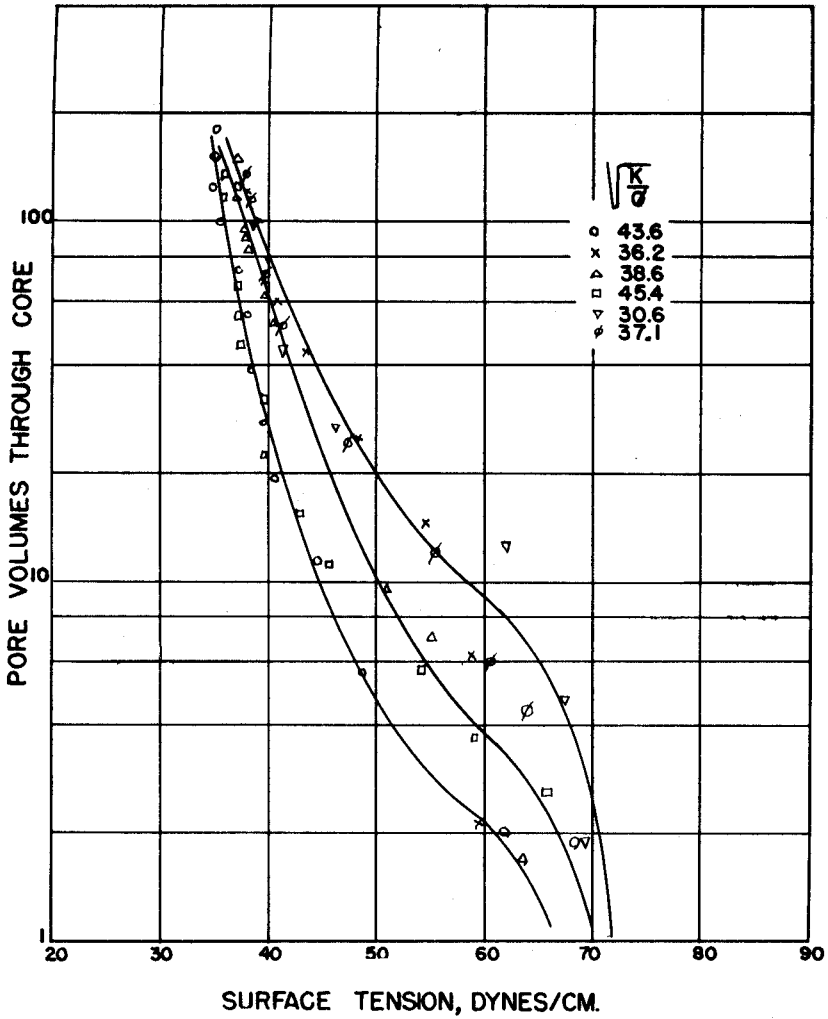

FIGURE 8. EFFECT OF CORE PROPERTIES ON PORE VOLUMES TO ATTAIN CONSTANT EFFLUENT STREAM CONCENTRATION

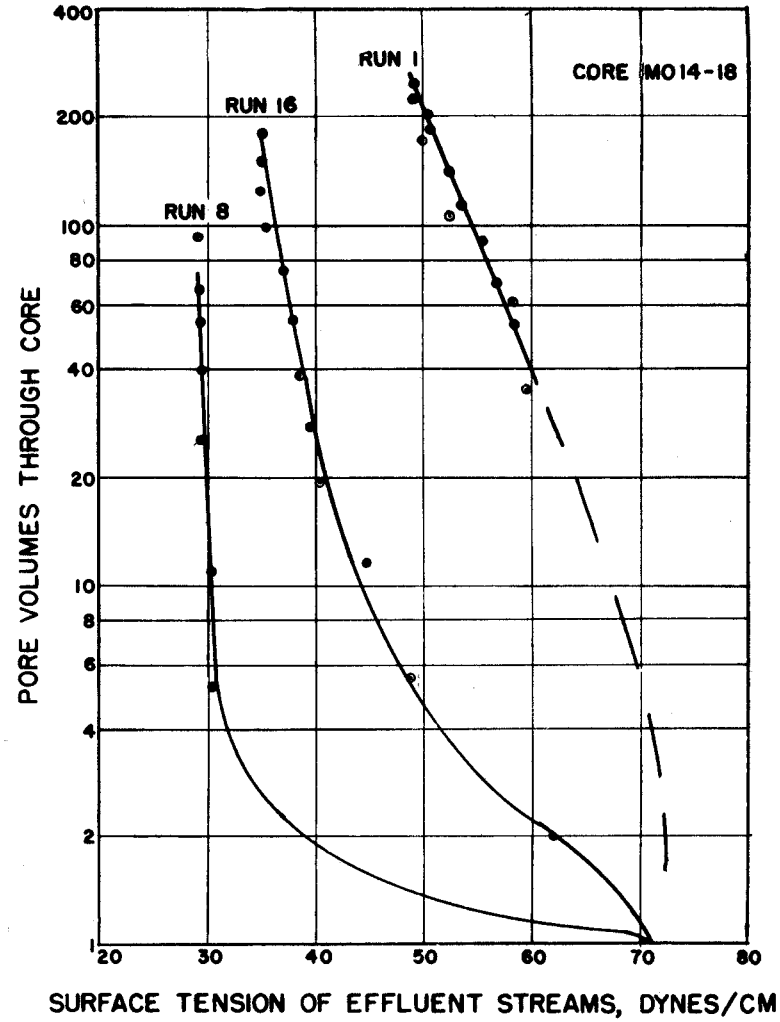

FIGURE 9 EFFECT OF AGENT CONCENTRATION ON PORE VOLUMES TO ATTAIN CONSTANT EFFLUENT STREAM CONCENTRATION

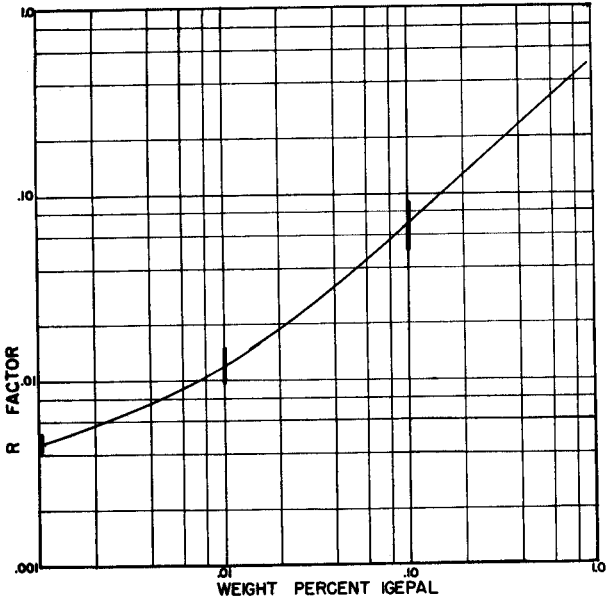

FIGURE 10. RATE OF AGENT AND WATER MOVEMENT

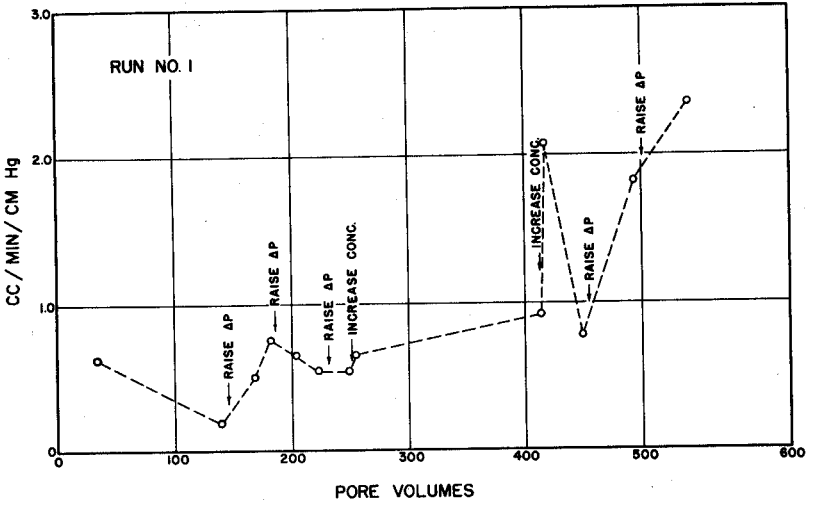

FIGURE 11 FLUID RATE PER UNIT OF APPLIED PRESSURE

PHASE EQUILIBRIA FOR MIXTURES OF CARBON DIOXIDE AND SEVERAL NORMAL SATURATED HYDROCARBONS

W. C. Stewart* and R. F. Nielsen**

Abstract

The solubility of carbon dioxide in n-octane, n-decane, n-dodecane, n-tetradecane, and n-hexadecane at 60°F and 90°F was measured over the entire composition range. Two liquid phases were encountered in the case of tetradecane and hexadecane. The trends in the degree of carbon dioxide miscibility with increasing molecular weight of the hydrocarbon, and with the nature of the hydrocarbon mixture are discussed. The use of "equilibrium constants" for phase calculations involving three phases is illustrated.

Introduction

The possibility that carbon dioxide may have some uses in the oil industry has been discussed from time to time for a good many years. These possibilities arise from its cheapness, its miscibility with hydrocarbons, and other properties. Pirson[1] in 1941 proposed the injection of carbon dioxide into a reservoir at fairly high pressures as a means of recovering part of the oil left after primary production. More recently the use of carbon dioxide in connection with water flooding has received a good deal of attention.[2,3] The fact that it is fairly soluble in water, coupled with its solvent properties for hydrocarbons seemed to justify field and laboratory experimentation involving the injection of carbon dioxide coincident with a water flood.

Among other properties of carbon dioxide which put it in a favorable light are its critical temperature and pressure, 88°F and 1072 psia. That is, it is condensible without excessive pressures at temperatures which might be encountered in many cases. At higher temperatures the compressed gas should have better solvent properties than methane at the same pressure. The vapor pressure is high enough to facilitate subsequent separation and recovery. The lesser degree of miscibility of heavy hydrocarbons in liquid carbon dioxide as compared with light hydrocarbons, suggests uses as a selective solvent.

A survey of the literature shows a limited amount of phase equilibrium data for hydrocarbon-CO_2 systems. It is known that light hydrocarbons are miscible in all proportions with liquid CO_2 in the room temperature range. It is also known that a crude stripped of most of its light ends is not. Thus if a CO_2-rich liquid phase exists in the presence of a more hydrocarbon-rich phase, the light hydrocarbons, such as propane and butanes will have more tendency to enter the CO_2-rich phase than will the heavier constituents. The prediction of such phase equilibrium compositions requires a large amount of systematic data.

While a large-scale use of carbon dioxide in production operations does not appear likely for economic reasons, it seems desirable to be able to predict its behavior with hydrocarbon mixtures. This work was undertaken to help build up fundamental data for these predictions. The present paper may be regarded as a progress report on data obtained so far.

Previous Work

The ethane-CO_2 system was investigated by Kuenen[4] in 1897 over a range of pressures and temperatures around the critical region. Dew point and bubble point curves were obtained for a series of mixtures. Reamer, Olds, Sage and Lacey[5,6,7] investigated binary mixtures of carbon dioxide with methane, ethane, propane and n-butane, dew point and bubble point curves being obtained in the case of the last two. Mixtures of carbon dioxide with propane, n-butane and n-pentane were studied by Poettmann and Katz [8] in the critical region as well as in the two phase region. Lara[9] made an investigation on a single mixture of carbon dioxide and n-heptane.

Contribution No. 53-18 , School of Mineral Industries, The Pennsylvania State College.

* Former Research Assistant, Division of Petroleum and Natural Gas Engineering, The Pennsylvania State College, now of The Ohio Oil Company.

**Division of Petroleum and Natural Gas Engineering, The Pennsylvania State College.

Materials

In the present investigation the solubility of carbon dioxide at 60° and 90°F was measured as a function of pressure in five normal saturated hydrocarbons: octane, decane, dodecane, tetradecane, and hexadecane. The hydrocarbons were obtained from Humphrey-Wilkinson, Inc., North Haven, Connecticut, and had a guaranteed purity of better than 95 per cent. Commercial liquid carbon dioxide was used. According to the distributors, Liquid Carbonic Corporation, the purity was about 99.9%.

Apparatus

The apparatus is shown in Figure 1. A double-windowed Jerguson Gage having a volume of about 100 cc and built to withstand 2000 psi at 100°F was used for the equilibrium cell. Two cylindrical trundles were bolted on opposite sides of the cell, slightly above the center of gravity. These extended through bronze supports. An adjustable arm on one of the trundles was connected by a rod to a reduction gear, so that the cell was rocked through a 90° arc by a small motor. Flexible stainless steel tubing was used to convey the fluids and transmit pressure. This was connected to the various pieces of equipment by welding it to nipples in Aminco high pressure fittings. The arrangement is shown in the figure. The Heise gage had been checked with a dead weight tester. To avoid an air cushion, the Bourdon tube was filled with oil, and the oil isolated from the rest of the system by a small U-tube filled with mercury. A large water bath with plate glass sides served for temperature control, which was within 0.05°F. The carbon dioxide cylinder was connected without a pressure regulator, so that the full pressure of the cylinder could be applied when desired.

Analytical Apparatus

Samples of the liquid phase were collected in simply constructed sample bombs. These bombs consisted of short lengths of high pressure 1/8 inch pipe with a high pressure needle valve on each end (see Figure 2). An Aminco high pressure fitting was connected to one valve and a 1/8 inch pipe-to-compression fitting connected to the other end. In this way, the sample could be collected by attaching the sampler to a high pressure fitting on the equilibrium apparatus and the sample could be released to atmospheric pressure by using the compression fitting. The volume of a sample bomb was about six cubic centimeters.

The analytical apparatus consisted essentially of a separator, a "Rotometer" to measure flow rates, and a carbon dioxide absorption tube. A short test tube fitted with a two-hole rubber stopper was used as the separator. A short length of Saran tubing with a compression fitting on one end was used to connect the sample bomb with the separator. The separator, Rotometer, and absorption tube were connected in series by short lengths of heavy-walled rubber tubing. The Rotometer itself was not used so much to accurately measure rates of flow, but to enable the operator to use a constant flow rate for the various analyses.

Several standard devices were tried for carbon dioxide absorption. The most satisfactory was a pyrex tube about an inch in diameter and 4 1/2 inches long, fitted with one-hole stopper through which short lengths of Saran tubing were passed. "Caroxite" was used as the absorbent.

Procedure

Before each run the equilibrium cell was cleaned and dried, and connection made at the bottom of the cell to the mercury pump. A few cubic centimeters of mercury were introduced. The hydrocarbon was introduced through the top of the cell, which had been disconnected. The amount introduced was determined by experience such that a gas phase would remain after establishment of equilibrium and yet as many samples as possible be obtained for analysis. After connections were made, the air was purged by pressuring and depressuring the cell a few times with carbon dioxide. Carbon dioxide was admitted into the equilibrium cell until a pressure somewhat above the equilibrium pressure desired was reached. Then the two-way valve was closed so that the pressure gage showed the pressure in the cell only. Thus, the carbon dioxide cylinder and lines were cut out of the system. After this was done, the cell was agitated for a period of 10 or 15 minutes, depending on the length of time necessary to obtain an equilibrium pressure. The action of the mercury rolling back and forth in the cell caused vapor-liquid equilibrium to be attained quite rapidly. When the pressure had remained constant for a period of five minutes or more, the agitation was halted and the cell placed in an upright position. The valve on the bottom of the cell was then opened to admit mercury from the mercury pump.

The carbon dioxide cylinder had previously been cut out of the system and the pressure released from the lines. The line to the cyclinder was disconnected at the two-way valve. The next step was to open the two-way valve to the atmosphere very slowly and at the same time start injecting mercury into the equilibrium cell with the mercury pump, the object being to eject all the vapor phase form the cell at constant pressure. This required considerable practice, but the manipulation was finally perfected so that the pressure did not vary by more than two or three psi. This was felt to be entirely satis-

factory, as no bubbles were observed to form in the liquid phase during the process. The first few cubic centimeters of liquid phase were ejected also, in case some slight change in composition might have taken place in the lines. Next, the nut and sleeve of an Aminco fitting were attached to the two-way valve where the line from the carbon dioxide cylinder had been removed. The sample bomb, previously weighed on an analytical balance, was then connected with the nut and sleeve, and the fitting tightened. The valve was again opened slightly and the liquid pumped from the cell into the sample bomb at a pressure above the bubble point of the liquid. The valves were closed, the connection broken, and the bomb was weighed again, after any liquid outside the valve had been removed. The difference between this weighing and the previous one gave the weight of the sample to be analyzed.

Analysis of Sample

The sample bomb was clamped in a horizontal position on the analytical apparatus and connected to the separator. The absorption tube was weighed and then clamped in position and connected to the system. The valve on the sample bomb was opened enough to give a predetermined flow rate on the Rotometer, the valve being so manipulated that this flow rate remained constant until the sample bomb was exhausted. Then a nitrogen cyclinder was connected to the other end of the sample bomb, the valve opened, and nitrogen was passed through the system for five minutes with agitation of the bomb. This was done to flush all remaining carbon dioxide from the system and cause it to be absorbed in the Caroxite tube.

The above procedure gave quite accurate results. Before it was adopted, tests were made to check the adsorption of nitrogen on the Caroxite. For a test period of five minutes the adsorption was found to be nil. Any nitrogen absorbed would have affected the results by less than 0.1 percent. Tests were run to see how much of the hydrocarbon vapor would be absorbed by the Caroxite. To do this, a sample bomb was weighed empty and then filled with pure carbon dioxide and weighed again. The carbon dioxide was then bubbled through octane, the most volatile of the hydrocarbons used, and absorbed in the Caroxite tube. There was no excess increase in weight recorded. This was repeated several times to check results.

Finally, to check the accuracy of the procedure, a known weight of hydrocarbon and a known weight of carbon dioxide were placed in the sample bomb together. The bomb was thoroughly agitated, and then a carbon dioxide analysis was run. Recovery was greater than 99 percent in each of the several tests made.

The percentage of carbon dioxide in the liquid phase was calculated by dividing the gain in weight of the absorption tube by the weight of the sample. Two samples of the liquid phase were taken at each pressure recorded. The percentage of carbon dioxide in each sample had to agree within $\pm$ 0.5 before a run was considered accurate. Most samples checked within 0.1 percent carbon dioxide.

Results

Complete miscibility was obtained with octane, decane, and dodecane at both 60° and 90°F. The solubility of carbon dioxide in each of these at 60° and 90° is shown as a function of pressure in Figures 3 and 4. As previously stated, the vapor phase was not analyzed. At the lower pressures the vapor phase composition can be estimated by applying Raoult's law to the hydrocarbon. The mole per cent of hydrocarbon in the vapor would thus be found to be very small, less than one percent at 50 psia. At the higher pressures the percentage of hydrocarbon in the vapor is greater than that given by Raoult's law due to the solvent effect of the dense gas, the same effect that gives rise to "retrograde vaporization". With so little of the hydrocarbon present, the analytical procedure would have yielded high relative errors with respect to the hydrocarbon percentages.

At 60° (Figure 3) the curves end at the vapor pressure of pure CO_2, 747.5 psia. A straight line drawn from this point to the origin of the graph (since the hydrocarbon vapor pressure is too small to be shown on the scale) shows what the curves would have been if Raoult's law were obeyed. The curves should approach this line at 100% CO_2. The critical temperature of CO_2 is 88.0°F, hence the curves for 90° (Figure 4) bend over abruptly near 100% CO_2 and merge into the dew point curves. These latter were not determined, as stated previously. If the vapor pressure—temperature curve for carbon dioxide were extrapolated above the critical point to 90°, the value 1099.6 psia is obtained. Hence a line from this pressure at 100% CO_2 to the origin gives the bubble point curve that would be obtained on the basis of Raoult's law.

It is apparent from the figures that the deviation from Raoult's law increases with molecular weight. The curves of Figures 3 and 4 show an inflection at the upper end. The inflection increases with molecular weight of the hydrocarbon and, in the case of n-tetradecane and n-hexadecane the curve becomes double-valued at a certain pressure (Figures 5 and 6). This means that there are two liquid phases in equilibrium with a vapor phase. According to the "phase rule", if the temperature is fixed, the system is invariant when three phases are present. In other words, at a given temperature, two

liquid phases and a vapor phase occur at only one pressure, and the compositions of all three phases are fixed. Adding or removing carbon dioxide from the cell over a certain range only changes the relative amounts of each phase but does not change the pressure or compositions in the phases. At 60° the curves continue from the point corresponding to the CO_2 rich liquid phase to the vapor pressure of pure carbon dioxide, approaching the line drawn to the origin from this point. At 90° (above the critical temperature) the curves do not continue to 100% carbon dioxide but Raoult's law is approximately obeyed in the CO_2 rich phases, on the basis of the extrapolated vapor pressure, as would be expected. The original data are given in Table I.

Equilibrium Constants

The so-called "equilibrium constants" for predicting hydrocarbon phase compositions have been defined as follows:

$$K_i = \frac{y_i}{x_i}$$

where y_i is the mole fraction of the i'th constituent in the vapor phase and x_i the mole fraction of that constituent in the equilibrium liquid phase. These "constants" vary with the constituent, with temperature and pressure, and to a certain extent with the composition of the mixture. They may be assumed constant over a sufficient range of compositions to allow phase calculations. When Raoult's law is obeyed, the value of K for a constituent is equal to the vapor pressure of the constituent when pure at the given temperature divided by the total vapor pressure of the mixture. Equilibrium constants for carbon dioxide have been computed from Figures 3 through 6, assuming the mole fraction in the vapor to be unity. These are shown in Figures 7 and 8. The value for the CO_2-rich liquid phase is shown by a circle at the pressure at which two liquid phases can exist.

If Henry's law is obeyed, the plot of K against pressure should be a 45 degree line on double log paper. Also a plot of log K, for a given pressure and a limited temperature range should be a linear function of 1/T, T being the absolute temperature, °R. Under these conditions, we can write,

$$\log K = a - \frac{b}{T} - \log \pi$$

π being the total pressure in psia. Recently Jacoby and Rzasa [10,11] determined equilibrium constants for the constituents of a typical condensate field reservoir mixture, carbon dioxide being one of the constituents. Their values for the carbon dioxide, which was present in very small amounts, are approximately given by the above equation at the lower pressures, with $\underline{a} = 4.7$, $\underline{b} = 813$. At higher pressures the trend depends entirely on the particular mixture at hand, since, by definition, all equilibrium constants become unity at the critical point. Figures 7 and 8 show a slight trend in the value of $\underline{a}$ with molecular weight of the hydrocarbon, from 5.32 for octane to 5.27 for hexadecane, with $\underline{b} = 1180$.

When "flash" phase calculations are to be made in a range in which two liquid phases and a vapor phase may form, equilibrium constants for each of the liquid phases must be known. It is more convenient, however, to employ the vapor-liquid constants for the hydrocarbon-rich phase and the distribution coefficients C for the liquid phases. At a given pressure and temperature let

y_i = M. F. of i'th constituent in vapor

x_i = M. F. of i'th constituent in hydrocarbon-rich liquid

x'_i = M. F. of i'th constituent in CO_2-rich liquid

$K_i = y_i/x_i$, $K_i' = y'_i/x'_i$ $C = K_i/K'_i = x'_i/x_i$

If one mole of mixture gives L moles of the hydrocarbon-rich phase, L' moles of the CO_2-rich phase, and V (= 1- L - L') moles of vapor and X_i is the mole fraction of a constituent in the entire mixture, a material balance gives.

$$X_i = Vy_i + Lx_i + L'x'_i$$

and substituting for y_i and x'_i

$$X_i = x_i (VK_i + L + L'C_i)$$

In general, L and L' must be found by trial and error. The calculation of a trial and error type (Table 2) is similar to that for two phases, except that "guesses" must be made for both L and L' simultaneously. These must be determined such that

$x_i = X_i / (VK_i + L + L'C_i) = 1$, and also that either

$Kx_i = y_i = 1$, or $Cx_i = x'_i = 1$. If one of these last two conditions is fulfilled the other will also be.

Table II illustrates the "flash" calculation for a mixture of CO_2, hexadecane and propane at 60°F and 700 psia. Three constituents, rather than two, were taken since, in the latter case, when the temperature is fixed, three phases can occur at only one pressure and one composition for each phase. Values of K and C for CO_2 and hexadecane (denoted by subscripts c and 16, respectively) were taken from the figures of this paper, although the presence of propane will undoubtedly lower the distribution coefficient for hexadecane and also slightly lower the K's for CO_2 in the hydrocarbon-rich phase. It was assumed that propane obeys Raoult's law in both liquid phases, so that $K_3 = K'_3 = 100/700$, the vapor pressure of pure propane at 60° being 100 psia.

As mentioned before, some kind of adjustments based on the relative amounts of heavy and light hydrocarbons would have to be made for multicomponent mixtures. Comparison of the butane-CO_2 system with the butane-ethane system[12] indicates distribution coefficients of the order of unity for light hydrocarbons such as propane and butanes, over a considerable composition range. Values of C apparently decrease with increasing molecular weight, other conditions being the same. The distribution coefficients necessarily are low if the equilibrium pressure for three phases is near the vapor pressure of pure carbon dioxide at the given temperature. It does not seem possible with the data so far available to set up any kind of correlation chart for estimating distribution coefficients for a given set of conditions.

Disregarding the economic side, carbon dioxide should be more effective than methane, in any solvent extraction method of oil recovery. The equilibrium constants found by Jacoby and Rzasa are about half way between those for methane and those for ethane. At temperature well above the critical temperature for CO_2, two liquid phases would not form, but solvent and "retrograde" effects should take place at a much lower pressure than with methane. In a "low pressure gas flood" a mixture of, say, propane and carbon dioxide with a given bubble point would contain more of the less volatile constituent than a mixture of propane and methane with the same bubble point. The former would, therefore, give a more efficient recovery of solvent on subsequent pressure reduction.

It is hoped that this work can be continued with multicomponent mixtures of hydrocarbons and carbon dioxide, so that more accurate phase predictions can be made.

Acknowledgment

The writers are indebted to the Pennsylvania Grade Crude Oil Association for the support of a part of this work.

References

1. Pirson, S. J., Unpublished Communication, 1941. "Tertiary Recovery of Oil," paper presented before the Central Appalachian Section, A.I.M.E., June 26, 1951.

2. Martin, J. W., "Field Data on Operation of the Arco Process Near Richburg, New York," Oil and Gas Journal, 50 (32), Dec. 13, 1951.

3. Neil, D. C., Johnson, W. E., Breston, J. N., and Macfarlane, R. E., "Laboratory Experiments with Carbonated Water and Liquid Carbon Dioxide as Oil Recovery Agents," The Pennsylvania State College, Mineral Industries Experiment Station Bulletin No. 60, 1952.

4. Kuenen, J. P., "Experiments on the Condensation and Critical Phenomena of Some Substances and Mixtures," Phil. Mag., V. 44, pp. 174-179, 1897.

5. Reamer, H. H., Olds, R. H., Sage, B. H., and Lacey, W. N., "Phase Equilibria in Hydrocarbon Systems. Volumetric Behavior of the Ethane-Carbon Dioxide System." Ind. Eng. Chem., 37, pp. 688-691, 1945.

6. Olds, R. H., Reamer, H. H., Sage, B. H., and Lacey, W. N., "Phase Equilibria in Hydrocarbon Systems. The n-Butane-Carbon Dioxide System," API, Fundamental Research on Occurrence and Recovery of Petroleum 1948-1949, pp. 9-16, 1950.

7. Reamer, J. H., Sage, B. H., and Lacey, W. N., "Phase Equilibria in Hydrocarbon Systems. The Propane-Carbon Dioxide System," API, Fundamental Research on Occurrence and Recovery of Petroleum 1950-1951, pp. 64-69, 1952.

8. Poettmann, F. H., and Katz, D. L., "Phase Behavior of Binary Carbon Dioxide-Paraffin Systems," Ind. Eng. Chem., 37, pp 847-853, 1945.

9. Lara, C., "Phase Diagram for Normal Heptane-Carbon Dioxide System," M. S. Thesis, The Pennsylvania State College, 1943.

10. Jacoby, R. H., and Rzasa, M. J., "Equilibrium Vaporization Ratios for Nitrogen, Methane, Carbon Dioxide, Ethane, and Hydrogen Sulfide in Absorber Oil-Natural Gas and Crude Oil-Natural Gas Systems," A.I.M.E Trans. 195, p 99, 1952.

11. Jacoby, R. H., and Rzasa, M. J., "Equilibrium Vaporization Ratios for Nitrogen, Methane, Carbon Dioxide, Ethane, and Hydrogen Sulfide in a Natural Gas-Condensate System," A.I.M.E. Petr. Tech., 198, p. 225, Sept., 1953.

12. Kay, W. B., "Vapor-Liquid Equilibrium Relations of the Ethane-n-Butane System," Ind. Eng. Chem., 32, p. 353, 1940.

TABLE I

DATA ON SOLUBILITY OF CARBON DIOXIDE IN NORMAL PARAFFIN HYDROCARBONS

60°F		90°F	
Pressure (psia)	Mole % CO_2	Pressure (psia)	Mole % CO_2
	n-Octane		
166	12.9	154	9.9
470	44.6	470	34.3
572	64.0	755	61.6
619	73.1	861	76.6
637	76.5	901	82.1
695	93.3	998	93.5
		1009	95.9
	n-Decane		
166	13.5	120	7.6
415	38.0	466	31.1
586	57.2	638	44.8
626	66.4	820	63.7
694	87.4	942	80.6
725	96.3	959	83.7
		1022	95.3
	n-Dodecane		
157	12.9	130	9.0
365	33.2	497	34.1
507	47.4	729	51.3
668	70.9	983	79.2
712	90.3	1020	89.0
723	95.5	1033	92.5
	n-Tetradecane		
183	17.1	120	8.7
425	39.1	547	38.4
661	63.9	918	65.7
700	69.9	1062	96.5
735	81.0	1062*	83.4
735*	94.5		
	n-Hexadecane		
146	14.1	132	9.7
420	38.8	465	31.6
614	55.5	814	54.7
710	68.0	1021	71.4
737	71.2	1064	74.8
737*	98.12	1080	98.95
		1080*	75.3

* Two liquid phases

TABLE II

SAMPLE "FLASH" EQUILIBRIUM CALCULATION FOR TWO LIQUID PHASES AND A GAS PHASE, COMPOSED OF CO_2, C_3H_8 AND $C_{16}H_{34}$ AT 60°F AND 700 PSIA

SUCCESSFUL "TRIAL" FOR V = .3, L = .3, L' = .4

Const.	Feed, X	K	C	.3K + .3 + .4C	$\frac{X}{.3K + .3 + .4C} = x$	xC=x'	xK = y
CO_2	.871	1.48	1.39	1.30	.670	.932	.990
C_3H_8	.037	.142	1.0	.743	.050	.050	.007
$C_{16}H_{34}$	.092	0	.0714	.329	.280	.020	0
					1.000	1.002	.997

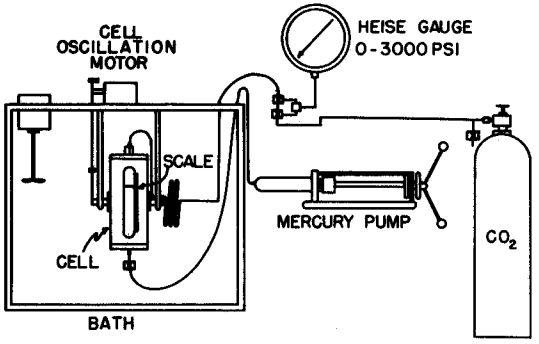

FIGURE I. SOLUBILITY APPARATUS.

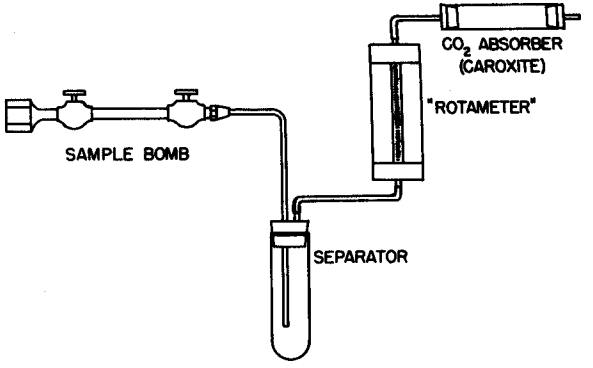

FIGURE 2. CARBON DIOXIDE ABSORPTION APPARATUS.

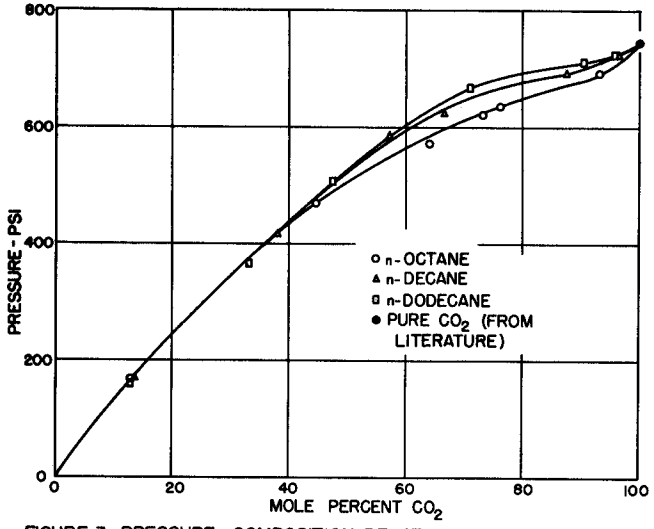

FIGURE 3. PRESSURE - COMPOSITION RELATIONS FOR LIQUID PHASE FOR CO_2 - n-OCTANE, CO_2 - n-DECANE, AND CO_2 - n-DODECANE SYSTEMS AT 60°F.

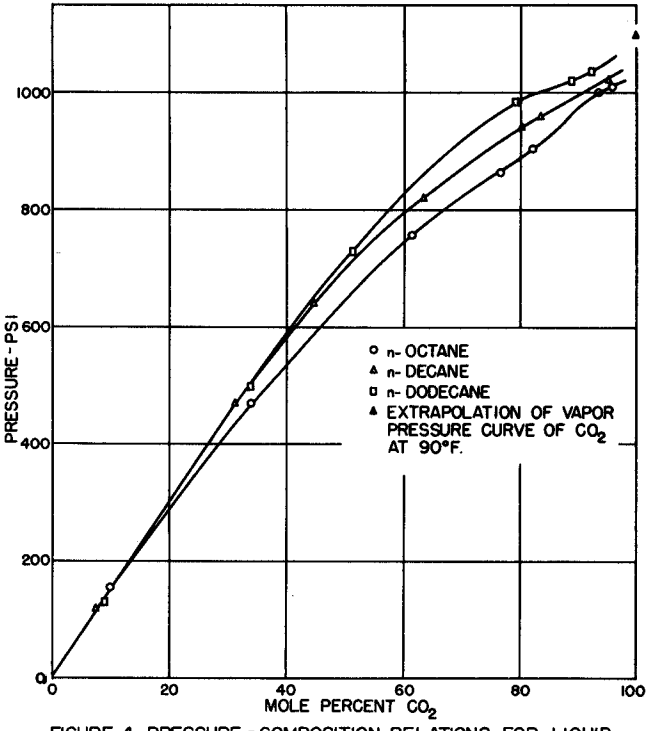

FIGURE 4. PRESSURE - COMPOSITION RELATIONS FOR LIQUID PHASES FOR CO_2 - n-OCTANE, CO_2 - n-DECANE, AND CO_2 - n-DODECANE SYSTEMS AT 90°F.

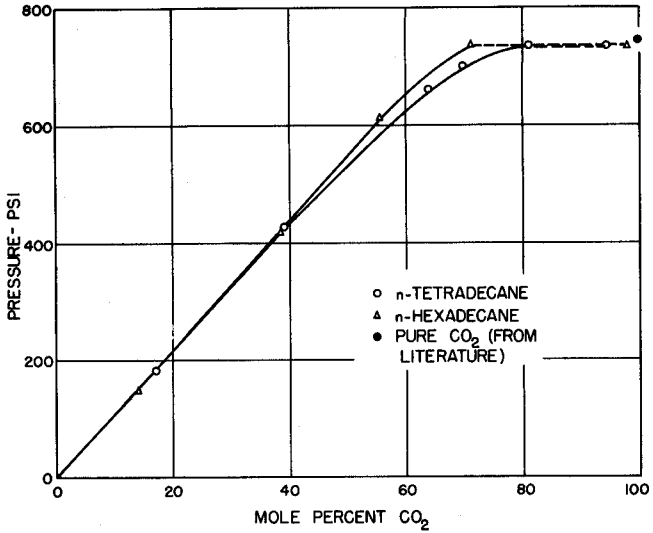

FIGURE 5. PRESSURE-COMPOSITION RELATIONS FOR LIQUID PHASES FOR CO_2 - n-TETRADECANE AND CO_2 - n-HEXADECANE SYSTEMS AT 60° F.

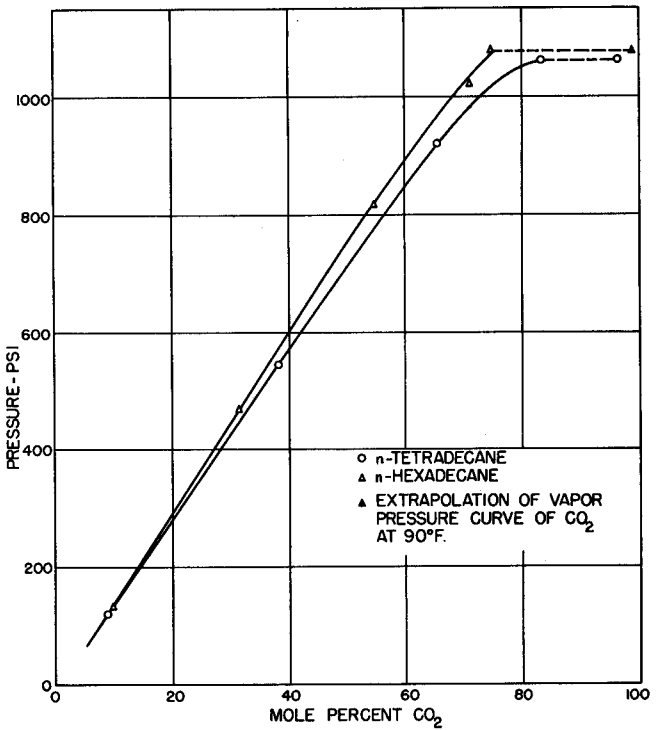

FIGURE 6. PRESSURE-COMPOSITION RELATIONS FOR LIQUID PHASES FOR CO_2 - n-TETRADECANE AND CO_2 - n-HEXADECANE SYSTEMS AT 90°F.

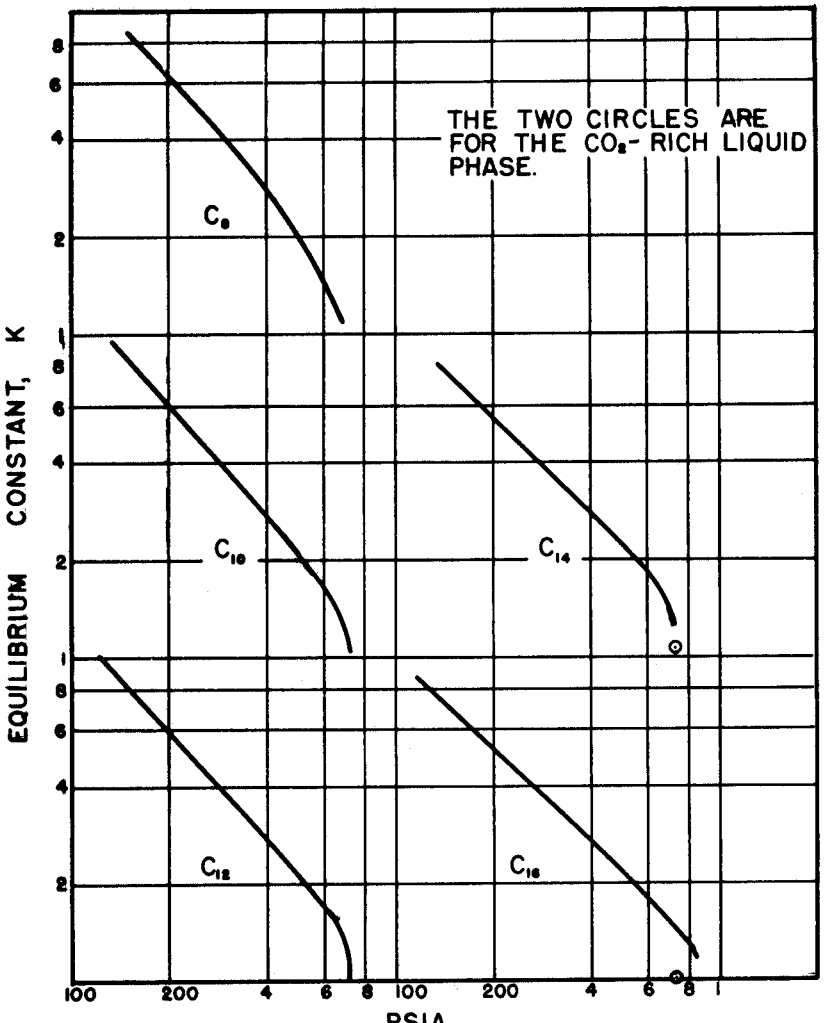

FIGURE 7. EQUILIBRIUM CONSTANTS FOR CARBON DIOXIDE IN FIVE PURE NORMAL HYDROCARBONS AT 60° F.

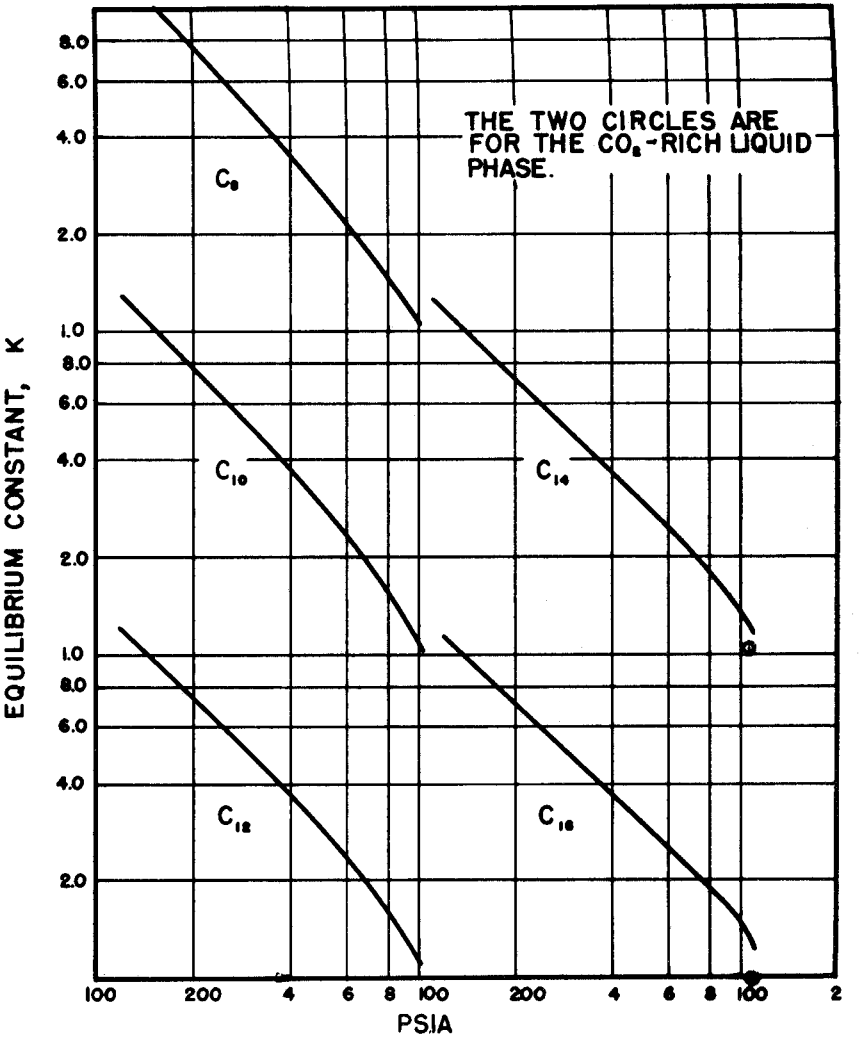

FIGURE 8. EQUILIBRIUM CONSTANTS FOR CARBON DIOXIDE IN FIVE PURE NORMAL HYDROCARBONS AT 90° F.

SELF-POTENTIALS OF RESERVOIR SANDS*

E. B. McConnell, Jr.**

Abstract

The self-potentials of oil reservoir rocks were measured in the laboratory to determine some of the factors and considerations necessary for the interpretation of well logs, particularly in the Bradford, Pennsylvania, area. Self-potentials were obtained by placing sand cores between salt solutions of differing concentrations and observing the potentials developed across the cores.

The research has confirmed that the self-potential generated by a sand core in the laboratory may often be represented by the equation $SP = K \log R_m/R_w$, where R_m and R_w refer to the resistivities of the bore hole and connate water respectively, and K is a factor depending on the clay content of the core. For Bradford, Pennsylvania, oil sands, the equation $SP = 45 \log R_m/R_w$ was found to give good approximations of the relation between the laboratory self-potential and the ratio of resistivities up to a concentration difference of 100:1.

For the accurate interpretation of the self-potential well log in terms of the connate water resistivity it is concluded that it may often be necessary to resort to laboratory determinations of the self-potential constant K.

Introduction

The self-potential measured in a well results from the interaction of the solutions in the bore hole and the adjacent rock structure, from the effects of ion active earth material such as clays in the reservoir, and from electrokinetic phenomenon. The potentials resulting from these three factors, the concentration differences, the quantity of ion active earth material, and the electrokinetics, are called the electrochemical, Mounce, and streaming potentials, respectively. Their quantitative effect on the self-potential log can vary considerably in any particular well and is dependent upon the nature and distribution of the rocks and fluids at the points of measurements.

In the absence of streaming potential, the self-potential well log can often be successfully interpreted to yield values of the connate water resistivity as well as to delineate some of the stratigraphic sequences down the well. However, in some oil fields, like Bradford, the physical and chemical characteristics of the reservoir rocks are such that it is difficult to make reliable interpretations.

The research discussed below was carried out with the aim of investigating some of the factors affecting the self-potential log, particularly in the Bradford, Pennsylvania, area.

Theory

Electrochemical potentials are a common phenomenon of physical chemistry (Glasstone, 1946). An electrochemical potential occurs whenever two solutions that have ions of differing mobilities are placed in contact with each other. This potential may be expressed by the relation:#

$$E = \frac{(v - u)}{(v + u)} \frac{RT}{nF} \ln \frac{a'}{a''} \qquad (1)$$

where v = cation mobility
u = anion mobility
R = gas constant, 8.314 joules
T = absolute temperature
n = ionic valency
F = Faraday, 96,500 coulombs
a', a" = mean activities of the solutions

Contribution No. 53-10, School of Mineral Industries, The Pennsylvania State College.

* This article is a summary of a thesis performed in partial fulfillment of the requirements for the M. S. degree in Geophysics at The Pennsylvania State College.

** Magnolia Petroleum Company

\# In this paper the symbol ln is used to represent the logarithm to the base e = 2.7183; log to represent the logarithm to the base 10.

At twenty-five degrees centigrade and with sodium chloride solutions, this equation may be simplified to read:

$$E_{mv} = -11.5 \log \frac{a'}{a''} \qquad (2)$$

For dilute solutions of sodium chloride (under one molal), the mean activities in equation (2) may be replaced by the equivalent conductances of the electrolytes (MacDougall, 1948). Since equivalent conductance is inversely proportional to resistivity, equation (2) may be expressed in terms more familiar to well logging as:

$$E_{mv} = -11.5 \log R_m/R_w \qquad (3)$$

where R_m and R_w refer to the resistivity of the bore hole fluid and connate water respectively.

The term Mounce potential is applied to any potential measured between solutions of differing concentrations when separated by earth materials such as clay, sandstone or shale, which enter into base exchange reactions with the ions in the connate water. Where such reactions occur, the rock acts as an ion selective membrane. Mounce potentials may be vizualized as resulting from sieving action in which cations move more easily through a system than anions. The resulting excess of cations in one part of the system results in a potential difference in the opposite sense to the electrochemical potential.

The relative magnitude of this Mounce potential of any substance depends on the quantity and distribution of its ion selective material. Since clays are the principal ion active substances in earth materials, the Mounce potential must be related to the clay content of a rock. For the case of an ideal ion selective material, such as a shale or pure clay, it has been empirically found (Wyllie 1949) that the potential may be represented by the Nernst equation:

$$E = \frac{RT}{F} \ln \frac{a'}{a''} \qquad (4)$$

With sodium chloride solutions at twenty-five degrees centigrade, and with resistivities instead of activities, this equation can be expressed as:

$$E_{sv} = 59 \log R_m/R_w \qquad (5)$$

Because sandstones contain smaller quantities of clay than shale, they will not act as ideal ion-membranes and the Nernst equation will not represent their self-potentials. Generally, the potential of a sandstone, or sand-shale, will range between the potentials predicted by the electrochemical and Nernst equations; and may be represented by the general relation:

$$SP = K \log R_m/R_w \qquad (6)$$

Observed Data

Measurements of self-potential generated across 56 cores of sandstone and other materials were made using the apparatus shown in Figure 1. Thirty of these cores were cut from sandstones from the Bradford area, and 26 were from other sandstones, shale-sands, and limestones. In most cases the concentration differances were 50,000/500 ppm NaCl. For six cores the concentrations were varied from 1,000 to 50,000 ppm NaCl on one side of the core, the concentration remaining constant at 500 ppm NaCl on the other side. Tests were also made to determine the effects of toluene extraction of hydrocarbons, electrodialysis, and drying on the self-potential.

Table I to VI and Figures 2 and 3 are a presentation of the measurements made in this research. The data have been grouped to bring together for comparison cores which had undergone similar treatment. The self-potentials were measured with sodium chloride solutions at approximately twenty-three degrees centigrade. To facilitate the interpretation of the data, the cores have been designated by a number and one or more letters. The letters following the core number are to distinguish its environment prior to measurement. The lettering system is as follows:

W- Core canned in water
P- Core canned in crude oil
A- Core canned in air
U- Core uncanned
L- Core lucite mounted.

The average potential and the deviation from the mean potential are listed for each group of

untreated cores. For the laboratory treated cores the differences in potential recorded both before and after treatment are given.

Tables I through VI present measurements of self-potentials using solutions of 50,000/500 parts per million sodium chloride at a temperature of approximately twenty-three degrees centigrade. In Table I are listed the potentials of a group of air-canned Bradford cores, while in Table II are potentials for Bradford area cores under differing canning conditions. In Table III are the potentials of a variety of cores taken from various oil reservoirs in the United States. A majority of the cores listed in Table III were received uncanned and lucite mounted.

In Tables IV through VI are listed potentials before and after laboratory treatments as follows:

Table IV - Toluene extracted cores
Table V - Electrodialysed cores
Table VI - Oven dried cores.

Figure 2 shows examples of the self-potential variation of Bradford cores for different salinity ratios. The salinity was varied between 1000 and 50,000 parts per million on one side of the core, while the solution on the opposite side remained constant at 500 parts per million.

The apparently consistent nature of potentials listed in Table I indicates that the rock properties influencing the self-potential in the Bradford area are quite uniform. Table II shows the variations of potentials of Bradford cores under differing conditions of canning and the potentials measured across a shale and a sandstone containing large streaks of shale, (53A and 52A, respectively). The variously canned cores listed in Table II have a wide scatter of self-potentials. This wide scatter should be expected, since Calhoun (1953) found that the physical properties of cores in the laboratory are dependent on the manner in which they are stored following coring, with cores canned in air being the most representative of the rock in situ of the systems tested.

Table III shows the variations of self-potential for different reservoir sands. In general, the self-potentials indicate that only relatively few sands over the country have strong Mounce potentials. Tables I and II, when compared to Table III, point out the unusual nature of the Bradford sand where strong Mounce potentials are the rule rather than the exception.

Table IV indicates that toluene extraction tended to lower the self-potential by an average value of six millivolts, but that the particular effect for an individual core is unpredictable. A potential change of thirty-six millivolts was noted for one core, while potential changes of ten percent or more occurred in thirty-eight percent of the cores. The extraction process produced such erratic potentials in some cores that it is unwise to rely on self-potential measurements on extracted cores as representative of their untreated condition.

Toluene extraction's effect on the self-potential is probably the result of removal or addition of materials coating the clays. Despite the unreliable nature of these potentials, extracted cores are still useful in indicating the general magnitude of the potential expected from the core before treatment. This is especially true in clay-free cores, or cores with very low Mounce potentials, where extraction does not alter the Mounce potential appreciably.

Table V shows that electrodialysis lowered the potential an average of three millivolts, the greatest deviation being plus twenty-seven millivolts. The potential of the untreated cores were undoubtedly influenced by ions such as sulfate and chloride, while the potentials of the electrodialysed cores were affected only by the H^+ and Cl^-ions. This is because electrodialysis removes all other free ions from the clays. On saturation with sodium chloride, the electrodialyzed clay particle will take on the chloride ion resulting in a negative clay charge.

Table VI illustrates the erratic nature of the self-potential of dried cores. Since the distribution of clay, oil and water in the cores influences the self-potential, drying might change the fluid distribution in such a way as to either add to or decrease the potential, depending on the accessibility of the brine to the clays when they are resaturated after drying.

Figure 2 shows self-potentials for 2 Bradford area cores under differing conditions of salinity. The plots of the ratio of the resistivity to self-potential are straight lines from a salinity ratio of 1/1 to 50,000/500 parts per million sodium chloride. This linearity for Bradford sand cores shows that equation (6), $SP = K \log R_m/R_w$ accurately represents the relation between the self-potential and the logarithm of the concentration difference.

Demonstration of the validity of the self-potential equation (6) for the Bradford area sands is important. McCardell, Winsauer, and Williams (1953) have shown that the potentials of some shales and clay-sands, under salinity differences of 50,000/500 parts per million sodium chloride, will not obey

it.

X-ray diffraction patterns were made for three sets of powdered samples of Bradford sandstone. Figure 3 is a sample of one of these. The diffraction patterns show peaks indicating qualitatively the relative amount of clay minerals in the samples. In Table VII the self-potential measurements are compared with the relative clay content of the cores as determined by X-ray diffraction studies. In each group of measurements the cores are listed in order of increasing clay content. It is plain to see that self-potential increases with increasing clay content.

Further research on this method of measuring clay content will have to be done before it becomes quantitative rather than only a relative measure of composition. Even with its present limitations, X-ray diffraction measurements of this sort are the best, rapid, inexpensive means of estimating clay content of a core. They are of particular value because they distinguish the different clay minerals from one another.

Application of Measured Self-Potentials

To make a self-potential well log, a single electrode traverses a bore hole. The potential difference is measured between this electrode and a similar electrode that is usually located in a mud pit at the surface. In well log interpretation the value of self-potential observed opposite shales is used as a base line, and all other values of potential are measured with respect to it.

The magnitude of the potential deflection from the shale base line may be used to determine the resistivity of the connate water by the relation:

$$SP = K' \log R_m/R_w \qquad (7)$$

where K', in the ideal case, would be expected to equal seventy (Wyllie, 1949). If the sand contains a certain amount of clay, then it will possess an ion sieving action and the potential recorded will not be of the magnitude expected for a clean sand, but will approach the shale potential as the clay content increases. The size of the sand deflection is then inversely related to the quantity of clay in the sand, all other factors being equal.

The ability of the self-potential well log to yield accurate values of connate water resistivity in a great many oil fields using a K constant of seventy seems to indicate that many sands logged contain little, if any ion active clay. However, in fields such as Bradford, Pennsylvania, the sands do contain appreciable quantities of clay (Krynine, 1940). The clay content of the Bradford sands would than be expected to reduce the sand deflections. To obtain connate water resistivities in this type of field it is necessary to use K values lower than seventy in order that the self-potential equation be valid for interpretation of logs in terms of interstitial water resistivity (Pirson, 1952).

In order to convert laboratory values of self-potential into the constant K of equation (6) for use with commercial well logs, it is necessary to consider the manner in which field self-potentials are measured. Consider any two values of self-potential as recorded on a well log. Their values will be called SP_1 and SP_2. Call the resistivities of the connate water associated with these self-potentials R_{w1} and R_{w2} respectively, and the resistivity of the fluid in the bore hole R_m. For this case equation (6) becomes.

$$SP_1 = K_1 \log R_m/R_{w1} \qquad (8)$$

$$SP_2 = K_2 \log R_m/R_{w2} \qquad (9)$$

In well logging, the difference , SP, between the shale base line and any deflection from this base line (usually in the negative direction) is used to determine the resistivity of the connate water (Schlumberger, 1953). If SP_1 is the value of the shale base line and SP_2 the value of some particular deflection, then:

$$SP = SP_1 - SP_2 \qquad (10)$$

It follows that:

$$SP = K_1 \log R_m/R_{w1} - K_2 \log R_m/R_{w2} \qquad (11)$$

Assuming that the resistivity of the connate water is the same in both formations, then $R_{w1} = R_{w2}$. In addition, let $K_2 = K_1 - K^*$. Substituting these relations in equation (11), the equation relating the self-potential deflection to the resistivities of the connate and bore hole water is obtained:

$$SP = K^* \log R_m/R_w \qquad (12)$$

Equation (12) shows that values of K* used in the field for self-potential well log interpretation are actually differences between two K values; for example, K' in equation (7).

The determination of the values of K from the laboratory measurements of self-potential follows from the analysis given below.

Assume that self-potential measurements with salt solutions of the same salinity constrast have been taken in the laboratory on three cores: (1) a shale, (2) a sand-shale, and (3) a clay free sand. The respective potentials of these three cores could be represented graphically as in Figure 4. If cores (1), (2), and (3) were now placed in the ground and the temperature, salinity differences and ions present were the same as in the laboratory, the record of a conventional self-potential well log traversing these cores could also be represented by Figure 4. (Assuming no streaming potential in the well) In this case the potential of the shale in the laboratory would now be that potential associated with the shale base line.

The relation between the potentials in the field and in the laboratory, Figure 4, can be given by the equation:

$$\Delta SP = SP - C \qquad (13)$$

The constant, C, is the difference between the laboratory reference potential and the field reference potential.

Wyllie (1952) has concluded that shales in their natural environment in the earth act as ideal ion selective membranes and that their potentials obey the Nernst equation. Thus, the difference, C, between the laboratory base line and the field base line is the self-potential of shale, which is given by equation (5). Equation (13) becomes, with the aid of equation (6):

$$\Delta SP = (K - 59) \log R_m/R_w \qquad (14)$$

and:

$$\Delta K = K - 59 \qquad (15)$$

Both K, as determined by equation (6), and ΔK, as determined by equation (15), have been calculated for Bradford cores, and are given in Tables VIII and IX. The cores of Table VIII are air-canned cores, and those of Table IX are miscellaneous non-air canned cores. The K's obtained apply only for sodium chloride solutions at twenty-three degrees centigrade.

Table VIII shows that the range of K's for the Bradford sand was from -41 to -51, the average being -45. The low deviation of the mean .69 is significant in that it shows the consistency of the Mounce potential, and resulting K constant, of these cores. The variously canned sandstone cores from Bradford have a wider spread of K's than those in Table VIII (-37 to -60). This is what would be expected, since the physical properties of cores are dependent on the manner in which they were stored following coring. Despite the variety of canning conditions, the sand cores, on the average, show a ΔK of close to -45.

K's have not been determined from the self-potential measurements of cores from outside of the Bradford area because it was not shown that the self-potential of these cores is a linear function of the logarithm of the concentration ratio. This linearity is essential to the use of equation (6) (McCardell, Winsauer, Williams, 1952).

Commercial use of K Constants

The application of the ΔK constants obtained in this research to equation (12), $\Delta SP = \Delta K \log R_m/R_w$, should make possible the determination of the resistivity of the connate water, where streaming potentials are either negligible, or a correction can be made for them. Because the determination of the connate water resistivity from the self-potential well log is one of the first steps in the quantitative interpretation of resistivity well logs, it is important that ΔK be properly evaluated.

There are two methods of obtaining ΔK: either by empirical field observations, or by laboratory experimentation. While empirical field methods are often applicable, the laboratory determination of ΔK is essential in oil reservoirs employing secondary recovery methods, such as Bradford, where water flooding continually disturbs the connate water and complicates the field evaluation of ΔK.

Once the interstitial water resistivity is obtained from the self-potential well log record,

it may be used in conjunction with the resistivity well log to find the porosity and water saturation of a sand (Pirson, 1952). Nomographs have been published that make use of the connate water resistivity and the resistivity log to determine porosity and saturation. For the Bradford field, Pennsylvania, the nomograph of Keller and Licastro (1951) is particularly useful.

Great care must be taken in the use of the equation (12). In certain oil fields, such as Bradford, where the stratigraphy consists of thin interbedded sands and shales, the observed self-potential values must be corrected for bed thickness, and the temperature and salinity within the bore hole must be taken into account.

Summary of Conclusions

From the studies discussed above, the following conclusions can be drawn:

1. For the Bradford, Pennsylvania, oil sands, the equation $SP = K \log R_m/R_w$ was found to represent the relation between self-potential and resistivity for ratios of salinity from 1:1 to 100:1, the salt being sodium chloride and the temperature twenty-three degrees centigrade.

2. For the Bradford, Pennsylvania, oil sands, the K constant as determined in the laboratory ranged in value from forty-one to fifty-two, with an average of forty-five.

3. The K factor depends on the clay content of a rock, as determined by X-ray diffraction studies.

4. Extraction of the hydrocarbons using toluene, electrodialysis, and drying are all likely to alter sand cores so greatly that self-potentials subsequently measured on them are not representative of those of an untreated core.

5. Laboratory determinations of K constants for reservoir sands containing clay appear to be essential to the evaluation of the connate water resistivity from the self-potential well log.

Acknowledgements

The writer would like to express his sincere appreciation to Professor B. F. Howell, Jr., for his counsel and guidance on all matters pertaining to this paper.

Gratitude is extended to the Pennsylvania Grade Crude Oil Association and the Petroleum Engineering Department of the Pennsylvania State College for the cores, core data, and equipment used in this research.

The writer is also indebted to the many people who took time to discuss with him matters pertaining to the work. In particular, Mr. P. H. Licastro's suggestions concerning the various aspects of self-potential well logging were very helpful.

Bibliography

Calhoun, J.C.
1953 "The intensive analysis of oil-field cores"
Presented at the spring meeting of the Eastern District A. P. I. Division of Production, Pittsburgh, Pa.

Glasstone, S.
1946 Elements of Physical Chemistry Ch 14:434-479 Van Nostrand.

Keller, C. V. and Licastro, P. H.
1951 " A progress report on the interpretation of differential resistivity logs" Producers Monthly, 16 (6), 27-38.

Krynine, P. D.
1940 "Petrology and genesis of the Third Bradford Sand" P.S.C. M. I. Exp. Sta., Bull. 29.

MacDougall, F. H.
1948 Physical Chemistry Ch XVIII 546-612 MacMillan

McCardell, W. M., Winsauer, W. V., William, M.
1953 "Origin of the electrical potential observed in wells"
Journ. Pet. Tech. 5 (2): 41-48

Pirson, S. J.
1952 Reference Manual on Electric Logging Pet. Pub. Co., Tulsa, Okla.

Schlumberger, C and M. and Leonardon, E. G.
1953 "A new contribution to subsurface studies by means of electrical measurements in drill holes" Trans A.I.M. E. 110:273-290.

Wyllie, M. R. J.
1949 "A quantitative analysis of the electrochemical component of the SP-curve" A.I.M.E. TF 2311. Journ. Pet. Tech. 1 (1): 17-26.

1952 "Clay technology in well log interpretation" Presented: National Conference on Clays and Clay Technology, July, 1952, Berkeley, Calif.

Table I

Core	Formation	State	Self-potential, mv
34A	Bradford Third	Pennsylvania	22
35A	"	"	25
36A	"	"	34
37A	"	"	21
39A	"	"	32
40A	"	"	32
41A	"	"	34
42A	"	"	32
43A	"	"	35
44A	"	"	29
45A	"	"	14
46A	"	"	28
47A	"	"	20
48A	"	"	33
49A	"	"	20
50A	"	"	21
51A	"	"	29

Average potential 27
Deviation of the mean 1.33

Table II

Core	Formation	State	Self-potential, mv
20U	Bradford Third	Pennsylvania	27
21U	"	"	23
22U	"	"	-2
52A	"	"	63
53A	"	"	100
55W	Scio Oil Sand	New York	20
56W	"	"	33
57P	"	"	20
58P	"	"	26
59P	"	"	22
60W	"	"	22
61W	"	"	42
62P	"	"	28

(Note: Core 53A is a shale, and core 52A is a sand core streaked with shale)

Average potential 33
Deviation of the mean 4.6

Table III

Core	Formation	State	Self-potential, mv
1UL	Tensleep	Wyoming	-4
2UL	"	"	-21
3UL	"	"	-20
4U	Warrior La.	Pennsylvania	-22
5UL	Missouri	Texas	-18
6UL	Glenn	Oklahoma	-20
7UL	Cypress	Illinois	-20
8UL	Smackover	Arkansas	-21
9UL	San Andreas	Texas	-16
10UL	Gibson Zone	Oklahoma	26
11UL	Wilcox	"	3
12UL	Weber	Colorado	41
13UL	Clearfork	Texas	-22
14UL	1750'	"	9
15UL	Cromwell	Oklahoma	-6
16UL	Rifenburg	Texas	9
17UL	"	"	-22
18UL	"	"	-22
19UL	Third	California	28
26A	Tensleep	Wyoming	23
27A	"	"	20
70A	Berea	Ohio	19
71A	"	"	13
73A	"	"	20

Average potential -1
Deviation of the mean 3.7

Table IV

Core	Untreated Potentials, mv	Toluene Extracted Potentials, mv	ΔE, mv
20U	27	26	-1
21U	23	1	-22
22U	-2	10	12
53U	46	56	10
44A	29	34	5
45A	14	19	5
46A	28	6	-22
47A	20	14	-6
48A	33	23	-10
49A	20	17	-3
57P	20	13	-7
55W	20	13	-7
56W	33	23	-10
58P	26	20	-6
51A	29	22	-7
52A	63	37	-26

Table V

Core	Untreated Potentials, mv	Electrodialyzed Potential, mv	ΔE, mv
34A	22	16	-6
35A	25	18	-7
36A	34	18	-16
37A	21	22	1
39A	32	32	0
40A	32	25	-7
41A	34	24	-10
42A	32	30	-2
26A	23	13	+10
70A	19	12	-7
71A	13	40	27
72A	15	13	-2
73A	20	36	16

Table VI

Core	Untreated Potentials, mv	Oven Dried Potentials, mv	ΔE, mv
59P	22	28	6
60W	33	34	1
61W	42	32	-10
62P	28	28	0

Table VII

Figure	Self-potential, mv	Relative Clay Content of Each Sample Increasing Downward
6	28	51A
	63	52A
	100	53A
7	20	47A
	29	46A
	33	48A
8	-22	3UL
	-2	54W

Table VIII

K and ΔK for Air Canned Bradford Cores

Core	SP	K	-ΔK
34A	22	11	47
35A	25	13	46
36A	34	18	41
37A	21	11	48
39A	32	17	42
40A	32	17	42
41A	34	18	41
42A	32	17	42
43A	35	19	41
44A	29	15	44
45A	14	7	52
46A	28	15	44
47A	20	10	48
48A	33	17	42
49A	20	10	48
50A	21	11	48
51A	29	15	44

Average K 45
Deviation of the mean .69

Table IX

K and ΔK for Miscellaneous Bradford Cores

Core	SP	K	-ΔK
20U	27	14	45
21U	23	12	47
22U	-2	-1	60
52A (shale-sand)	63	33	26
53A (shale)	100	51	8
55W	20	10	48
56W	33	17	42
57P	20	10	48
58P	26	14	45
59P	22	11	47
60W	22	11	47
61W	42	22	37
62P	28	15	44

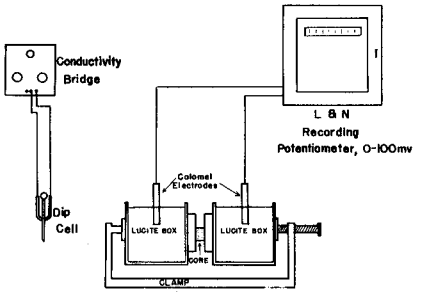

FIGURE 1. DIAGRAM OF SELF-POTENTIAL MEASURING EQUIPMENT USED IN THE LABORATORY

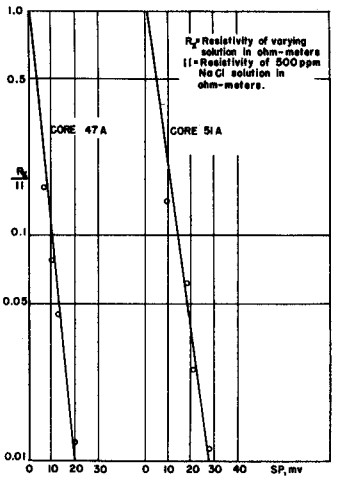

FIGURE 2. PLOT OF RESISTIVITY RATIO VS SELF-POTENTIAL FOR CORES 47A, 51A.

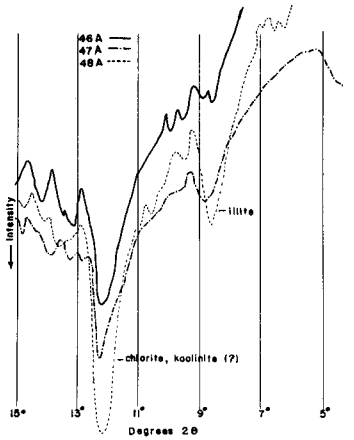

FIGURE 3. X-RAY DIFFRACTION PATTERNS OBTAINED WITH CORES

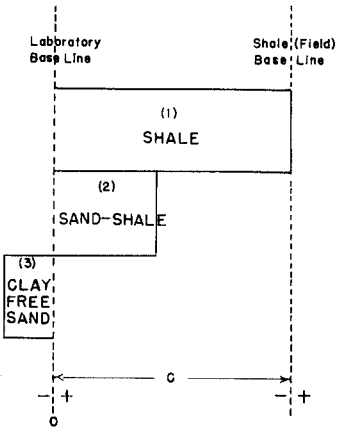

FIGURE 4. DIAGRAM OF THE RELATION BETWEEN FIELD AND LABORATORY SELF-POTENTIAL MEASUREMENTS

THE EFFECT OF SOLVENT EXTRACTION ON THE DETERMINATION OF POROSITY BY SATURATION

P. H. Licastro* and J. C. Griffiths**

Porosity is frequently used as one of the bases for the calculation of reserves in oilfield development; any error in porosity determination is, therefore, magnified considerably when applied over a whole field. The first step, in increasing the precision of porosity determination, is to evaluate the relative importance of different factors which enter the experimental procedure. The second step is to decide the sampling plan to be used in obtaining the final weighted average porosity figure used for a large volume of rock. These two aspects cannot be elucidated separately, but must be taken simultaneously into account in one and the same experiment if they are to be successfully applied to field conditions. The present experiment concerns both, but is only a preliminary stage in achieving the final objective.

During some recent experiments on the porosity of the Bradford Sand, determined by saturation techniques, it was found that porosity to water was lower than that to kerosene or tetrachloroethane, the difference being of the order of three per cent on sands varying in porosity from less than one to 23 per cent (Rosenfeld, 1950, Rosenfeld and Griffiths, 1950). Among the reasons for this difference is the possibility that the Bradford Sand is oil wet and therefore cannot be fully saturated with water. On the other hand as the samples analyzed had all been extracted prior to the porosity experiments the wettability may have been induced by pretreatment i.e. solvent extraction. It was decided to set up a series of experiments on sands of different mineral compositions, including oil bearing and barren samples, to determine whether there were any other such effects and to evaluate their magnitude.

One of the difficulties involved in experiments of this kind is that the treatment, including the determination of porosity by fluid saturation, may affect the rock irreversibly and, strictly, a single sample can then only be used once. In such a case it is necessary to use a number of samples of similar character and perform the different experiments on different subsamples of a single sample. It has been shown in previous investigations that variation in the Bradford Sand from inch to inch along the "bedding" is negligible. (Rosenfeld and Rosenfeld and Griffiths, op.cit.) Nevertheless this may not be true for other sediments, and one of the main difficulties in designing such an experiment concerns the elimination or separate evaluation of subsample variation as such differences may well be confounded with the variation due to treatment. The final experimental design for a comprehensive series of experiments aimed at a general solution to these problems can only be evolved by testing various combinations of sampling plans and experimental treatments on different rocks; the final choice will, of course, be made in terms of efficiency, i.e. amount of information per unit cost in time and energy. The present experiment is therefore a preliminary skirmish aimed at finding the weak spots rather than at the solution to any specific problem.

The rock chosen was a sandstone, the Oswego low rank graywacke from an outcrop at Skytop on route 322, central Pennsylvania. This rock is most unlikely to be oil wet and has been weathered at the surface for some considerable time. A low rank graywacke (Krynine, 1948) was chosen deliberately as most oil sands are of this type, and the order of magnitude of effects in these rocks are therefore likely to be most informative. Furthermore, the Bradford Sand previously analyzed is generally similar and comparison is therefore possible. Nevertheless, there are sufficient variations in proportions of minerals within the group low rank graywacke to yield a wide range of effects in behavior.

Six samples from the outcrop at Skytop were used for the analysis and these six were initially split into four subsamples each yielding 24 subsamples which were randomly sampled for the experimental treatments. The sampling plan is illustrated in Figure 1 and, as is the case with most experiments, extra samples were taken in case of loss. Fortunately there were no losses in the present series of of experiments and so extra information accrued. In general, it is prudent to use equal numbers of samples in experiments of this type unless there is a very definite reason for using an unbalanced sampling plan. Equal numbers of samples usually lead to a simpler and more efficient statistical analysis of the resulting data whereas unequal sampling generally results in difficulties in handling the data. In the present case, however, the statistical analysis gained in precision from the increase in the number of samples and, it was found that the use of more than four subsamples for each treatment is a very definite advantage. It appears from this result that a minimum of six subsamples is necessary unless it is known beforehand that the magnitude of the effects is sufficiently large to be detected by less information.

Contribution No. 53-12, School of Mineral Industries, The Pennsylvania State College.

*Division of Geophysics, The Pennsylvania State College.

**Division of Mineralogy, The Pennsylvania State College.

Experimental Design and Procedure

The group of 24 subsamples had been assigned numbers at random and was first split into two sets originally of 12 each. It will be noted from the experimental plan (Fig. 2) that the additional 6 subsamples were added to one set only and although this was actually fortuitous and not purposive, it fortunately did not affect the final comparisons. All 30 subsamples were oven dried at 100 degrees centigrade and brought to equilibrium by evacuation. The first set of 12 subsamples were solvent extracted in toluene and then assigned by number i.e. randomly, to the three different saturating fluids, distilled water, 5000 parts per million sodium chloride solution and oil, pentachloroethane. The second set of 18 subsamples were given no extraction treatment and were also assigned by number to the same saturating fluids respectively. The porosities of all 30 subsamples were thus determined and this completed Stage I of the experiment. Subsequently they were all brought to equilibrium again by oven drying and evacuation. In the second stage of the experiment the original set of 12 were given no further extraction treatment but the same subset of 4 subsamples was saturated with sodium chloride solution as a control. The subsets which were assigned to distilled water and oil in the first stage were now, however, reversed.

In the second stage of the experiment the second set of 18 subsamples were solvent extracted in toluene and the same subsets used in the first stage again assigned to the three saturating fluids.

The object of this rather elaborately complicated design was to obtain porosity values for sets of subsamples which could be compared in such a way as to yield a very sensitive statistical test which it was believed would be capable of detecting very small changes in the data. It is fortunate that this was deliberately planned because the effects were very small indeed and only a very efficient analytical technique could have detected them. In fact it appears from this experiment that the method of paired comparisons (Snedecor, 1946, p. 75) is particularly suited to this kind of experiment.

Analysis of the Porosity Determinations of 30 Subsamples from the Oswego Graywacke

The mean porosity of the 30 subsamples of Oswego graywacke based on two determinations for each subsample is 5.290 per cent porosity with a standard deviation of 0.337 per cent porosity. The coefficient of variation of the entire experiment is Cv%=6.36 indicating good experimental control and small magnitude variation. The entire range of porosity values is 4.456 - 5.856 porosity per cent. This serves to emphasize the small differences to be expected in the data and the demand of sensitivity in the tests used to detect real differences.

The 12 subsamples of Set 1 yielded 24 porosity determinations and their mean is 5.310 per cent porosity with a standard deviation of 0.378 units. The coefficient of variation of this set is Cv%=7.12 and the range 4.456 -5.855 per cent. The 18 subsamples of the second set yielded 36 determinations with a mean of 5.276, standard deviation of 0.311 and a coefficient of variation of 5.89%. Their range is 4.677 - 5.856 porosity per cent.

On the basis of these results the sets may be compared and no significant difference was found between the means (80>P>70), i.e. on the basis of a "t" test (Snedecor, p. 62) such a difference would occur less than 80 but more often than 70 times in every 100 even if the two sets of subsamples were in fact drawn from the same population. There is then little difference in porosity between these sets of subsamples irrespective of treatment. Evidently the original samples do not differ much in porosity. The statistical test used in the above comparison is an omnibus test in the sense that it does not discriminate between differences in means or variances of a set of data and hence in order to establish a difference between means exists it is advisable to test the variances of the two sets of data. Incidentally this test is also informative in a physical sense because if there is a big difference in variance, literally variabilities, of the two sets, then some change has come about during the experiment or the subsamples were different initially in their degree of variability. In this case a variance ratio test (Snedecor, 1946, p. 218) indicated no significant difference (20<P>10).

The next step is to compare the two stages of the experiments on the same set of subsamples. In both cases neither the first set of 12 or the second set of 18 showed a mean difference or a difference in variance between the two stages of the experiment. On the basis of this series of tests it can be seen that there is no difference between the sets of subsamples or between the general results of the different experimental treatments. It must of course, be emphasized that no very great differences could be expected as the range of porosities over the whole experiment is small and the porosity of these six Oswego samples low.

The next stage in the analysis is to test the effects of the different saturating fluids on the same sets of samples and as there were an equal number of subsamples involved in each case, the method of paired differences could be used. This is considerably more sensitive than a straightforward test of means but used the same kind of statistical device a "t" test (Snedecor, p.77). In each case a test of the variances preceded a test of the means in order that any "mean difference" that showed up should be

unambiguously attributed to differences between means and not to variances or both means and variances; this precaution should always be followed because the physical meaning of a difference in variance carries a different implication than a difference in means.

The second set of 18 subsamples was first analyzed because these should yield the largest differences due to treatments. For example in the case of distilled water used as a saturating fluid before and after extraction four of the six subsamples took less water after extraction than before and two took more. The basis of the paired difference test is the assumption that no real difference exists, then it follows that the differences found are accidental and the mean difference expected in a large number of trials would be zero. The test consists of comparing the mean difference observed with the expected value zero and, on the basis of the variance of the differences, deciding how likely such a value is to occur. In the case of distilled water the mean difference is 0.066 porosity per cent and the variances of the two sets of values are not significantly different (P>20). Such a difference would arise by chance in sampling a set of values with zero difference more often than 60 times and less than 70 times in every 100. When sodium chloride solution was used as the saturating fluid before and after extraction five out of the six subsamples took less water after the extraction and one took more. In this case the variances were again not significantly different and the mean difference was 0.228 porosity per cent. Such a difference would occur more than 5 but less than 10 times in 100 from a group in which no difference exists. The conventional level for accepting real differences is generally taken at the 5 per cent level, i.e. if the difference is large enough to be expected less than five times in every 100 it is regarded as likely to signify a real difference. In the case of a sodium chloride, therefore, the difference may be considered suggestive, particularly as we are dealing with such small orders of magnitude. The five subsamples saturated with oil before and after extraction all took less oil after extraction than before and the mean difference (0.156 porosity units) is significant in this case (1<P>.1). It is noteworthy that in using all three fluids the greater number of subsamples took less fluid after extraction than before, and that this was significantly less in the case of oil and approached significance in the case of sodium chloride solution. These results may be accumulated and, of course, the accumulated difference over all treatments (0.150 units) is highly significant. Apparently then in the case of the Oswego graywacke the rock takes less fluid, irrespective of kind, after extraction than before.

We may now turn to the results of Set 1 subsamples in which the subsamples were first extracted and subsequently saturated. The subsamples from this set, saturated with sodium chloride, showed very small differences between the first and second saturation, the mean difference being not significant (60 P 50) as would be expected. For those samples which were first saturated with water and subsequently with oil, all samples took less oil than water but the difference (0.350 units of porosity) was not significant (20 P 10). In the subset of subsamples which after extraction were saturated first with oil and then with water, the differences were quite irregular and the mean was not significant (40 P 30).

A number of other comparisons could be undertaken between subsamples and treatments but unless the data admitted of the use of paired differences then it is almost certain that the small differences which exist between means of the sets would not be significant.

Conclusion

The first consideration is that this experiment has shown that the magnitude of the differences due to various treatments including extraction, and the use of different saturating fluids has negligible effect on the determination of porosity values in sediments which have porosities of the order of 5 per cent. Unfortunately, this is not very informative because most of the rocks dealt with by petroleum engineers possess considerably higher porosities and it cannot be decided whether these effects would be equally unimportant in rocks with higher porosities. In addition, of course, the Oswego graywacke may be a fairly stable type of graywacke in respect to the interaction between saturating fluids, solvents used for extraction and mineral surfaces. What then has the experiment demonstrated? Firstly, it has shown that effects exist and that these effects can be detected by suitable experiments even when they are very small. In fact, it may be stated that this experiment has achieved at least limited success under the most unfavorable conditions that are likely to be found. These techniques, therefore, this sampling plan, and the statistical device of paired differences are likely to be most fruitful in subsequent experimentation along these lines.

Finally the experiment has demonstrated that there are real effects which must be attributed to treatment and particularly to fluid extraction and this has confirmed the need for more exhaustive and more comprehensive investigation of the effect of pretreatment upon the determination of porosity by fluid saturation.

It may be of interest to note that the Bradford Sand samples previously investigated took less water than oil and this was after extraction. The Oswego samples took less fluid, whether that fluid was distilled water, sodium chloride solution or oil after extraction. From the results of the present experiment there are fourteen subsamples saturated with oil after extraction and fourteen with water un-

der the same conditions; the mean differences between these sets is not significant and hence the Oswego samples took as much oil as water after extraction. Such differences of behavior between the rocks is to be attributed to different response of mineral surfaces to wetting fluids and perhaps implies different wettabilities in the original state.

References

Krynine, P. D., The Microscopic Study and Field Classification of Sedimentary Rocks, Jour. Geol., 56.2, 130-165, 1948.

Rosenfeld, M. A., "Porosity", Unpublished M. S. thesis, Division of Mineralogy, The Pennsylvania State College, 1950.

Rosenfeld, M. A., and Griffiths, J. C., "A New Approach to the Problems of Porosity Measurement," The Pennsylvania State College, Mineral Industries Experiment Station Bulletin, No. 56, 163-201, 1950.

Snedecor, G. W., Statistical Methods, Iowa State College Press, Ames, Iowa, 1946.

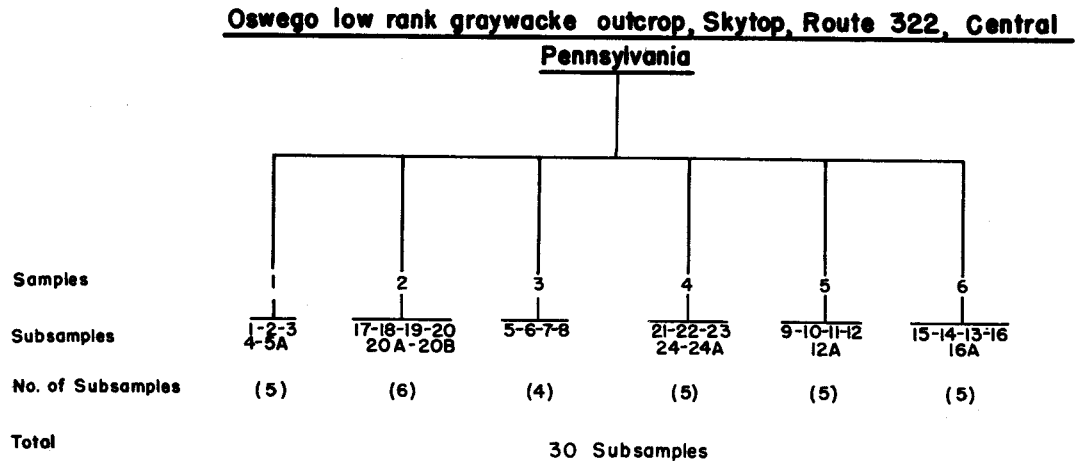

FIGURE 1 Sampling Plan For Evaluation Of Porosity Variation

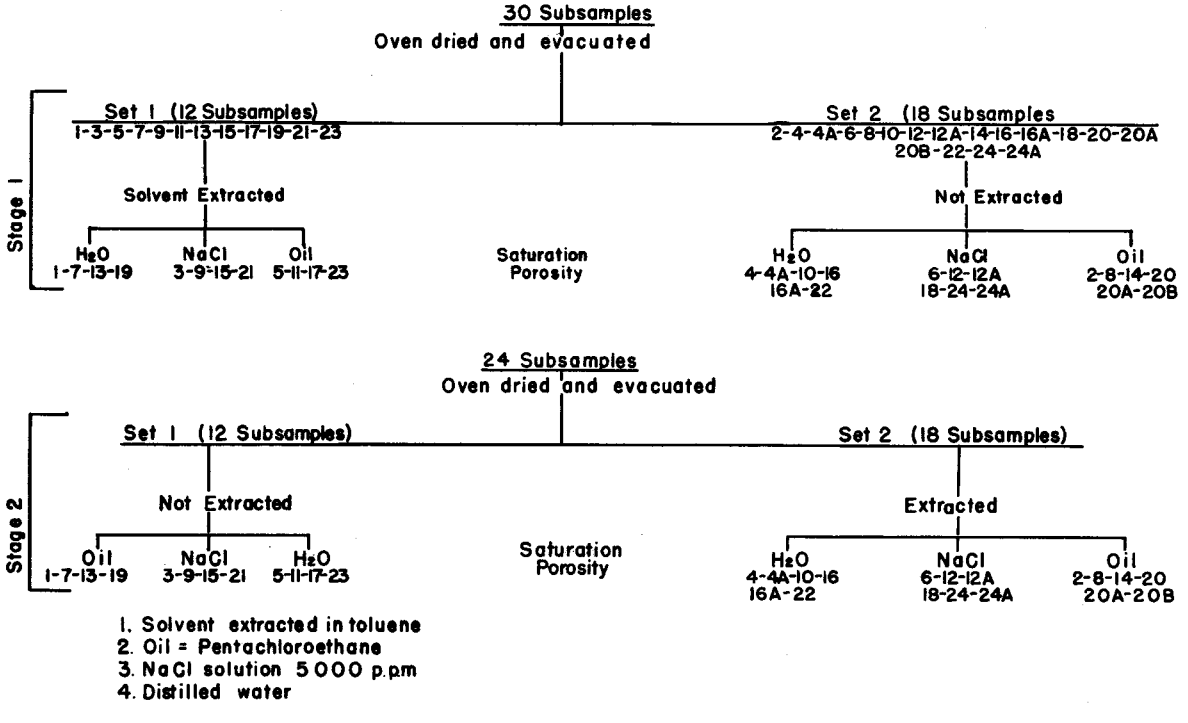

FIGURE 2 Experimental Design For Evaluation Of The Effect Of Solvent Extraction On Porosity Determination By Fluid Saturation

PROGRESS IN ELECTRIC LOGGING RESEARCH AT THE PENNSYLVANIA STATE COLLEGE DURING 1952-1953

Charles R. Holmes*

Abstract

Three phases of the logging research program for the past year are reviewed. The first problem studied was an evaluation of the effects of related paramaters on the measurement of core resistance in the laboratory, particulary in their effect on determinations of the saturation index. The value of core resistance measured is shown to reflect critically the distribution of fluid within the core. A method of core preparation which will allow reliable resistance measurements to be made is described. The second phase of the work was an investigation of the resistance variation with water saturation of especially prepared Bradford Sand cores. Limiting values are presented for the saturation indices of extreme types of water-wet and water-repellent cores. The departure of the values of the saturation index for natural Bradford Sand cores from the limiting values obtained is interpreted as reflecting the ratio of water-wet to water-repellant pores inside the core. The third phase of the work, which was devoted to a study of the effect of load and formation pressures on the electrical properties of oil bearing rocks, is reviewed briefly.

The electric logging research program for the past year has been divided into three phases. One phase of the effort was devoted to a study of laboratory methods of measurement of the resistance of reservoir rocks. This investigation of the effect of techniques of measurement on the values of the resistivity parameters recorded was conducted in an effort to provide control for the second phase of the work which was an investigation of the resistance variation with water saturation of especially prepared Bradford Sand cores. The third phase of the research was concerned with the effect of load and formation pressures on the electrical properties of oil bearing rocks, and with the construction and evaluation of the apparatus necessary to a study of this type.

Measuring Techniques

In the measurement of the variation of core resistance with the amount of contained water the usual practice is to express the values recorded in terms of the dependence of a resistance ratio on a corresponding water saturation value. This dependence has been previously expressed (Archie, 1942) as

$$I = S_w^{-n}$$

where S_w is the water saturation (fraction of the voids in the core filled with water).
I is the resistivity index (ratio of the resistivity of a core partially saturated to the resistivity of that same core at 100% water saturation).
n is an exponent called the saturation index.

Values of the saturation index determined in the laboratory for the above empirical relation have been used in an attempt at field determinations of fluid saturations from electrical well logs, but with limited success in the Bradford Field. It is believed that failure to correlate saturations as determined by core analysis may result from the values of the saturation index used.

Standard procedure in the laboratory determination of rock resistance is to make the current and voltage measurements on a sample cut from the rock into a regular geometric shape (usually a right cylinder) with the ends connected in any of a variety of ways to the measuring electrodes. Errors in measurement then might arise from: electrical resistance at the contacts as a result of poor connection between contact and core; polarization effects at the electrodes (as conduction is primarily electrolytic); electrical reactances that result from the use of currents that are other than direct; variations in resistance with temperature; and variations that result from changing fluid distributions within the core. The fluid distributions in turn depend on methods of core treatment preparatory to saturation as well as on the time element necessary to achieve equilibrium distributions. In addition, there is the difficulty of correlating any resistance measurement with the correct water saturation since these measurements cannot be made simultaneously. All of these variables might adversely affect

Contribution No. 53-11, School of Mineral Industries, The Pennsylvania State College.

*Research Assistant in Divisions of Geophysics and Geochemistry.

the resulting determination of the saturation index, and the investigation was conducted primarily to determine their relative importance, and to determine particularly if any of them were critical.

The importance of contact resistance probably has concerned everyone who has attempted the measurement of true rock resistance. In the present program several known types of core contacts were tested for their effect on the measured resistance as the water content of the core was varied, and for reproducibility of measured value when contact was broken and then remade, other factors being kept constant. A comparison was made between electrodes constructed of pliable, absorbent blotting paper wet with the same fluid used to saturate the core, foil electrodes of silver, aluminum, tin, and gold, and electrodes formed by painting the core ends with silver paint. Reproducible results were obtained with the blotter electrodes only on cores at full water saturations. In the case of partially saturated cores, the resistance appears to decrease with time implying that water from the blotters was entering the core. It is felt that blotter electrodes can be used successfully on partially saturated cores only when the core length is large compared to its diameter, and the measurements can be completed in short time intervals on cores at near equilibrium fluid distributions. The foil electrodes were formed to the core ends by pressure applied to a rubber backing. The rubber backing was cut to the diameter of the core and enclosed in a ring pressure plate to prevent diametral expansion. Thus when pressure was applied the foil was formed closely into the grain structure of the core. Of the foils tested, only the aluminum disintegrates so rapidly from electrochemical action as to be unusable. Gold foil electrodes are most satisfactory when the contact is to be maintained unbroken over long time intervals as they are little affected by the corrosive action of the brine. It is difficult to remake a satisfactory contact with any of the foil electrodes after temporary removal when the core is not fully saturated; particularly on those cores where the porelets are not readily wetted by the brine water. Silver painted core ends minimize contact resistance but are affected by electrochemical action. However, the effect of electrochemical action at the contacts on the measured resistance is not discernible if the initial salinity of the saturating fluid is high.

Wettability Studies

The resistance of a core measured in the laboratory depends in part on the fluid distribution in the core. This fluid distribution depends in turn on the degree of wettability of the porelets with water. Thus, if water adheres well to its pore surfaces, a core is termed 'water-wet', but if not is called water-repellant*. Artificial extremes of these types have been previously prepared from cores by boiling them in chromic acid to render them water-wet (Ryder, 1949) or by flooding them with a solution of Dri-film to make them oil-wet,(Licastro and Keller, 1953). However, the attempt to render a core uniformly water-wet by following the accepted treatment was completely unsuccessful. Whether the cores were boiled in chromic acid or flooded with acid and then allowed to stand in it for as long as a week, the net result was to preferentially water-wet the thin surface layer of the core with respect to its interior. The only successful method of preparing the cores found was flushing under pressure. The most satisfactory reagent found for cleaning a core was a 30% solution of hydrogen peroxide (Superoxyl). This treatment renders the core water-wet to a high degree while altering the appearance of the core but little. Chromic acid was found to be a satisfactory cleaning agent, but is much too viscous to allow easy migration through the core at the moderate pressures used except on cores previously treated with Superoxyl.

In order to evaluate the dependence of the core resistance on temperature and to allow resistance measurements to be made as a function of fluid distribution at constant saturations, individual desiccators as shown in Figure 1 were designed to hold the cores. The cores are pressure fitted with rubber backed gold foil electrodes and held in a pyrex glass tube by means of a spring and adjustable stoppers. A rubber stoppered escape hole allows the removal of moisture without otherwise disturbing core or contacts. Five such units can be contained in a pair of temperature controlled lucite boxes as shown in Figure 2. Provision for the measurement of variations of core temperature was made by contacting one of the cores about mid-section with a platinum-platinum rhodium thermocouple. The individual desiccators can be easily removed from the temperature controlled box for weight determinations on the cores without loss of contained moisture. At the higher water saturations the humidity of the atmosphere in the core holders surrrounding each core is near the saturation point and any slight decrease in the temperature of the core holder causes moisture to precipitate out on the glass. This effectively prevents the determination of the resistance dependence of a core on temperature as the temperature decreased, and all resistance measurements made with this apparatus were on the upward swing of a temperature cycle, at which time, any moisture migration was into the core. The resistance measurement made for any given temperature of the rising part of a temperature cycle was always greater than one made at the same temperature after sufficient time had elapsed to allow near equilibrium conditions to arise. The difference between this value and the equilibrium value results from both the temperature

*Rocks which are water-repellant are commonly assumed to be preferentially oil-wet, and spoken of as such. The latter term is used as synonymous with water-repellant in this paper.

inertia of the core and the non-equilibrium distribution of the contained moisture. However, the magnitude of the difference is small and even though the moisture distribution within the core may not have been at equilibrium, resistance measurements made at constant moisture values were duplicated for the same temperature over more than one temperature cycle so that the dependence of the determinations of the saturation index on temperature were minimized.

The electrical conductance of an electrolytic solution has been expressed approximately by the relation

$$R_t = R_o/(1 + mT)$$

Where R_t is the resistance at any temperature T and R_o is the resistance at 0°C., and 'm' has the value 0.022. This value for 'm' differed slightly from that computed from data taken on cores over a temperature range from 25 to 45 degrees centigrade. The value obtained on all cores and at all saturations during the evaporation process was, within the limit of error of the measurements, 0.020. Although this difference was not shown not to depend on such rock properties as solid conduction or porosity it is thought more probably a reflection of the thermal inertia of the cores.

The dependence of the resistivity index on saturation for cores measured in the apparatus previously described is shown in Figure 3. Curve number I represents a typical curve for artificially water wetted cores and curve number II one for artificially oil wetted cores. It was noted in particular during the evaporation process that at the very low saturations the resistance of the oil wetted cores depended greatly on the humidity of the atmosphere surrounding the core. Thus, if the desiccator holding the core was closed and the humidity of the atmosphere surrounding the core increased slightly by the addition of moisture from within the core, the magnitude of the resistance would drop to a value much less than that previously recorded. It was felt that this effect was probably the result of conduction over the surface, which might be of importance in the deviations of the curves for the water-wet and oil-wet types from each other, and might help explain the wide difference between the curve obtained for either of these two extreme types and one such as curve Number III for a natural core.

The elimination of the effect of surface conductance was accomplished by taking measurements on cores wtih diameters large compared to core length. After extraction, the lateral core surface was sealed with a hard transparent plastic coating. Desaturation of the core was accomplished by evaporation through the end surfaces after removal of the foil electrodes. Some difficulty was experienced in remaking the electrical contact on the artificially oil-wetted cores at the lower water saturations once the contact was broken. In order to overcome this it was necessary to coat the ends of the core with a thin permeable film of silver paint. The foil contacts were then formed to the silvered ends of the core with rubber faced pressure plates and maintained under pressure until the next cycle of evaporation. With this procedure all the core surfaces were isolated from the atmosphere and sufficient time could be given to allow the fluid distribution within the core to approach equilibrium without the deleterious effects of excessive moisture loss or surface conductance. This last method is the most satisfactory of all those tried for the treatment and handling of cores in the determination of the saturation index. The effects of contact resistance and surface conductance are minimized, and those due to changes in core temperature and moisture content can be evaluated or controlled. In addition, the apparatus required for making the measurements is not complicated, and a core may be easily flushed at low to moderate pressures once the lateral surface is sealed with the plastic sealant. The resistivity index determinations made in this manner are illustrated in Figure 4. The curve numbered IV is a curve for resistivity index versus water saturation for a core rendered artificially water wet by flushing first with Superoxyl and then with chromic acid. The difference between this curve and that for the water wet case in Figure 3 should be noted. The slope of curve IV is constant at about -2.5, but for curve number I changes from -2.0 for high saturations to about -2.5 for the low saturations. The curves determined for the oil-wet case deviate only at the lower saturations. Curve V would approximate a limiting line of slope about -3.1 drawn tangent to curve II at the high saturations.

It is believed that an explanation for the difference between the curves of Figures 3 and 4 can be given in terms of the effects of surface conduction and in the degree of wettability of the pore surfaces themselves in the different types of cores. If at the very low water saturations an oil wet core is subjected to a humid atmosphere, any condensation of moisture on the lateral core surface would produce a short, highly saline conductive path that would effectively shunt the high resistance represented by the interior of the core. This picture becomes more plausible if one considers that even a very high resistance shunt becomes effective at the low water saturations. This shunting effect results in resistivity index determinations that are too low for the observed water saturations and a deviation of the slope of the curve from the -3.1 value of curve V. The departure of curve I from a straight line in Figure 3 for the water wet case also results from values of core resistance that are too low for the observed water saturations, but at the medium rather than the very low saturations. Although this variation in slope might possibly reflect uneven fluid and salt distributions within the cores, this is not believed to be the case in view of the dimensions of the cores used. Again it is felt that surface conductance effects afford a more plausible explanation. If moisture migration from the

core interior to the surface is sufficient to keep the surface moist in spite of evaporation an effective shunt could be formed from the short current path on the core surface even though the interior core resistance is not as high as for the oil-wet case at the low saturations. This explanation is substantiated by the fact that the maximum deviation of the saturation index from a constant value was observed on a core on which the surface had been made preferentially water wet with respect to the interior by boiling the core in chromic acid. The shunting effect of a humid atmosphere would be much less effective at the very low saturations since any water condensed out on the surface of water-wet cores would migrate rather rapidly to the relatively dry interior of the core. The resulting uniform distribution of moisture would result in only slightly lowered resistance values.

The higher values of the saturation index observed for the oil-wet case over that of the water-wet is a direct reflection of the nature of the pore surfaces themselves. Any given departure from total water saturation will result in more interruptions of current paths and correspondingly higher resistance in an oil-wet than in a similar water-wet core as the water tends to coalesce into discreate droplets on an oil wet surface but uniformly cover one that is hydrophilic. The discrepancy between the value of the saturation index observed for cores rendered artificially water wet and the accepted value of about -2 for naturally water-wet cores is not yet explained but is not believed to result merely from any effects of surface conductance. The results presented are based on studies made on nineteen cores. It is possible that the treatment used left the cores uniformly but only partially water wet and that the observed value of saturation exponent is high. This possibility will be checked by measurements on cores in which the degree of wetness is successively changed from an initial condition.

The curve numbered III on Figure 3 represents the typical dependence of resistivity index on water saturation that was observed for the natural Bradford cores that were extracted only. As is illustrated, values of the saturation index obtained for natural cores do not lie between the expected limiting values given by the oil and water wet indices, except at high saturations. An explanation for this departure may be that the cores are not partially but uniformly wettable relative to some limiting condition, but contain pores some of which exhibit a relatively high degree of water wetness, while others are water-repellant. These pores then will be kept saturated by capillary pressures as desaturation progresses until all the moisture that can migrate from the oil-wet to the water-wet porelets has done so. At that point, desaturation of the water-wet pores of the core would begin. In the initial desaturation of the core the decrease in moisture in the oil wet pores would result in a dependence of resistance on water saturations that would be much the same as for the limiting type oil wet core. However, as the moisture loss progressed the shunting effect of the saturated water wet pores would become more and more effective and result in values of the saturation index much less than those for either limiting case. When desaturation of the water-wet pores finally begins nearly all of the moisture must come from these pores. Then core resistance rises very rapidly and results in a sharp break in the resistivity index curve in the saturation range of 8% to 13%*. The conclusions presented are based on relatively few data. It is planned to investigate this departure of the saturation index from the limiting cases for a large number of natural Bradford cores and to try to relate it to some range of 'wettability ratio' of the pores as well as to the degree of uniform wetness of all the pores. It would then be possible with such a relative scale to devise a standard procedure for the determination of wettability of Bradford cores from routine laboratory measurements. This in turn may make possible more accurate determinations of fluid saturations from electric well logs.

Pressure Studies

Measurements of rock resistivity which are made in the laboratory are generally carried out under conditions of atmospheric pressure and the room temperature. The validity of the results based on these measurements depends on how well they reflect the conditions imposed by the temperatures and pressures prevailing at depth. During the past year pressure apparatus has been designed and constructed that will allow measurements to be made for the determination of the magnitude and possible significance of pressure variations with depth upon the resistivity parameters. Figure 5 is a schematic diagram of the set-up used to make the measurements. Gas pressure may be supplied from a tank to the three fluid reservoirs in such a manner that it is possible to either flood the core or maintain fluids in it under pressure. The details of the pressure bomb in which the core is contained are shown in Figure 6. The core is held in the constriction in the teflon liner and maintained in position between the stainless steal stem end electrodes by means of stainless steel spacers which are not shown. The spacers also serve to prevent flowage of the teflon under pressure. A recession cut 1/16 inch deep from the outer surface of the teflon liner and slightly longer than the core makes it possible to apply load pressures through the teflon to the cylindrical core surface independently of the fluid pressures within the core. This arrangement permits independent variation in either of the two pressures over the working range used. In the case of the external load pressures actual pressures applied to the teflon were not the actual pressures exerted upon the rock. This pressure difference can be corrected for by subtracting from the observed

* This is not shown on the curve illustrated as the break occurred at a lower saturation than could be plotted.

load pressures the pressure difference obtained with the bomb filled only with water. Although results are as yet incomplete the effect of variations in both internal and external pressures on core resistance has been investigated for a few cores. Measurable variations in resistivity are apparent and for the cores measured are believed to result from surface conduction and compaction effects. The effect of surface conductance was evaluated by making measurements on a core rendered impermeable by saturating it with melted paraffin under pressure. It was observed that this effect is negligible provided the effective load pressures are kept higher than the internal pressures. An increased core resistance was observed with load pressures for any given internal pressure and is believed to reflect a decrease in porosity that results primarily from closure of incipient fracture systems and the sealing of interconnecting capillaries in shaley portions at the lower pressures. At the higher pressures, the resistance increase is believed to result primarily from the effect of elastic compaction.

Acknowledgment

The research on which this discussion is based was conducted under the sponsorship on the Pennsylvania Grade Oil Association whose support of this work is sincerely appreciated. The author is grateful also for help received from other members of the staff of the Division of Geophysics and Geochemistry and to Dr. Elner Denson who supervised the project and conducted the pressure experiments this past year.

References

Archie, G. E., 1942, "The Electrical Resistivity Log as an Aid in Determining Some Reservoir Characteristics," A.I.M.E. Tech. Paper No. 1422. Trans. A.I.M.E., Vol. 146, pp. 54-67.

Ryder, H. M., 1949, "Characters of Pores in Oil Sands," Quarterly of The Colorado School of Mines, Vol 44, No. 3, pp. 583-595.

Licastro, P. H., and Keller, G. V., 1953, "Resistivity Measurements As a Criteria for Determining Fluid Distribution in the Bradford Sand," Producers Monthly, Vol. 17, No. 7, pp. 17-23.

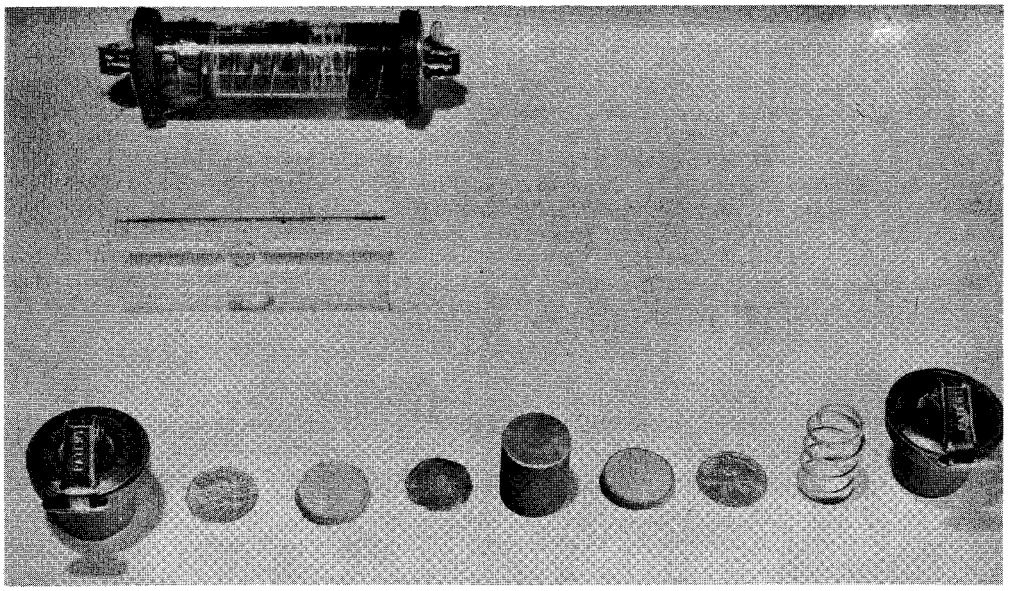

FIGURE 1 CORE HOLDER AND UNASSEMBLED COMPONENTS

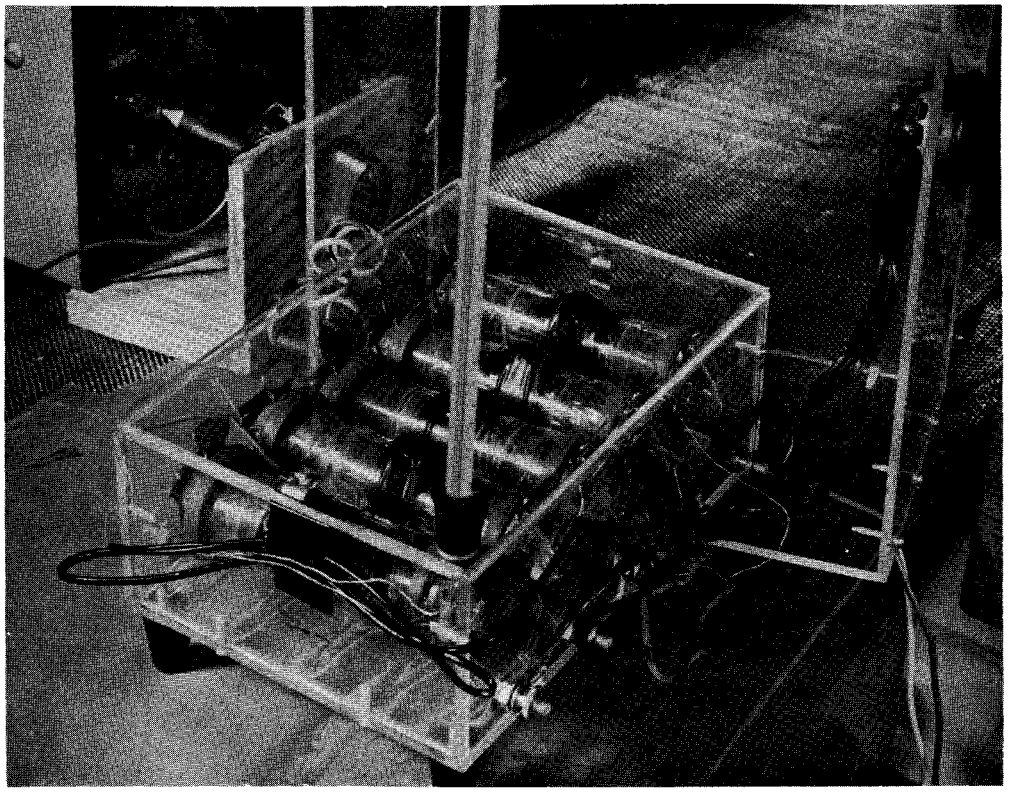

FIGURE 2 CORE HOLDERS ASSEMBLED IN TEMPERATURE BOX

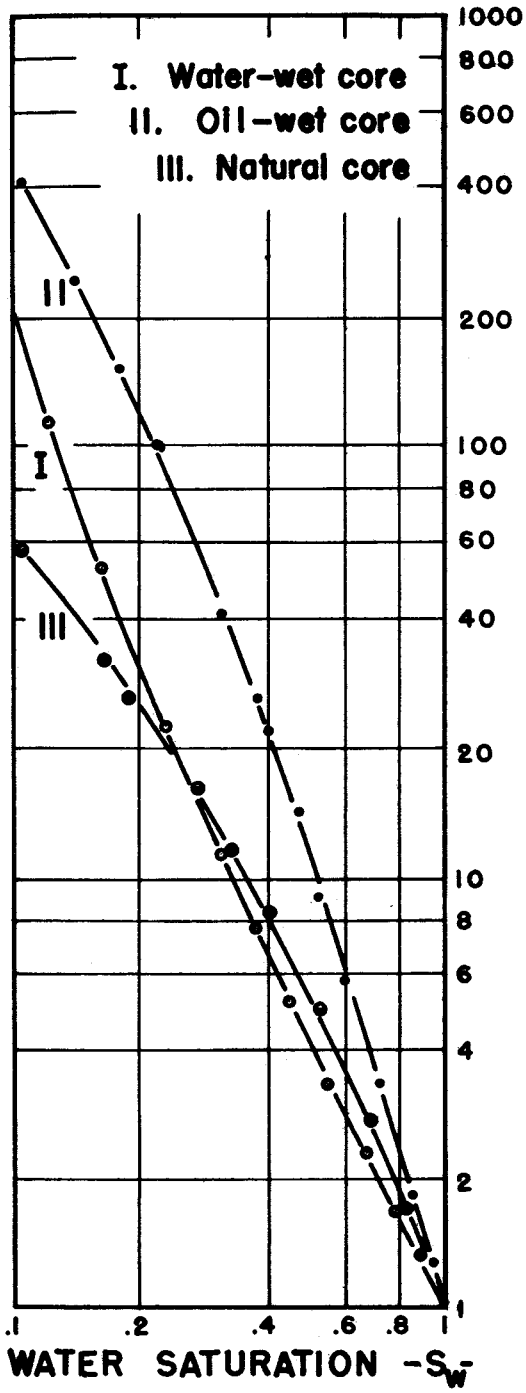

FIGURE 3

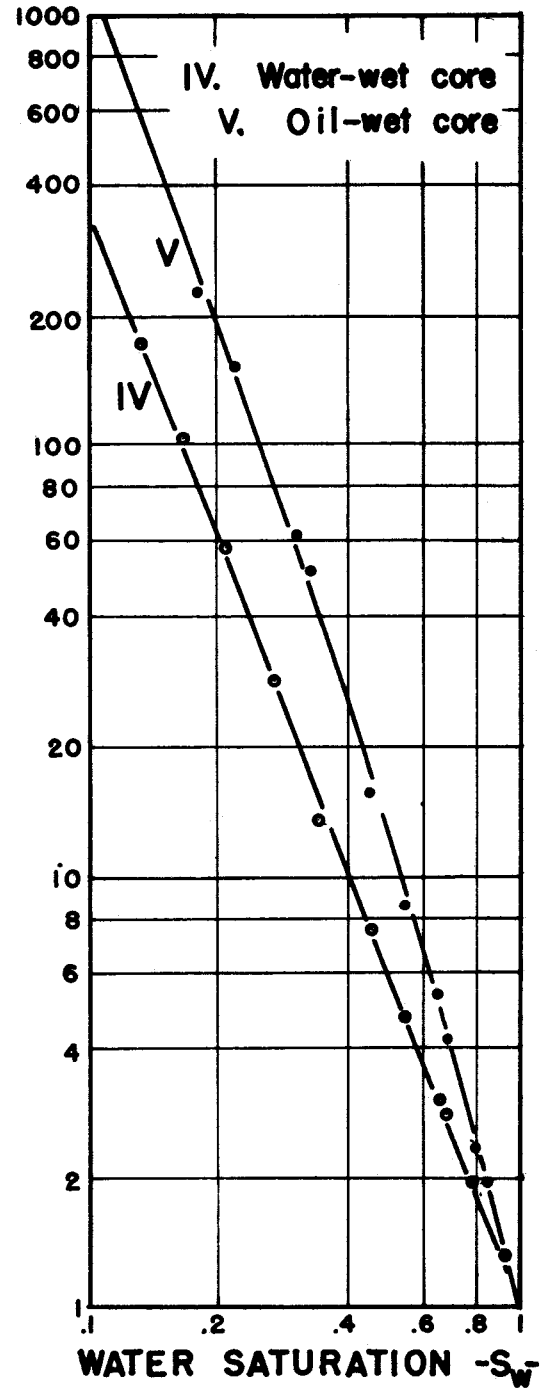

FIGURE 4

SATURATION INDEX DEPENDENCE ON WETTABILITY

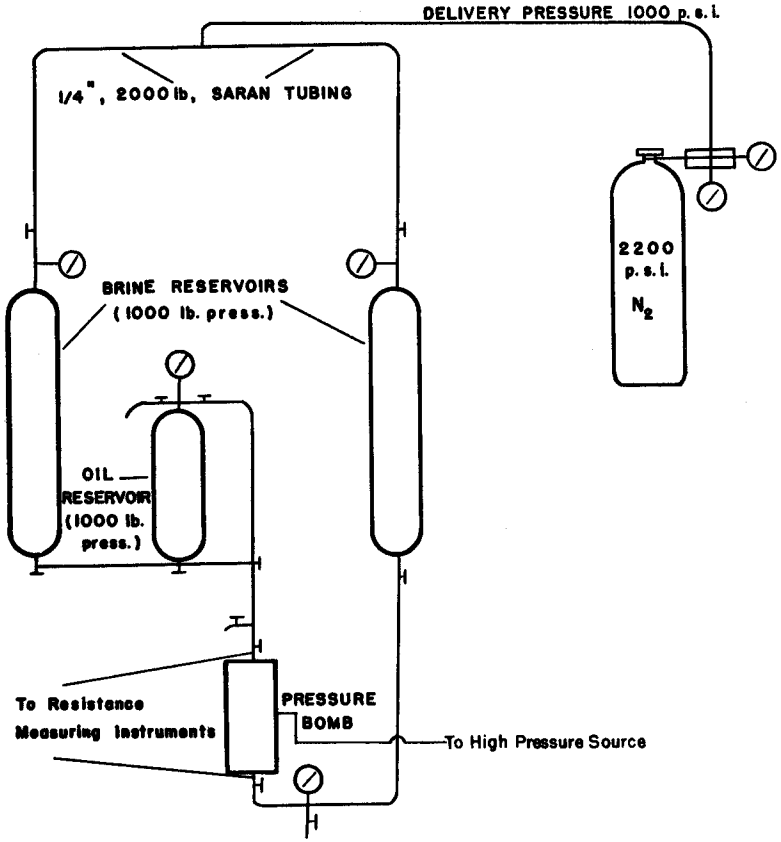

FIGURE 5 SCHEMATIC DIAGRAM OF PRESSURE APPARATUS

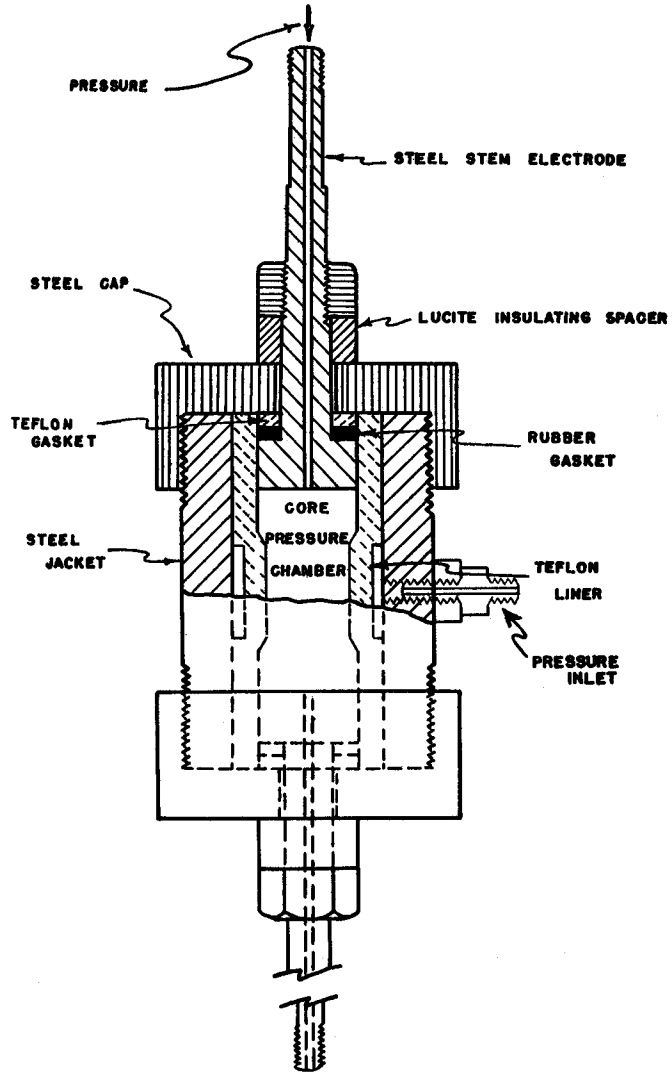

FIGURE 6 DIAGRAM OF CORE HOLDER USED WITH PRESSURE APPARATUS

CAPILLARY DESATURATION AND IMBIBITION IN POROUS ROCKS

C. R. Killins*, R. F. Nielsen** and J. C. Calhoun**

Introduction

The recognition of hysteresis in capillary measurements is almost as old as the recognition of the capillary forces themselves. In single capillary experiments, there have been discussions of hysteresis based upon the differences between advancing and receding contact angles and the alternate rise and fall of liquids in capillary tubes of non-uniform cross-sectional area. In the techniques of measuring the capillary properties of porous rock systems, hysteresis has also been established. Leverett[1], in his pioneering article on capillary properties of porous material, gave data on and discussed relationships between height of water rise and water saturation for the drainage of water from a sand as well as for the imbibition of water into the sand.

Welge[2] presented relationships between fluid saturation and capillary pressure both for the displacement of a wetting fluid by a non-wetting fluid and the displacement of a non-wetting fluid by a wetting fluid on natural porous systems. Subsequent to his publication several technical notes on the subject appeared in the literature. The first, by Rose[3] argued that it was impossible to obtain the type of experimental results shown by Welge and at the same time maintain capillary equilibrium between the various fluids in the porous system. The second, by Purcell[4] argued that it was possible to have capillary equilibrium and at the same time produce the experimental results which were shown by Welge. In a subsequent technical note, Jones-Parra[5] has indicated that the argument developed by Purcell did not apply because it did not take into consideration the presence of residual wetting liquid during the process of displacing the non-wetting liquid by the wetting liquid. Jones-Parra held that the argument of Purcell, when applied to the situation where a residual wetting liquid did exist, supported Rose rather than Welge.

In the meantime there have been several other publications of experimental capillary pressure data in which hysteresis has been discussed. Stahl[6], Kinney[7], and Kinney, Killins and Nielsen[8] have presented relationships between fluid saturation and capillary pressure for certain natural porous rocks in which data have been determined not only by displacing a wetting liquid by a non-wetting liquid but also by displacing a non-wetting liquid by a wetting liquid. In the majority of these experiments the porous rock was brought into contact with the non-wetting liquid before the wetting liquid was used as a displacing media. There was no attempt to carry on a cycle of measurements so that the displacement of a non-wetting liquid by a wetting liquid took place in the presence of irreducible wetting liquid.

Still more recently Arman[9] has undertaken capillary pressure measurements in porous glass bead systems. The cycle of displacement which he used was non-wetting fluid (gas) into wetting liquid followed by wetting liquid into non-wetting fluid without resaturating the porous matrix and with a continuous change of capillary pressure in small increments.

Hassler, Brunner and Deahl[10] discussed hysteresis at length and indicated several possible types, but did not offer experimental proof for their hysteresis ideas. They define two types of hysteresis, which they call "optional hysteresis" and "trap hysteresis". The first, they say, "arises from the complex geometry of the porous medium that allows the fluids to be in equilibrium with different distributions at different capillary pressures. The particular distribution that the fluids will assume and hence the capillary pressure that will obtain will naturally depend on the immediately preceding distribution. In the various states of distribution considered here it is supposed that both phases are continuous throughout the porous medium. The states are then stable. They represent true equilibrium."

Trap hysteresis, according to the definition of Hassler et al, is that which occurs when small globules or bubbles of the non-wetting fluid become separate from the main body of fluid and are trapped either in dead end interstices or in interstices with narrow necked openings. They go on to

Contribution Number 53-16, School of Mineral Industries, The Pennsylvania State College.

* Former staff member, Division of Petroleum and Natural Gas Engineering, The Pennsylvania State College, now with The Ohio Oil Company.

** Division of Petroleum and Natural Gas Engineering, The Pennsylvania State College.

point out that this type of hysteresis does not represent an equilibrium. The trapped globule will eventually dissolve and emerge, after diffusion, in the connected portion of the fluid in question. They recognize that this diffusion process is slow and that for practical purposes the hysteresis due to trapping of isolated globules might be a phenomenon of importance in actual oil field production.

It is the intent of the present paper to enumerate some capillary pressure studies made for the specific purpose of learning the nature of hysteresis loops. These hysteresis data are internally consistent and consistent with an understanding of the nature of the porous materials as learned from other tests. It is possible to deduce from the nature of the hysteresis loops the means by which one fluid will displace another within the pores of a capillary system.

In order to establish uniformity of thought on this problem and to eliminate the use of wordy phrases it is proposed that two terms be adopted for the upper and lower portions of the hysteresis loop. Capillary desaturation will be used to refer to that process whereby a non-wetting fluid is displacing a wetting fluid from the porous material (the upper portion of the loop). Capillary imbibition will be used to indicate the process under which the wetting fluid is displacing the non-wetting fluid (the lower portion of the loop). In general there will be different relationships between capillary pressure and fluid saturation during the desaturation and imbibition processes.

Experimental Work

Capillary pressure information has been obtained on samples of the Bradford, Venango, Tensleep and Berea formations. In addition to analyses made on the extracted samples of these formations some analyses were made after the samples were treated with dri-film in order to render them oil wet. Capillary pressure information was also obtained on unconsolidated systems of glass beads and anthracite coal.

Consolidated formation samples were cylindrical plugs which had been cut from larger cores. They were approximately 1/2 inch in diameter and from 1 to 1 1/2 inches long. All formation samples were extracted in toluene for a period of 24 hours or longer, after which they were dried, prior to saturation for any capillary pressure tests.

The oil phase used in all cases was a mixture (50-50 by volume) of mineral oil and Kensol 18*, a close cut hydrocarbon. The density of this mixture was 0.837 gms/cc at 30°C. Distilled water was used in all cases for the aqueous phase. Liquids were degassed prior to being used. The interfacial tension between the oil and water phases was 38.2 dynes per centimeter at 30°C, the temperature at which all tests were made.

Two types of apparatus were used. The first, similar to that commonly used in restored state tests, consisted of a glass Buchner funnel with a fritted glass capillary diaghragm of ultra-fine grade. The formation sample in question was placed on this diaphragm which had been rendered either oil wet or water wet depending upon the liquid which was to be displaced. The sample was then surrounded with the other liquid, to which air pressure was supplied. Generally, the test sample was held in place by a spring in compression between the top of the sample and the neoprene stopper which served as a cap for the funnel. The entire assembly was clamped in place so that the applied air pressure would not force the stopper. To complete a desaturation-imbibition cycle with this particular type of apparatus it was necessary, upon completing a desaturation cycle, to permit imbibition back to atmospheric pressure and then transfer the sample to a similar apparatus having a diaphragm of wettability opposite to that first used.

The second type apparatus is shown in Figure 1. Two capillary diaphragms were used, one in each end of a lucite tube, with the sample to be tested lying between the diaphragms. When the sample was unconsolidated the entire space between the two diaphragms was packed with the sample. One diaphragm was oil wet and the other water wet so that desaturation or imbibition tests could be performed merely by reversing the direction of pressure. When the sample was consolidated, the entire space between the diaphragms was not filled with the sample. Consequently, the two diaphragms were of equal wetting properties and the displacing liquid occupied the space surrounding the sample and between the diaphragms. Air pressure was supplied to the displacing liquid. With the use of this second apparatus it was also necessary, in completing a capillary pressure cycle, to permit the imbibition to proceed to atmospheric pressure and then change the sample to an apparatus where the wettability of the diaphragms was opposite to that used for the desaturation process.

* Manufactured by the Kendall Refining Company, Bradford, Pennsylvania.

In most instances it was necessary to use a finely divided powder to maintain capillary contact between the samples and the diaphragms. A water paste of Silene EF was used when a water wet diaphragm was required and dri-film treated Silene EF, mixed in oil, was used when an oil wet diaphragm was required.

All changes in saturation of the samples were determined from the volumes of liquid measured in accurate volumetric pipettes into which the liquid displaced from the samples was forced. The pore volumes of the individual samples were taken to be the volumes of wetting fluid required to fully saturate the samples.

Capillary pressure-saturation relationships are shown in Figures 2-16. In each instance the saturation scale used is that of the liquid considered to be wetting. Numbered arrows indicate the sequence of paths taken during the test cycles.

Interpretation of Test Results

In order to interpret each of the hysteresis cycles shown in Figures 2-16, it will be necessary to refer to other work and develop some theoretical concepts. For this purpose Figure 19 shows a number of different possible cycles which could occur in running desaturation and imbibition capillary pressures.

When desaturation occurs under circumstances such that the wetting liquid maintains continuity, each increase in pressure permits entry into a new set of pores and further reduces the amount of pendular wetting liquid in pores already entered. After irreducible wetting liquid is reached and imbibition is permitted, each decrease in pressure may be thought of as accomplishing the reverse process, i.e. increase in pendular wetting liquid in those pores not fully entered and the reentry into other pores. In the ideal homogeneous porous system, the imbibition into individual pores would proceed in the exact reverse order of desaturation of the pores. Thus, in this ideal system the imbibition curve would be the reverse of the desaturation curve.

Even in the ideal system, however, adjustment must be made for differences in advancing and receding interface curvatures. Although the order of re-entry into capillaries by imbibition may be the reverse of the order of desaturation, the capillary pressure path may differ due to the interface curvature change. This situation could still demand that all pores be re-entered so that the end point of imbibition be full saturation of the wetting liquid, but with the capillary pressure at a given saturation lower on the imbibition cycle than on the drainage cycle. An imbibition displacement pressure should exist and successive tests should always produce the same cycle in this type situation. Paths numbered 1 and 2a in Figure 19 are the result.

Capillary pressure desaturation and imbibition curves of this nature have been reported in the literature. Puri[11], for example, shows many desaturation-imbibition cycles on sands and soils wherein the imbibition cycles return to full saturation and exhibit imbibition displacement pressures. One of Puri's experiments in which the capillary pressure cycle was repeated five times with water on a silt sample is reproduced here as Figure 17. Arman[9] has also reported desaturation-imbibition cycles for glass beads. One set of his curves, reproduced here as Figure 18, shows the return to full saturation at the end of the imbibition cycle.

Arman's data is also useful to show the magnitude of the relationship between the desaturation and imbibition paths of the hysteresis loop. In the data duplicated here, (Figure 18) a solid curve has not been drawn through the imbibition data. Rather, the solid imbibition curve shown is such that the imbibition capillary pressure is 0.56 times the desaturation capillary pressure at a given saturation. For two other glass bead packs, Arman gives additional data and the ratios of 0.625 and 0.630 bring the imbibition and desaturation data together. Thus, for three sets of glass beads, Arman not only shows imbibition to full saturation but shows a rather constant ratio of imbibition to desaturation capillary pressures. Constant ratio between the desaturation and imbibition capillary pressures suggest that the change in interface curvature might be due to a difference between the advancing and receding contact angles. However, the concept of advancing and receding angles becomes rather ambiguous when a continuous film of wetting liquid exists throughout the pore structure.

Of course, the differences between desaturation and imbibition capillary pressures might be due to re-entry of pores in an order different from the order of desaturation. This would be the "optional" hysteresis described by Hassler. If 100% saturation were reached, however, the imbibition displacement pressure under this situation should be equal to the desaturation displacement pressure.

If one postulates that the re-entry of pores during imbibition is not in the reverse order of pore displacement during desaturation, the wetting liquid saturation at full imbibition may be less than 100%. It is conceivable that within the porous structure there will be large pores sufficiently surrounded by small pores that when the pressure is reduced low enough to effect entry into the large

pores, the act cannot be done because there is no path by which the non-wetting liquid can escape. The differentiation between large and small pores in this discussion is only one of degree, and isolation of non-wetting liquid might occur in any size pore as soon as imbibition is started. As soon as such non-wetting liquid is isolated, the capillary pressure is no longer uniform throughout the porous structure. The imbibition curve can never, under these circumstances, be an equilibrium curve.

This is the "trap" hysteresis referred to by Hassler.[10] Because of the nature of this hysteresis, it is not obvious that the imbibition curve under these conditions has a distinct meaning unless it can be duplicated each time it is run. The percentage of pore space occupied by globules trapped during imbibition might have some significance in determining pore size distribution. It appears that if conditions for trap hysteresis are present, the hysteresis would be increased by the heterogeneity of the porous structure, the degree of preferential wetting by the wetting liquid and the speed at which the imbibition was allowed to proceed. It would also seem obvious that true trap hysteresis could not be removed by the application of excessive pressures against the non-wetting fluid.

In Figure 19, cycles numbered 1, 2b, 3b and 4b show the path taken by this type hysteresis. Figures 2-4 and 8-10 of the present experimental work are felt to be examples of capillary pressure cycles wherein the preferential wetting is sufficiently pronounced to give desaturation and imbibition curves on the positive scale of capillary pressure but pore distributions, and/or rates of imbibition are such as to produce trap hysteresis.

Perhaps the best and most complete illustrations of this are Figures 8 and 9, the first an untreated Berea sample (water wet) and the second a treated Berea sample (oil wet). It will be noted that the isolated non-wetting liquid after imbibition was slightly greater than that indicated after pressure was applied to the wetting liquid. Approximately 10% additional pore space was invaded by application of pressure to the wetting liquid, after which the isolated non-wetting liquid saturation was definite as indicated by the vertical lines for cycles 3 and 4.

What would happen to the desaturation curve if it were repeated after trap hysteresis was formed? Present experimental data does not permit an evaluation of this. In one instance (Figure 10) glass beads were saturated with a non-wetting liquid, the wetting liquid imbibed without application of pressure until trapping was almost completely effected. A pressure was applied to complete the trapping, and after its removal a desaturation curve was made. However, there is no available data for comparison of this desaturation curve with that which would have resulted without the presence of trapped non-wetting liquid.

In the considerations thus far, a condition has been that the wetting liquid maintains continuity so that imbibition may proceed. Let it be supposed that, as pendular rings are formed during desaturation, they become isolated. Such a situation has been proposed before and Bethel[12] has given supporting evidence. If the pendular rings become isolated they do so because the wetting of the solid is not definitely in favor of the original wetting liquid. Upon release of pressure there may be no increase in wetting fluid saturation because the advancing contact angle may be greater than 90°. In Figure 19 this is shown by paths 1 and 2d. Upon subsequent application of pressure to the original wetting liquid, the change in contact angle requires the development of a displacement pressure. Under such circumstances the presumed imbibition loop would actually be a desaturation loop of a new cycle of capillary pressures with a different wetting fluid, but with isolated pendular rings of the first wetting liquid already in place. Upon reaching the irreducible minimum saturation of this secondary desaturation loop in turn, a secondary imbibition could proceed, or the desaturated liquid might again lose continuity so that imbibition could not proceed. In Figure 19, these possible paths have been numbered 3d and 4d; and 3d and 4b.

Figures 11, 12 and 13 are examples of capillary pressure cycles where apparently the continuity of the original wetting fluid is broken during desaturation. All of these show the characteristics discussed. Not only does the wetting liquid saturation increase by only a small amount, if at all, upon release of pressure, but a displacement pressure is necessary to force oil (the original wetting liquid) into water (the original non-wetting liquid). The oil into water curve (cycle 3), therefore, properly becomes a desaturation curve with a portion of the porous matrix filled with non-communicative residual oil. After this secondary desaturation, a secondary imbibition (cycle 4) occurs, indicating that the porous systems could properly be termed water wet, in the presence of the original residual oil (original wetting liquid). During the secondary imbibition cycles there may also be a trap hysteresis of water as indicated by the failure of cycle 4 to return to the same saturation as cycle 3 at zero capillary pressure. This point is not proven because each of these imbibitions was carried on at a rapid rate. Bradford sand samples were used for the data in Figures 11, 12 and 13. This sand is known to be quite neutral in its wettability and previous tests on the sand have often shown displacement pressures both for water into 100% oil saturated samples and oil into 100% water saturated samples.

Other Bradford sand tests, reported by Stahl[6], are duplicated here as Figures 20 and 21. They show imbibition of oil when the samples were fully saturated with water and show water isolated by trap hysteresis. This indicates that there must be a fundamental difference between that situation wherein oil attempts to displace water from pores where no oil is in contact with the surface and that situation wherein oil attempts to displace water from pores in which isolated oil already is in contact with the surface. Figures 20 and 21 are also interesting because they show desaturation curves in the presence of trapped non-wetting fluid (similar to Figure 10). In Figure 20 there is a partial comparison between desaturation curves run from full saturation and from partial saturation (trapped non-wetting phase).

When the original desaturation of a wetting phase occurs, some but not all pendular rings may be isolated, the advancing angle may be high but not sufficiently so to cause the complete loss of imbibition. Neither may it be low enough to support complete imbibition. Therefore, an imbibition curve could fall almost anywhere between the two extremes which have already been illustrated. In Figure 19 the sequence shown by 1, 2c, 3c and 4c is of this nature.

Figures 5-7 and 14-16 are presented as a group of tests in which the capillary pressure cycles are of this in-between type. Figures 14-16 lean quite strongly to the Bradford sand type. These are Berea cores treated with dri-film to render them oil wet. Apparently, however, the treatment was insufficient to produce the complete oil wettability which would give a performance as indicated in Figure 9. Upon release of pressure to permit imbibition (cycle 2) the increases in saturation were slight. Furthermore, upon application of pressure to the wetting liquid, slight displacement pressures were observed. The shapes of the capillary pressure-saturation relationships on this part of the test (cycle 3) suggest a desaturation process. Upon reaching the end of cycle 3, the release of pressure produces little imbibition, however. The pressure goes to zero (cycle 4) with very little change in saturation, which suggests a break in the continuity of the fluid previously being displaced (water). Consequently, these sequences are not like Figures 8 and 9 nor like Figures 11, 12 and 13. The wetting characteristics of these surfaces (treated Berea) apparently are more oil wet than Bradford, but no so oil wet as they could be (see Figure 9, for example).

Figures 5-7 lean quite strongly to the examples of Figures 8 and 9. However, in Figures 5-7 trapping of the non-wetting liquid was not nearly so complete when pressure was removed for the imbibition cycle as in Figures 8 and 9. Since these are Berea samples and, in general, Berea samples are so definitely water wet, it is possible that the deviation from complete imbibition could be blamed on the speed with which the imbibitions were made (i.e. there are fewer steps of pressure release shown in Figures 5-7 than in Figures 8 and 9).

Of the samples tested, therefore, with the fluids used, anthracite coal and Tensleep sand were quite oil wet; Bradford sand was oil wet but close to neutral; Venango and Berea samples were water wet, the former probably being closer to neutral than the latter.

General Discussion

The experimental work presented permits the delineation of several degrees of hysteresis. During the measurement of a capillary pressure under hysteresis conditions it is not claimed that capillary equilibrium is achieved throughout an entire porous system. In this sense capillary pressure curves may be meaningless. However, the type of hysteresis loop gives an insight into what may be happening to fluid interfaces within the porous systems. Hysteresis capillary pressure curves may well have a meaning in this sense.

One of the chief conclusions from the experiments is that a desaturation or imbibition curve by itself tells little about the wetting properties of a porous system. To gain a true picture of wetting it is necessary to obtain rather complete hysteresis data. Undoubtedly, a scale of wetting might be possible by expanding hysteresis measurements in a quantitative direction.

Capillary pressure hysteresis itself does not appear to be chargeable to any one cause. Apparently trap hysteresis is a rather well founded concept and easily recognized. Optional hysteresis, under conditions of complete equilibrium, may be possible but the condition is not obviously demonstrated. A hysteresis, similar to trap hysteresis of the non-wetting liquid, is possible for the wetting fluid. In some instances, it is probable that all these effects occur. The limiting situations which have been discussed here and illustrated are of help, however, in delineating the causes for hysteresis in a specific instance.

There are a number of practical applications which come to mind. The cycle of fluids used in reservoir control may be a very important consideration if hysteresis is important. Certainly, also, any hysteresis in capillary pressure should mean that a hysteresis would exist in relative permeability, in fluid displacement by water flooding, or in electrical resistivity measurements.

Not the least important of the factors considered here is the rate at which imbibition processes are carried on. In instances where capillary forces are important in field recoveries this could also be an important factor.

Acknowledgements

Acknowledgement is made to the research program of the Penn Grade Crude Oil Association at Penn State under which much of the experimental work was performed. The detailed data are also reported in the M. S. thesis of C. R. Killins at Penn State which was relied on heavily in preparation of the manuscript.

References

1. M. C. Leverett, "Capillary Behavior in Porous Solids," Trans. AIME, Vol. 142, p. 159 (1941).

2. Henry J. Welge, "Displacement of Oil from Porous Media by Water and Gas", AIME T. P. 2433, Pet. Tech. (Sept. 1948).

3. W. Rose, "A Note on the Application of the Capillary Pressure Method for the Determination of Oil Recovery", Pet. Tech., Section 1, p. 30 (March 1949).

4. W. R. Purcell, "Interpretation of Capillary Pressure Data", Trans. AIME Vol. 189, p. 369 (1950).

5. J. Jones-Parra, "Comments on Capillary Equilibrium", Journal Petroleum Technology, Vol. V, 502 (Feb. 1953).

6. C. Drew Stahl, "An Investigation of Capillary-Pressure Saturation Relationships", M. S. Thesis, The Pennsylvania State College, State College, Pa. (1949).

7. P. T. Kinney, "Some Theoretical Aspects of Correlations of Capillary Pressure Data on the Bradford and Venango Sands", M. S. Thesis, The Pennsylvania State College, State College, Pa. (1951).

8. P. T. Kinney, C. R. Killins and R. F. Nielsen, "Some Applications of Capillary Pressure Measurements on Pennsylvania Sands", Producers Monthly, Vol. 16, No. 3, (Jan. 1952).

9. I. H. Arman, "Relative Permeability Studies", M. S. Thesis, University of Oklahoma, Norman, Okla. (1952).

10. G. L. Hassler, E. Brunner, and T. J. Deahl, "Role of Capillarity in Oil Production", Trans. AIME, Vol. 155, p. 155-174 (1945).

11. A.N. Puri, Soils, Their Physics and Chemistry, Reinhold Publishing Corp., New York (1949), p. 346-469.

12. F. T. Bethel and J. C. Calhoun, "Capillary Desaturation in Unconsolidated Beads", Journal of Pet. Tech., Vol V., No. 8 (Aug. 1953).

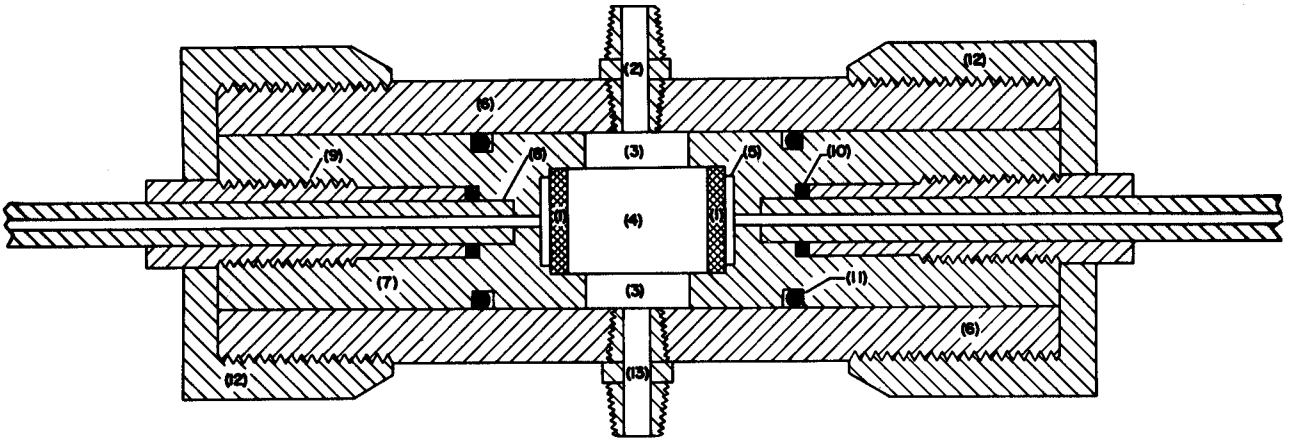

1. CAPILLARY DIAPHRAGMS
2. INLET
3. ANNULAR RESERVOIR
4. CORE
5. RESERVOIR
6. OUTER SHELL
7. PLATE HOLDER
8. PIPETTE
9. PIPETTE FOLLOWER
10. O-RINGS
11. O-RINGS
12. METAL CAP
13. OUTLET

FIGURE 1 CAPILLARY PRESSURE CELL

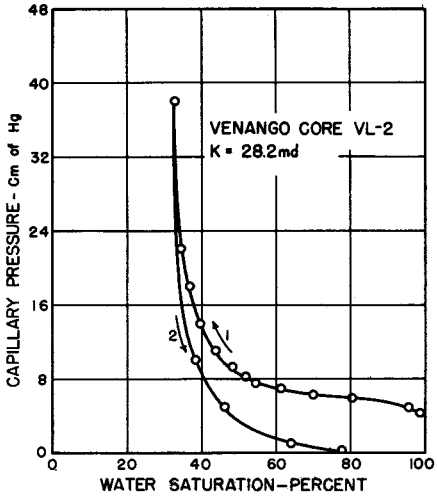

FIGURE 2. CAPILLARY PRESSURE VS. WATER SATURATION.

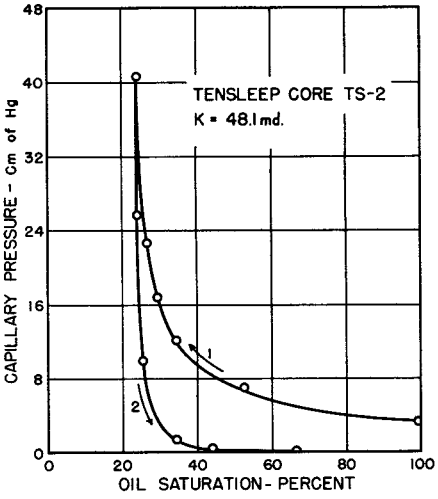

FIGURE 3. CAPILLARY PRESSURE VS. OIL SATURATION.

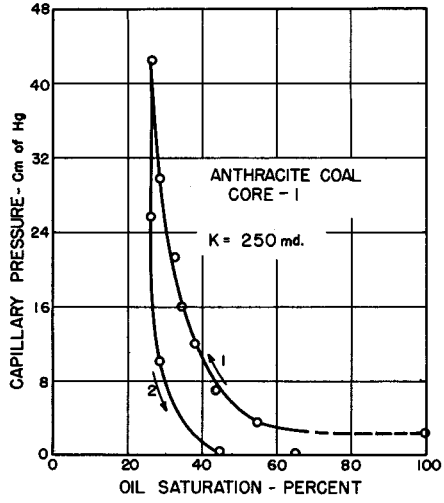

FIGURE 4. CAPILLARY PRESSURE VS. OIL SATURATION.

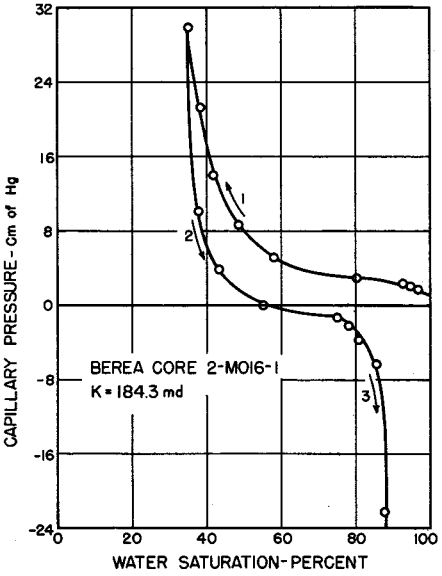

FIGURE 5. CAPILLARY PRESSURE VS. WATER SATURATION.

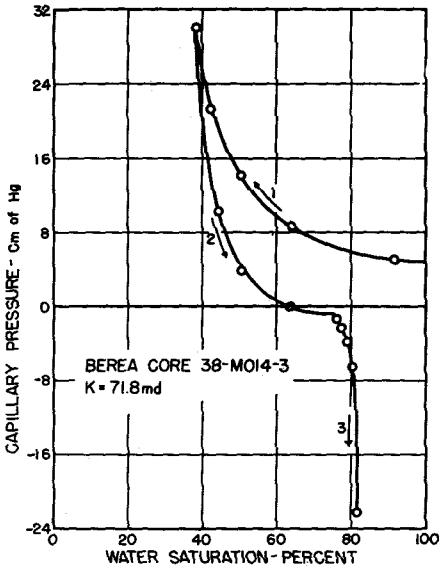

FIGURE 6. CAPILLARY PRESSURE VS. WATER SATURATION.

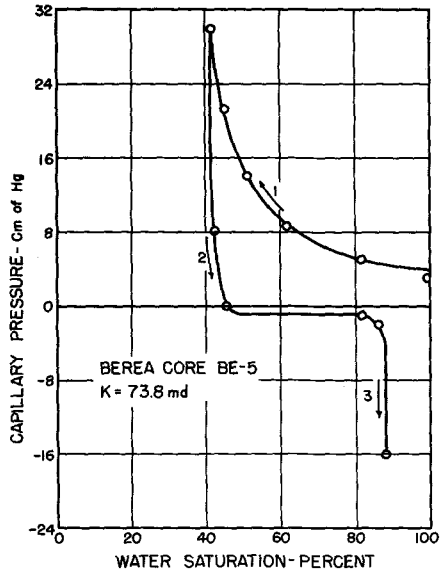

FIGURE 7. CAPILLARY PRESSURE VS. WATER SATURATION.

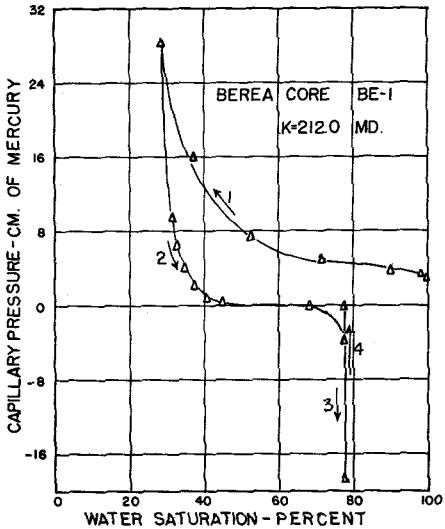

FIGURE 8. CAPILLARY PRESSURE VS. WATER SATURATION

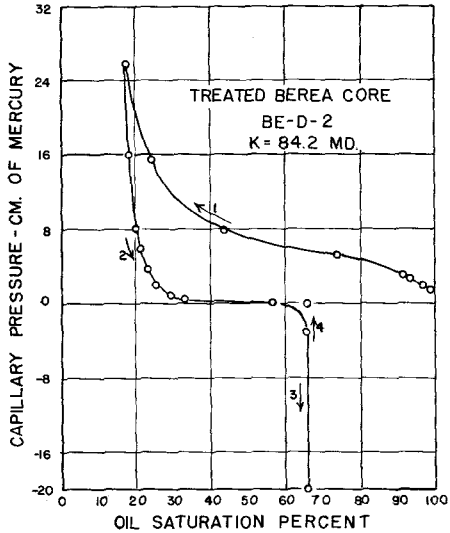

FIGURE 9. CAPILLARY PRESSURE VS. OIL SATURATION

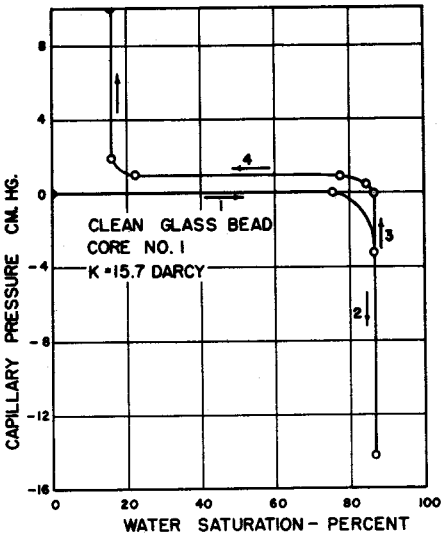

FIGURE 10. CAPILLARY PRESSURE VS WATER SATURATION

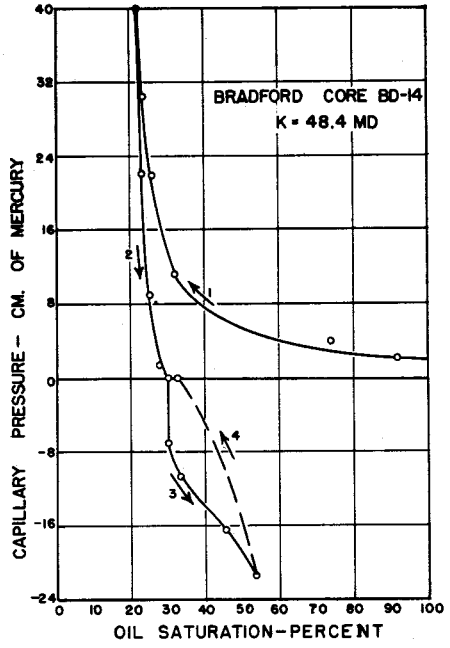

FIGURE 11. CAPILLARY PRESSURE VS. OIL SATURATION

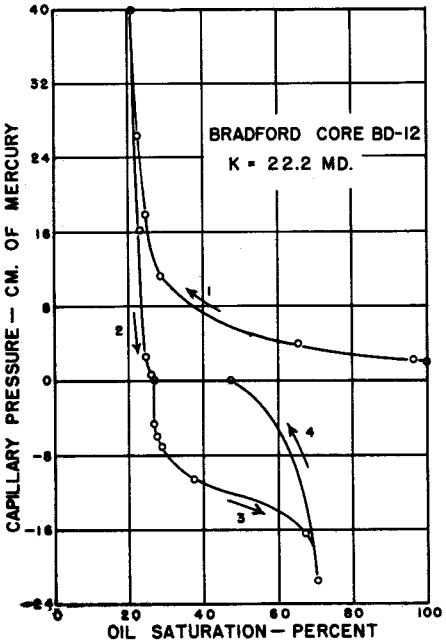

FIGURE 12. CAPILLARY PRESSURE VS. OIL SATURATION

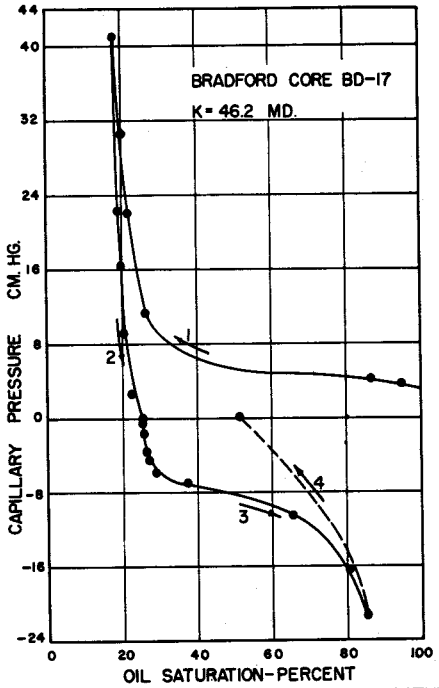

FIGURE 13. CAPILLARY PRESSURE VS OIL SATURATION

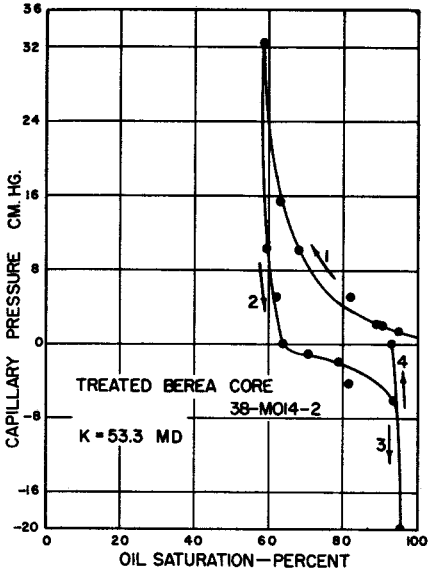

FIGURE 14. CAPILLARY PRESSURE VS OIL SATURATION

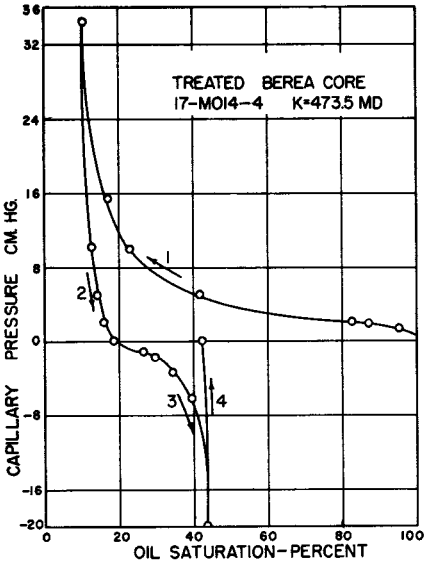

FIGURE 15. CAPILLARY PRESSURE VS OIL SATURATION

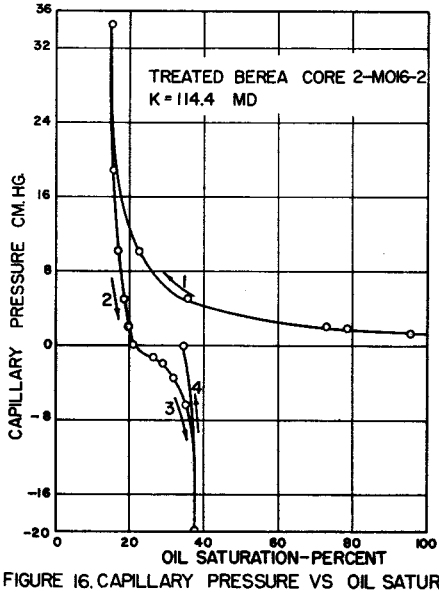

FIGURE 16. CAPILLARY PRESSURE VS OIL SATURATION

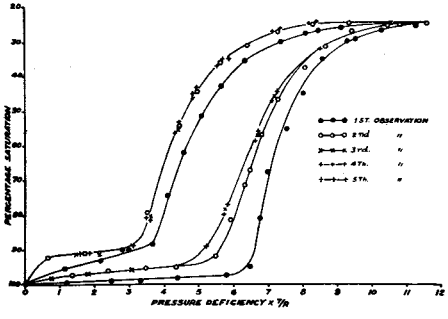

FIGURE 17. CAPILLARY PRESSURE CURVES FOR SOILS — AFTER PURI[11].

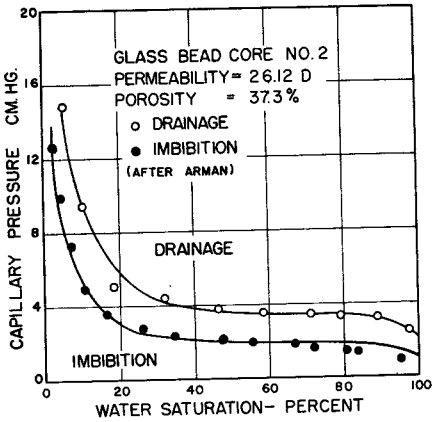

FIGURE 18. CAPILLARY PRESSURE VS WATER SATURATION

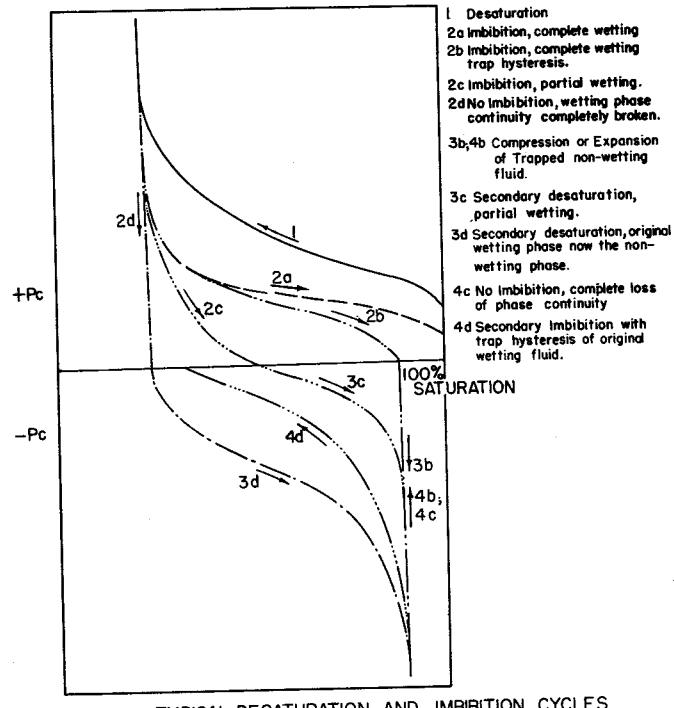

FIGURE 19. TYPICAL DESATURATION AND IMBIBITION CYCLES

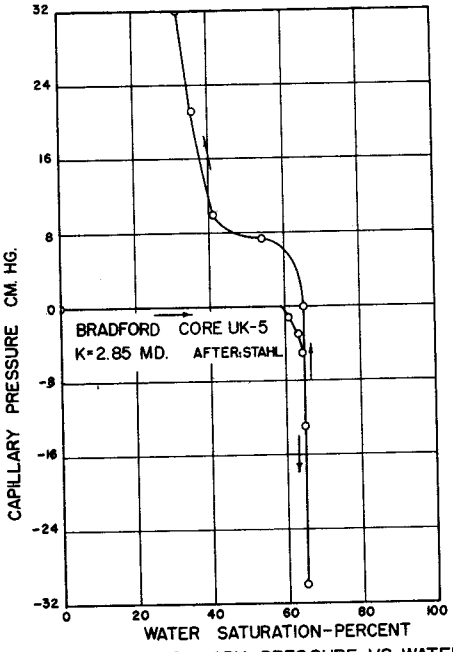

FIGURE 20. CAPILLARY PRESSURE VS WATER SATURATION

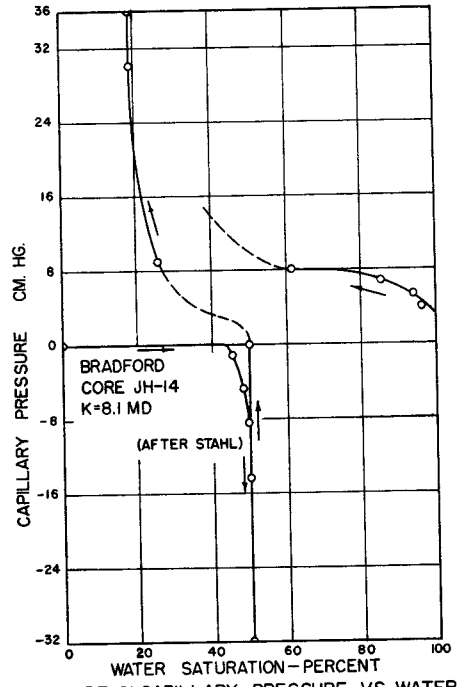

FIGURE 21. CAPILLARY PRESSURE VS WATER SATURATION

RECONNAISSANCE INVESTIGATION INTO RELATIONSHIPS BETWEEN BEHAVIOR AND PETROGRAPHIC PROPERTIES OF SOME MISSISSIPPIAN SEDIMENTS

J. R. Emery* and J. C. Griffiths*

This investigation represents the first step in a comprehensive program of study of the petrography of Mississippian sediments of Pennsylvania. The program has three main objectives, the first, to describe the degree of variation encompassed in a geological system. How variable are the rocks in a geological unit the size of a system? Are the formations in the system uniform in petrographic properties, or is there any petrographical basis for such subdivisions? In other words, is a formation, defined on lithological properties as a "mappable unit", reducible to objective quantitative specification in terms of petrographic properties? Secondly there are facies differences in the Mississippian sediments; can these be reduced to operationally defined quantitative parameters? If so what is the significance of such differences? Thirdly can oil reservoir rocks be differentiated from barren sediments within the Mississippian unit? If so what is the magnitude of the differences and what characteristics most clearly lead to the differentiation?

To achieve these objectives it is necessary to decide what properties are measurable and how many measurements on how many samples are necessary; such information may be translated, at least approximately, into cost, in terms of time and size of organization for such an investigation. The program is ambitious and, as it is a pioneering investigation, it is best to proceed in steps; the present article describes the results of the first step.

Sixteen samples were chosen at random from a large number of Mississippian sediments collected from various localities in Pennsylvania and the petrographic properties, composition size, shape, orientation and packing as exhibited by these samples was measured. The techniques have been reduced to relatively simple routines and for this reconnaissance approach only those items considered to be most important were investigated. The immediate objective is to ascertain the degree of variation shown by a random set of samples and with this as basis decide which properties should be evaluated on a much larger number of samples and which are not particularly informative for the purposes of the main program.

The Properties of Sediments and Their Investigation

The initial investigation of a sedimentary rock must encompass a specification of the items of which the rock is composed and, if such information is to be of real value, the relative proportions of these constituent items must also be included; hence the first step in analyzing a sediment is to identify the constituents and obtain an estimate of their proportions Subsequently each constituent is considered as an individual class of items (i.e. particles) and the range of size and shape of these individual particles within the classes must also be estimated. This completes the description of the individual items but a rock achieves individuality only as an aggregate and the behavior of this aggregate is the subject of interest to petroleum geologists and engineers. It is necessary, therefore, to characterize the set of constituents as an aggregate and for this purpose the relative position of the items is important. This aspect is known as the fabric of the rock and the operational techniques which describe fabric comprise a measure of orientation of each grain and an estimate of the proximity of each grain to its neighbor- generally designated as the packing of the grains.

To characterize a rock, then, five separate properties are investigated, namely, mineral composition, size, shape, orientation and packing and techniques have been evolved for measuring each of these properties. These fundamental properties and their interrelationships lead to a characteristic behavior of a rock estimated by its bulk density, porosity, permeability and fluid saturation. One of the goals of this research program is to attempt to express these behavior characteristics as functions of the five fundamental properties of the rock in an equation of the type (Griffiths, 1952 a and b):-

$$P = f(m,s,sh,o,p) \qquad (1)$$

where the five properties are represented by the initials m = mineral composition, s = size, sh = shape, o = orientation, p = packing and the index "P" is the value of behavior, such as porosity, bulk density, etc. To this end the bulk density and porosity of the 16 samples were also measured.

The immediate objective of this analysis is to estimate the magnitude of variation shown by the 16 samples and to evaluate the interrelationships between the various measured properties. To understand

Contribution Number 53-13, School of Mineral Industries, The Pennsylvania State College.

* Division of Mineralogy, The Pennsylvania State College.

this aspect it is necessary to describe the techniques and the data accruing therefrom and then attempt to relate one set of measurements to the other. A description of this procedure follows.

The Mineral Composition of the "Pocono" Samples

The "Pocono" sediments are largely low rank graywackes (Krynine, 1948), and the mineral constituents comprise quartz, feldspar, rock fragments, micas, chlorite, matrix and cement. The following notes briefly outline the classes of constituents used for estimation of the proportions of the minerals in the 16 thin sections. The technique - point count - has been described by Chayes (1949).

The class called quartz for purposes of quantitative estimation comprises detrital quartz grains, proably the most typical constituent of most sedimentary rocks. It also includes clear untwinned feldspar which cannot be readily distinguished from quartz during counting procedures; in the "Pocono" sediments this untwinned feldspar is unlikely to have affected the proportions because feldspar generally is not too common.

The feldspar includes grains which show twinning and those which show characteristic dusty decomposition products, probably largely kaolinite. As secondary criteria for feldspar identification the evidence of rectangular morphology i.e. cleavage steps, refractive index and shagreened surface were also used to classify clear quartz-like grains as feldspar.

Two kinds of rock gragments were identified, the class called quartzite and chert and the class composed of shale, phyllite and schist. Quartzite grains are of the same size as individual detrital quartz and are composed of aggregates of quartz crystals which show sutured borders, mortar or mosaic texture. They are probably metaquartzite fragments. The chert grains are also similar in size to detrital quartz grains but possess cryptocrystalline aggregate polarisation. As the size of the individual crystals in the aggregate vary these rock gragments show a complete transition from quartzite to chert fragments. The second class containing shale, phyllite and schist is difficult to differentiate from matrix as both are ultimately composed of micaceous aggregates. As a basis for operational definition of rock fragment the most important criterion is the existence of a clear outline to the grain containing this micaceous aggregate. From this optimum, decreasing definition of outline to an extreme of unity of orientation of the mica constituents over a small area is classified as a rock fragment. If the parallelism of the mica shreds is not evident the mica aggregate is classified as matrix material.

In addition to mica aggregates there also occur larger individual grains of muscovite, chlorite and biotite which are presumably detrital in origin. These were separately counted.

Matrix is a term used to include micaceous aggregates which could not be definitively classified as rock fragments of shale, phyllite or schist. In most cases a large part of the mica aggregate could be designated as matrix without ambiguity but as the source of the matrix material is disintegrated rock fragments of mica aggregate a complete transition exists and the boundary is largely arbitrary. Matrix material is an important factor in determining rock behavior and hence an estimate of its proportions is essential. The exact identification of matrix constituents is largely beyond the limitations of the light microscope hence the convenient term "mica aggregate" which certainly includes muscovite-illite-chlorite and various intermediates of the clay minerals group.

Another constituent of importance in determining rock behavior is cement but here again much ambiguity must be introduced during analysis. The two important cements are the various carbonates of calcium, magnesium and iron and silica and while the presence and sometimes the variety of carbonate can often be specificed the silica cement is much more difficult to identify. In the present investigation "secondary" silica cement was observed as an outgrowth around quartz grains but never entered the count, hence the volume must be less than 0.1 per cent. However, some cementitious silica is almost certainly present along with some carbonate in the matrix material and no separate estimate of its volume can be made in this case. The estimation of the proportion of cement, therefore, refers solely to the recognizable carbonate content in these thin sections.

Finally there are always some items which occur outside these classes such as, for example, pores, pyrite and heavy mineral grains. These are counted as a single class called miscellaneous but a separate record is kept of the specific kind of item which enters the miscellaneous class. As a general rule if any item in the miscellaneous class exceeds 3 per cent of a single 100 point traverse it is given the status of a separate class. Usually the fractional proportion in this class is so small that its value has little effect on the estimates of the proportions of the constituents.

On the basis of this classification thin section analysis of the 16 samples is summarized in per cent in Table 1. and the variation in composition is obvious. Quartz and matrix together account for the greater proportion of the material in most samples. In only one sample carbonate accounted for a very

large percentage (Loyalhanna sample 6846-1, 49.4 per cent). For purposes of this study the two classes matrix and quartz are the most important compositional elements.

The percent of quartz is plotted against the percent of matrix in Figure 1 and if these two items accounted for the whole rock the plot would result in a straight diagonal across the graph from 100 percent quartz to 100 percent matrix. On the other hand if there are large variations in any of the other constituents the relationship between quartz and matrix would not be linear. For these 16 samples all but three fall on a line parallel to the diagonal which indicates the small but relatively constant admixture of other components. Three samples depart from this general trend; sample number 6320 is from the Olean conglomerate and possesses very little matrix material which is in accord with its quartzite composition. Sample 6846-1 is a sample of Loyalhanna sandly limestone and contains no matrix; it is composed of quartz, quartzite and chert and "cement", i.e. carbonate. 6845 is a conglomeratic sediment from the Mauch Chunk with an unusually large proportion of calcareous clay pebbles, quartzite and chert.

Such a figure serves to illustrate that the main source of variation in mineral composition of "Pocono" type sediments is the reciprocal fluctuations of quartz and matrix i.e., the "Pocono" sediments vary from typical low rank graywackes towards quartzite with removal, perhaps by winnowing, of matrix material. On the basis of this reciprocal relationship, the correlation of variation in proportions of mineral constituents with variation in other petrographic properties may be simplified by confining attention to the variation in proportion of quartz content. Any positive association found between percent quartz and some other measured property will imply a negative association with proportions of matrix.

Variation in Grain Size and Shape of Quartz Grains in "Pocono" Sediments

Grain size and shape may be measured by a large number of different techniques and the choice of technique depends on the objective of the analysis. For purposes of comparison of one sample with another merely to emphasize differences, any of the various techniques may be used and in the present investigation measurement of the longest intercept of quartz grains in thin section was chosen as the most convenient. The longest intercept of quartz grains in thin section yields a measure of size which is affected by orientation of the thin section and orientation of the grains within thin sections. It is, therefore, difficult to interpret what a change in size between samples implies when size is measured by this technique. Nevertheless as the measurements are restricted to quartz grains the mineral composition variable is removed (Griffiths, 1952b). Thin section size analysis is advantageous when shape and orientation are also measured during the same procedure and on the same grains and this is the main reason for the choice of this technique in the present investigation.

The size distribution of the longest intercept of 50 quartz grains in each of the 16 thin sections is illustrated as a histogram in Figure 2. The arithmetic mean is 2.67 phi units[1] (157 microns) and the standard deviation 1.36 phi units. As the modal value of 3.25 phi (105 microns) differs from the mean the frequency distribution is skewed. The skewness and kurtosis were estimated from the cumulants (Fisher, p. 73) and the skewness, $g_1 = 1.17$, while the kurtosis $g_2 = 5.93$. The advantage of the "g" statistics is that they may be tested for significance and in the present case both skewness and kurtosis are highly significant ($P < 0.001$). This departure from a symmetrical normal distribution is in large part due to a limitation of technique, the grains yielding maximum intercepts of less than 6 phi units (15.6 microns) cannot be measured and hence there is a cut-off at the fine end of the distribution. The physical interpretation of these statistics is, therefore, somewhat obscure and we may confine our attention to the two statistics, mean and standard deviation as estimates of average size and degree of sorting respectively.

The mean size and standard deviation in phi units of each sample is listed in Table 2 and there is a wide range in both average size and degree of sorting in these 16 samples. 6845 from the Mauch Chunk is noteworthy in being among the coarsest and most poorly sorted and as it contains pebbles of calcareous mudstone this must be a detrital conglomerate. The Olean conglomerate (sample 6320) is the coarsest and the second most poorly sorted sample and these two samples suggest that there may be a relationship between size and sorting of quartz grain intercepts. When the average grain size and the sorting of the quartz grains is plotted, however, no systematic trend appears and on the basis of these 16 samples size is independent of sorting except in the two coarsest sediments of the set. For purposes of correlation among petrographic properties it will be necessary, therefore, to use both size and sorting as independent properties of these sediments. An estimate of the shape of the quartz grains in thin section is obtained by measuring the longest intercept and the longest axis perpendicular to this intercept; axial ratio, a two dimensional measure of sphericity, is then equal to the ratio of the shorter to the longer axis. The range in axial ratio is thus limited to 0.0 to 1.0 axial ratio units. The 800 measurements comprising

1. The phi scale proposed by Krumbein (1938) represents a change in scale from arithmetic (millimeters or microns) to logarithmic (phi) units; the standard deviation cannot be translated into millimeters or microns because it is a logarithmic measure.

50 quartz grains from each of the 16 thin sections yields a frequency distribution which like that for size shows a cut-off in this case at 1.0 units. The mean axial ratio is 0.657 units with 0.170 unit standard deviation. The mean and standard deviation of axial ratio for each sample is also included in Table 2. The range in means is from 0.604 to 0.721 axial ratio units and at first sight this may appear to be small but variation in sphericity of quartz grains in sediments is seldom large (Curray, 1949). These figures may be compared with some similar measurements made on Bradford sand (Griffiths and Rosenfeld, 1950, 1953) as in Table 3 and it may then be realized that the variation among the 16 samples of "Pocono" sediments is much greater than among 10 thin sections from 3 samples of Bradford sand. Similarly the standard deviations of axial ratio are more variable in the "Pocono" samples than in those of the Bradford sand. It must be emphasized that no attempt has been made to interpret the physical meaning of these values of shape and size and the only information to be obtained from measurements of this type is by comparison with similar measurements on other rocks.

Orientation and Packing of Quartz Grains in "Pocono" Sediments

Measurement of dimensional orientation has recently been reduced to a routine operation and the general procedure is described in our earlier publications (Griffiths, 1949, 1953, Griffiths and Rosenfeld, 1950, 1953). Some minor but important changes in technique were used in the present experiment. The inclination of the longest intercept of quartz grains was used as the basis of measurement and a change was made in the choice of reference plane from which inclination is measured. In our previous work no obvious structural attitude of the sediment could be observed and hence horizontality was generally chosen as a base line. In the present case the thin sections were classified in terms of parallelism of structure, i.e. bedding or other lineation, before microscopical examination and this direction is taken as reference zero. Where no direction could be observed horizontality was used as reference zero.

The 100 inclination measurements per thin section were then classified as deviations from the reference zero in 10 degree intervals both positive and negative between 0 and 90 degrees. From the resulting frequency distributions the variance and standard deviations of the 100 measurements from each slide were calculated and tested for significance[1] (op. cit., Griffiths 1953 and Griffiths and Rosenfeld 1953). The relevant figures are summarized in Table 4.

The degree of parallelism of quartz grain intercepts is estimated by the standard deviation in Table 4, and varies from 20 to 51 degrees. Most of the sediments show a high degree of preferred orientation when compared with our previous results (op. cit.). Three samples, 6227, 6837 and 6857 showed no orientation on the basis of the statistical test of significance. It is interesting to note that the megascopic classification is a very poor guide to the degree of parallelism measured and in particular the terms "massive" and "doubtful lineation" are misleading in the present case.

The property of packing of grains in sediments is important in determining such behavior characteristics as porosity and bulk density and means for measuring this property would be of considerable value in interpreting the behavior of sedimentary rocks. Unfortunately no suitable technique appears to exist at present although a few have been proposed (Taylor 1950, Shearin et al 1952 and Gaither, 1953). Counting grain contacts along traverses through a thin section was chosen as the basis of the present investigation and the specific contacts counted were those between detrital grains. Essentially this reduces to counting contacts between quartz grains. In traverses of unit length the number of quartz/quartz contacts is a function of the size, shape, and orientation of the grains and in order to remove, at least partially, the effect of these other variables the length of traverse was divided by the mean grain size of the quartz grains. In rocks composed entirely of quartz the number of contacts is a function of the length of traverse and the size of grains, shape and orientation being assumed equal. The expected number of contacts under ideal conditions is therefore:-

$$\text{Number of contacts} = \text{Length of traverse/mean grain size} \qquad (1)$$

1. In our previous work the significance tests were based on the use of 150 to 800 grain measurements per thin section (Griffiths 1953) but in the present investigation only 100 measurements per slide were made and the significance test using the same notation as before (op. cit. p. 53) becomes:-

Probability level	P	< 0.05	< 0.01
$n_1 = n_2 = 100$	F	1.39	1.59
	s_2^2	1942.4	1698.1
	s_2	44.07	41.21

If both traverse length and mean size is expressed in millimeters the number of contacts is dimensionless. If this value may be considered the expected number then a packing index may be expressed as the expected divided by the observed:-

$$P.\ I. = (L.\ T./\ \bar{X})/\ Q.\ Q. \qquad (2)$$

where L. T. = length of traverse, $\bar{X}$ = mean grain size, and Q. Q. = quartz/quartz contacts. For convenience we may take the reciprocal of this value and express it as a percentage when the packing index (P. I.) becomes:-

$$P.\ I. = (Q.\ Q.)(\bar{X})/\ L.\ T. \qquad (3)$$

This packing index varied from 6.1 to 99.8 per cent in the 16 samples of "Pocono" sediments. At least a part of this variation in packing index is a reflection of variation in proportion of matrix because as the amount of matrix decreases the number of quartz to quartz contacts must increase. Nevertheless on a priori considerations if the amount of matrix is constant the packing index is a reflection of arrangement and particularly contiguity of quartz grains. In future analyses, therefore, this measure of packing should be adjusted for variations in proportions of matrix and then the residual variation in packing index will be independent of both size and mineral composition. All measures of packing so far proposed suffer from the same difficulties i.e. they are a function of composition, size, shape, orientation and packing; it seems evident that to obtain a meaningful measure of this property more detailed analysis and a number of different approaches must be tried.

Bulk Density and Porosity of "Pocono" Sediments

The bulk density of the 16 samples was determined by means of the mercury balance and in order to evaluate separately the different sources of variation an experiment was arranged to yield an analysis of variance of the results (see Griffiths and Rosenfeld, op. cit.) Each sample was split into three subsamples and the bulk density of each subsample run three times. From the analysis of variance (Table 5) it can be seen that the experimental error variation is small (approximately 0.007 bulk density units) and the variation between subsamples is very much greater (0.02 units). Despite this large subsample variation differences between different samples is still larger (0.15 units) and from the analysis it seems clear that we may neglect experimental error (i.e. replicate runs) in future experiments and concentrate on subsample variation.

The average bulk density for all 144 determinations is 2.510 gm/cm^3 and the range 2.070 - 2.642 gm/cm^3.

Porosity was determined by saturation with tetrachlorethane and each determination repeated four times on each sample; from the analysis of variance of Table 6 it can be seen that the differences between samples far exceeds the experimental error (variation arising from replicate runs). The average variation due to experimental error is of the order of 0.26 porosity per cent. The average porosity for all samples and all runs is 4.43 per cent and the range 1.04 - 13.08 per cent. The majority of the samples possessed porosities less than 5 per cent.

Interrelationships Between the Properties

One of the main objectives mentioned in the introduction is to differentiate oil reservoir rocks from barren sediments and as the differences are likely to be small and no one property sufficient the ultimate approach will be by way of multiple regression (Fisher, p. 156); in order to determine which factors are important to this approach it is necessary to eluciadate the interrelationships between the different properties. It has already been mentioned that there is an approximately linear reciprocal (inverse) relationship between proportions of quartz and matrix and as these two constituents make up the bulk of these "Pocono" sediments they are among the most important characters in determining rock behavior. For correlation of composition with other sedimentary properties, however, because of the inverse relationship (see Figure 1) variation in only one of these constituents need be used and the relationship of the other variables may be deduced. On the other hand grain size ($\bar{X}$) appears to be independent of sorting (s = standard deviation) and hence both these factors may have to be taken into account.

A very approximate linear relationship appears to exist between mean grain size and per cent quartz (inverse in phi terms, see Figure 3) which indicates that increasing quartz content is associated with increasing coarseness of quartz grains on average. In this case the relationship is far less clearly defined and is not sufficient grounds for rejection of either variable in forming a complex function. Nevertheless, in what follows, any relationship between mean quartz per cent and some other property will be at least approximately applicable to mean grain size. For example a similarly diffuse relationship of increasing per cent quartz and increasing sphericity (axial ratio) of quartz grains is mainly a reflection of the much closer relationship between increasing mean grain size and increasing sphericity.

In each case if the relationship is presumed linear the spread around the line of best fit is large. This is the kind of relationship which is to be expected among interdependent interacting variables (Girffiths, 1952b).

Perfection of orientation decreases with increase in quartz per cent (Figure 4) and the trend is reasonably linear. Both size and shape show more diffuse trends in which as size increases perfection of orientation decreases and similarly orientation becomes poorer with increasing sphericity (axial ratio). Closeness of packing as would be expected increases with increasing amount of quartz (Figure 5).

From qualitative judgment of these relationships it seems clear that each variable is connected with the other and the whole set of properties forms a group of interdependent variables. 16 samples are insufficient to evaluate the relationships statistically with any worthwhile degree of precision but they are sufficient to suggest that a combination of these measurements may be of value in predicting rock behavior.

When per cent quartz is compared with bulk density (Figure 6) no systematic trend appears and as bulk density is closely and positively associated with effective porosity the same lack of relationship is to be expected. Grain density is a weighted average specific gravity dependent on mineral composition and particularly their mutual proportions. An estimate of grain density of these samples may be obtained by calculation from the bulk density and porosity measurements[1] and when this value is plotted against the per cent of quartz (Figure 7) no systematic relationship appears. Apparently then effective grain density, i.e. grain density calculated from effective porosity and bulk density, is not entirely dependent on mineral composition. No obvious association between either per cent matrix or per cent quartz can be deduced from the graph. This suggests that it is necessary to take into account the other variables, size, shape orientation and packing if a satisfactory relationship between rock behavior and petrographic properties as measured in thin section is to be established.

Discussion

In most cases where reservoir behavior has been investigated on the basis of laboratory analysis of cores of reservoir rock the variations in the petrographic properties of the rock have been encompassed by introducting a constant into the equation relating reservoir behavior and the properties measured. Generally the laboratory determinations show discrepancies of various kinds when compared with actual field performance. It seems clear from the present investigation that these discrepancies may be due in no small part to the fact that the constant introduced into the engineering equations is expected to account for too great a magnitude variation in too many variables. Mention has been made before of the peculiar interdependence and interactions characteristic of the variations in petrographic properties of rocks and their behavior characteristics (Griffiths 1952a,b). The investigations here described confirm the theoretical analysis already deduced and it seems likely that when enough information has been compiled i.e. enough samples analyzed, the discrepancies between laboratory analysis of rock behavior and the field performance of oil reservoirs may be materially reduced. At least the feasibility of inventing a "constant" to cover the interdependent variation of the petrographic properties of sediments may be evaluated from studies such as these. If all the properties so far analyzed were completely dependent then a constant would perhaps be sufficient to account for the limited variation likely to be encountered but as the above investigation has emphasized the relationships are not dependent, neither are they independent and the only mode of approach which we can use in this case is statistical analysis and an experimental design which will embrace all the variables of importance in one and the same experiment - and without attempting to oversimplify the conditions by holding some of the properties constant and allowing one or two to vary at a time.

It seems likely that the solution to problems of this kind lie in the use of the statistical technique called multiple regression which is specifically designed to take into account variables which show interdependent relationships. The above petrographic analysis has illustrated the kind of variation to be expected and by adding to our information by the analysis of more samples it may be possible to elucidate the conditions which decide whether a rock is likely to behave as a favorable reservoir rock or not.

One other problem which can be partially evaluated from the present analysis concerns sampling; ultimately the number of samples analyzed is a function of the degree of variability and by arranging the experiment to encompass multistage sampling, as in the case of bulk density and porosity determination, the stage at which the major proportion of variation is to be expected can be specified. Thus in the bulk density experiments the replicate runs on the same subsample contribute negligible variation to the determination and it would be more informative to increase the number of subsamples anddecrease the runs.

1. Through the relationship, Grain density = Bulk density/(1 - porosity).

Most of the other experimental analyses were arranged to evaluate similar sampling stages in thin section, size, axial ratio, orientation and packing techniques. By this means we can decide how many outcrops, how many samples and how many subsamples must be used to achieve a certain degree of precision.

It appears from this petrographic investigation that achievement of the objectives described in the introduction is possible and practicable and the variation discovered is of the type best evaluated by statistical analysis and, specifically, by the use of multiple regression techniques.

References

Chayes, F. (1949), A simple point counter for thin section analysis; Am. Mineralogist, 34, 1-11.

Curray, J. R. (1951), An analysis of sphericity and roundness of quartz grains, Unpublished M. S. Thesis Division of Mineralogy, The Pennsylvania State College.

Fisher, R. A. (1948), Statistical methods for research workers, 10th Edn., Oliver and Boyd, Edinburgh, Scotland.

Gaither, A. (1953), A study of porosity and grain relationships in experimental sands, Jour. Sed. Petro., 23, 3, 180-195.

Griffiths, J. C. (1949), Directional permeability and dimensional orientation in Bradford Sand, The Pennsylvania State College, Mineral Industries Experiment Station, Bull. 56, 202-236.

Griffiths, J. C. (1952a), Grain-size distribution and reservoir rock characteristics, Amer. Assoc. Petro. Geol. Bull. Vol. 36, 2, 205-229.

Griffiths, J. C. (1952b), Measurement of the properties of sediments, Abstr. Bull. Geol. Soc. Amer., 63, 12, pl. 2, 1256.

Griffiths, J. C. (1952c), A review of dimensional orientation of quartz grains in sediments, The Pennsylvania State College, Mineral Industries Experiment Station, Bull. 60, 47-55.

Griffiths, J. C. and Rosenfeld, M. A. (1950), Progress in measurement of grain orientation in Bradford Sand, The Pennsylvania State College, Mineral Industries Experiment Station, Bull. 56, 202-236.

Griffiths, J. C. and Rosenfeld, M. A. (1953), A further test of dimensional orientation of quartz grains in Bradford Sand, Amer. Jour. Sci., 251, 192-214.

Krumbein, W. C. (1938), Size frequency distribution of sediments and the normal phi curve, Jour. Sed. Petrol. Vol. 8, No. 3, 84-90.

Krynine, P. D. (1948), The megascopic study and field classification of sedimentary rocks, Jour. Geol., 56, 2, 130-165.

Shearin, H. M., Jr., Masson, P. H., Williams, M. (1952), Resistivity of Brine-saturated sands in relation to pore geometry, Bull. Amer. Assoc. Petrol. Geol., 36, 2, 253-277.

Taylor, J. M. (1950), Pore-space reduction in sandstones, Bull. Amer. Assoc. Petrol. Geol., 34, 4, 701-716.

TABLE 1

Mineral Composition of 16 Samples of "Pocono" Sediments Estimated by Point Count in Thin Section

Sample No.	Quartz	Rock Fragments Quartzite and Chert	Shales Schists	Matrix	Feldspar	Micas	Carbonate	Misc.
	%	%	%	%	%	%	%	%
6225	77.6	1.0	7.6	13.4	—	4	—	—
6227	79.1	2.4	5.8	12.2	0.1	—	—	—
6229	53.8	5.8	2.0	35.2	1.0	2.2	—	—
6269	52.0	3.6	3.0	37.8	0.2	3.6	—	—
6272	59.5	8.3	0.7	29.5	0.8	1.0	—	0.2
6275	56.8	10.0	2.4	37.4	0.6	2.6	0.2	—
6283	62.8	5.9	1.7	25.6	0.7	3.3	—	—
6285	63.0	5.4	6.8	23.8	0.2	0.8	—	—
6220	66.0	0.5	19.1	3.5	1.2	—	—	9.8*
6323	46.0	1.0	0.4	47.8	—	4.8	—	—
6834	64.4	4.3	4.8	23.7	0.4	1.4	—	—
6837	83.2	2.6	4.0	9.8	0.2	0.2	—	—
6845	17.25	0.1	23.8	53.6	—	0.1	5.25	—
6846	46.8	—	2.6	—	0.8	0.2	49.4	0.2
6851	56.6	2.8	5.6	33.0	0.6	1.2	—	0.2
6857	57.4	4.4	3.2	32.4	1.2	1.0	—	—

Sample numbers refer to the catalogue in Division of Mineralogy, The Pennsylvania State College.

* Pores.

TABLE 2

Size and Shape of Quartz Grains in "Pocono" Sediments

Sample No.	Grain Size		Axial Ratio (Shape)	
	$\bar{X}$ phi units	s	$\bar{X}$ dimensionless	s
6225	1.62	0.98	0.671	0.151
6227	1.44	0.43	0.687	0.159
6229	3.30	0.41	0.626	0.183
6269	3.10	0.58	0.604	0.162
6272	3.99	0.45	0.618	0.176
6275	3.55	0.51	0.685	0.195
6283	3.36	0.45	0.616	0.180
6285	2.79	0.44	0.636	0.178
6320	0.76	1.60	0.680	0.152
6323	3.75	0.79	0.629	0.174
6235	2.86	1.07	0.635	0.199
6837	1.76	0.31	0.721	0.152
6845	0.82	3.14	0.668	0.159
6846-1	2.64	0.91	0.651	0.192
6851	3.28	0.46	0.637	0.142
6857	3.68	0.22	0.681	0.156
All Samples	2.67	1.36	0.657	0.170

$\bar{X}$ = averages; s = standard deviation

TABLE 3

Comparison of Axial Ratio of Quartz Grains From Bradford Sand and "Pocono" Sediments

	$\bar{X}$	s
"Pocono" (16 samples)	0.657	0.170
Range	0.604 - 0.721	0.142 - 0.199
Bradford Sand		
Sample 5820[1]	0.6505	0.150
Range (5 thin sections)	0.630 - 0.6565	0.142 - 0.164
P4-(1) Range (4 thin sections)[2]	0.655 - 0.682	0.148 - 0.150
PNY 22-2 (1 thin section)[2]	0.650	0.147

1. Griffiths and Rosenfeld, 1950
2. Griffiths and Rosenfeld, 1953

TABLE 4

Dimensional Orientation of Quartz Grains in 16 Samples of "Pocono" Sediments

Sample	N	s^2	s	P	Megascopic Structure
6225	100	992.73	31.51	0.01	Doubtful Lineation
6227	100	2595.60	50.95	0.05	Doubtful Lineation
6229	100	1011.25	31.80	0.01	Bedded
6269	100	935.67	30.59	0.01	Bedded
6272	100	1651.21	40.64	0.01	Doubtful Lineation
6275	100	510.58	22.60	0.01	Bedded
6283	100	1310.07	36.19	0.01	Doubtful Lineation
6285	100	1517.34	38.95	0.01	Doubtful Lineation
6320	100	1852.81	43.04	0.05 70.01	Doubtful Lineation
6323	100	429.31	20.72	0.01	Cross Bedded
6834	100	1077.53	31.76	0.01	Massive
6837	100	2055.96	45.34	70.05	Doubtful Lineation
6845	100	1538.91	39.23	0.01	Coarse Poor Bedding
6846-1	100	702.54	26.51	0.01	Bedded
6851	100	626.36	25.03	0.01	Bedded
6857	100	2417.68	49.17	0.05	Massive

TABLE 5

Analysis of Variance of Bulk Density Determinations of 16 "Pocono" Sediments

Source of Variation	Degrees of Freedom	Sum of Squares	Mean Square	F
Samples	15	3,048,308.7	203,220.58	155.73***
Subsamples	32	41,759.8	1,304.99	26.04***
Runs	96	4,811.5	50.12	
Total	143	3,094,880		

*** Significant at the 0.1 per cent level.

TABLE 6

Analysis of Variance of Porosity Determinations on 16 Samples of "Pocono" Sediments

Source of Variation	Degrees of Freedom	Sum of Squares	Mean Square	F
Samples	15	5,824,832.44	388,322.16	592.7***
Replicates	48	31,446.50	655.14	
Total	63	5,856,278.94		

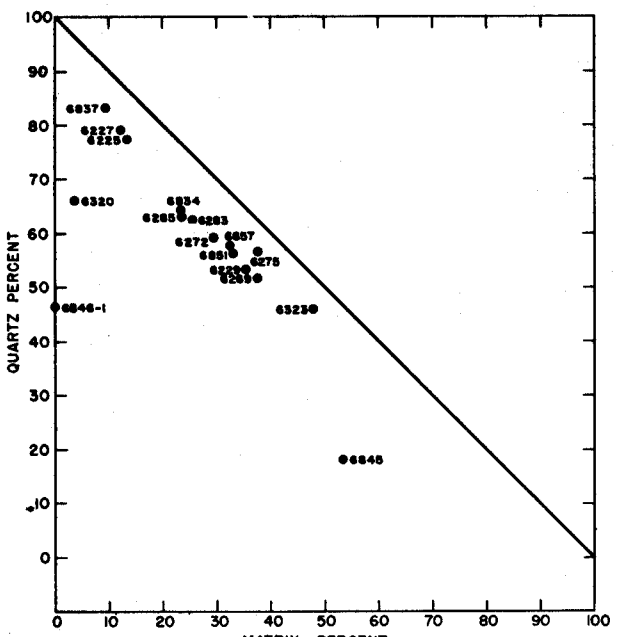

Figure 1. VARIATION IN PROPORTION OF QUARTZ AND MATRIX IN THIN SECTION

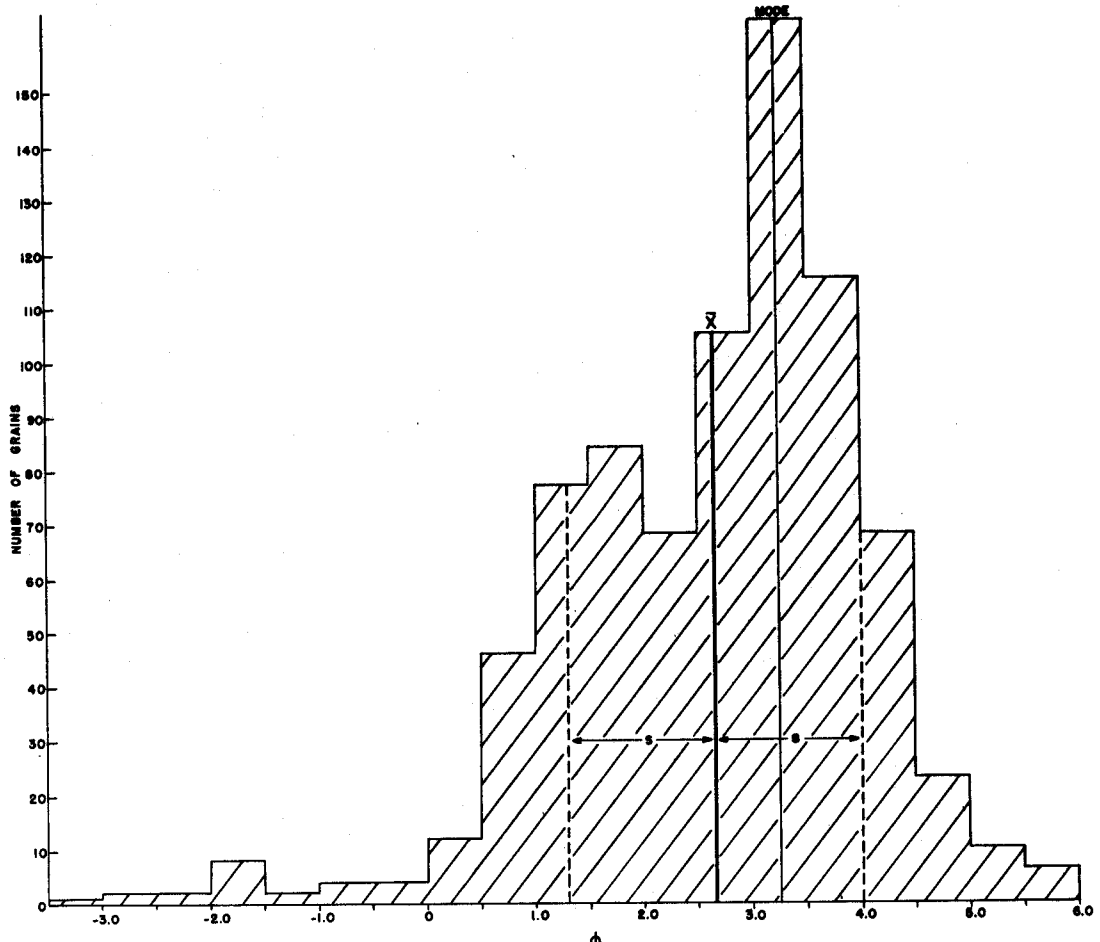

Figure 2. SIZE DISTRIBUTION OF QUARTZ GRAINS IN 16 "POCONO SEDIMENTS" AS MEASURED IN THIN SECTION

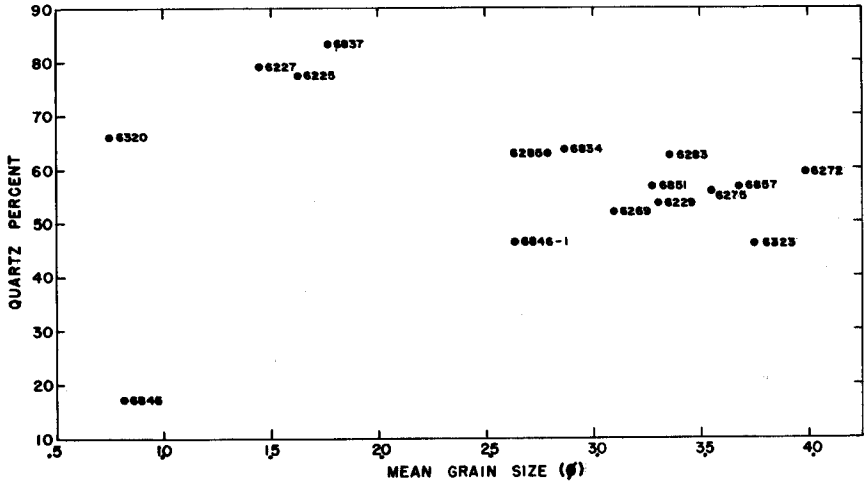

Figure 3. MEAN GRAIN SIZE VERSUS QUARTZ PERCENT

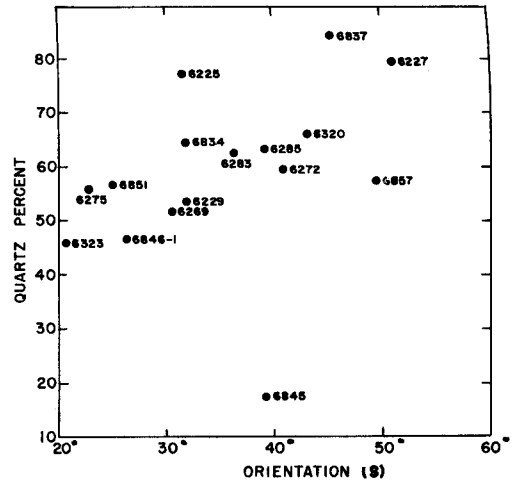

Figure 4. QUARTZ PERCENT VERSUS ORIENTATION

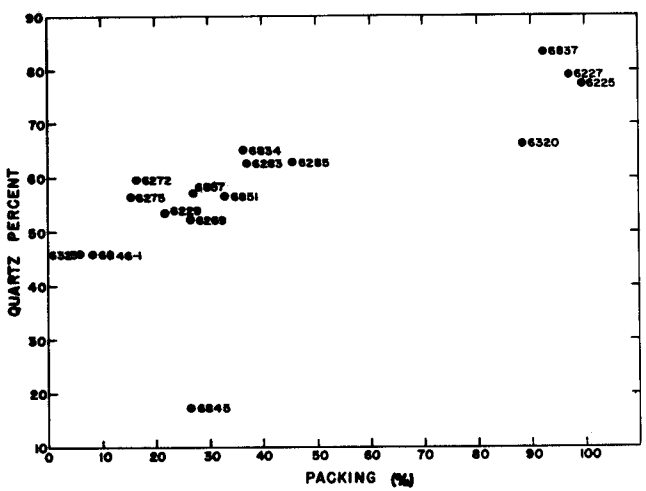

Figure 5. QUARTZ PERCENT VERSUS PACKING

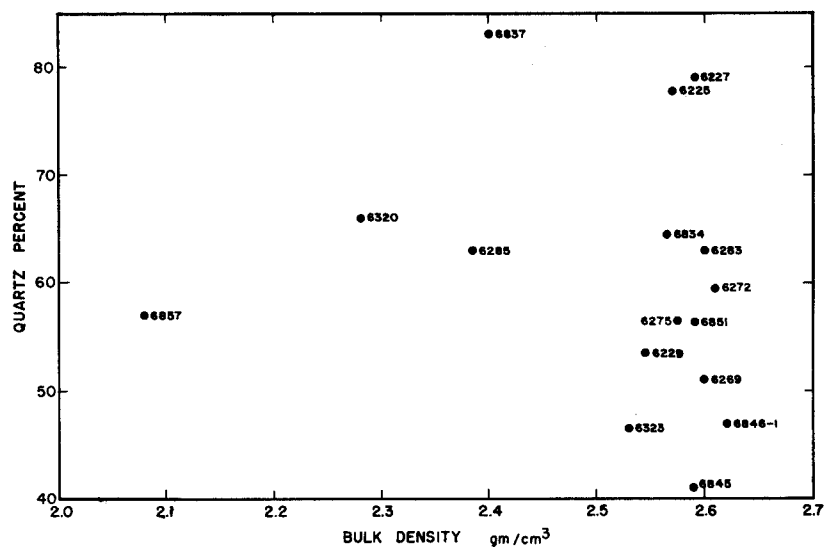

Figure 6. MEAN QUARTZ PERCENT VERSUS BULK DENSITY

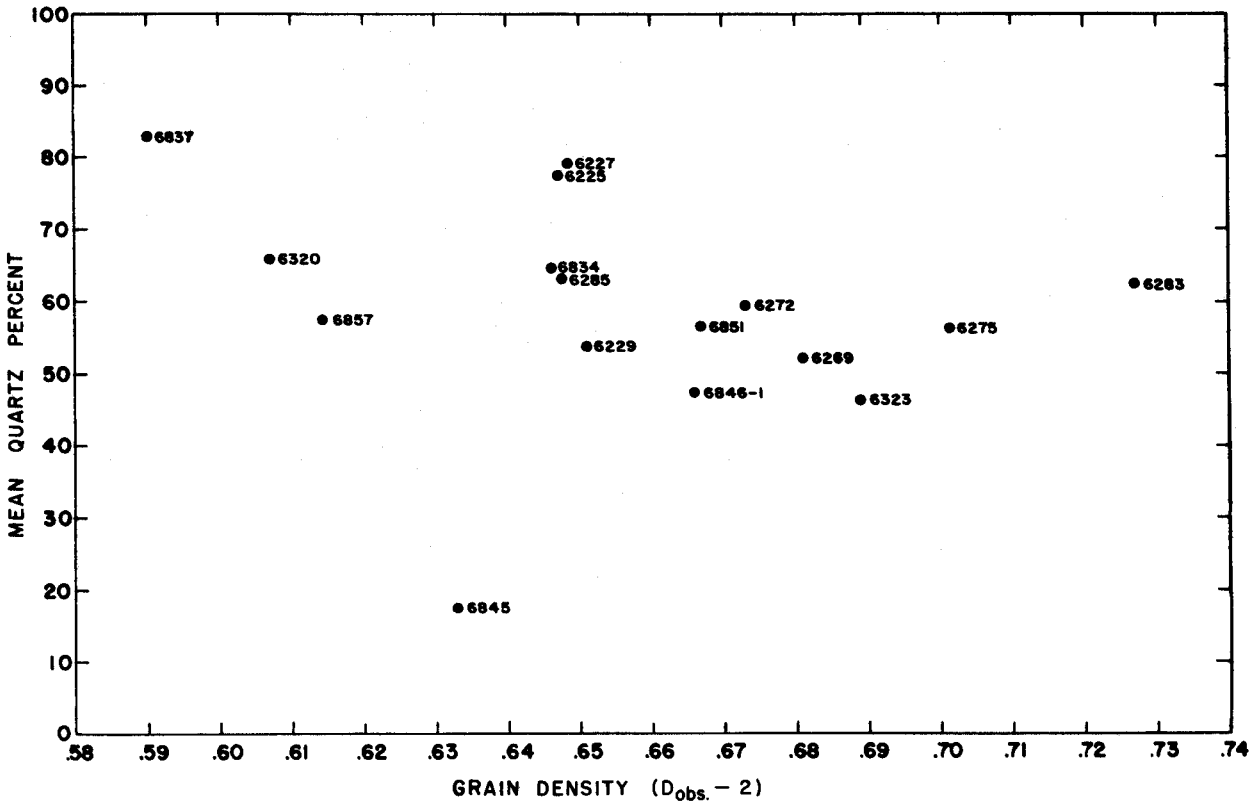

Figure 7. MEAN QUARTZ PERCENT VERSUS GRAIN DENSITY

FURTHER STUDIES ON HEAT TRANSFER IN UNCONSOLIDATED SANDS DURING WATER INJECTION

Floyd W. Preston* and Richard D. Hazen**

Introduction

In any petroleum field practice in which fluids are injected into a reservoir, the possibility exists that the reservoir temperature would be altered. These temperature changes are important in that they affect oil production and yield useful information regarding reservoir operation. The change in the geothermal gradient near a well caused by fluid injection into the formation is now the basis for a method of determining fluid movement profiles within the well.[11]. More recently, a method of oil recovery has been described which is based upon heat transfer processes.[12] The combustion of crude oil and the heating of the reservoir during this process are both dependent upon heat transfer within the reservoir. Studies have also been made of the influence of injected water upon the reservoir temperature. This problem is significant where wax is precipitated from oil by lowering the oil temperature below the initial reservoir temperature.[13].

In all of the above problems, emphasis has so far been on qualitative interpretations. Little information is available concerning procedures for predicting temperature changes within a reservoir. This lack of quantitative relations is in large part a reflection of the complex nature of fluid flow and displacement processes within a reservoir. In addition, very little work on heat transfer has been done in any system at the very low Reynolds numbers characteristic of fluid flow in reservoirs.

This exploratory investigation on heat transfer in porous media has been limited to a study of simplified systems. The primary objective has been to determine and correlate significant variables so that heat transfer within the simplified system is predictable. Whether reservoir heat transfer is predictable from these data depends, at least for the present, upon whether field conditions may be assumed equivalent to conditions used in this investigation, or could be extrapolated from the laboratory conditions.

Theory of Heat Transfer in Porous Media

Heat transfer theory as applied to the present problem has as its objective prediction of sand and water temperature as a function of time and distance during heating and cooling of the porous medium.

Before describing the temperature history of a porous medium mathematically, consider the heating process qualitatively. An insulated linear porous sand bed is saturated completely with cold water at temperature T_o. The bed is at thermal equilibrium so that the sand is also at temperature T_o. Let hot water be injected at a constant rate and constant temperature, T_i such that T_i is greater than T_o. As water is injected, it loses heat to the sand. The temperature of any given volume increment of water continually decreases as it moves through the bed. At all times and all positions the water temperature will be above that of the sand. Also at any particular time, the sand and water at the inlet are hotter than at the exit. With continued injection of hot water, the entire sand bed tends to attain the temperature of the inlet stream. The above qualitative picture may be visualized by reference to Figure 3. Here the temperature versus length along a sand bed is shown for a particular time after the beginning of hot water injection. This temperature gradient or temperature profile existing within the bed may be considered as a heat "wave" or "front".

Equations describing the movement of a heat wave in a porous medium have been proposed by several writers. The first work was done by Anzelius[1] and by Nusselt[2]. Differential equations describing the operation were presented but solutions were not general, being applied only to particular problems of interest to them. The first complete analytical solution was presented by Schumann[3]. He derived equations describing the movement of the temperature "wave" through a linear porous medium. The assumptions which he made were:

1. Temperature of injected fluid is constant.

2. Flow rate is constant.

Contribution No. 53-14, School of Mineral Industries, The Pennsylvania State College.

*Division of Petroleum and Natural Gas Engineering, The Pennsylvania State College.

**Graduate Student, Division of Petroleum and Natural Gas Engineering, The Pennsylvania State College.

3. The porous medium is initially at a uniform temperature.

4. The physical constants (i.e. density, specific heat, and thermal conductivity are constant within the temperature range employed.)

5. The rate of heat transfer between solid and fluid at any point is proportional to the average temperature difference between solid and fluid at that point.

6. No temperature gradient exists within a particle.

7. No heat is transferred from one point to another within either phase by conduction. This implies that heat is transferred only between solid and fluid.

8. The heat transfer coefficient is independent of temperature.

These assumptions were used together with a heat balance equation to determine the temperature of the porous medium and the fluid at any point within the medium as a function of time. Schumann's derivation [3] of the basic differential equation describing the process is presented by Greenstein and Preston[4]. The solution corresponding to the boundary conditions implied by the above assumptions is: (Nomenclature at end of paper)

$$\frac{T_s - T_o}{T_i - T_o} = e^{-Y-Z} \sum_{n=1}^{n=\infty} Z^n M_n(YZ) \qquad (1)$$

$$\frac{T_w - T_o}{T_i - T_o} = e^{-Y-Z} \sum_{n=0}^{n=\infty} Z^n M_n(YZ) \qquad (2)$$

Where:

$$Y = \frac{ha}{C_{pw}\varphi} \frac{x}{v} \qquad (3)$$

$$Z = \frac{ha}{C_{ps}(1-\varphi)} \left(\theta - \frac{x}{v}\right) \qquad (4)$$

$$M_n(YZ) = \frac{d^n[M_o YZ]}{d(YZ)^n} \qquad (5)$$

$$M_o(YZ) = J_o(2i\sqrt{YZ}) = 1 + YZ + \frac{(YZ)^2}{(2!)^2} + \frac{(YZ)^3}{(3!)^2} + \cdots\cdots \qquad (6)$$

The function $M_o(YZ)$ is the Bessel function of the first kind and zeroth order, $J_o(2i\sqrt{YZ})$, values for which may be found for known values of the product YZ.

The function $\frac{d^n[M_o(YZ)]}{d(YZ)^n}$

is the n-th derivative of $M_o(YZ)$ taken with respect to YZ. The terms in Equations (1) through (6) are dimensionless grouping of the variables which influence the solid and fluid temperatures. A numerical solution of Equations (1) and (2) is usually made under the circumstances that Y and Z are known. Even for this situation, the solution is laborious because it involves the summation of the terms $M_n(YZ)$ each of which is itself an infinite series defined by Equation (5). Evaluation of the series at high values of YZ is particularly onerous because of the slow convergence of the series.

Klinkenberg[5] has proposed an alternate and much more easily used solution to Schumann's differential equation. With his equation, a numerical solution is readily available without the need of evaluating infinite series. His equations are:

$$\frac{T_w - T_o}{T_i - T_o} = \frac{1}{2}\left[1 + \frac{2}{\sqrt{\pi}} \int_0^{\left(\sqrt{Z} - \sqrt{Y} + \frac{1}{4\sqrt{Z}}\right)} e^{-u^2} du\right] \qquad (7)$$

$$\frac{T_s - T_o}{T_i - T_o} = \frac{1}{2}\left[1 + \frac{2}{\sqrt{\pi}} \int_0^{\left(\sqrt{Z} - \sqrt{Y} - \frac{1}{4\sqrt{Z}}\right)} e^{-u^2} du\right] \qquad (8)$$

The integral, $\frac{2}{\sqrt{\pi}} \int_0^{\left(\sqrt{Z}-\sqrt{Y} \pm \frac{1}{4\sqrt{Z}}\right)} e^{-u^2} du$

also known as the error function, can be evaluated for known values of the upper limit by a set of mathematical tables such as Pierce[10]. Likewise, if the temperatures are known, then the value of the upper limit may be determined such that Equations (7) and (8) are satisfied.

Equations (1) and (2) or (7) and (8) could be immediately used to calculate the amount of heating which a reservoir undergoes upon injection of heated water using average data for specific heats of reservoir rocks and fluids, if it were not for the lack of numerical data for values of h and a in Equations (3) and (4). In dealing with heat transfer in porous media, the general procedure is to combine h and a into a single coefficient, ha. This alleviates the necessity of separately evaluating h and a for each porous medium. This approach is particularly useful because we do not know what fraction of the total internal surface area contributes to heat transfer. Previous to the study which was initiated by Greenstein[4], no values were available for this product ha. The experimental work of this project is directed to determining this product, ha. To eliminate confusion, the product, ha, will be hereinafter referred to as the heat transfer coefficient.

Experimental Procedure

The experiments consisted of forcing hot water vertically downward at a constant rate and constant temperature through an insulated sand-packed tube initially saturated with cold water at a constant temperature. The temperature of the exit stream was measured as a function of water throughput. A flow diagram of the apparatus is shown in Figure 1. A cross section of the flow column is presented in Figure 2. The variables which were investigated were flow rate, column length, and sand size. The range of experimental conditions investigated are listed in TABLE I.

TABLE I

Flow Rate	2 to 25 ft/hr
Sand size	20 to 170 U.S.mesh
Column Length	6.03", 11,7", 24.0"
Column Diameter	3.0"
Water Inlet Temperature	120° to 180°F
Column Initial Temperature	Approximately 80°F

The apparatus was designed to fulfill as nearly as possible the following requirements.

1. Negligible heat loss from the sand.
2. Negligible heat content of the sand retainer tube.
3. Flow of water per unit area should be the same at all points across the face of the sand.
4. Flow rate and temperature of injected water should be constant with time.
5. Continous measurement of temperature of the exit stream.

To insure a minimum heat loss, the column was insulated with granulated cork. This material was chosen because of its low thermal conductivity, low density (and therefore low heat capacity) and its ease of handling. A low heat capacity for the sand retainer was achieved by using .005 inch brass sheet formed into a tube 3 inches in diameter. Ends for the column were formed from sheets of 0.021" soft copper. The tube heat capacity was less than 4 percent of the total heat capacity of the sand saturated with water. The choice of a sand retainer tube with negligible heat capacity was made as the best alternative to finding a tube material that is a non-conductor of heat.

A constant flow rate was maintained by manually controlling the air pressure to the water reservoir. Flow rate was indicated by a rotameter. During a run the air pressure was slowly decreased to maintain a constant flow as the column was heated. A constant flow rate per unit cross sectional area was obtained by use of small headers consisting of a monel 8-mesh screens at the tube exit and a 1/8" free space at the tube entrance. A 200 mesh sand retaining screen was placed next to the sand at each end of the column. Water entered the header through three 1/4 inch tubes placed circumferentially on the tube 90° apart. A single, centrally located 1/4 inch tube was the exit from the lower end of the sand column.

Temperatures of the exit and inlet streams were determined by 30 gauge iron-constantan thermocouples placed in the streams with approximetely two inch immersion and with the bead within 1/16 inch of the ends of the sand retainer screen. Very small thermocouple beads were formed by shorting the wire ends

with an electrical current while they were submerged in oil. Calibration of the thermocouples with a precision potentiometer indicated that they were accurate to within 1°F without calibration. Temperatures were recorded automatically with a Brown Electronic Strip Chart Potentiometer.

The porous media were angular, unconsolidated quartz sands from 20 to 170 mesh, U.S. Sieve Series. These sands were boiled in hydrochloric acid, washed with distilled water, and dried at 140°C. The sand was packed into the column with a pneumatic jolter, operating at approximately 30 cycles per minute. Sand was allowed to fall through a constant depth of water and the sand level rose at about 1" per minute. The properties of the sands used are listed in TABLE II. Permeabilities were determined with water. At the start of a run the top header and flow lines to the column were flushed out with hot water for about 1 minute to bring them to constant temperature. This flushing water did not enter the sand but instead was removed through an outlet at the top of the column. At the moment when hot water was switched from the flushing operation to displacing of the cold water in the column, the chart of the temperature recorder was started. A run was concluded when the exit stream was approximately 5 degrees below the inlet temperature.

Determination of Heat Transfer Coefficients From Experimental Data

By the use of Equations (2) or (7) a numerical value of the heat transfer coefficient, ha, can be assigned to each particular run for which temperature of the exit stream is known as a function of the volume of water injected. Because of the complex nature of these equations the value of, ha, cannot be determined algebraically. Perhaps the simplest procedure for computing, ha, is the one first suggested by Furnas[7]. He employed the concept of accomplished temperature fraction used by Schumann[3].

$$\text{accomplished temperature fraction, (for water)} \quad T_{rw} = \frac{T_w - T_o}{T_i - T_o}$$

$$\text{accomplished temperature fraction, (for sand)} \quad T_{rs} = \frac{T_s - T_o}{T_i - T_o}$$

Either T_{rw} or T_{rs} occurs on the left side of Equations (1), (2), (7) and (8). Accomplished temperature fraction for either sand or water represents the change in temperature of the particular phase compared to its maximum possible temperature change. This definition shows why the physical limits of the temperature fraction are 0 and 1. Furnas'[3] method to compute the heat transfer coefficient using this temperature fraction is as follows:

1. Construct a plot of accomplished temperature fraction versus Z with Y as a parameter. This is done using Equation (2) or (7) and assuming numerical values of Z and Y. The calculated results are plotted on semi-log paper with Z on the log scale and accomplished temperature fraction on the cartesian scale.

2. Using exactly the same size and type of semi-log coordinates on tracing paper, plot the experimental data as $(\theta - x/v)$ versus accomplished temperature fraction, the time function being plotted on the log scale.

3. Slide the experimental curve over the family of curves prepared in (1) above, keeping the accomplished temperature fraction scales in coincidence. Determine which member in the family of curves matches the experimental curve.

4. The value of, ha, is determined using Equation (3) and the value of Y corresponding to the curve which matched the experimental curve.

This method is possible because multiplication of Z by a constant does not alter the shape of the Z versus temperature fraction curve so long as Y is held constant. Furnas[7], Saunders and Ford[6] and Lof and Hawley[8] plotted time, θ, versus temperature fraction. They used this procedure because in their work x/v was small compared to θ. The term x/v is the time required to pass a single pore volume of fluid through the porous medium. In heating porous media with gas, many pore volumes are required, whereas in the present experiments with water, seldom were more than four pore volumes needed. Thus omission of x/v is permissible only when working with gases. In gaseous heat transfer it is also frequently possible to assume that the quantity of heat in a single pore volume of gas is small compared to the quanitity of heat which the solid can hold. This assumption permits a simplification in the differential equation describing the heating process so that a graphical solution is possible. This method is described in detail by Ledoux[9].

For data in this study it was found convenient to rewrite Equation 4 as:

$$\angle = \frac{ha}{C_{ps}(1-\Phi)} \frac{x}{v}\left[\theta\frac{v}{x} - 1\right] \qquad (9)$$

and to plot temperature fraction versus $(\theta v/x - 1)$. The term $\theta v/x$ represents the number of pore volumes of fluid which has passed through the sand tube. A typical curve is shown in Figure 4. The data for this curve are given in TABLE III. The family of curves of Z versus temperature fraction are shown in Figures 5 and 6, the data for which are given in TABLE IV. Using Figure 5, the value of Y, for the data of Figure 4 was found to be 10 and, ha was calculated as 1,160 Btu/hr°F ft^3 at a velocity of 5.54 ft/hr.

A limitation to use of the curve matching method is that for values of Y above 100, difficulty is encountered in determining which curve matches the experimental data most closely. Fortunately, few runs had a Y greater than 100. However, a mathematical method was devised to solve for large values of Y. It was observed that at large values of Y, the curve of Z versus accomplished temperature fraction was a straight line when plotted on logarithmic-probability paper. Typical curves are shown in Figure 7. Each curve corresponding to a given Y can be uniquely described by a number which we shall call the temperature variation.

$$\text{Temperature Variation} = V_t = \frac{Z_{.80} - Z_{.20}}{Z_{.50}} \qquad (10)$$

Here the subscripts on Z refer to the value of Z at the particular value of accomplished temperature fraction. All parallel lines on the graph have the same Temperature Variation. Because the Z scale is logarithmic, Z or any value proportional to it can be plotted. Thus V_t will be the same whether temperature fraction is plotted versus Z or versus $(\theta - x/v)$. As a consequence of this, Temperature Variation can be defined also as:

$$V_t = \frac{(\theta - \frac{x}{v})_{.80} - (\theta - \frac{x}{v})_{.20}}{(\theta - \frac{x}{v})_{.50}} \qquad (11)$$

Equation (11) is used to compute V_t for an experimental run. The value of Y for a given Temperature Variation is a unique function of Y and is a straight line on log-log paper. The relation is

$$Y = 5.87\, V_t^{-1.98} \qquad (12)$$

Equation (12) was obtained using data of TABLE IV in the range Y = 80 to Y = 200 and is plotted in Figure 14. The error introduced in computing Y by use of this equation rather than by use of the curve matching method to obtain Y is shown in TABLE V.

The greatest usefulness of Equation (12) is in the compution of temperature versus volume throughput for a column in which Y and Z are known. Only a single point need be computed by Equation (7). This point can be put on a logarithmic-probability graph of Z versus accomplished temperature fraction. A line is then drawn through the point such that V_t has the value calculated from Equation (12) for the known value of Y.

Equation (10) is not the only possible definition of Temperature Variation. Limits other than .20 and .80 could be used for accomplished temperature fraction. However, each new set of temperature limits results in a new set of constants for Equation (12). The larger the temperature fraction spread, the higher is the minimum value of Y which can be used.

To show the accuracy of the curve matching method in determining the heat transfer coefficient, experimental data for two runs were compared with curves calculated from the experimentally determined coefficient. The curve matching method makes difficult the interpolation of Y values in Figures 5 and 6. An experimental curve whose true Y value is 17 might be matched with either the curve corresponding to a Y of 16 or 18 since no curve for a Y of 17 was drawn. For Run No. 66, shown in Figure 12 a Y value of 16 was determined by the curve matching procedure. As seen from this figure the experimental curve is bracketed by the curves for the determined Y value (i.e. Y = 16) and the next higher Y curve given in Figure 5 (i.e. Y = 18). The same situation exists in Figure 13. By the curve matching method a Y value of 8 was determined and Figure 5 gives the next higher value to be Y = 9. The experimental data are again bracketed by these two curves.

Correlation of Heat Transfer Coefficients

Heat transfer coefficients for 60 runs were determined by the curve comparison method previously described. A list of all coefficients is given in TABLE VI. Plots of coefficients versus velocity are shown in Figures 8, 9, 10, 11 and 15. For all runs, the heat transfer coefficient has been expressed as Btu of heat transferred per hour, degree Fahrenheit temperature difference between fluid and solid

per cubic foot of sand bulk volume.

The coefficient of heat transfer is very sensitive to flow velocity. This is observed in Figures 7, 8, 9, and 10. The results of all runs are plotted in Figure 15. A single trend is evident. The curve may be represented by the equation

$$h_a = 54.5\ v^{1.82} \qquad (13)$$

The extreme sensitivity of the coefficient to flow velocity is shown by the velocity exponent, 1.82. The similar exponent for gaseous heat transfer is approximately 0.7 as reported by Lof and Hawley[8] and by Furnas[7]. Their gas flow was definitely in the turbulent regime. Experiments of Furnas covered a Reynold's Number range from 3000 to 30,000. Lof and Hawley determined their coefficients in the Reynolds Number range 5 to 2800. The present experiments had Reynold's Numbers from .02 to 100. The transition from viscous to turbulent flow in porous media occurs near $R_e = 1$. It is felt that the difference in velocity sensitivity of the heat transfer coefficient in gaseous and liquid systems may be a reflection of the difference in heat transfer mechanism rather than a difference in Reynolds Number.

As can be seen from Figures 8 and 9 all sand sizes give the same relation between heat transfer coefficient and flow rate. This implies that within the range of permeabilities studied, the heat transfer coefficient is independent of permeability.

From Figures 10 and 11 it is evident that length of the porous medium has no influence on the heat transfer coefficient. Columns of three different lengths gave the same velocity versus heat transfer coefficient curve. This result signifies that the influence of length on the time versus temperature curve is adequately accounted for by the existing theory. It is felt that the dependence of the coefficient upon length obtained in the earlier paper of Greenstein and Preston[4] was due to heat losses occuring during the runs.

Example Problems

To show how the coefficients obtained in the laboratory can be applied directly to field problems, two sample calculations are presented. The first problem involves determination of the temperature of water produced from a formation into which heated water is being injected. The second problem is to determine for the above problem the temperature throughout the reservoir after injection of water for a certain time. In making these calculations it is of course assumed that the reservoir will behave as did the sand columns of the present experiments.

1. Exit Temperature Versus Time and Pore Volumes of Water Produced.

Determine the temperature of water coming from a linear reservoir with producing and inlet faces 100 feet apart under the following conditions:

Flood front advance	=	1 ft/hr
Sand Porosity*	=	25%
Specific heat for sand* (for silica)	=	.19 Btu/lb.°F = 31.5 Btu/ft³,°F
Specific heat for water	=	1.00 Btu/lb,°F = 62.4 Btu/ft³,°F
Inlet water temperature	=	200°F
Initial reservoir temperature	=	60°F

By use of Equation (13), the heat transfer coefficient, ha, is computed to be 54.5 Btu/hr, ft³,°F. The calculation could be made at a more realistic water advance rate (i.e. 0.1 to 1.0 ft/day) if it is felt that extrapolation of Equation (13) is justified. Knowing, ha, and all the physical properties of the system, compute Y from Equation (3).

$$Y = \frac{h_a}{C_{pw}\,\phi}\left(\frac{x}{v}\right) = \left(\frac{54.5\ \text{Btu}}{\text{hr,ft}^3,{}^\circ\text{F}}\right)\left(\frac{{}^\circ\text{F,ft}^3}{62.4\ \text{Btu}}\right)\left(\frac{1}{.25}\right)\left(\frac{100\ \text{ft}}{1\ \text{ft/hr}}\right) = 359$$

*If residual oil is present, these values may be adjusted to express effective porosity to water and total specific heat of the immobile phases on a volumetric bases. However, at present we do not know the influence of residual oil on the heat transfer coefficient.

Several solutions for this problem are now possible:

a. Choose values for θ, evaluate Z from Equation (4) and using the values of Z and Y in Equation (2), determine T_w. This method is the most precise but is very laborious.

b. Choose θ and proceed as in (2) above but use Equations (7) rather than Equation (2). This procedure is fairly rapid and is sufficiently precise for most engineering work.

c. Use a simplified graphical procedure based on three observations. First, as pointed out by Ledoux[9], for large values of Y, the terms Y and Z are equal at an accomplished temperature fraction of 0.50. Second, for large values of Y, the accomplished temperature fraction Z is a straight line on log-probability paper. Third, the "temperature variation" as defined by Equation (10) is a logarithmic function of Y at large values of Y. This latter relation is expressed by Equation (12). These three observations are combined to allow calculations of time versus temperature.

The method referred to in (c) will be used. From Ledoux's approximation, Y = Z = 349 at an accomplished temperature fraction of 0.50. This point is plotted as shown in Figure 16. From Equation (12) we compute the temperature variation, V_t, to be 0.106.

$$Y = 5.87\ V_t^{-1.98}$$

$$349 = 5.87\ V_t^{-1.98}$$

$$V_t = .106 = \frac{Z_{.80} - Z_{.20}}{Z_{.50}} = \frac{Z_{.80} - Z_{.20}}{349} \qquad (14)$$

By use of a simple trial and error process, find the straight line through the point Z = 349, accomplished temperature fraction = 0.50, which satisfies Equation (14). This curve drawn in Figure 16 gives Z for all values of temperature fraction for conditions under which Y is 349. These values of Z are used in Equations (4) and (9) to get time or pore volumes as a function of temperature fraction and temperature. For this problem, these equations are

$$\frac{Z(1-\phi)}{ha} + \frac{x}{v} = \theta = \frac{Z(.75)(31.5\,Btu)_{hr,ft^3,°F}}{ft^3,°F\,(54.5\,Btu)} + \frac{100\,ft}{1\,ft/hr} \qquad (15)$$

$$\theta = (0.433Z + 100) \quad \text{hours}$$

$$\frac{Z(1-\phi)C_{ps}}{ha}\frac{v}{x} + 1 = \frac{Qv}{x} = \text{Pore volumes of water produced}$$

$$Z(.75)\left(\frac{31.5\,Btu}{ft^3\,°F}\right)\left(\frac{hr,ft^3,°F}{54.5\,Btu}\right)\left(\frac{1\,ft/hr}{100\,ft}\right) + 1 = \text{Pore volumes of water produced.}$$

$$0.00433\,Z + 1 = \text{Pore volumes of water produced} \qquad (16)$$

In TABLE VII, the Z and accomplished temperature fraction values are recorded as taken from Figure 16. Temperature of the produced water, T_w, is computed from the following relation.

$$\text{Accomplished Temperature Fraction} = \frac{T_w - T_o}{T_i - T_o} = \frac{T_w - 60}{200 - 60}$$

Calculations are carried out as indicated in TABLE VII. The results are plotted in Figures 17 and 18.

2. Temperature Distribution Within Reservoir

In the previous problem the temperature of produced water was predicted as a function of time. Let us now calculate the temperature throughout the reservoir of Problem 1, after injecting water for 100 hours.

The problem must be solved somewhat differently from Problem 1 because here Y will have a different value at each position. It would not be practical to construct a curve similar to Figure 16 for each value of Y. We shall use the method based on procedure (b) above. All physical properties and the heat transfer coefficient will be the same as in Problem 1.

Use Equations (3) and (4) to define Y and Z in terms of the known constants of the system and the varible distance x.

$$Y = \frac{hq}{C_{pw}\Phi}\left(\frac{x}{v}\right) = \left(\frac{54.5\,Btu}{hr,ft^3,^\circ F}\right)\left(\frac{ft^3\,^\circ F}{62.4\,Btu}\right)\left(\frac{1}{.25}\right)\left(\frac{x\,ft}{1\,ft/hr}\right) = 3.49\,x \qquad (17)$$

$$Z = \frac{hq}{C_{ps}(1-\Phi)}\left(\theta - \frac{x}{v}\right) = \left(\frac{54.5\,Btu}{hr\,ft^3\,^\circ F}\right)\left(\frac{ft^3\,^\circ F}{35.5\,Btu}\right)\left(\frac{1}{.75}\right)\left(100 - \frac{x\,ft}{1\,ft/hr}\right) = 2.31\,(100-x) \qquad (18)$$

Equation (7) is now written as:

$$\frac{T_w - 60}{200-60} = \frac{1}{2}\left[1 + \frac{2}{\sqrt{\pi}}\int_0^{\sqrt{Z}-\sqrt{Y}+\frac{1}{4\sqrt{Z}}} e^{-u^2}\,du\right] \qquad (19)$$

Now choose values of x and evaluate Y and Z from Equation (17) and (18) respectively. Use these values to compute the value of the upper limit in the integral used in Equation (19). For known values of this upper limit the value of the integral can be obtai ed from mathematical tables[10]. Water temperature, T_w, is then computed from Equation (19). Calculations ior this problem are presented in TABLE VIII and the results are shown in Figure 3.

Conclusions

A study was made of the heating of completely water saturated unconsolidated sands from 20 to 170 mesh (U.S. Sieve), by injection of hot water. The heating rate was characterized by a heat transfer coefficient expressed as Btu of heat transferred between water and solid per unit of bulk volume, time, and temperature difference. This coefficient was found to be independent of sand size and length of sand column but it increased with interstitial fluid velocity raised to the 1.8 power. Sample calculations are shown in which the temperature of water in a reservoir may be computed as a function of time and distance.

Acknowledgments

The authors wish to express their appreciation to the American Petroleum Institute for their sponsorship of this work through a Research Grant-In-Aid. The authors are also grateful to Dr. John C. Calhoun, Jr., for his guidance and constructive criticism of this project. The data for this paper are taken from a thesis presented by Mr. Richard D. Hazen in partial fulfillment of the degree of Master of Science in the Division of Petroleum and Natural Gas Engineering, The Pennsylvania State College. The authors also wish to express their appreciation to Mr. Taher A. R. Hadidi who did the drafting for this paper.

References

1. Anzelius, A., Z. Angew. Math. Mech., 6, 291,(1926).

2. Nusselt, W., Z. Ver. Deut. Ing. 71, 85,(1927).

3. Schumann, T. E. W., J. Franklin Inst., 208, 405,(1929).

4. Greenstein, Robert I., and Preston, Floyd W., Heat Gain by Unconsolidated Sands During Hot Water Injection, Producers Monthly, Vol. 17, No. 4, pp. 16-23, February 1953.

5. Klinkenberg, A., Ind. Eng. Chem. 40, 1992, (1948).

6. Saunders, O. A. and Ford, H. J., J. Iron and Steel Inst. (London) 141, 291,(1940) .

7. Furnas, C.C., U.S. Bureau of Mines Bulletin, No. 361, (1932).

8. Lof, G. O. G. and Hawley, R. W. Ind. Eng. Chem. 40, 1061, (1948).

9. Ledoux, E., Ind. Eng. Chem. 40, 1970, (1948).

10. Peirce, B.O., A Short Table of Integrals Third Revised Edition, Ginn and Company, Boston, 1929, p. 116.

11. Nowak, T. J., The Estimation of Water Injection Profiles From Temperature Surveys, J. Petroleum Technology, Vol. 5, No.8, pp 203-212, August 1953.

12. Kuhn, C. S. and Koch, R. L., In-Situ Combustion-Increasing Oil Recovery, Oil and Gas J., Vol 52, No.14, pp 92-96, August 10, 1953.

13. Calhoun, J. C. and Yuster, S. T., Wax Saturations in Oil Sands, Producers Monthly, Vol. 10, No.1 pp 20-26, November, 1945.

Nomenclature

a = surface area of solid, ft^2/ft^3 of bulk volume.

C_{pw} = specific heat of water Btu/ft^3,°F.

C_{ps} = specific heat of solid Btu/ft^3,°F.

h = heat transfer coefficient Btu/hr.ft.^{2},°F.

T_i = inlet temperature of hot water, °F.

T_o = initial temperature of bed, °F.

T_s = Temperature of solid at any point, °F.

T_w = Temperature of water at any particular point, °F.

v = Linear velocity, ft./hr. based on effective flow area.

x = Distance from inlet end of system, feet.

θ = Time in hours, measured from introduction of first hot water.

φ = Fractional porosity

T_{rs} = Accomplished temperature fraction for solid and equal to $(T_s - T_o)/(T_i - T_o)$.

T_{rw} = Accomplished temperature fraction for liquid and equal to $(T_w - T_o)/(T_i - T_o)$.

w,s, = subscripts referring to water and solid respectively.

i,o, = subscripts referring to inlet stream and initial fluid respectively.

ha = heat transfer coefficient based on a unit of bulk volume, Btu/hr,°F,ft^3.

u = an arbitrary variable used in expression of probability integral.

V_t = temperature variation.

Y = A dimensionless parameter defined by Equation 3.

Z = A dimensionless parameter defined by Equation 4.

TABLE II

PHYSICAL PROPERTIES OF SAND AND SAND COLUMNS

COLUMN PROPERTIES

Length Inches	U.S. Mesh Size	Porosity %	Permeability darcys	Pore volume cc
6.03	50-70	37.4	23.6	258
	100-140	33.8	5.61	233
11.7	20-30	32.4	57.0	430
	50-70	39.3	23.2	521
	100-140	35.5	4.78	470
	Misc.	33.7	2.43	447
24.0	50-70	39.2	35.5	1078

SAND PROPERTIES

Mesh Size	Average Particle Diam*
20-30	.0282 inches
50-70	.0100
100-140	.0050
Misc.	.0045 Approx.

*Arithmetic Average of Screen Openings

ANALYSIS OF MISCELLANEOUS SAND

Mesh	Weight Percent
-70	1.2
70-80	1.1
80-100	32.1
100-140	12.7
140-170	21.8
170-200	3.2
200+	27.9

Specific gravity of sand, 2.65 gm/cm^3
Specific heat of sand, .19 Btu/lb°F

TABLE III

HEATING RUN DATA
RUN NO. 57 20-30 MESH SAND
VELOCITY = 5.54 ft/hr.

Time Units 2/3 min.	Pore Volume Injected	Tw °F	Trw
0	0	81.0	0
1	0	81.0	0
4	0	81.0	0
5	0	81.0	0
6	1.150	81.2	.003
7	1.34	84.0	.046
8	1.53	89.8	.134
9	1.72	98.9	.272
10	1.92	110.0	.441
11	2.11	120.3	.598
12	2.30	129.0	.731
13	2.49	135.8	.834
14	2.68	141.0	.913
15	2.87	144.3	.963
16	3.07	146.8	1.00
17	3.26		

T_i = 146.7 T_o = 81.0 Column: 3.00" Diam. by 11.7" Long.

TABLE IV

ACCOMPLISHED TEMPERATURE FRACTION FOR LIQUID PHASE

AS FUNCTION OF Y AND Z (From Equation 7)

Z Values for Various Temperature Fractions

Y	.05	.10	.20	.30	.40	.50	.60	.70	.80	.90	.95
2	—	—	—	.34	.96	1.46	2.01	2.66	3.52	4.87	6.13
3	—	—	.49	1.31	1.88	2.47	3.14	3.91	4.90	6.45	7.87
4	—	—	1.43	2.12	2.79	3.48	4.23	5.11	6.22	7.94	9.49
5	.56	1.22	2.16	2.96	3.71	4.49	5.32	6.29	7.51	9.37	11.05
6	1.10	1.85	2.97	3.80	4.64	5.49	6.40	7.45	8.76	10.75	12.55
7	1.66	2.50	3.69	4.66	5.57	6.49	7.47	8.59	10.05	12.11	14.00
8	2.25	3.18	4.47	5.53	6.51	7.49	8.54	9.73	11.21	13.44	15.43
9	2.85	3.86	5.27	6.40	7.45	8.49	9.60	10.86	12.42	14.75	16.83
10	3.48	4.58	6.08	7.28	8.39	9.49	10.66	11.98	13.61	16.05	18.21
12	4.78	6.13	7.72	9.06	10.29	11.49	12.77	14.20	15.97	18.60	20.91
14	6.13	7.53	9.39	10.86	12.19	13.50	14.87	16.41	18.30	21.10	23.55
16	7.54	9.06	11.09	12.67	14.09	15.50	16.96	18.60	20.61	23.57	26.16
18	8.98	10.61	12.80	14.49	16.01	17.50	19.05	20.78	22.90	26.01	28.72
20	10.44	12.21	14.53	16.32	17.93	19.50	21.13	22.95	25.17	28.42	31.25
22	11.94	13.82	16.27	18.56	19.85	21.50	23.21	25.11	27.43	30.82	33.76
24	13.45	15.44	18.02	20.00	21.70	23.50	25.28	27.27	29.68	33.20	36.25
26	14.99	17.08	19.78	21.85	23.70	25.50	27.36	29.42	31.92	35.56	38.74
28	16.54	18.22	21.55	23.71	25.63	27.50	29.42	31.56	34.15	37.91	41.16
30	18.11	20.39	23.33	25.55	27.57	29.50	31.49	33.69	36.37	40.25	43.59
40	26.14	28.86	32.33	34.22	37.27	39.50	41.80	44.33	47.38	51.78	55.57
60	42.83	46.28	50.63	53.89	56.76	59.50	62.31	65.38	69.07	74.36	78.87
80	60.06	64.11	69.21	73.00	76.33	79.50	82.74	86.27	90.50	96.53	101.7
100	77.59	82.69	87.95	92.22	95.95	99.50	103.1	107.1	111.8	117.6	124.1
120	95.37	100.5	106.8	112.5	115.6	119.5	123.5	127.6	132.9	140.2	146.3
140	113.3	119.1	125.8	130.9	135.3	139.5	143.8	148.4	153.9	162.0	163.4
160	131.4	137.4	144.8	150.3	155.0	159.5	164.1	169.0	174.9	183.2	190.3
180	149.6	156.0	163.9	169.7	174.7	179.5	184.3	189.6	195.8	204.6	212.1
200	168.0	177.6	183.0	189.1	194.5	199.5	204.6	210.1	216.7	226.0	233.7

TABLE VI

HEAT TRANSFER COEFFICIENTS

IN UNCONSOLIDATED SANDS

Run	Sand Mesh	Length ft	Velocity ft/hr	ha Btu/hr,ft²,°F
99	150-170	.502	7.11	2,400
89			6.55	1,930
90			8.45	3,560
87			3.24	411
98			14.0	7,080
91			11.9	5,030
94			14.3	7,250
97			19.3	13,000
93			20.2	13,700
95			22.1	18,600
61	50-70	.502	2.88	402
62			4.86	1,130
63			7.38	2,390
64			12.70	6,460
68			19.0	24,800
66			25.4	21,200
37	50-70	.980	6.95	1,780
41			2.75	351
44			23.4	17,940
39			12.1	4,940
38			4.65	826
40			9.95	4,570
42			17.90	10,050
43			14.60	7,460
60	20-30	.980	3.36	494
58			10.1	3,830
56			16.5	7,630
59			25.3	12,800
52			11.9	4,060
53			20.5	9,750
54			7.16	1,810
57			5.54	1,160
26	100-140	0.98	8.41	2,730
30			23.2	15,500
33			2.96	377
27			7.06	1,950
31			9.70	3,570
32			6.58	1,510
24			10.90	4,520
25			12.3	5,660
29			19.0	11,400
36			12.4	5,720
28			15.0	7,590
73	100-140	0.502	26.4	24,400
74			15.7	9,240
75			8.19	2,750
77			3.26	411
14	Misc.	0.980	24.2	6,390
17			2.92	395
18			12.7	3,340
19			6.78	1,330
21			15.7	2,940
22			12.4	3,020
23			15.1	3,990
20			8.90	2,160
16			5.20	920
15			18.4	7,290
85	50-70	2.00	2.90	354
79			12.3	4,210
83			6.93	1,530

TABLE V

Error Caused By Use Of Equation
Relating Y and Temperature Variation
As A Means Of Calculating Y

Y	Percent Error in Y
10	7.2
20	2.7
40	.5
60	.2
80	.05
140	.04
200	.02

TABLE VII

Calculations For Problem 1

Accomplished Temperature Fraction	Produced Water Temperature, T_w	Z	Time From Start Of Injection θ	Pore Volumes Of Water Produced
.01	61.4	305	232	2.32
.10	74.0	324	240	2.40
.20	88.0	333	244	2.44
.40	116.0	345	249	2.49
.50	130.0	349	251	2.51
.60	144.0	355	254	2.54
.80	172.0	368	259	2.59
.90	186.0	377	263	2.63
.99	198.6	402	274	2.74

TABLE VIII

Calculations For Problem 2

x ft.	Y	Z	$\sqrt{Y}$	$\sqrt{Z}$	$\frac{1}{4\sqrt{Z}}$	$\sqrt{Z} - \sqrt{Y}$	$k = \sqrt{Z} - \sqrt{Y} + \frac{1}{4\sqrt{Z}}$	$A = \frac{2}{\sqrt{\pi}} \int_0^k e^{-u^2} du$	$\frac{A+1}{2}$	T_w °F
30	104.7	161.7	10.23	12.69	.020	2.46	2.48	1.000	1.000	200.0
32	111.7	157.1	10.57	12.53	.020	1.96	1.98	.995	.997	199.6
34	118.7	152.5	10.89	12.35	.020	1.46	1.48	.964	.982	197.5
36	125.6	147.8	11.21	12.16	.021	.95	.97	.830	.915	188.1
38	132.6	143.2	11.52	11.97	.021	.45	.47	.494	.747	164.6
40	139.6	138.6	11.82	11.78	.021	-.04	-.02	-.023	.489	128.5
42	146.6	134.0	12.11	11.58	.022	-.53	-.51	-.529	.236	93.0
44	153.6	129.4	12.39	11.38	.022	-1.01	-.99	-.839	.081	71.3
46	160.5	124.7	12.67	11.17	.022	-1.50	-1.48	-.964	.018	62.5
48	167.5	120.1	12.94	10.96	.023	-1.98	-1.96	-.995	.003	60.4
50	174.5	115.5	13.21	10.74	.023	-2.47	-2.45	-1.000	.000	60.0

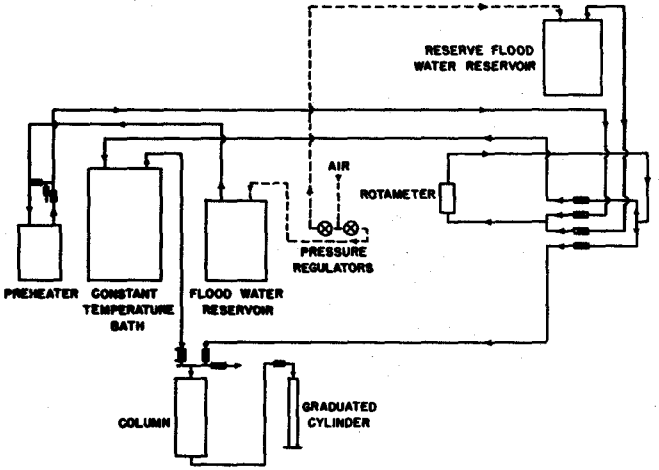

FIGURE 1 FLOW DIAGRAM

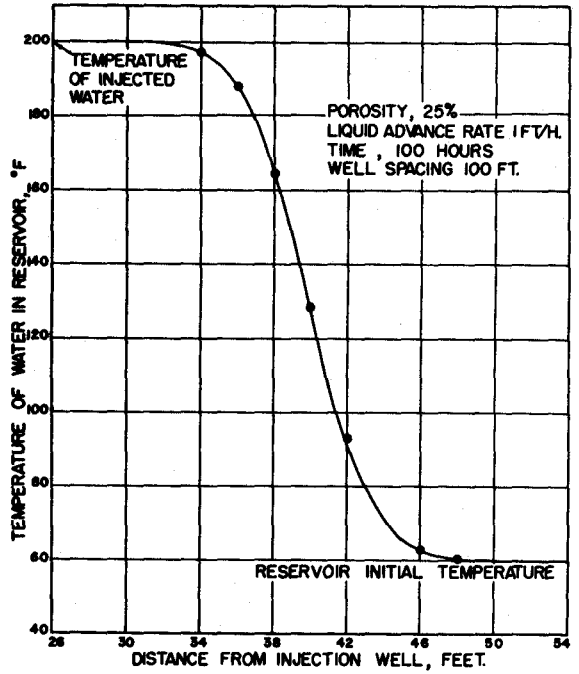

FIGURE 3. TEMPERATURE OF WATER IN LINEAR RESERVOIR AS FUNCTION OF DISTANCE FROM INJECTION WELL.

(SOLUTION TO PROBLEM 2)

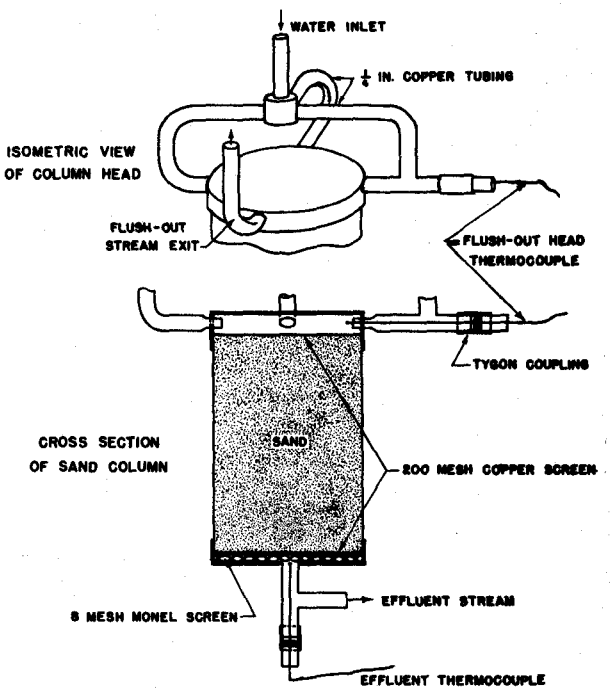

FIGURE 2 VIEW OF SAND RETAINING TUBE

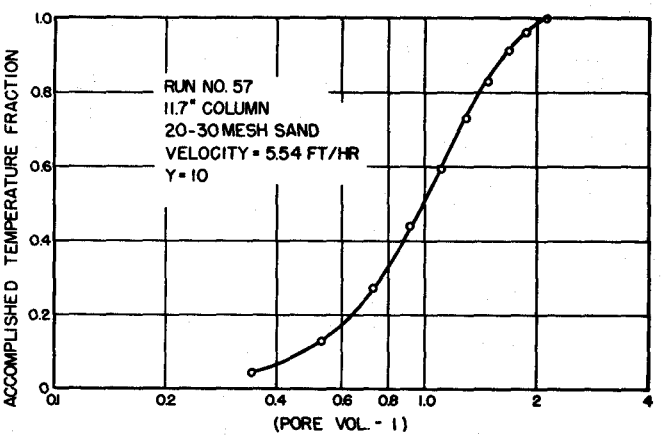

FIGURE 4. EXPERIMENTAL DATA FOR TYPICAL RUN.

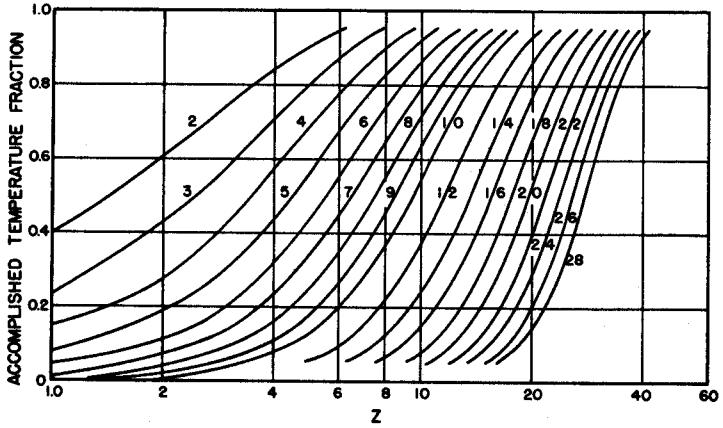

FIGURE 5. MASTER CURVES FOR ACCOMPLISHED TEMPERATURE FRACTION VS. Z AND Y FOR LIQUID TEMPERATURE AND LOW VALUES OF Y.

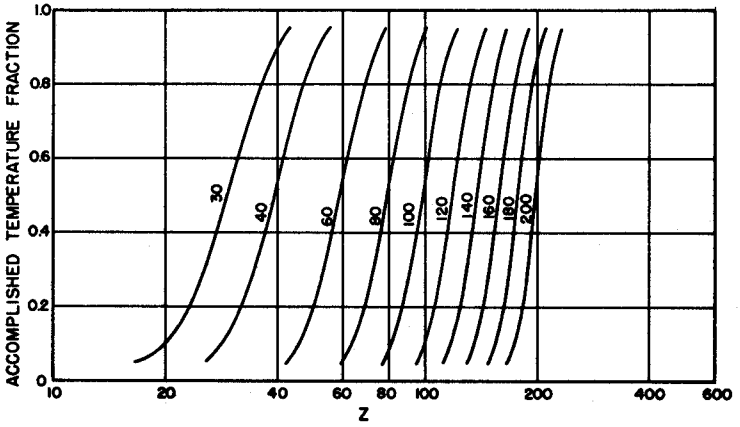

FIGURE 6. MASTER CURVES FOR ACCOMPLISHED TEMPERATURE FRACTION VS. Z AND Y FOR LIQUID TEMPERATURE AND HIGH VALUES OF Y.

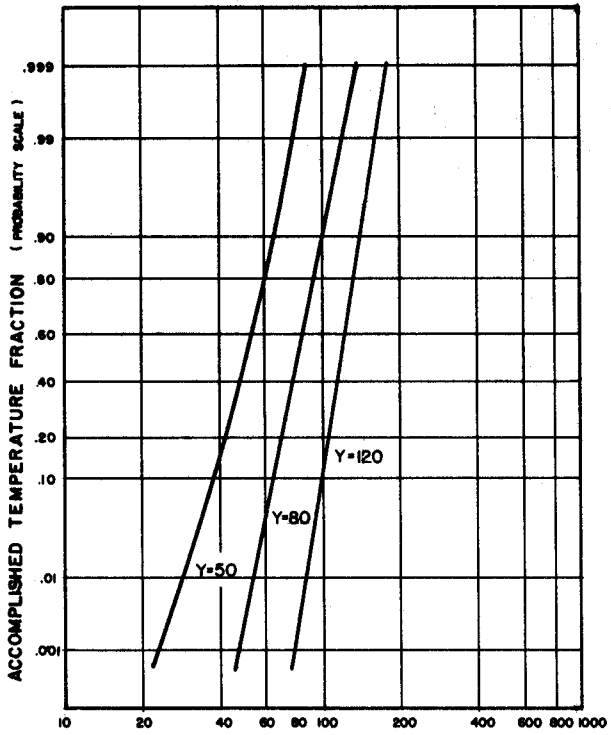

FIGURE 7. ACCOMPLISHED TEMPERATURE FRACTION AS A FUNCTION OF Y & Z

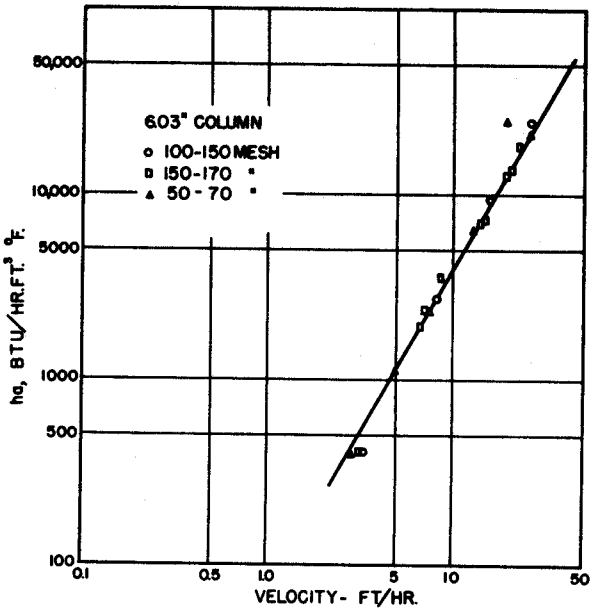

FIGURE 8. EFFECT OF SAND SIZE ON HEAT TRANSFER COEFFICIENT IN 6.03" COLUMN.

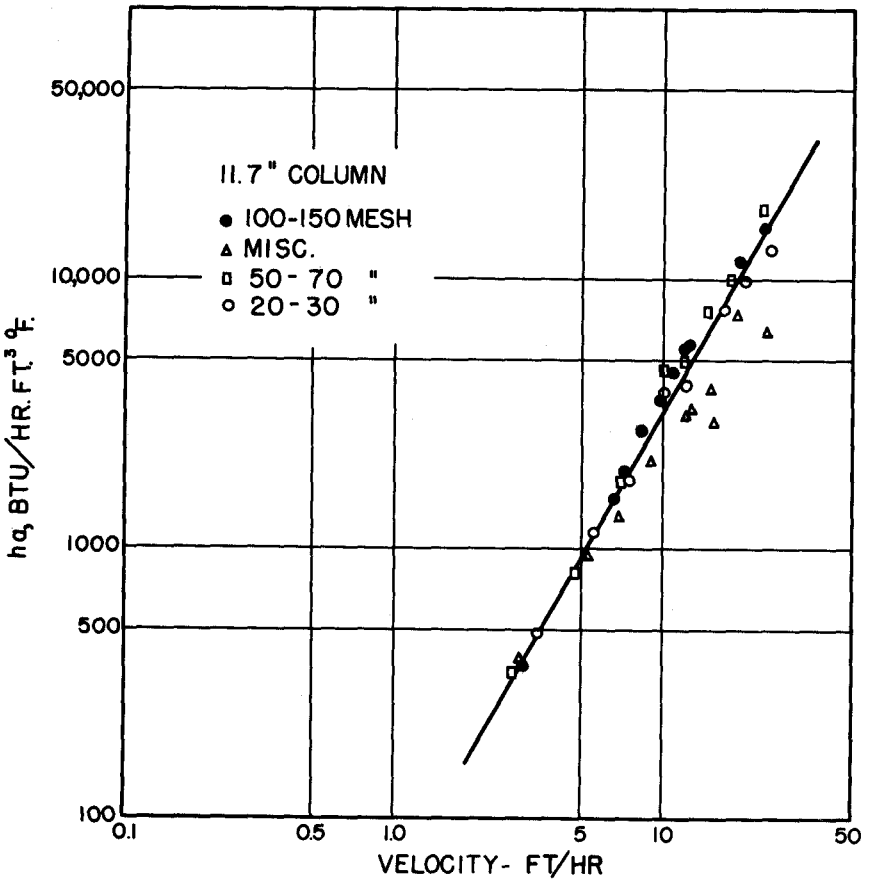

FIGURE 9. EFFECT OF SAND SIZE ON HEAT TRANSFER COEFFICIENT IN 11.7" COLUMN.

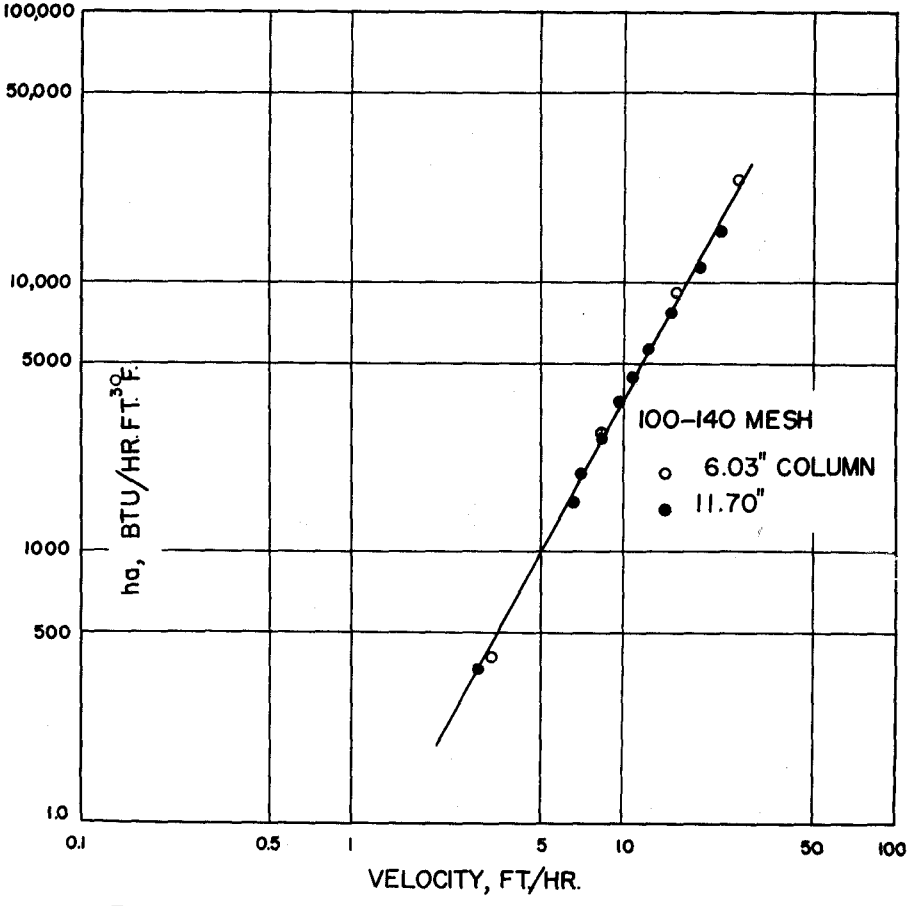

FIGURE 10. EFFECT OF COLUMN LENGTH ON HEAT TRANSFER COEFFICIENT FOR 100-140 MESH SAND.

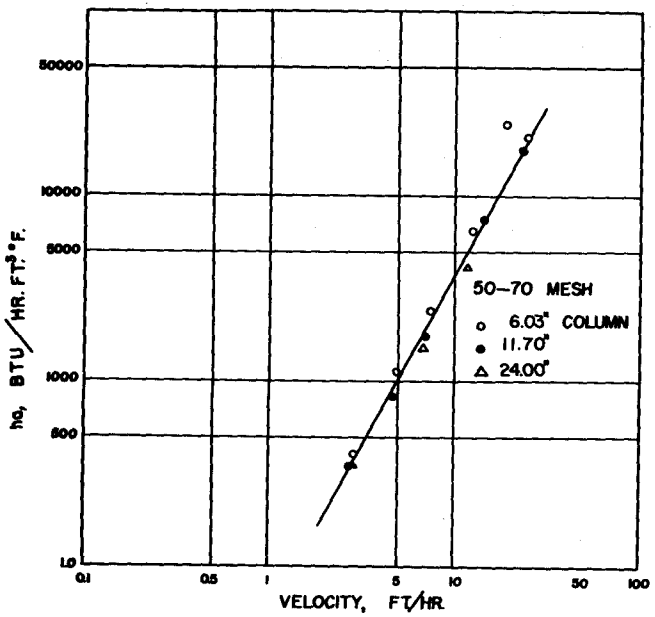

FIGURE 11. EFFECT OF LENGTH ON HEAT TRANSFER COEFFICIENT FOR 50–70 MESH SAND.

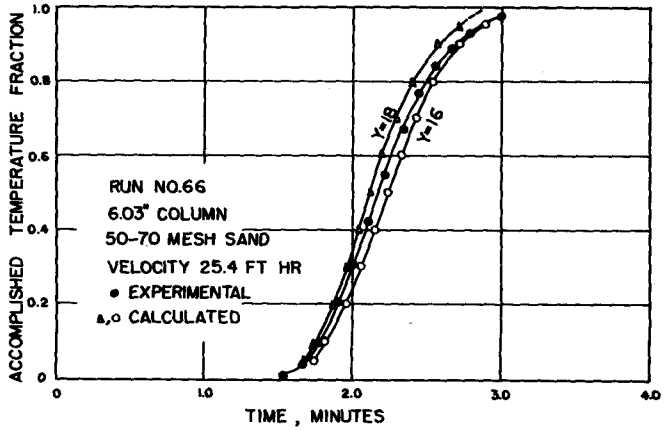

FIGURE 12. COMPARISON OF EXPERIMENTAL AND CALCULATED TEMPERATURE — TIME CURVES

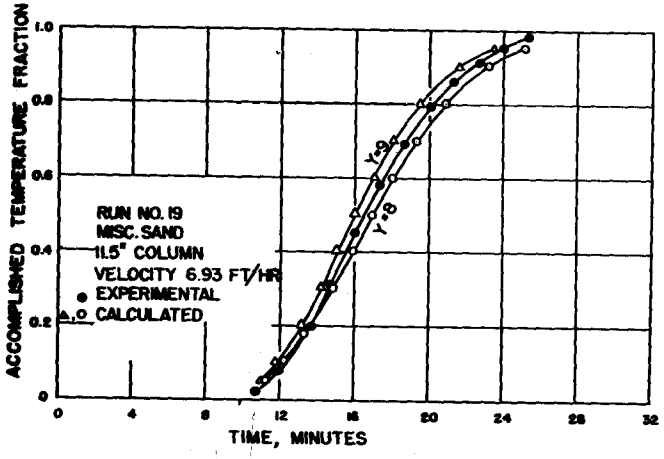

FIGURE 13. COMPARISON OF EXPERIMENTAL AND CALCULATED TEMPERATURE — TIME CURVES

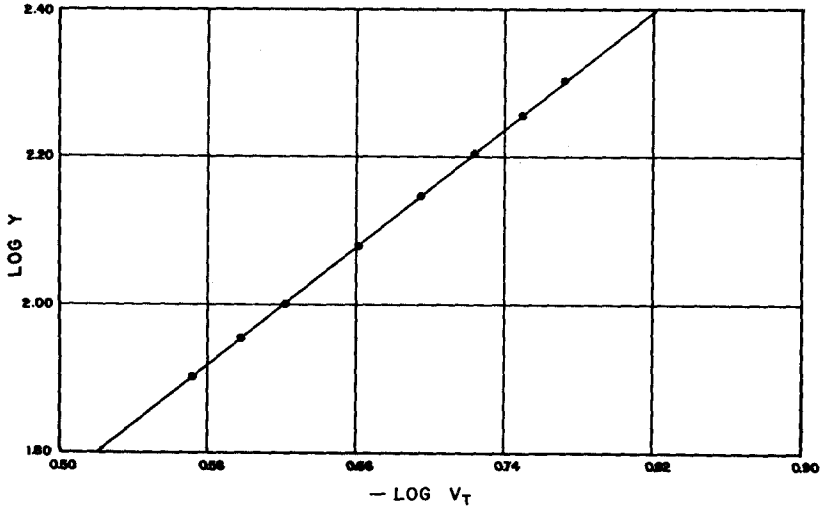

FIGURE 14. CALCULATED DATA FOR Y VERSUS TEMPERATURE VARIATION, V_T.

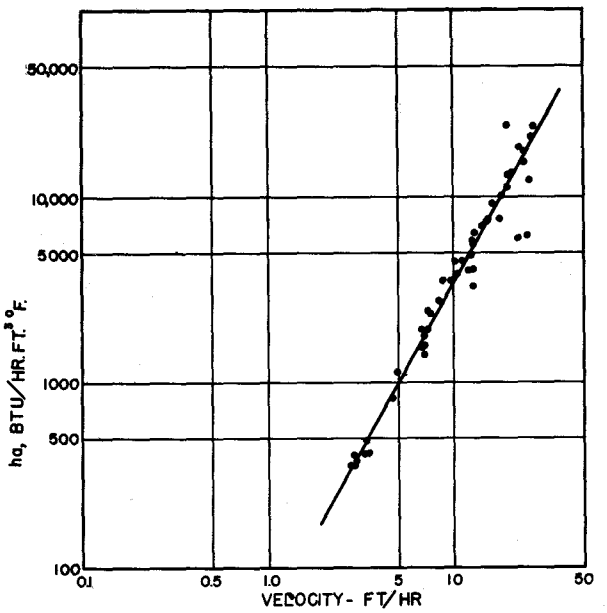

FIGURE 15. HEAT TRANSFER COEFFICIENTS FOR ALL RUNS.

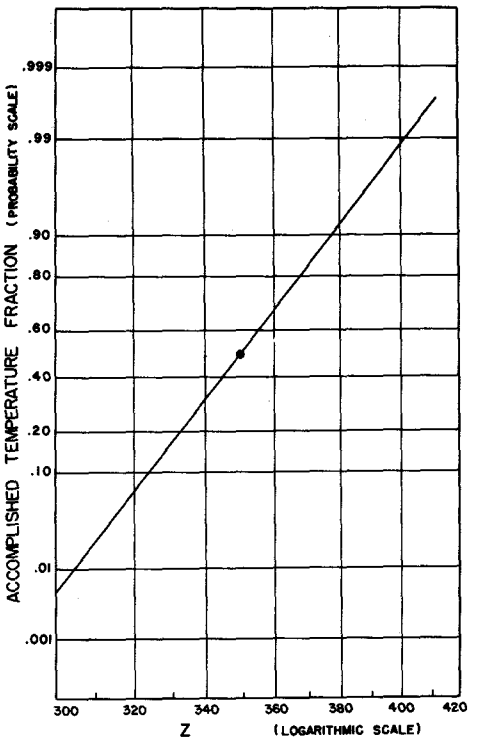

FIGURE 16. Z VS ACCOMPLISHED TEMPERATURE FRACTION (FOR PROBLEM I)

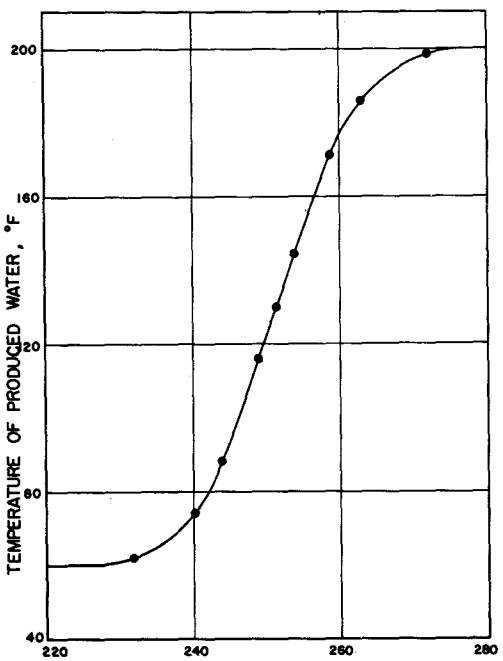

FIGURE 17. TEMPERATURE OF PRODUCED WATER AS A FUNCTION OF TIME (FOR PROBLEM I)

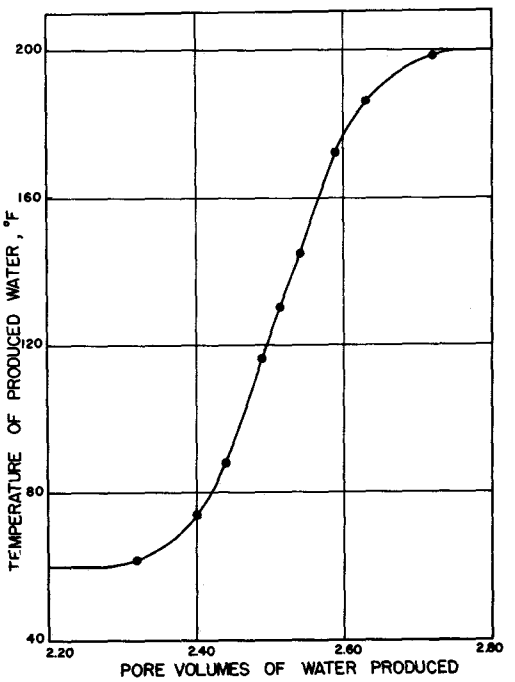

FIGURE 18. TEMPERATURE OF PRODUCED WATER AS A FUNCTION OF PORE VOLUMES OF WATER PRODUCED. (FOR PROBLEM I)

A THEORETICAL AND EXPERIMENTAL STUDY OF CONSTANT RATE DISPLACEMENTS IN WATER WET SYSTEMS

J. Jones-Parra*, C. D. Stahl** and J. C. Calhoun**

Introduction

Most of the early experimental investigations in which oil was displaced by water from a porous medium were carried on to obtain information as to the floodability of specific reservoirs. Consequently, as many as possible of the actual reservoir properties were reproduced in the laboratory floods. Such flooding results were often the basis of sweeping generalizations. It soon became apparent that results of specific flooding tests were in conflict so far as general applications were concerned, and when a theoretical analysis of flooding was possible, it became apparent that for the theory to gain thorough acceptance, a tremendous number of empirical observations, some of which were contradictory in nature, had to be taken into account. The thorough acceptance of a theory has not yet resulted because a complete accounting of experimental observations has not been made.

The analysis of the displacement of oil by water was made possible by the theory and associated equations developed by Leverett (1) and Buckley and Leverett (2). Pirson (3) made an extensive analysis of the variables involved in the Buckley-Leverett equations. The validity of the Buckley-Leverett theory was clearly demonstrated by the excellent experimental and theoretical study of Terwilliger et al (4).

In the meantime, some of the controversial results obtained in laboratory floods were cleared up by the investigation of Rapoport and Leas (5). They indicated that in systems which were not strongly wet by one of the fluids, the velocity might affect values of the relative permeability and the capillary pressure, implying, although no data were given, that experiments with porous media of different wetting properties did not confirm their theory so well as the oil-wet system which they used. However, Levine (6) has shown that in systems of such neutral wettability the velocity does not affect the relative permeability. Furthermore, Engelberts and Klinkenberg(7) show data to the effect that at certain high viscosity ratios the recovery decreases as the rate increases, a result directly opposite to the Rapoport-Leas correlation.

The present report is concerned with both the experimental and theoretical phases of the oil displacement problem. Experimental work has been done to furnish basic facts and demonstrate points resulting from theoretical considerations. The theory of Buckley-Leverett is relied upon and extended so that the composite more nearly conforms to the total of reported experimental facts. Those experimental data which show behavior contrary to the LVU_w correlation of Rapoport-Leas will be explained on the basis of the time dependency of the saturation gradient and of the fractional flow function. Although this possibility has been acknowledged by most investigators it has been promptly neglected by all but Terwilliger et al, who, unfortunately for the solution of the problem, were working on a type of displacement which included this transient behavior as a minor point. It will also be established theoretically that steady-state relative permeabilities do not always apply to transient flow processes.

Experimental Work:

The principal barrier to the deduction of generalizations from laboratory work has been the lack of control over important variables. The experimental work reported here was initiated, therefore, to yield basic information under circumstances of known control. At the time the work was initiated, the scaling of length had not been proposed in the literature, but the importance of length was deduced from reported work (9). Inasmuch as constancy of fluid rates was a part of the Buckley-Leverett theory this was set as an experimental condition. In order to have consistency of surface properties and to work in the range where capillary and viscous forces were both important, water-wet systems were adopted. Shortly after the experimental work was begun publication of information on water-wet systems(7), showing apparently anomalous behavior, made it imperative that experimental data on this type system be checked before facts could be completely fitted to a theory.

The porous matrices used throughout were lucite tubes, 2.5 inches inside diameter, packed with unconsolidated glass beads. Packed tubes were of three different lengths, 19.0, 25.4, and 38 centimeters.

Contribution No. 53-15, School of Mineral Industries, The Pennsylvania State College.

*Graduate Student, The Pennsylvania State College, Sponsored by Ministry of Mines and Hydrocarbons, Venezuelan Government.

**Division of Petroleum and Natural Gas Engineering, The Pennsylvania State College.

The beads, of 140-170 mesh size, were almost perfectly spherical in shape. After being treated with cleaning solution, the beads were found to be preferentially water wet. They were poured into lucite tubes, which were vibrated by means of a hydraulic tamper. The rate of packing was kept less than one centimeter of height per minute. Following the packing procedure the assembled tubes were dried and porosity and permeability tests were run. A summary of these results is given in Table I.

A constant injection rate pump* was used for fluid injection. In order to reduce slippage, the pump was used to meter motor oil which displaced brine from an outside reservoir. A small mounted sandstone core plug was found sufficient to eliminate the pump pulsations at the injection end of the core. The pump assembly gave output rates ranging from 0.30 to 0.005 cubic centimeters per second. Injection pressures were measured at the core inlet by means of a liquid-filled mercury manometer.

Early in the experimental work it was realized that an accurate method for determining displacing-phase breakthrough would be necessary. Therefore, electrodes were inserted in the lucite endplates to contact the fine mesh screen at the core ends. Line current across these electrodes was wired in series with a small neon bulb so that a light would show the time electrical conductivity through the porous body. This was taken as the true point of breakthrough of displacing brine.

A displacing liquid of 0.920 centipoise viscosity was obtained with a 0.5% by weight sodium chloride solution. Other 0.5% by weight sodium chloride solutions blended with chemically-pure glycerol produced displacing liquids of 3.25 and 5.2 centipoises. It was found impossible to adjust the viscosity of the displacing phase without altering the specific gravity.

The displaced-phase liquids were made up of inert water-white petroleum derivatives together with sufficient carbon tetrachloride to adjust the liquid specific gravities to unity. Care was exercised in the selection of the oil-phase mixtures to insure that unsaturated polar compounds would not be encountered. Mixtures having viscosities of 0.957, 1.85, 2.4, 3.25, and 5.2 centipoises were used. Commercial products including mineral oil were used as listed in Table II. The interfacial tensions of those liquids were determined against the appropriate brine solution. Those values are also listed in Table II. Only liquids which did not react with any part of the flow system were adopted for use.

The experimental procedure consisted of displacing the oil phase from the saturated unconsolidated beads at constant displacing fluid injection rates. The injection rates were varied from run to run. Tests were made at the maximum output rate of the pump or less excepting that no runs were made at a rate less than 15% of the maximum. Injection pressures and produced-volumes of liquid were recorded. An average injection rate was determined by timing the run from the beginning up to breakthrough and dividing into the total produced oil at breakthrough. Two breakthrough values were recorded. The first was that indicated by electrical conductivity through the length of the flooded core; the second was taken as the point at which the displacing phase first appeared in the graduated cylinder at the outlet end of the core. Some tests were carried past breakthrough although most were terminated at that point. There was always a difference between the breakthrough determined electrically and by produced fluid. This difference was generally smallest at the high velocity runs and highest at the low velocity runs.

The packed tubes were cleaned by flushing with distilled water and naphtha. They were then dried to constant weight and resaturated. At the completion of each series of runs, the cores were dismantled and repacked with new beads. No tubes ever gave evidence of having changed wettability between runs.

Ninety four separate runs were made. The general results are given in Tables III, IV, and V wherein the variables of each test run and the breakthrough recovery values are listed. In all instances except those marked by an asterisk, the breakthrough recoveries are those given by the electrical circuit. In those instances marked with an asterisk the breakthrough recovery is the visually-observed breakthrough reduced by an amount which would make it equivalent to an electrically-measured breakthrough. This was felt to be justified because the experience in all instances where both breakthroughs were measured showed a rather constant set of differences.

The recovery of oil at breakthrough was used as the correlating parameter in all these tests. In each series of runs, length of system and fluid viscosities were constant; velocity was the variable. In some instances breakthrough recovery increased with velocity, but in other cases breakthrough recovery decreased with velocity. In those instances where breakthrough recovery increased with velocity the curve had a characteristic "S" shape as indicated by the example data of Figure 1. This type curve was obtained for all cases where the ratio of oil to water viscosity was unity.

Plots of breakthrough recovery versus velocity for those instances wherein the viscosity ratio was greater than unity are shown in Figure 2. For viscosity ratios of 1.85 and 2.4 centipoises the curves are still "S" shaped; for viscosity ratios of 3.25 and 5.2 centipoises the curves not only are not "S"

* A Milton Roy Mini-Pump.

shaped, but over the range of velocities tested show a decrease in recovery at breakthrough with increased velocity. This is the same type relationship reported in one instance by Engelberts and Klinkenberg. After theoretical considerations so indicated, as will be pointed out on subsequent discussion, selected runs were made to extend one of these reversed curves to higher velocities and it was found that the increase of breakthrough recovery with velocity was obtained.

All combinations of variables were tried in an effort to scale experimental data to a common curve. In particular, LVu_w and LVu_w/γ were used. As can be seen immediately from Figure 2, it would be impossible to obtain a general scaling, but even the data for all runs where the oil-water viscosity ratio was unity could not be completely scaled as is seen in Figures 3 and 4. In Figures 3A, 3B, and 3C, LVu_w/γ has been plotted versus recovery for varying lengths of column at constant viscosity conditions. In Figures 4A, 4B, and 4C, LVu_w/γ has been plotted versus recovery for varying viscosities at constant length. These experimental data indicate that the scaling of LVu_w as proposed by Rapoport and Leas is not general, nor is it even applicable to water wet systems for a viscosity ratio of unity.

It should be pointed out that visual observations were made continuously during each experimental run. Sharp lines of demarcation between oil and water were observed at the flood fronts at high velocities when the viscosity ratio was unity and at some high velocities even when the viscosity ratio was not unity. In these instances breakthrough was observed to coincide with the arrival of this line of demarcation at the outlet of the system. On the other extreme, at low velocities and high viscosity ratios, intense fingering was observed. It was difficult to tell when the first fingers reached the outlet end, but generally electrical breakthrough coincided with estimates based on fingering. Under these conditions, there was observed to be a counterflow of oil at the inlet end of the system in the early runs. Although the oil which counteflowed always reentered the system later during the flood, it was deemed advisable to keep this to a minimum by redesigning the inlet end of the packed column so that very little backflow could result.

It was obvious from these observed fingers and sharp flood fronts that the length of the core is important. In many instances (at intermediate viscosity ratios or rates) the fingers could be seen to establish themselves, but after a time the flood front would coalesce into a sharp line of demarcation. This suggested that in many instances breakthrough recoveries were low only because the flooding system was not sufficiently long to permit the effects of initiating the flood to be obliterated before the outlet end of the system was reached by the initiating fingers. Thus, it seems important that an entry "end effect" is present in experimental observations and a complete theory must take this end effect into account.

It becomes apparent, therefore, that a theoretical development of displacement will be required to explain the failure of LVu_w to correlate breakthrough recoveries in some instances but not in others; to account for the decrease of recovery with velocity at high viscosity ratios; to explain the failure of length to scale data even when the viscosity ratio is unity; and to account for a fingering at the inlet.

Theoretical Consideration

Buckley and Leverett have presented equations for the solution of oil recovery by water flooding. Their equations are complete and suffice for general solutions of the problem. Unfortunately, those who used the Buckley Leverett equations immediately made simplifications which were not originally intended and which introduced many inconsistencies which the original equations do not possess. The most unfortunate of these simplifications involves the dropping of the capillary pressure term. In the original paper this simplification was not justified by the authors; the capillary pressure term was dropped because no data were available. Subsequently many investigators have attempted to justify their disregard of the capillary pressure term by stating that by increasing the rate the term can be made arbitrarily small. (See Equation 3). As it happens, as the rate is increased the term cannot be made arbitrarily small because $\partial S/\partial x$ for the saturation at the front approaches infinity so that the ratio of the satution gradient to the velocity becomes indeterminate. The capillary pressure term can be dropped only if $\partial S/\partial x$ approaches zero, as it does at high water saturations for long enough systems. Had this been recognized earlier, the double-valued saturation distribution obtained by dropping the capillary pressure term would not have confused so many investigators and driven others to such explanations as considering the double valued part of the curve "imaginary".

The flow equations developed by Rapoport and Leas(5) have received considerable attention. However, these equations are not subject to formal solution. Inasmuch as the Buckley-Leverett equations have been handled successfully for a rather complex case(4), it seems advisable to point out the equivalence between the two sets of equations and then refer only to those developed by Buckley and Leverett.

The flow equation derived by Rapoport and Leas

$$\phi \frac{\partial S_w}{\partial t} + V \frac{dF_w}{dS_w} \frac{\partial S_w}{\partial x} = \frac{K}{c\mu_w} \frac{\partial}{\partial x}\left[K_o F_w \frac{dP_c}{dS_w} \frac{\partial S_w}{\partial x}\right] \quad (1)$$

Is equivalent to

$$\phi \frac{\partial S_w}{\partial t} + V \frac{\partial f_w}{\partial x} = 0 \quad (2)$$

where, for an oil wet system,

$$f_w = F_w \left[1 - \frac{K K_o}{V \mu_o} \frac{d P_c}{d S_w} \frac{\partial S_w}{\partial x}\right] \quad (3)$$

and the boundary condition of Rapoport and Leas

$$K_o\left[V + \frac{K K_w}{\mu_w} \frac{d P_c}{d S_w} \frac{\partial S_w}{\partial x}\right] = 0 \quad \text{at } x = 0 \text{ for any } t \quad (4)$$

is equivalent to

$$f_w = 1.00 \text{ at } x = 0 \text{ for any } t \quad (5)$$

Equation 2) can be transformed (2) to

$$\frac{dx}{dt} = \frac{V}{\phi}\left[\frac{\partial f_w}{\partial S_w}\right]_t \quad (6)$$

Equations 3) and 6) are generally referred to as the Buckley-Leverett equations.

The Buckley-Leverett equations are so-called point equations, applicable at a given time at a given distance. A solution of the equations to apply at some significant time, such as water breakthrough, can be obtained only if the complete saturation-distance history is known from time zero up to the time in question. In the event that the saturation-distance relationship, i.e. $\partial S/\partial x$ is independent of time the conditions for solution are met. If $\partial S/\partial x$ is not independent of time, then the time variation must be known to permit solution. The saturation gradient is a function of time, at least for part of the duration of the flood. This can be shown by solving equation 3) for the gradient:

$$\frac{\partial S}{\partial x} = \frac{F_w - f_w}{\frac{K K_o F_w}{V \mu_o} \frac{dP_c}{dS_w}} \quad (7)$$

Consider the time when any saturation for which K_o is not zero is located at the inlet, i.e. at $x = 0$. For the saturation at that time and at that particular location, $f_w = 1.00$. By introducing this value of f_w into equation (7) it is possible to solve for the gradient, since all the other quantities involved are fixed by the saturation. At a later time during the displacement process, the saturation in question will be located not at $x = 0$ but somewhere within the porous medium. The value of f_w at this saturation will no longer be unity, and the value of $\partial s/\partial x$ will be changed accordingly.

Now, although $\partial s/\partial x$ is a function of time, the form of equations 3 and 6 is such that solution for a significant time can be made if an initial saturation-distance distribution is available. Also, if a flood tends to equilibrium values of $\partial s/\partial x$ over a short interval of time, solution can be approximated very well if the time to come to equilibrium is ignored; this is equivalent to assuming that the equilibrium value of $\partial s/\partial x$ is attained instantaneously. In the gravity drainage system investigated by Terwilliger, et al, they not only found that equilibrium values of $\partial s/\partial x$ were achieved at some rates before gas breakthrough, but they were also able to obtain a solution for the transient period before the flood attained equilibrium. Their problem was simplified by the fact that the initial distribution covered the whole range of saturations and hence a starting point was available for numerical solutions of the equations.

Once a stable front has been shown to exist, then the application of Terwilliger's method of solution is valid. The equilibrium form of f_w versus S_w is given by a straight line from the initial water saturation drawn tangent to the curve defined by F_w and along F_w from the point of tangency on.

This assumes that for saturations above those comprising the stable front $\partial S/\partial x$ approaches zero as the distance travelled by the flood increases. The point of tangency of the straight segment of f_w and F_w defines S_{wd}, the saturation dividing the stabilized zone from the saturations in the elongated portion, which comprise the variable zone.

Jones-Parra and Calhoun [8] applied Terwilliger's method of solution to the problem of water flooding under the conditions that an equilibrium saturation-distance profile was attained instantaneously. They made an appeal to empirical observations to justify the existence of an equilibrium distribution of saturations at the front. It can be shown analytically however, that there is only one equilibrium distance separating any two saturations at the flood front. This is given in Appendix A. This analytical proof then permits the general use of Terwilliger's method, if the equilibrium flood front is reached instantaneously.

Inasmuch as the Terwilliger method, based on the existence of an equilibrium flood front permits the determination of a saturation distribution at a specific time the breakthrough recovery can also be computed. Jones-Parra and Calhoun[8] obtained the saturation distribution over the entire length of the flood, and derived an equation for the recovery by dividing the total amount of injected water in the system at breakthrough by the pore volume. The following equation was obtained: (See Appendix B)

$$\text{Rec. \% P. V.} = \left[S_{w_{avg_V}} - S_{w_i}\right] - \left[S_{w_{avg_V}} - S_{w_{avg_S}}\right] \frac{\gamma \cos\theta \sqrt{K\phi}}{CLV\mu_w} \psi(S_{w_D}) \qquad (8)$$

This equation should permit the calculation of breakthrough recoveries only so long as the system has attained equilibrium before breakthrough.

The fact that the saturation-distribution must be in equilibrium before equation 8 can be applied, explains in part the scatter of points when the recovery is plotted versus the scaling coefficient, whether it be LV_{uw}, $LV_{uw}/\sqrt{K}$ or $LV_{uw}/\gamma\cos\theta\sqrt{K\phi}$. This scatter is apparent in the correlations presented by Engelberts and Klinkenberg and those obtained here (Figures 3 and 4), but is not at all present in the data of Rapoport and Leas. The existence of an exact correlation of recoveries versus the scaling coefficient implies a saturation distribution which is independent of time. This can best be shown by referring to Figure 5. The average saturation of curve A is equal to that of curve B for all values of L, V, and S_w only if the shape of curve A is equal to that of curve B. This only occurs when the front has achieved equilibrium, so that in laboratory floods an exact correlation would not generally be found. It is obvious that the longer the system the greater the chance that the equilibrium distribution will be achieved before breakthrough. This particular point will be considered further; but for the time being, it should be pointed out that in the present experiments there is a definite improvement in the correlation as the length is increased. This is shown in Figure 4, where A, B, and C correspond to lengths of 19, 25.4 and 38 cms.

It remains then to establish the conditions under which a flood will or will not reach equilibrium conditions for the system being studied at the rate used, the viscosity ratio prevailing and the length to be flooded. Very little is known about the behavior of the flood during the time prior to the attainment of equilibrium. Study of this behavior is in progress, but there is sufficient information available at this time to attempt a qualitative analysis.

An idea of how a non-equilibrium distribution behaves can be obtained from the data presented by Terwilliger et al. Their non-equilibrium distributions resulted at high rates, but this might not be a general condition because of the nature of their system. However, it is apparent that the non-equilibrium distribution exhibits much lower saturation gradients for the low saturations than would be expected under equilibrium conditions; that is, the low saturations tend to finger.

Another hint can be obtained from the data presented by Levine[6]. The variables in the expression for f_w (Equation 3) were measured independently by him and when f_w was plotted versus S_w an S-shaped curve was obtained. When Equation 6 is applied to this S-shaped curve the result is that intermediate saturations have higher linear velocities than low saturations. Obviously the f_w curve is a non-equilibrium curve, because if the S-shape is retained indefinitely then intermediate saturations will eventually run down and pass the lower saturations which is a physical impossibility. However, the fact that the intermediate saturations at breakthrough had the higher linear velocities indicates that they were in the process of reducing the distance separating them from the low saturations. In short, it again appears as if the non-equilibrium saturation gradients are smaller than the equilibrium gradients.

An obvious measure of non-equilibrium is the saturation at the inlet. Under equilibrium conditions, $f_w = 1.00$ only when $K_o = 0.0$ and this is true only at S_{w_m}, the maximum water saturation that can be achieved in the porous medium. When the water saturation at the inlet is not S_{w_m}, f_w for that saturation at the inlet is equal to unity although its equilibrium value must be smaller. Since the equilibrium value of f_w decreases as the saturation decreases, it follows that the lower the saturation at the

inlet the further away from equilibrium the system must be.

Engelberts and Klinkenberg presented evidence to the effect that for equal volumes of water injected, the water saturation at the inlet was lower the higher the injection rate. By simple material balance, it is clear that at the higher rate the given volume of water penetrated further into the porous medium than at the lower rate. These experimenters made these observations for high viscosity ratios. In the present work the behavior reported by Engelberts and Klinkenberg has been found at viscosity ratios of 3.25 and 5.2. A plot of recovery versus rate is shown in Figure 6, for a column of 25.4 cms and a viscosity ratio of 3.25. Typical of these runs also was the tendency of the water saturation at the inlet to remain low as evidenced by the counterflowing tendencies which were observed.

It was felt that if the decrease in recovery with an increase in rate was due to the fact that saturation distributions had not yet reached equilibrium, a simple proof would be to increase considerably the length of the system, thus giving the water saturation at the inlet at the time breakthrough occurred a chance to increase. The result of this test, conducted on a core 129 cm. long and using the same fluids as in Figure 6, is shown on Figure 7. The points labeled A and B were obtained with the 129 cms. column. It was also felt that the decrease in recovery with rate was true only for some undetermined range in rate, because it was difficult to picture the water saturation always becoming lower at the inlet as the rate increased indefinitely. It seemed logical that at some extremely high rate, the water saturation at the inlet should rise almost instantaneously to a very high value. To investigate this possibility, a run was made on the 25.4 cms. column at an average rate of 10 cc/sec. The test was successful, and increase in recovery resulting. This is shown by point C on Figure 7.

Thus, the results obtained at high viscosity ratios although at first glance appearing to contradict the Buckley-Leverett theory, can in fact be explained on the basis of their equations if one recognizes the need for including the transient history into the solution of the equations to obtain behavior at a given time.

The dilemma posed by these considerations was postulated by Rapoport and Leas when discussing extraneous velocity effects: It appears as if laboratory floods in some cases will not be at all representative of field floods. Rapoport and Leas suggest that in this case the recoveries should be calculated. This poses other problems. In particular it can be shown that steady-state relative permeabilities are not necessarily applicable to transient flow processes. If transient flow must be evaluated, what relative permeability data should be used poses a problem.

Consider a flood conducted at some high rate such that the stablized zone can be neglected and of length such that $\partial S/\partial x$ is very small at breakthrough in the variable zone. Applying equation (6) to the highest saturation at the front, to S_{wD}, at breakthrough, and integrating,

$$L = \frac{Vt}{\phi}\left(\frac{\partial f_w}{\partial S_w}\right)_t \tag{9}$$

the recovery at breakthrough is given by

$$\text{Rec. \% P.V.} = \frac{Vt}{\phi L} = \frac{1}{\left[\frac{\partial f_w}{\partial S_w}\right]_{S_{wD}}} \tag{10}$$

but the recovery at breakthrough is also given by

$$\text{Rec. \% P. V.} = S_{w_{avg}} - S_{w_i} \tag{11}$$

so that

$$S_{w_{avg}} - S_{w_i} = \frac{1}{\left[\frac{\partial f_w}{\partial S_w}\right]_{S_{wD}}} \tag{12}$$

since $\frac{\partial f_w}{\partial S_w}$ is a constant from S_{wi} to S_{wd},

$$\left[\frac{\partial f_w}{\partial S_w}\right]_{S_{wi}} = \left[\frac{\partial f_w}{\partial S_w}\right]_{S_{wD}} \tag{13}$$

so that

$$S_{w_{avg}} - S_{w_i} = \frac{1}{\left[\frac{\partial f_w}{\partial S_w}\right]_{S_{wi}}} \tag{14}$$

however, Calhoun (10) has shown that

$$Sw_{avg} - Sw = \frac{1 - fw}{\left[\frac{\partial fw}{\partial Sw}\right]} \qquad (15)$$

so that

$$(fw)_{Swi} = 0 \qquad (16)$$

Now the value of f_w is zero in the general case being considered, only when $K_w = 0$ so that the relative permeability to water is zero at the initial water saturation regardless of how low this saturation might be, which is not the case under steady-state conditions. Recently, Levine(6) presented experimental data to this effect for the case of zero initial water saturation. Terwilliger et al (4) showed that steady-state relative permeabilities were applicable in their particular system; however, the initial saturation in their system was zero and the relative permeability went to zero at 2 per cent saturation, so that the two values were very close. The interesting point is that there is a definite possibility that if the steady-state relative permeability goes to zero at the initial water saturation, then the relative permeabilities might apply. Obviously when a laboratory flood is carried out at zero initial displacing phase saturation, it is not to be expected that calculations based on steady state relative permeabilities will predict the behavior.

Conclusions

From the experimental work and the theoretical considerations made it is concluded that there can be no all inclusive generalization as to the direction in which recovery will change in laboratory floods over wide ranges of variables. Nor does it appear possible to arrive at a scaling factor which will correlate all flooding information on laboratory floods for a complete range of variables on a given system. The principal reason for this lack of generality is that there is always a time required for a flood to reach a stabilized saturation configuration, and this time may be much longer than the time required to complete the flooding of the system in question to the point of break through.

Correlations of flooding recoveries are possible only on systems that have reached saturation-distribution equilibrium prior to the time that breakthrough occurs. In such instances the scaling coefficient $LV\mu_w/\gamma Cos\theta\sqrt{K\phi}$ can be utilized and suffices as a basis for predictions.

Under the conditions of an equilibrium saturation distribution, the Buckley-Leverett equations can be solved by the method of Terwilliger to produce the complete flood history.

When calculating any flood behavior from correlations there is danger in not utilizing the correct relative permeability information, because the steady-state relative permeabilities do not necessarily apply. There is the possibility that the use of such permeabilities is proper if the relative permeability to the wetting phase goes to zero at the initial water saturation.

Because of the inadequacy of laboratory tests to yield a general correlation of recoveries the calculation of field performances based on laboratory recoveries must be approached with care. As field dimensions are approached the conditions which lead to equilibrium saturation-distributions are approached. It is always possible, however, that field dimensions might not be sufficient to remove the flood behavior from the transient region in the flooding times available.

References

1) Leverett, M. C. " Capillary Behavior in Porous Solids" Trans. A.I.M.E., 1941

2) Buckley, S. E. and Leverett, M. C. "Mechanism of Fluid Displacement in Sands" Trans. A.I.M.E., 1942

3) Pirson, S. J. "Elements of Reservoir Engineering" McGraw-Hill Publishing Co., Inc., 1950

4) Terwilliger et al, "An Experimental and Theoretical Investigation of Gravity Drainage Performance" Trans. A.I.M.E. , 1951

5) Rapoport, L. S. and Leas, W. J. "Properties of Linear Water Floods" J. of Petroleum Technology, May, 1953

6) Levine, J. S. "Displacement Experiments in a Consolidated Porous System" Publication No. 38, Shell Development Co., Houston, Texas. (To be presented at the Fall Meeting 1953, Petroleum Branch A.I.M.E.)

7) Engelberts, W. F. and Klinkenberg, L. J. "Laboratory Experiments on the Displacement of Oil by Water from Packs of Granular Material" Annals of the Third World Petroleum Congress, The Hague, 1951.

8) Jones-Parra, J. and Calhoun, J. C. "Computation of a Linear Water Flood by the Stabilized Zone Method" Cont. No. 53-6, School of Mineral Industries, The Pennsylvania State College, 1953 (Submitted to Petroleum Technology)

9) Calhoun, J. C. and LaRue, J. W. "The Effect of Velocity in Water Flooding" Prod. Monthly, April, 1951

10) Calhoun, J. C. "Engineering Fundamentals" The Oil and Gas Journal Series

Nomenclature

V = total rate of flow per unit cross-sectional area, followed by subscript referes to flow of fluid indicated.

μ = viscosity

C = μ_o/μ_w

t = time

F_w = $\left(1 + \frac{K_o}{K_w C} \right)^{-1}$

x = distance along direction of flow

L = length of system

K = permeability, followed by subscript indicates relative permeability

ϕ = porosity

P_c = pressure drop across the oil-water interface

f_w = V_w/V

$\frac{dx}{dt}$ = linear velocity of a plane of constant saturation

S_{wi} = initial saturation

S_{w_m} = saturation at $K_o = 0$

S_{wD} = saturation dividing variable zone from stabilized zone

$S_{w_{avg}}$ = average water saturation; $S_{w_{avg}V}$, in variable zone; $S_{w_{avg}S}$, in stabilized zone

γ = interfacial tension

θ = contact angle

$$\psi(S_{w_D}) = \int_{S_{w_i}}^{S_{w_D}} \left[\frac{F_w K_o \frac{\partial J}{\partial S_w}}{F_w - f_w} \right] dS_w$$

J = Leverett's J function = $\frac{\sqrt{K/\phi}\, P_c}{\gamma \cos \theta}$

Appendix A

Consider the constant rate flow of oil and water through a porous medium. Ignoring for a moment capillary forces.

$$V = V_o + V_w = \left[\frac{K_o}{\mu_o} + \frac{K_w}{\mu_w}\right] K \frac{\partial P}{\partial x} \qquad (A\text{-}1)$$

Now assume that the saturation at x_1 is S_{w_1} and that at x_2 it is S_{w_2}.

$$\Delta P = \frac{V}{K} \int_{x_1}^{x_2} \left(\frac{dx}{\frac{K_o}{\mu_o} + \frac{K_w}{\mu_w}}\right) \qquad (A\text{-}2)$$

The value of the integral obviously depends on the manner in which the saturation range S_{w_1} to S_{w_2} is distributed between x_1 and x_2. The most stable distribution is that which offers the least resistance to flow. At constant rate, this means that the equilibrium distribution is that which leads to the lowest pressure. It can be easily verified that the minimum value of the integral in Equation 9 results when both saturations, S_{w_1} and S_{w_2} are found at either x_1 or x_2, depending upon the viscosity ratio, the relative permeability characteristics, and the saturations S_{w_1} and S_{w_2}. In fact, it is in this manner that saturations at the flood front arrange themselves at very high injection rates.

The actual potential causing flow is the applied pressure plus the capillary pressure, and the capillary pressure is not the same at saturations S_{w_1} and S_{w_2}. The excess total pressure acts on the lower saturation to place them slightly ahead of the higher ones such that the excess resistance balances the excess pressure. The actual distance separating any two saturations therefore depends on the ratio of applied pressure to the capillary pressure but since the ratio is fixed, the distance is fixed. This ratio of viscous forces to capillary forces was determined by Engelberts and Klinkenberg to be given by

$$\frac{LV\mu_w}{\gamma\sqrt{K}} \qquad (A\text{-}3)$$

A similar coefficient was obtained by Rapoport and Leas from a dimensionless form of their equation, and by Jones-Parra and Calhoun (8) from the Buckley-Leverett equations. The applicability of the coefficients has been proven experimentally by correlating recoveries. (5)(6)

Appendix B - Derivation of Recovery at Breakthrough

Using the equilibrium value of f_w from S_{w_1} to S_{wD}, the saturation distribution can be obtained by numerical integration of Equation (7). From the saturation distribution the average saturations, S_{wavgS}, can be obtained; and the total length of the stabilized zone obtained by solving Equation (7) for $\partial x/\partial S$ and integrating from S_{w_1} to S_{wD}. This total length, Xt, after substitution of Leverett's J function for the capillary pressure, is given by

$$X_t = \frac{\gamma \cos\theta \sqrt{K\phi}}{V \mu_o} \int_{S_{w_1}}^{S_{wD}} \left[\frac{F_w K_o \frac{\partial J}{\partial S_w}}{F_w - f_w}\right] dS_w \qquad (B\text{-}1)$$

By making the substitutions

$$\psi(S_{wD}) = \int_{S_{w_1}}^{S_{wD}} \left[\frac{F_w K_o \frac{\partial J}{\partial S_w}}{F_w - f_w}\right] dS_w \;, \quad C = \frac{\mu_o}{\mu_w} \qquad (B\text{-}2)$$

$$X_t = \frac{\gamma \cos\theta \sqrt{K\phi}}{C V \mu_w} \psi_{(S_{wD})} \qquad (B\text{-}3)$$

The total volume of injected water in the stabilized zone is given by

$$\phi A X_t (S_{wavgS} - S_{w_1}) \qquad (B\text{-}4)$$

The average saturation in the variable zone can be obtained by graphical solution of Equation (15) at S_{wD}. This is done by extending the straight line portion of f_w versus S_w, from S_{w_1} to S_{wD}, to

$f_w = 1.00$. The saturation at the intersection of the extended line and $f_w = 1.00$ is S_{wavgV}. The volume of injected water in the variable zone at breakthrough is given by

$$\phi A\ (L - Xt)\ (S_{wavgV} - S_{wi}) \tag{B-5}$$

The recovery at breakthrough is given by the total amount of water injected divided by the pore volume

$$\text{Rec. \% P. V.} = \frac{Xt\ (S_{wavgS} - S_{wi}) + (L - Xt)(S_{wavgS} - S_{wi})}{L} \tag{B-6}$$

Simplifying and substituting (A-3)

$$\text{Rec. \% P. V.} = (S_{wavgV} - S_{wi}) - (S_{wavgV} - S_{wavgS}) \frac{\gamma \cos\theta \sqrt{K\phi}}{L\ V/\mu_w\ C} \psi_{(S_{wD})} \tag{B-7}$$

TABLE 1

Core Properties

Core No.	Length, cm	Permeability, d	% Porosity
1	25.4	7.04	37.10
2	25.4	6.98	37.06
3	25.4	6.95	37.60
4	25.4	7.01	37.80
5	19.0	7.0	37.52
6	38	7.18	37.58
7	19	Not Run	38.03
8	19	7.03	38.4
9	25.4	6.50	37.05
10	38	7.5	37.10

TABLE II

Interfacial Tension (Du Nuoy) Values at 25°C

Apcothinner-Carbon Tetrachloride against 0.5% NaCl
35.8 dynes/cm

Soltrol 180-Carbon Tetrachloride against 0.5% NaCl
31.1 dynes/cm

XCT White Oil-Carbon Tetrachloride against 0.5% NaCl
35.2 dynes/cm

Mineral Oil-Apcothinner-Carbon Tetrachloride against 0.5% NaCl
37.7 dynes/cm

Bayol 50-Carbon Tetrachloride against 0.5% NaCl
35.8 dynes/cm

Mineral Oil-Apcothinner-Carbon Tetrachloride against 3.2 cp. glycerol
25.5 dynes/cm

Soltrol 180-Carbon Tetrachloride against 1.85 glycerol solution
18.6 dynes/cm

TABLE III

Tabulation of Results For Floods
With Viscosity Ratio Not Unity

Run#	Lenth cms.	Velocity cc/min/cm^2	Oil Viscosity cps.	Water Viscosity cps.	γ dynes/cm	Breakthrough Recovery %
1	25.4	.412	3.25	0.92	36.5	59.4*
2	25.4	.271	3.25	0.92	36.5	58.4*
3	25.4	.098	3.25	0.92	36.5	63.9*
4	25.4	.030	3.25	0.92	36.5	74.1*
6	25.4	.545	3.25	0.92	36.5	60.5*
7	25.4	.598	1.85	0.92	31.1	75.8*
8	25.4	.294	1.85	0.92	31.1	77.1*
10	25.4	.151	1.85	0.92	31.1	64.6*
11	25.4	.071	1.85	0.92	31.1	68.7*
12	25.4	.075	1.85	0.92	31.1	66 *
14	25.4	.043	1.85	0.92	31	61.2*
20	25.4	.573	2.4	0.92	35.5	77.7*
21	25.4	.280	2.4	0.92	35.5	82.5*
22	25.4	.196	2.4	0.92	35.5	74.8*
23	25.4	.129	2.4	0.92	35.5	68.7*
24	25.4	.063	2.4	0.92	35.5	83.9*
25	25.4	.007	2.4	0.92	35.5	55.3*
26	25.4	.069	2.4	0.92	35.5	68.2*
27	25.4	.161	2.4	0.92	35.5	77.8*
28	25.4	.153	2.4	0.92	35.5	77.4*
29	25.4	.473	5.2	0.92	35.8	49.2
30	25.4	.259	5.2	0.92	35.8	53.1
32	25.4	.188	5.2	0.92	35.8	50.3
33	25.4	.126	5.2	0.92	35.8	62.6
34	25.4	.059	5.2	0.92	35.8	64.0
35	25.4	.029	5.2	0.92	35.8	63 *
36	25.4	.129	5.2	0.92	35.8	56.5*
37	25.4	.003	5.2	0.92	35.8	59.5*
38	25.4	.745	5.2	0.92	35.8	47.7*

TABLE IV

Tabulation of Results For Floods
With Viscosity Ratio Unity

Run#	Length cms.	Velocity ccs/min/cm²	Oil Viscosity cps.	Water Viscosity cps.	γ dynes/cm	Breakthrough Recovery %
15	25.4	0.421	0.957	0.920	24.6	94.0*
16	25.4	0.306	0.957	0.920	24.6	90.0*
17	25.4	0.161	0.957	0.920	24.6	82.3*
18	25.4	0.061	0.957	0.920	24.6	81.8*
19	25.4	0.784	0.957	0.920	24.6	95.6*
45	38	0.486	0.957	0.920	24.6	92.3
46	38	0.277	0.957	0.920	24.6	91.6
47	38	0.182	0.957	0.920	24.6	89.3
48	38	0.116	0.957	0.920	24.6	85.3
49	38	0.051	0.957	0.920	24.6	84.9
50	38	0.479	0.957	0.920	24.6	92.1
51	38	2.549	0.957	0.920	24.6	94.9
53	19	0.467	0.957	0.920	24.6	86.9
54	19	0.279	0.957	0.920	24.6	82.5
55	19	0.179	0.957	0.920	24.6	76.5
56	19	0.112	0.957	0.920	24.6	72.8
57	19	0.057	0.957	0.920	24.6	72.0
59	19	0.012	0.957	0.920	24.6	72.5
61	38	0.606	1.688	1.756	18.6	90.7
62	25.4	0.453	1.688	1.756	18.6	84.1
63	19	0.598	1.688	1.756	18.6	83.5
64	38	0.271	1.688	1.756	18.6	89.0
65	25.4	0.290	1.688	1.756	18.6	85.7
66	19	0.286	1.688	1.756	18.6	72.3
67	38	0.175	1.688	1.756	18.6	85.0
68	25.4	0.176	1.688	1.756	18.6	79.2
69	19	0.175	1.688	1.756	18.6	68.5
70	38	0.104	1.688	1.756	18.6	80.5

TABLE IV (cont)

Tabulation of Results For Floods
With Viscosity Ratio Unity

Run#	Length cms.	Velocity $\frac{ccs/min}{cm^2}$	Oil Viscosity cps.	Water Viscosity cps.	γ dynes/cm	Breakthrough Recovery %
71	25.4	0.114	1.688	1.756	18.6	77.5
72	19	0.104	1.688	1.756	18.6	68.0
73	38	0.058	1.688	1.756	18.6	67.5
74	25.4	0.054	1.688	1.756	18.6	63.6
75	19	0.055	1.688	1.756	18.6	73.3
76	38	0.602	3.169	3.170	25.5	94.2
77	25.4	0.537	3.169	3.170	25.5	92.3
78	19	0.581	3.169	3.170	25.5	81.7
79	38	0.282	3.169	3.170	25.5	89.7
80	25.4	0.294	3.169	3.170	25.5	86.8
81	19	0.277	3.169	3.170	25.5	81.6
82	38	0.188	3.169	3.170	25.5	87.8
83	25.4	0.188	3.169	3.170	25.5	87.9
84	19	0.192	3.169	3.170	25.5	82.2
85	38	0.117	3.169	3.170	25.5	87.4
86	25.4	0.117	3.169	3.170	25.5	85.2
87	19	0.061	3.169	3.170	25.5	80.0
88	38	0.071	3.169	3.170	25.5	81.5
89	25.4	0.051	3.169	3.170	25.5	78.8
90	19	0.090	3.169	3.170	25.5	73.0
91	19	0.027	3.169	3.170	25.5	74.4

TABLE V

Run	Length	Velocity	Oil Viscosity	Water Viscosity	γ	Breakthrough Recovery
A	129	.090	3.25	.92	36.5	59.5
B	129	.535	3.25	.92	36.5	63.8
C	25.4	19.61	3.25	.92	36.5	73.0

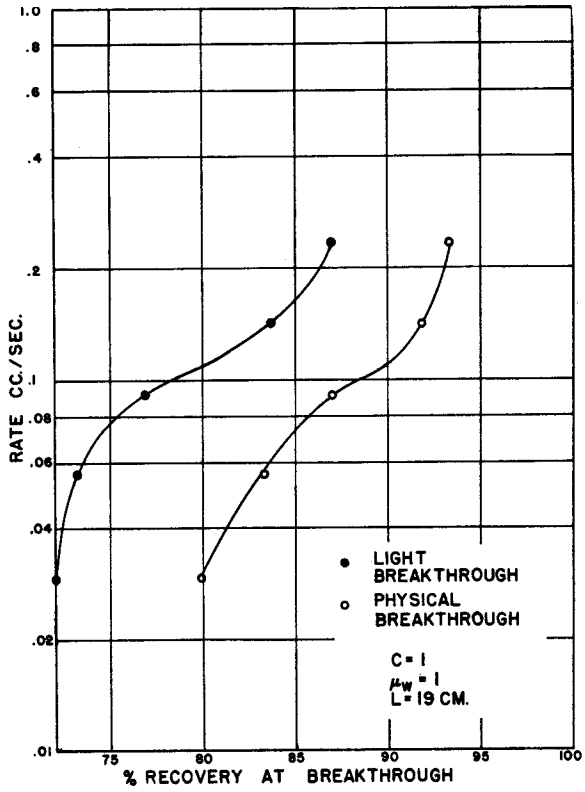

FIGURE 1. TYPICAL CURVE FOR LOW VISCOSITY RATIO

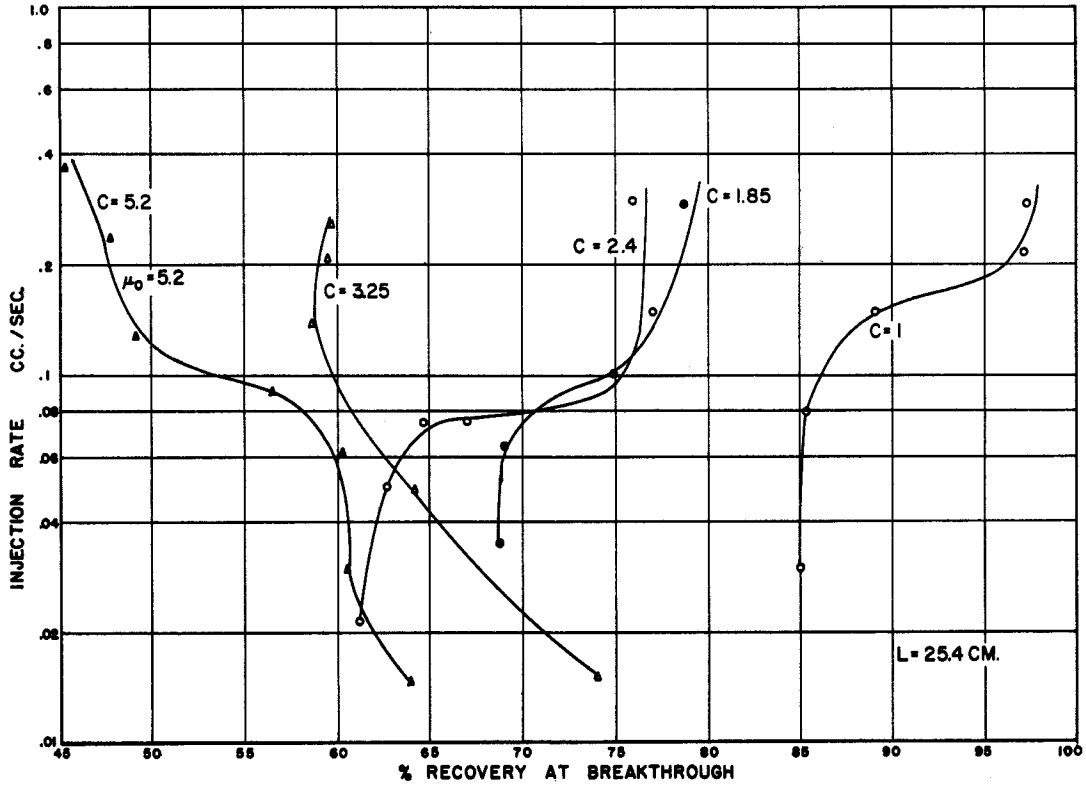

FIGURE 2. EFFECT OF VISCOSITY RATIO AT CONSTANT LENGTH

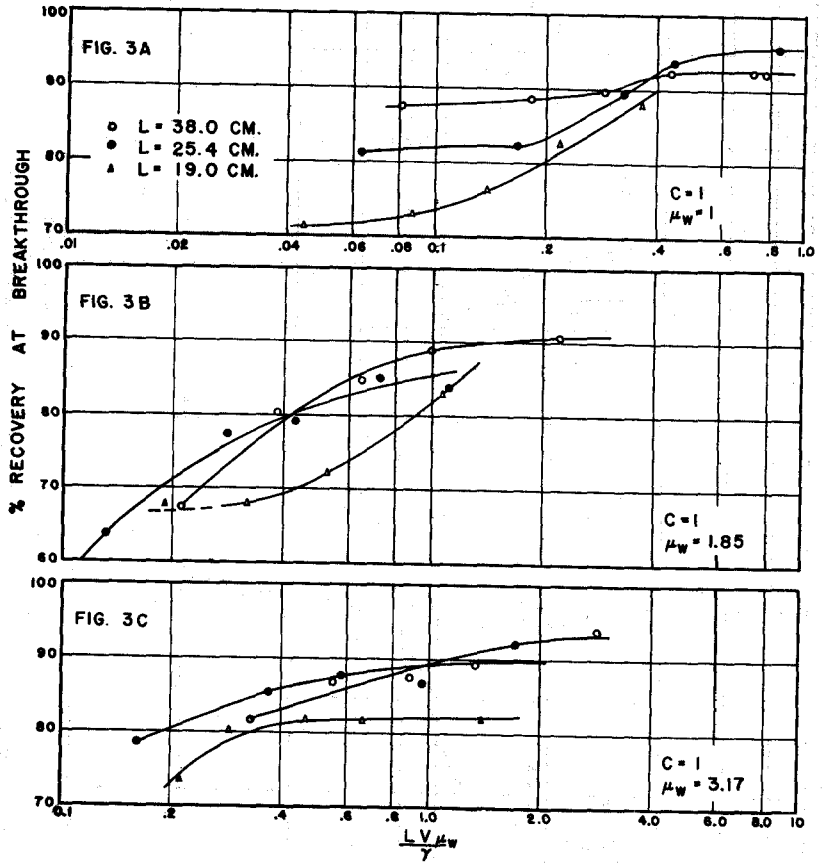

FIGURE 3. EFFECT OF LENGTH FOR VARIOUS μ_w

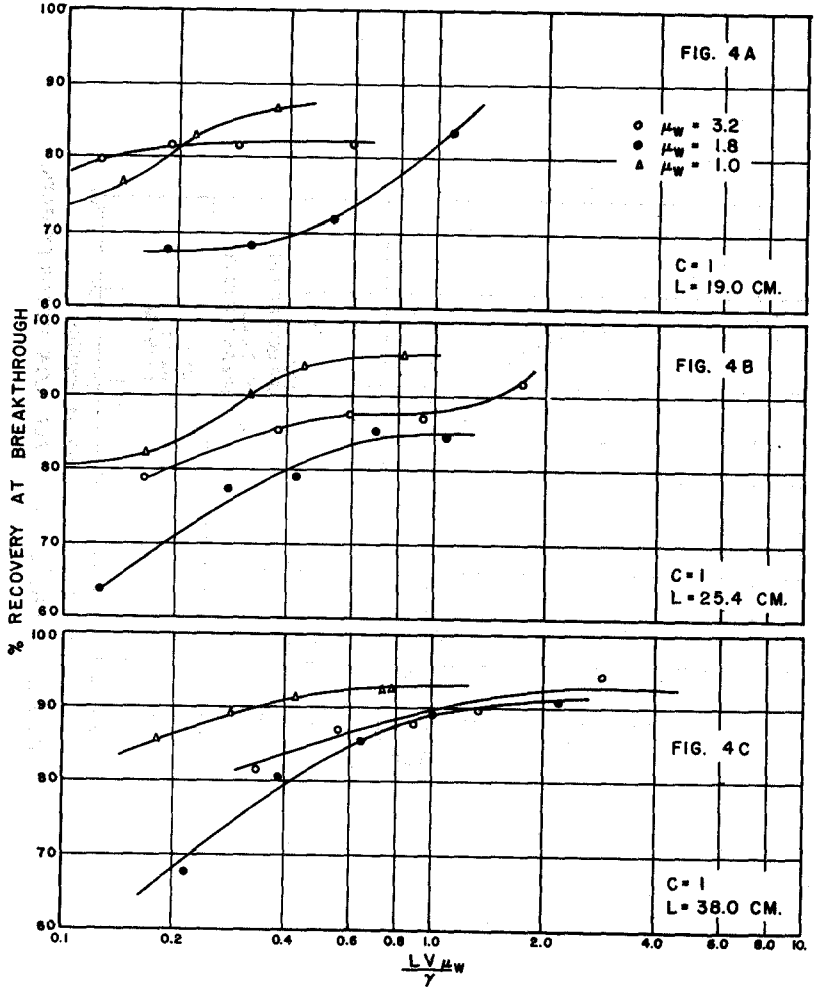

FIGURE 4. EFFECT OF μ_w FOR VARIOUS LENGTHS

HOT WATER INJECTION TREATMENT OF WELLS TO INCREASE WATER INTAKE RATES

J. N. Breston* and B. R. Pearman*

Introduction

One of the major obstacles to the economic recovery of oil in the Bradford and Allegany oil fields is the low permeability of much of the sand. Water injection rates are low and consequently the rate of oil recovery is low. As a result some parts of the reservoir cannot be flooded economically right from the start, and in other cases leases are abandoned prematurely because the production cannot cover operating expenses.

Since greater well density, heavier shooting, and higher pressures have not proved to be a complete solution to the problem, other methods of increasing water injection rates have been and still are being sought. Some years ago a natural born experimenter named Kenneth Barton, who was working for the Forest Oil Company in the Bradford fields, decided to see what would happen if very hot water was injected into a well for awhile. He rigged up some gas burners under the water line going to an injection well and turned on the gas. Reportedly he heated the water so hot that the straw in the water box which came into contact with the pipe caught on fire. The intake rate of the well increased considerably during the period of hot water injection. When the heating was stopped and the well was allowed to cool, the intake rate did not return to its former value but remained 100% higher. Due to the danger involved in the method employed to heat the water, the experiment was discontinued and apparently forgotten.

Ever since its inception the Bradford Laboratory of the Pennsylvania Grade Crude Oil Association has been experimenting with various means of increasing water intake rates. In 1949 it turned its attention to hot water. Accordingly, some simple laboratory experiments were devised whereby radial core specimens could be flooded with cool water to an equilibrium value, then with hot water to an equilibrium value, and then again with cool water. In the case of several cores this flooding cycle was repeated and each time the hot water temperature was raised 20°F.

The experiments showed that definite increases in water intake rates were effected by hot water flooding. The effect did not take place until water temperature of 140° to 170°F were reached, and then continued to increase with each increase in temperature. The experiments were not carried above 250°F due to limitations of the apparatus. Of eight core samples with air permeabilities ranging from 0.1 to 2.0 md seven showed increased intake rates after hot water flooding. The increases ranged from 10% to 400%. Most significantly, in several of the cores there was an increase in water intake rate without any apparent oil production. Even in the case of the other cores there was little oil production since they were already thoroughly flooded out before the hot water flooding. A summary of the data from these tests is listed in Table 1.

The results appeared so convincing that it was decided to go right to the field with any further experiments. In that way the tests could be carried to higher pressures and temperatures, and the results would be more significant from the practical viewpoint. It appeared that a field test would not be difficult to perform provided a means could be found to deliver hot flood water to the sand. Two prime considerations were involved. First, would it be possible to heat the water on the surface and expect a reasonable amount of heat to remain in the water when it reached the bottom of the well (average depth 1500 ft.)? Second, if heating the water on the surface was not applicable, could a method be devised to heat the water at the bottom of the well while the well was taking water under normal sand face pressure (average, 1800 psig)?

After much debate the idea of heating the water on the surface was abandoned in favor of heating it at the bottom of the well. This was to be accomplished by a bottom hole electric heater.

The Heater

Through the joint collaboration of the Pennsylvania Electric Company, Quaker State Oil Refining Corporation, Woessner-McKnight, Inc., and the laboratory staff, a plan was devised whereby an electric resistance heater would be constructed that could be lowered through the 2 inch tubing to the bottom of the well on 3/4 inch pipe. An adaptation using commercial rod heaters was constructed and tested but failed under the high pressures at the bottom of the well. The heater that finally worked was made of #12 nichrome resistance wire strung with ceramic beads and laced back and forth through the

* Pennsylvania Grade Crude Oil Association, Bradford, Pennsylvania.

four quadrants of a steel cross support. The assembly was slipped into 1 inch copper pipe, and the voids filled with magnesia. One end of the resistance wire was welded to the copper pipe and the other end brought out of the top of the heater to a jackknife connector. A sketch with the construction details is found in Figure 1. The heater was 26 ft. long and rated at 24 kw. when operating on 440 volts A.C.

Electricity was supplied to the heater by a one-wire insulated cable running down through the 3/4 inch pipe, with the 3/4 inch pipe serving as the return. The hookup is diagrammed in Figure 2. The cable was cut to pipe joint lengths and fitted with jackknife connectors (see Figure 1) so it could be run with the pipe. Thus the heater's interior and the cable were kept dry. Extreme caution was taken to insure against leakage at all threaded joints since little more than a drop of water was sufficient to short out the 400 volts. In two of the three tests the 3/4 inch pipe was pressured with nitrogen to partly balance the water pressure on the outside. This necessitated a special adapter and packing gland at the top of the 3/4 inch string of pipe to bring out the cable.

The arrangement just described worked surprisingly well and was used in all three of the well tests. In addition to the electrical equipment, the wells were equipped with volume and pressure recorders as shown in Figure 2, to provide complete performance data during the tests.

Test Procedure

The general procedure consisted of observing the well's equilibrium intake rate before installing the heater, after installing the heater, during hot water injection, and after hot water injection. In the case of two of the three wells no cleaning or other operations were performed prior to running the heater. In the third test the well was cleaned with sodium hypochlorite solution before installing the heater. The equilibrium intake rate was carefully checked after installing the heater to make sure that disturbing the well did not effect its injection behavior.

There were at least two periods of hot water injection for each well with sufficient time between to determine the cold water injection rate. The periods of hot water injection lasted from 3 to 10 weeks, or at least until the intake rate stopped climbing while the heat was still on. Several periods of hot water injection were experimented with to determine if successive treatments would continue to change the injection rate or whether one treatment alone would perform the ultimate.

In order to further analyze the effect of hot water injection treatments, pressure fall-off and injectivity tests were performed on the wells before and after treatment. In the case of one well temperature logs were run before treatment and again just after the heater was turned off and pulled out.

Upon termination of the heat treatments the intake rate behavior of the wells would be charted for at least six months to determine how permanent the change in intake rate would be.

Test I - McManus Lease Well W-18

McManus Well W-18 is drilled into the Bradford Third Sand in an area where the sand is quite "broken" and where about half of the sand has a permeability of 1 md. or less. As a result the intake rate was low ever since the start of the flood about nine years ago. This well may be considered typical of many in the Bradford field. The producer tried various cleaning operations without much effect on the intake rate. The lease production is still profitable but could be made more profitable if it were possible to increase intake rates and speed up the flood.

Before heat treatments the equilibrium intake rate of the well was determined as 16.8 bbl/day at an average well-head pressure of 1080 psig. The heater was installed and after several weeks the intake rate of the well was still 16.8 bbls/day. The heater was turned on and left on for a period of 21 days. The intake rate went up sharply for about 15 days and then started to level off. A complete intake rate and pressure history on the well is found in Figure 3. After 21 days the intake rate stood at 21.1 bbls. per day or an increase of 26 per cent. The average bottom hole water temperature was calculated at 250°F.

The electricity was then turned off and after several days the intake rate started falling. Within ten days it appeared to be leveling off at about 19 bbls. per day. For the next month there was a series of disturbances on the lease causing erratic operation and low pressures. About the 65th day the plant was again functioning fairly smoothly although the pressure was still a little low. The heater was turned on again on the 75th day and the intake rate started climbing. After 20 days the intake rate appeared to be leveling off at 22.7 bbls./day for an increase of 35 per cent over the original cold water injection rate of 16.8 bbls./day.

For the next 80 days the experiment was erratic for various operational reasons and the heater was on only about half the time. On the 178th day the heater was shut off and the well allowed to cool. The intake rate came down slowly and then appeared to settle at about 21 bbls/day at a pressure of 1070

psig. for a net increase in intake rate of 25 per cent. One year later the intake rate was still 19 bbls/day or 13 per cent higher than before hot water injection treatment.

Although not spectacular, the results are quite significant and bear out the results indicated by the laboratory tests. The second treatment appeared to have boosted the intake rate higher than the first one. From this it may be surmised that a series of treatments may be the most effective way of boosting intake rate by hot water injection treatment.

Well head pressure decline curves before, during and after treatment of the well are shown in Figure 4. A longer time for pressure fall off may be attributed to either more water backflowing from the less permeable sand or less water flowing into the more permeable sand. Whichever of the two explanations is considered it appears that the hot water injection treatment did change the water permeability characteristics of the well as reflected in the pressure decline curves.

Injectivity curves were also obtained on the well before, during and after treatment. These are shown in Figure 5. The curves taken during and after treatment are displaced downward at the lower injection pressures and are higher at the higher injection pressures when compared to the curve before treatment. Offhand, there is no ready explanation for the breaks in the curves. They may or may not be the result of the treatment. Although the change was not marked, the treatment did improve the injectivity characteristics of the well at least at the higher pressures.

Test II - Booth Lease Well DW-5

The second test was performed on another well drilled into the Bradford Third sand. The diamond core analysis on this well showed over 50 ft. of formation broken into many sand layers two thirds of which had permeabilities of 1 md. or less. The permeability log on the well is shown in Figure 6. The core also showed that the upper half of the formation had the bulk of the more permeable sand. The well is in an area where water by-passing between wells is fairly common. To be sure that none of the water injected into this well was by-passing into neighboring producers, about 15 lbs. of fluorescein dye was injected and tests made for the dye in the produced water of the four surrounding wells. Tests for 68 days failed to detect any fluorescein so it was assumed that there was no by-passing.

The heater was then installed in the well opposite the lower or less permeable portion of the formation so that most of the heat would be directed to the less permeable sand. Immediately after installation the heater was tested and found to be short circuited. The heater was pulled from the well and found to have a short circuit at the first connector.

While the heater was being repaired a temperature survey was run on the well by Bird Well Surveys, Inc. As shown in Figure 6 it indicated that most of the water was going into the upper part of the formation. An obstruction prevented the instrument from going below 1620 ft. A shut-in pressure decline curve and an injectivity rate curve were also determined for the well at the time it was at equilibrium.

The heater was installed again and the well allowed to come to equilibrium. After ten days the intake rate was down to about 31 bbls/day and the heater was turned on. As is shown in Figure 7 the intake rate rose to about 34 bbls/day and remained there for about 20 days. Then the intake rate dropped to about 33 bbls/day for about 20 days due to lower plant pressures. When the plant pressure went up to its normal value the intake rate went back up to about 34 bbls/day. After 57 days of hot water injection the heater was turned off. The intake rate dropped slightly over the next ten days, and would have dropped more had the plant pressure been down to normal.

As soon as the heater was turned off measurements were made of the well's pressure decline rate when shut in, and the injectivity rates when turned back on. The values are plotted in Figures 8 and 9. When compared to the curves before heating they show little change.

The increase in intake rate of 3.5 bbls/day or about 11% appears rather small. However, since only about half of the total water was being heated, the increase in intake rate to the lower sands could have been greater than 11%. From the core log it can be estimated that about 55% of the injection water was going to the formation opposite and below the heater. Thus 16.7 bbls/day of the original 30.5 bbls/day were heated. Assuming the increased intake rate of 3.5 bbls/day is all attributable to the lower section, then the increase in intake rate could possibly be 21%. Continuing on the same assumptions, it was calculated that the temperature of the heated water at the sand face could have been as high as 350°F.

It was then decided to raise the heater so that all of the water would be heated. Accordingly the heater was raised so that 22 of its 26 ft. length were above the top of the sand (see Figure 6). After the well had settled for 17 days and the intake rate appeared to be steady, the heater was turned on

again. After 5 days the intake rate started rising and it reached a maximum of 34.5 bbls/day after 20 days. Then it started to decline for some unknown reason and leveled off at approximately 33.2 bbls/day as shown in Figure 7.

After 67 days of hot water injection the heater was turned off and pulled from the well. As soon as the heater was out of the well, which was about 6 hours, a temperature log was run on the formation while the well was backflowing. The log is plotted in Figure 6 and indicates that heated water had permeated and was backflowing from all of the permeable formation. As would be expected from the permeability profile, most of the heated water was injected into the more permeable upper formation from whence it backflowed at the highest temperature (110°F). The calculated temperature of the heated injection water was 221°F. Since the backflow water was only 110°F there is evidence to assume that there was a large heat loss to the formation and the temperature gradient away from the well bore was steep.

After taking the temperature log, the water was turned back into the well. After fill-up the well settled down to 32.6 bbls/day where it remained for the next few months. The net increase in intake rate due to treatment may be estimated at 2.1 bbls/day or 6.5% which was disappointingly small.

About a month after the well was allowed to cool off, shut-in pressure decline rates and injectivity rates were measured again. These are plotted in Figures 8 and 9 along with those taken before hot water injection and those taken during hot water injection. The curves differ only slightly, which was to be expected since the increase in water intake rate was small.

Test III - McManus Well W-21

This well is adjacent to and in the same five spot as McManus Well W-18 on which Test I was performed. It has the same broken sand character and showed a low input rate right from the start. Before anything was done to the well its intake rate was about 7.5 bbls/day.

In the other two tests hot water treatment was applied without cleaning the wells in any way. To determine whether a clean well would respond differently to hot water treatment, it was decided to thoroughly clean the well in Test III before treatment. Accordingly the tubing was reamed and the well flushed. Then it was treated with 30 gallons of concentrated sodium hypochlorite solution, and again thoroughly flushed. As is noted in Figure 10 this succeeded in raising the intake rate from 7.5 to 9.2 bbls/day.

Then the heater was installed which disturbed the well again. However, after about a week the intake rate had again settled down to 9.2 bbls/day. The heater was turned on and within five days the intake rate rose to 10.6 bbls/day. About that time a serious leak developed at the adaptor on the well tubing. In order to repair it, it was necessary to withdraw the heater from the well. It was two weeks before the leak was repaired and the heater was back in the well. After another week the intake rate was back down to 10.4 bbls/day, and the heater was turned on again.

The heater was on for 43 days during which time the intake rate rose steadily to about 13.7 bbls/day where it appeared to level off. Since the intake rate rose an unprecedented 50% and it was feared that there might be a leak down in the well, the heater was turned off. The intake rate then dropped slowly and appeared to be leveling off at 13.2 bbls/day. Unfortunately, there was pump and engine trouble at the plant from then on for the next 40 days.

All the troubles were corrected about the 170th day, and by that time the well's intake rate had slipped to about 11.8 bbls/day. The heater was turned on again and the intake rate started rising. Just before this paper was typed the intake rate was back up to 13.8 bbls/day and still rising.

Assuming that the final equilibrium intake rate does not go any higher than 11.8 bbls/day, even though it looks very much as if it will, the net increase in intake rate of this well can be estimated to be about 28%. This is higher than for the other two wells even though it had but one treatment to this point.

As in the case of the other tests, shut-in pressure fall-off rates and injectivity rates were determined on the well before and during treatment. In Figure 11 we see that the pressure fall off rate is a little less rapid during treatment than before treatment. Figure 12 shows the injectivity rates to be considerably higher during hot water injection than before hot water injection. Due to erratic plant pressures it was impossible so far to obtain pressure fall-off and injectivity rates after the first hot water injection treatment.

On a basis of heater output and a water injection rate of 13 bbls/day it was calculated that the water in the well was as high as 440°F. On a basis of 9.2 bbls/day it could have been as high as 600°F.

Discussion and Conclusions

The results obtained in a way confirm those obtained in the laboratory as well as those obtained in the field by Kenneth Barton. However, they were affected on a much reduced scale.

Offhand, an increase in intake rate of 11 to 28 per cent does not seem spectacular. Nevertheless if such an increase in intake rate could be translated to a proportionate increase in production, it would be very significant from an economic standpoint. Of course, the cost and frequency of treatment will have to be reasonable if the application is to be practical. Cost figures were not considered in these experiments, but it was estimated that the electricity costs alone ran from $50 to $200.

It is more interesting to note that the response of the wells was inversely proportional to the original intake rates and directly proportional to the temperature rise. This is illustrated graphically in Figure 13. If the BTU output of the heater was not limited, it would have been interesting to see what would have happened at temperatures above those reached in these tests.

It is also interesting to speculate on the mechanism or reasons for the increased intake rates after hot water injection treatment. The first suggestion that comes to mind is a removal of some of the residual oil with an attendant increase in relative permeability to water. Another possibility is the solution or modification of some of the unnatural plugging materials that may have found their way to the sand face and shot cracks during previous flooding. However, this would hardly be the reason for obtaining results in the laboratory where the flood water was clean and stable.

A more interesting possibility would be the solution or modification of some of the cementing materials in the sand. This has some credence when considered in the light of the results of some experiments(1) in which the permeability of limestones were increased considerably by heating them in water to moderate temperatures while under high pressure. The cementing materials of Bradford sand do contain slightly soluble minerals, and it is reasonable to assume that their solubility would be increased at higher temperatures. Also, it is not entirely unreasonable to assume that the lower permeability sand may have more cementing material and hence more of the soluble minerals.

The authors feel that although the results of the experiments just described were not spectacular, further experiments, particularly at much higher temperatures, are warrented.

Acknowledgments

The authors wish to acknowledge the co-operation of the many people that make these experiments possible. In particular we wish to thank, Quentin Wood, Kenneth Barton and Dr. E. T. Heck of the Quaker State Oil Refining Corporation, Arthur Simmons and Stanley Grove of the Simmons Oil Co., Col. P. J. Stevenson and William Rindlaub of the Pennsylvania Electric Company, Roy McKnight of Woessner-McKnight, Inc., and James Bird of Bird Well Surveys, Inc. Other members of the Pennsylvania Grade Crude Oil Association Laboratory who helped in these experiments were Joseph Saxon, Jr., D. Thomas Byrne, Robert Neal and Willard Miller.

We wish to thank the Production Research Technical Advisory Committee of the Pennsylvania Grade Crude Oil Association for their guidance and for permission to publish the results of these experiments.

Bibliography

(1) "Expansion and Increase in Permeability of Carbonate Rocks", J. C. Maxwell and Peter Verall, TRANS. AM. GEOPHYSICAL UNION, Vol. 34, No. 1, February 1953.

TABLE I

EFFECT OF HOT WATER TREATMENT ON INTAKE RATES

OF BRADFORD SAND CORES

Core No.	Approximate Air Perm. In Md.	Water Intake Rate, ml/min.		% Change In Intake Rate
		Before Treatment	After Treatment	
97	2.0	0.44	1.30	+ 195
99	1.0	0.35	0.47	+ 34
101	0.5	0.0035	0.013	+ 270
102	0.5	0.19	0.21	+ 10
103	1.0	0.60	0.54	- 10
104	0.1	0.002	0.010	+ 400
105	1.5	0.45	0.51	+ 13
106	0.1	0.12	0.16	+ 33

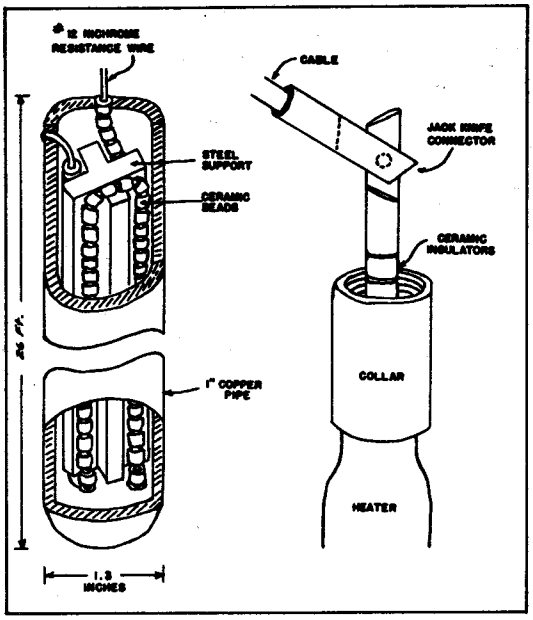

FIG. 1 – CONSTRUCTION OF ELECTRIC HEATER AND CABLE CONNECTORS

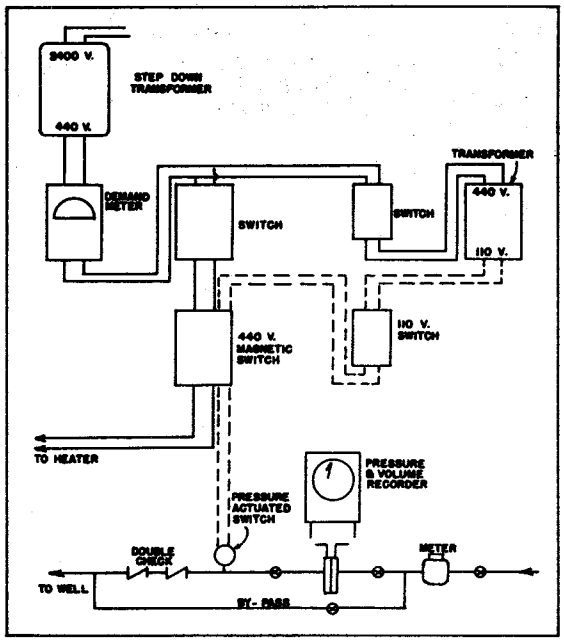

FIG. 2 – DIAGRAM OF ELECTRICAL HOOKUP AND ARRANGEMENT OF EQUIPMENT FOR BOTTOM HOLE HEATER EXPERIMENTS

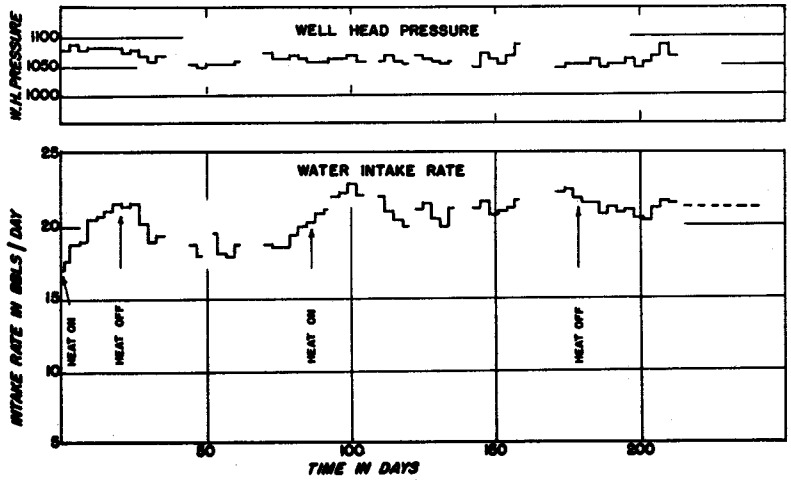

FIG. 3 – EFFECT OF HOT WATER INJECTION ON INTAKE RATE OF McMANUS WELL W-18

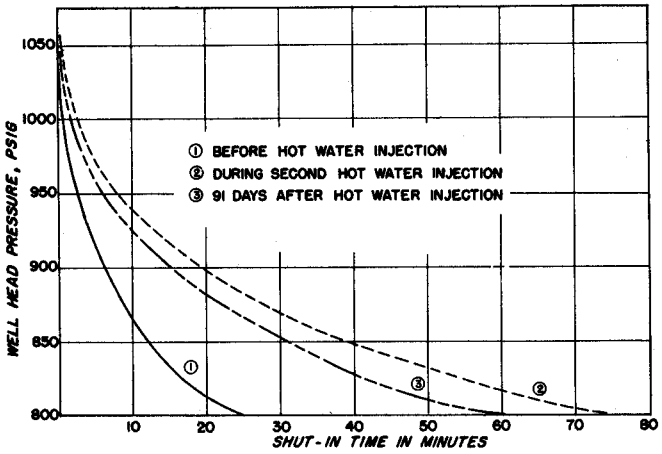

FIG. 4. - PRESSURE DECLINE CURVES AFTER SHUTTING IN McMANUS WELL W-18

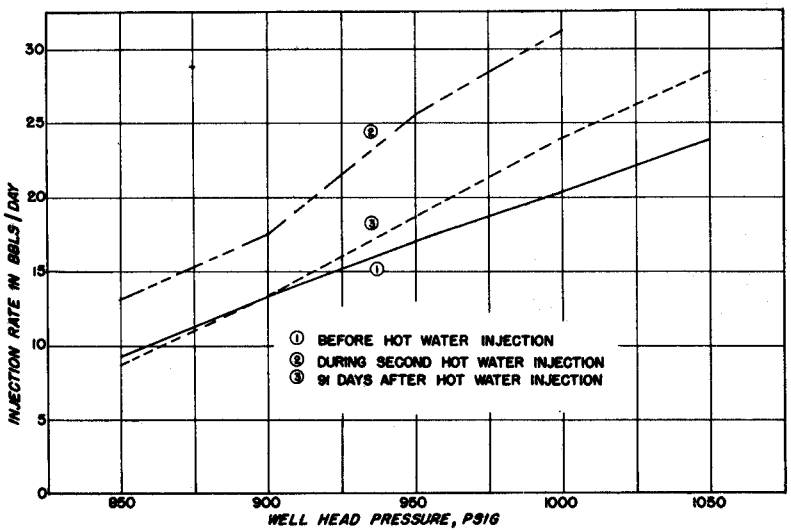

FIG. 5 - WATER INJECTIVITY CURVES ON McMANUS WELL W-18

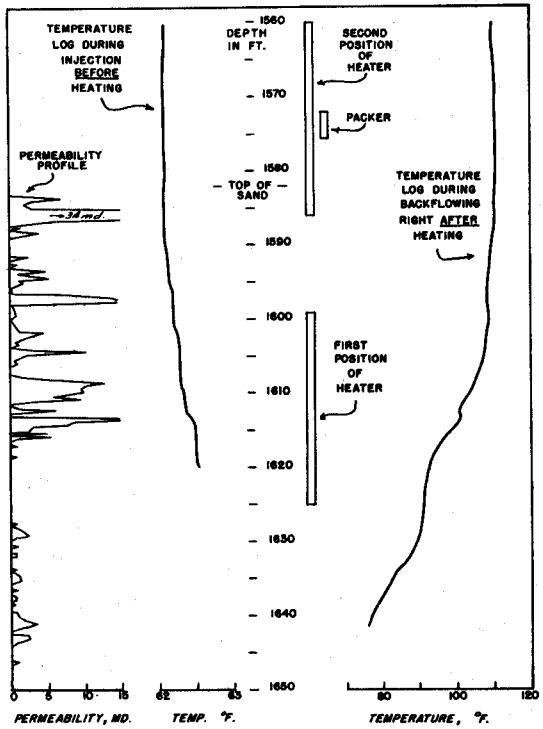

FIG. 6 - PERMEABILITY AND TEMPERATURE LOGS ON BOOTH WELL DW-5

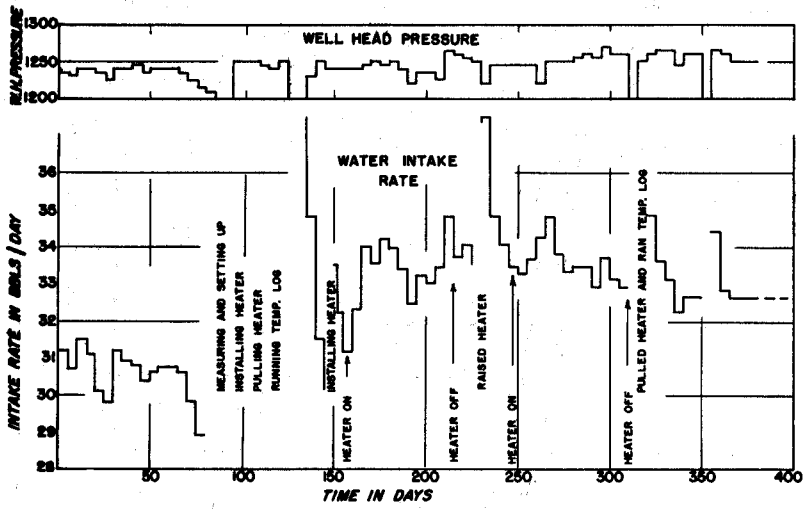

FIG. 7 – EFFECT OF HOT WATER INJECTION ON INTAKE RATE OF BOOTH WELL DW-5

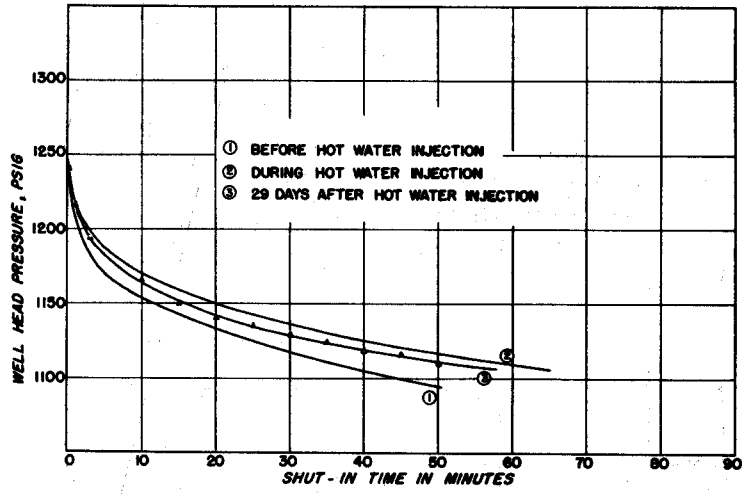

FIG. 8 – PRESSURE DECLINE CURVES AFTER SHUTTING IN BOOTH WELL DW-5

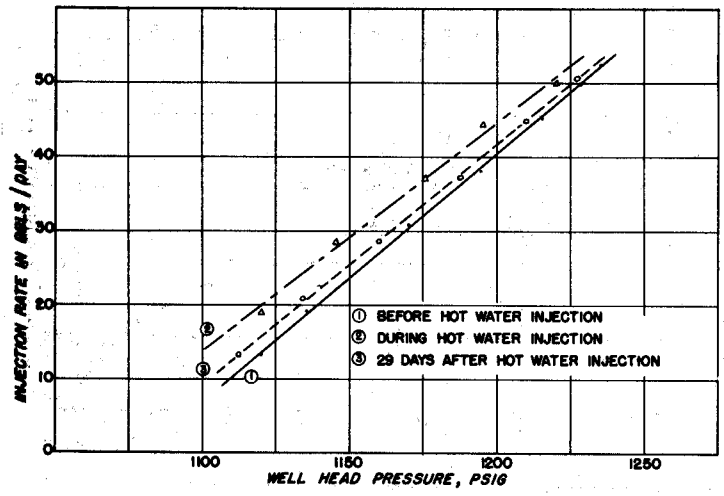

FIG. 9 - WATER INJECTIVITY CURVES ON BOOTH WELL DW-5

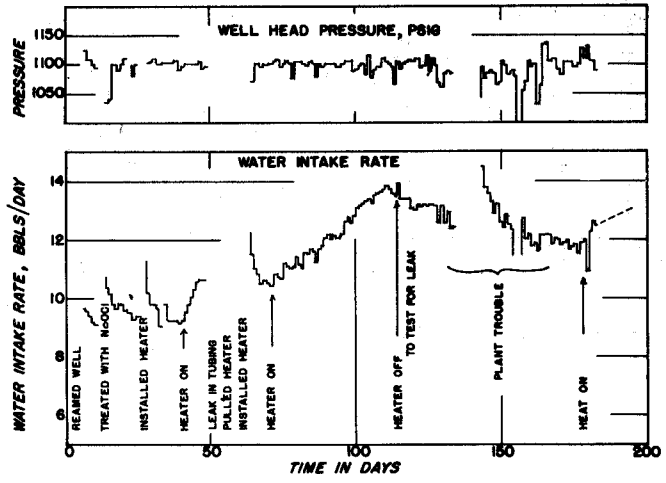

FIG. 10 – EFFECT OF HOT WATER INJECTION ON INTAKE RATE OF McMANUS WELL W-21

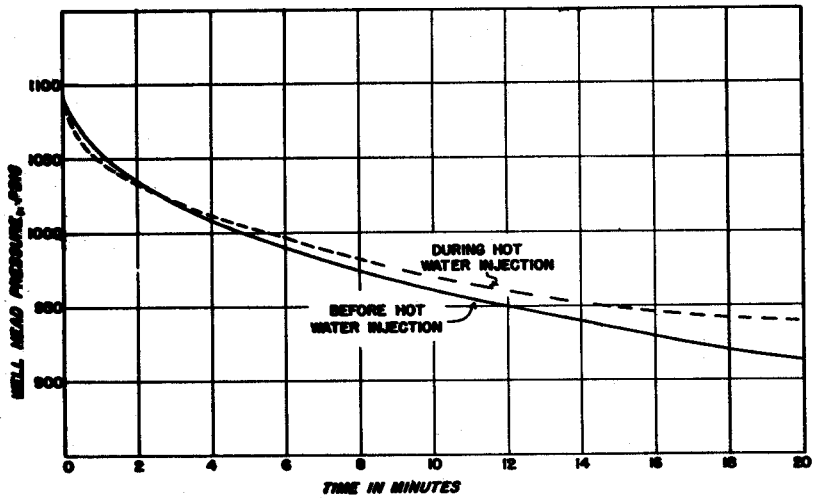

FIG. 11 – PRESSURE DECLINE CURVES AFTER SHUTTING IN McMANUS WELL W-21

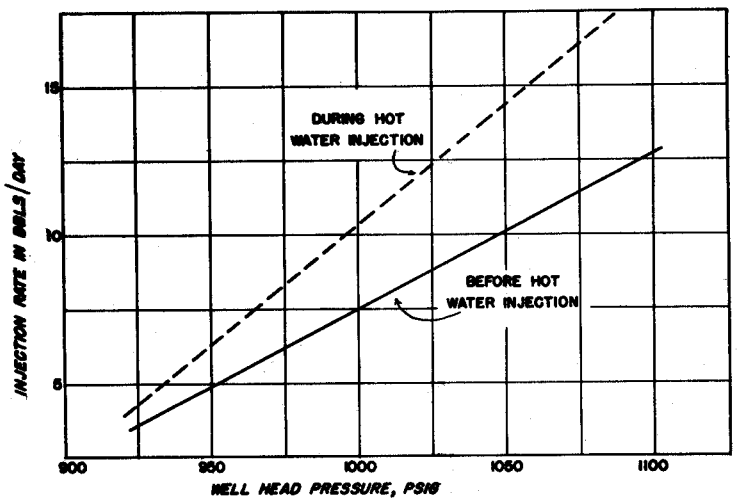

FIG. 12 – WATER INJECTIVITY CURVES ON McMANUS WELL W-21

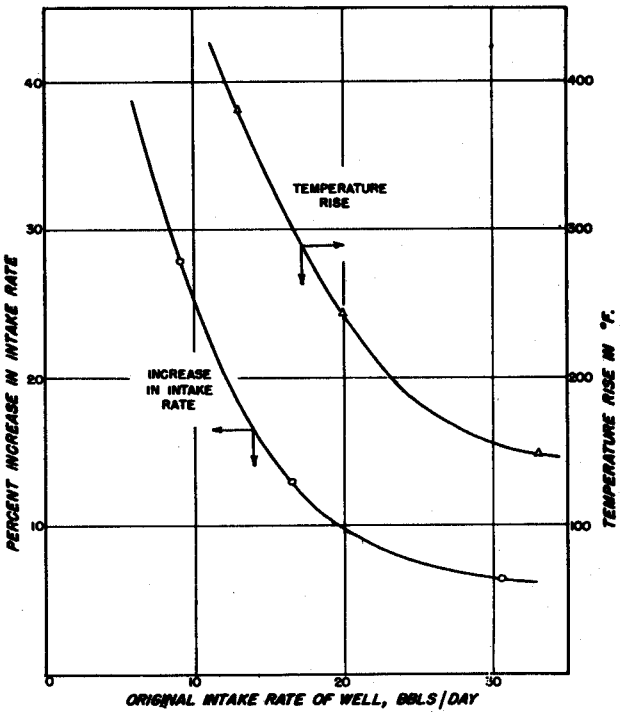

FIG. 13 – INCREASE IN INTAKE RATE AND TEMPERATURE RISE vs ORIGINAL INTAKE RATE

Seventeenth Technical Conference

Registration

Name	Company	Address
Alexis, Carl	Kendall Refining Co.	Bradford, Pa.
Austin, M. E.	Sun Oil Company	Mt. Pleasant, Michigan
Bail, Paul T.	U. S. Bureau of Mines	Bradford, Pa.
Barker, George E.	Atlas Powder Co.	Wilmington, Delaware
Barley, Roy E.	Wolf's Head Oil Refining Co.	Oil City, Pa.
Barnes, Kenneth B.	Oil and Gas Journal	Tulsa, Oklahoma
Barnett, Russell	Kendall Refining Co.	Bradford, Pa.
Bauer, G. G.	Producers Monthly	Bradford, Pa.
Beadell, D. A.	General Aniline & Film Corp.	New York, N. Y.
Bird, James M.	Bird Well Surveys	Bradford, Pa.
Bissey, Luther T.	The Pennsylvania State College	State College, Pa.
Black, Joseph L.	The Ohio Oil Co.	Terre Haute, Indiana
Blanchard, Miles B.	Quaker State Oil Refining Co.	Titusville, Pa.
Bobek, Jack E.	Carter Oil Co.	Tulsa, Oklahoma
Bohne, Henry J.	Thornton Co.	Wellsville, N. Y.
Booth, A. E.	M. D. Booth & Co.	Bradford, Pa.
Brandner, J. D.	Atlas Powder Co.	Wilmington, Delaware
Breston, J. N.	Penna. Grade Crude Oil Ass'n	Bradford, Pa.
Brewster, Frank	Belmont Quadrangle	Bradford, Pa.
Bridges, Harry B.	Shell Oil Co.	Centralia, Illinois
Bryner, E. James	Andrus & Bryner	Bradford, Pa.
Buchanan, D. W.	Preston Oil Co.	Columbus, Ohio
Burcik, Emil J.	The Pennsylvania State College	State College, Pa.
Calhoun, John C.	The Pennsylvania State College	State College, Pa.
Carlson, O. C.	South Penn Oil Co.	Bradford, Pa.
Castner, J. D.	Sohio Petroleum Co.	Oklahoma City, Oklahoma
Chipman, Charles	Penn Grade	Bradford, Pa.
Clark, A. P.	Independent	Wichita Falls, Texas
Cochran, Karney	Bradley Producing Corp.	Wellsville, N. Y.
Coley, Frank H.	The Pennsylvania State College	State College, Pa.
Cone, Earl H.	Hercules Powder Co.	Wilmington, Delaware
Convers, Frederick L.	University of Pittsburgh	Pittsburgh, Pa.
Cook, Michael	Bradley Producing Corp.	Wellsville, N. Y.
Corey, Arthur T.	Gulf Research & Development	Harmarville, Pa.
Crego, Bill	Tenn. Prod. Co.	Victoria, Texas
Danielson, Harlan H.	South Penn Oil Co.	Bradford, Pa.
Davies, James Allen	Thornton Co.	Wellsville, N. Y.
DePetro, John	Self	Bradford, Pa.
Dew, John	Continental Oil Co.	Ponca City, Oklahoma
Dunning, H. N.	Bureau of Mines	Bartlesville, Oklahoma
Edele, R. H.	West Virginia University	Morgantown, W. V.
Elicker, R. E.	South Penn Oil Co.	Bradford, Pa.
Ellenberger, Dick	Bradford Laboratories	Bradford, Pa.
Emery, J. R.	The Pennsylvania State College	State College, Pa.
Fancher, George	University of Texas	Austin, Texas
Feldmiller, Charles H.	Valvoline Oil Co.	Pittsburgh, Pa.
Felley, D. L.	Rohm & Haas Co.	Philadelphia, Pa.
Fisher, Henry B.	Phillips Petroleum Co.	Bartlesville, Oklahoma
Flower, Earl G.	Wolf's Head Oil Refining Co.	Oil City, Pa.
Freeman, James P.	The Texas Co.	Wichita, Kansas
Fulton, Paul F.	University of Pittsburgh	Pittsburgh, Pa.
Garin, T. J.	Penn Grade Crude Oil Ass'n	Oil City, Pa.
Grant, Bruce F.	Sinclair Research Labs.	Tulsa, Oklahoma
Gregory, A. R.	Gulf Research & Development	Pittsburgh, Pa.
Griffin, Wm. C.	Atlas Powder Co.	Wilmington, Delaware
Griffiths, J. C.	The Pennsylvania State College	State College, Pa.
Haas, George E.	Sun Oil Co.	Mt. Pleasant, Michigan
Hadidi, Taher A. R.	The Pennsylvania State College	State College, Pa.
Hardison, Eugene D.	U. S. Bureau of Mines	Washington, D. C.

Name	Company	Address
Harnish, Douglas H.	West Virginia University	Morgantown, W. V.
Headlee, A. J.	West Virginia Survey	Morgantown, W. Va.
Heck, E. T.	Minard Run Oil Co.	Bradford, Pa.
Heller, John P.	Magnolia Petroleum Co.	Dallas, Texas
Hindus, Richard F.	United Gas Corp.	Shreveport, La.
Hipple, J. A.	The Pennsylvania State College	State College, Pa.
Hogg, Paul J.	Quaker State Oil Refining Corp.	Titusville, Pa.
Holmes, Charles R.	The Pennsylvania State College	State College, Pa.
Howell, Ben F.	The Pennsylvania State College	State College, Pa.
Huntington, H. M.	Kendall Refining Co.	Bradford, Pa.
James, E. G.	Kendall Refining Co.	Bradford, Pa.
Johnson, F. Arthur	Reg. Prof. Eng'r.	Oil City, Pa.
Johnson, W. E.	Penn Grade Crude Oil Assn	Bradford, Pa.
Jones, J. P.	Penn Grade Crude Oil Ass'n	Bradford, Pa.
Jones-Parra, Juan	The Pennsylvania State College	State College, Pa.
Jukes, Harry R.	Gulf Research & Development	Pittsburgh, Pa.
Kennedy, Tracy J.	Magnolia Petroleum Co.	Electra, Texas
Kern, Curtis R.	Atlas Powder Co.	Houston, Texas
Killins, C. R.	Ohio Oil Co.	Terre Haute, Indiana
Kumpf, Fred W.	Socony-Vacuum Oil Co.	Worland, Wyoming
Lang, W. E.	Ashland Oil Refining Co.	Ashland, Kentucky
Latimer, Warren E	James A. Lewis Eng'r Inc.	Winchester, Kentucky
Lembche, Richard	Cities Service Research & Development	Tulsa, Oklahoma
Lent, L. G.	Andrus, Lent & Daggett	Bradford, Pa.
Lent, Raymond	Andrus, Lent & Daggett	Bradford, Pa.
Levine, J. S.	Shell Oil Co.	Houston, Texas
Lewis, Arthur	Bradley Producing Co.	Wellsville, N. Y.
Lewis, Roger	Bradley Producing Co.	Wellsville, N. Y.
Licastro, P. H.	The Pennsylvania State College	State College, Pa.
Lineman, Myron M.	Bradley Producing Co.	Wellsville, N. Y.
Lyons, Frank E.	Wolf's Head Oil Refining Co.	Oil City, Pa.
Lyon, Richard B.	Messer Oil Corp.	Olean, N. Y.
Lytle, William S.	Pa. Topographic & Geologic Survey	Butler, Pa.
MacFarlane, Robert	Penn Grade Crude Oil Ass'n	Bradford, Pa.
McClintock, C. B.	Wolf's Head Oil Refining Co.	Oil City, Pa.
McConnell, E. B.	The Pennsylvania State College	State College, Pa.
Marsden, Sullivan S.	The Pennsylvania State College	State College, Pa.
Meadors, V. G.	Carter Oil Co.	Tulsa, Oklahoma
Meldrum, Alan H.	The Pennsylvania State College	State College, Pa.
Monzingo, A. J.	Magnolia Petroleum Co.	Salem, Ill.
Neil, Don C.	Penn Grade Crude Oil Ass'n	Bradford, Pa.
Newman, Robert C.	The Pennsylvania State College	State College, Pa.
Newton, Richard R.	Smith Newton Oil Co.	Bradford, Pa.
Nielsen, Ralph F.	The Pennsylvania State College	State College, Pa.
Noonan, John F.	Bureau of Mines	Franklin, Pa.
O'Leary, Fred T.	Continental Oil Co.	Ponca City, Oklahoma
Paez. Jose G.	The Pennsylvania State College	State College, Pa.
Parrish, David R.	Stanolind Oil and Gas Co.	Tulsa, Oklahoma
Paulsell, William G.	The Pennsylvania State College	State College, Pa.
Paynter, Warren T.	South Penn Oil Co.	Bradford, Pa.
Pearman, Benjamin R.	Penn Grade Crude Oil Ass'n	Bradford, Pa.
Platt, H. O.	R. B. Moore Supply Co.	Bolivar, N. Y.
Powell, W. E.	Larkin & Co.	Olney, Illinois
Preston, Floyd W.	The Pennsylvania State College	State College, Pa.
Pyle, Foster M.	D. D. Feldman Oil & Gas	Dallas, Texas
Richards, R. G.	Bradford Supply Co.	Wichita Falls, Texas
Reed, Philip W.	The Pennsylvania State College	State College, Pa.
Riegle, Warren E.	National Supply Co.	Winchester, Kentucky
Rindlaub, W. T.	Penna. Electric Co.	Bradford, Pa.
Rogers, Douglas	South Penn Oil Co.	Bradford, Pa.
Rose, Herbert E.	Superior Oil Co.	Bakerfield, Calif.
Sayre, A. T.	Pure Oil Co.	Crystal Lake, Illinois
Scott, A. W.	Wolf's Head Oil Refining	Oil City, Pa.
Sherman, Carl W.	The Ohio Oil Co.	Terre Haute, Ind.

Name	Company	Address
Simmons, Arthur C.	Arthur C. Simmons	Bradford, Pa.
Skow, Clifton S.	Hercules Powder Co.	Wilmington, Delaware
Smith, Dale C.	Preston Oil Co.	Columbus, Ohio
Spencer, Oscar F.	The Pennsylvania State College	State College, Pa.
Stahl, C. Drew	The Pennsylvania State College	State College, Pa.
Stockwell, Clifford	The Pennsylvania State College	State College, Pa.
Sturm, Paul W.	Ashland Oil & Refining Co.	Ashland, Kentucky
Sweeney, Albert E.	Interstate Oil Compact Com.	Oklahoma City, Oklahoma
Szasz, Stephen E.	Sinclair Research	Tulsa, Oklahoma
Taylor, Berne E.	Kendall Refining Co.	Bradford, Pa.
Taylor, S. S.	Bureau of Mines	Franklin, Pa.
Thompson, W. E.	Sun Oil Co.	Norwood, Pa.
Tomlinson, John B.	Gulf Refining Co.	Laurel, Miss.
Vaughn, J. C.	Stanolind Oil & Gas Co.	Tulsa, Oklahoma
Villarreal, Juan	The Pennsylvania State College	State College, Pa.
Walchli, John	Richardson Petroleum Corp.	Wellsville, N. Y.
Warren, Joseph E.	The Pennsylvania State College	State College, Pa.
Waterman, James C.	Thornton Company	Wellsville, N. Y.
Weeks, H. J.	Sun Oil Co.	Philadelphia, Pa.
Wertman, Wm. T.	Bureau of Mines	Franklin, Pa.
White, Chester N.	Sun Oil Co.	Newtown Square, Pa.
Wiesner, Gale M.	Quaker State Oil Refining	Bradford, Pa.
Wise, Dennis	South Penn Nat. Gas	Parkersburg, W. Va.
Wood, Quentin E.	Quaker State Oil Refining Co.	Bradford, Pa.
Wygal, R. J.	Gulf Research & Development	Harmarville, Pa.
Young, Wilber H.	Bradley Producing Corp.	Wellsville, N. Y.